Characterization of the Isoforms of the Multiple Sclerosis Risk Protein, IL-22 Binding Protein (IL-22BP)

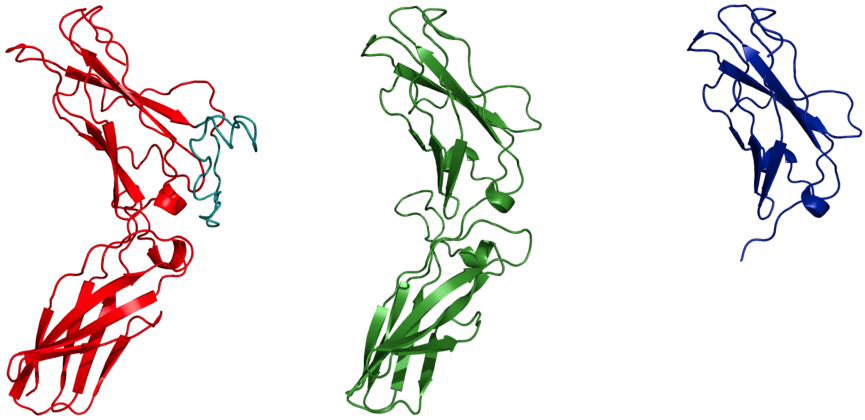

Paloma Gómez Fernández

eman ta zabal zazu

(c)2021 PALOMA GOMEZ FERNANDEZ

Characterization of the Isoforms of the Multiple Sclerosis Risk Protein, IL-22 Binding Protein (IL-22BP)

Author:

Paloma Gómez Fernández

Director:

Koen Vandenbroeck

Co-director:

Iraide Alloza

Departamento de Neurociencias, Facultad de Medicina y Enfermería

2021

eman ta zabal zazu

Universidad del País Vasco

Euskal Herriko Unibertsitatea

INDEX

List of figures

List of tables

List of abbreviations

Abbreviation	Definition
17-DMAG	17-dimethylaminoethylamino-17-demethoxygeldanamyin
17AAG	17-allylamino-17-demethoxygeldanamycin
aa	Amino acid
ANN	Artificial neural network
AP	Acetone precipitates
APC	Antigen processing and presenting cell
ATP	Adenosine triphosphate
B Lymphocytes	Bursal or bone-marrow-derived lymphocyte
B1	Follicular B cells
BCR	B-cell receptor
BLAST	Basic Local Alignment Tool
βME	Beta mercapthoethanol
bp	Base pair
CD	Crohn's disease
CD	Cluster of designation
cDC	Conventional dendritic cell
CIS	Clinically isolated syndrome
CL	Cell lysates
CM	Conditioned media
CNS	Central nervous system
CRC	Colorectal cancer
CsA	Cyclosporine A
CTD	C-terminal domain
DAMP	Damaged associated molecular pattern
DC	Dendritic cell
DM	Differentiation medium
dsRNA	Double-stranded

Endo H	Endoglycosidase H
ER	Endoplasmic reticulum
FBS	Foetal bovine serum
Fo	Follicular B cells
GA	Geldanamycin
GM-CSF	Granulocyte-macrophage colony-stimulating factor
GWAS	Genome-wide association study
h-region	Hydrophobic region
HMM	Hidden Markov model
HPA	Human Protein Atlas
HSP	Heat shock protein
IBD	Inflammatory bowel disease
IDR	Intrinsically disordered region
IFNγ	Interferon gamma
IL-10Rb	Interleukin 10 receptor, beta subunit
IL-22	Interleukin 22
IL-22BPi1	Interleukin 22 binding protein isoform-1
IL-22BPi2	Interleukin 22 binding protein isoform-2
IL-22BPi3	Interleukin 22 binding protein isoform-3
IL-22R	Interleukin 22 heterodimer receptor
IL-22RA1	Interleukin 22 receptor, alpha 1
IL22RA2v1	Interleuin 22 receptor, alpha 2, variant 1
IL22RA2v2	Interleuin 22 receptor, alpha 2, variant 2
IL22RA2v3	Interleuin 22 receptor, alpha 2, variant 3
ILC	Innate lymphoid cell
iNKT	Invariant natural killer T cell
IP	Immunoprecipitation
Leu	Leucine
LPS	Lipopolysaccharide
LTi	Lymphoid tissue-inducer cell
MD	Middle domain

MHC	Major histocompatibility complex
MRI	Magnetic resonance imaging
mRNA	Messenger RNA
MS	Multiple sclerosis
MZ	Marginal zone B cells
NAbs	Naturally occurring antibodies
NCR	Natural cytotoxicity receptor
NCR	Natural cytotoxicity-triggering receptor
NET	Neutrophil extracellular trap
NK	Natural killer cell
NKT	Natural killer T cell
nt	Nucleotide
NTD	N-terminal domain
O-GlcNAc	O-linked N-acetylglucosamine
ORF	Open reading frame
PAMP	Pathogen-associated molecular pattern
PBMC	Peripheral blood mononuclear cell
PCR	Polymerase chain reaction
PDB	Protein Data Bank
pDC	Plasmocytoid dendritic cell
PI	Proteasome inhibitor
PNGase F	Peptide:N-Glycosidase F
PPMS	Primary progressive multiple sclerosis
Pro	Proline
PTM	Post-translational modifications
qPCR	Quantitative polymerase chain reaction
RA	Rheumatoid arthritis
RIS	Radiologically isolated syndrome
RRMS	Relapsing-remitting multiple sclerosis
RT	Room temperature
SLE	Systemic lupus erythematosus
SNP	Single nucleotide polymorphism

SP	Signal peptide
SPMS	Secondary progressive multiple sclerosis
SS	Sjogren syndrome
ssRNA	Single-stranded RNA
T Lymphocytes	Thymus-derived lymphocyte
TC	Cytotoxic T cell
TCR	T-cell receptor
TGFβ	Transforming growth factor beta
TH1	T helper 1 cell
T_H2	T helper 2 cell
TLR	Toll-like receptor
TM	Transmembrane
TNFα	Tumour necrosis factor alpha
UC	Ulcerative colitis
UPR	Unfolded protein response
WB	Western blot

1. Abstract

1 Abstract

The human *IL22RA2* gene co-produces three protein isoforms in dendritic cells (IL-22 binding protein isoform-1 [IL-22BPi1], -2 [IL-22BPi2], and -3 [IL-22BPi3]). Two of these, namely, IL-22BPi2 and IL-22BPi3, are capable of neutralizing the biological activity of IL-22. The function of IL-22BPi1, which differs from IL-22BPi2 through an in-frame, 32-amino-acid insertion provided by an alternatively spliced exon, remains unknown.

This thesis focuses on the biochemical characterization of the three isoforms, as well as the potential pharmacological targeting thereof. Additionally, it addresses the functionality of the non-synonymous single nucleotide polymorphism (SNP), rs28385692, which is located in *IL22RA2* and has been found to be associated with multiple sclerosis (MS).

The present work demonstrates that IL-22BPi1 is secreted detectably, but at much lower levels than IL-22BPi2, and unlike IL-22BPi2 and IL-22BPi3, it is largely retained in the ER. In contrast to IL-22BPi2 and IL-22BPi3, IL-22BPi1 is incapable of neutralizing or binding to IL-22. To disclose the mechanism underlying the poor secretion of IL-22BPi1, interactome analysis were performed, and GRP78, GRP94, GRP170, and calnexin were identified as main interactors. IL-22BPi1 and IL-22BPi2 were also found to be bona fide clients of the ER chaperones GRP78 and GRP94. However, only IL-22BPi1 activates an unfolded protein response (UPR) resulting in increased protein levels of GRP78 and GRP94. Furthermore, this study investigated whether secretion of the IL-22BP isoforms could be modulated by pharmacological targeting of GRP94 and cyclophilin B, either by means of geldanamycin (GA), which binds to the ADP/ATP pocket shared by HSP90 paralogs, or by cyclosporin A, which causes depletion of ER cyclophilin B levels through secretion. It was found that GA and its analogues did not influence the secretion of IL-22BPi2 or IL-22BPi3, but significantly enhanced the intracellular and secreted levels of IL-22BPi1. The secreted protein was heterogeneously glycosylated, with both high-mannose and complex-type glycoforms present. In addition, cyclosporine A augmented the secretion of IL-22BPi1 and reduced that of

IL-22BPi2 and IL-22BPi3. These data indicate that the ATPase activity of GRP94 and cyclophilin B are instrumental in ER sequestration and degradation of IL-22BPi1 and that blocking these factors mobilizes IL-22BPi1 towards the secretory route.

The laboratory where this thesis was developed, in an SNP screen of this locus in a Basque population, found the non-synonymous SNP (rs28385692) of a rare coding variant substituting leucine (Leu) for proline (Pro) at the 16th position to be associated with MS. This variant is located in the signal peptide (SP) shared by the three secreted protein isoforms. In the present thesis, *in silico* and in vitro analyses were also performed to study the effect of this variant. *In silico* analyses predicted both disruption of the alpha helix of the h-region of the SP and decreased hydrophobicity of this region, ultimately affecting the SP cleavage site. The *in vitro* effect of the p.Leu16Pro variant on the secretion of IL-22BPi1, IL-22BPi2, and IL-22BPi3 revealed that the Pro16 risk allele significantly lowers the secretion levels of each of the isoforms to around 50%–60% in comparison to the Leu16 reference allele.

These results suggest that genetically coded decreased levels of IL-22BP isoforms are associated with augmented risk for MS and that therapeutic modulation of the production of IL-22BPi2 and IL-22BPi3 variants may be beneficial in IL-22-dependent disorders, including autoimmune diseases, infection, and malignancy.

2. Introduction

2 Introduction

The work presented in this thesis has its roots in a previous study by our group in which a non-synonymous single nucleotide polymorphism (SNP), rs28385692, located in the *IL22RA2* gene was found to be significantly associated with multiple sclerosis (MS). This revealed the *IL22RA2* gene as a new player in our quest to understand the polygenic basis of the risk of contracting MS. *IL22RA2* codes for a soluble receptor that binds and blocks interleukin 22 (IL-22) activity. The scarcity of available data on the properties and biochemical characteristics of this protein and its associated isoforms triggered the research in this thesis. The following sections provide background information on the immune system, with an emphasis in IL-22 biology, its function and regulation, and its role in different diseases.

2.1 Overview: The human immune system

The human immune system consists of a complex network of biochemical and cellular mechanisms that defend the body from pathogens such as viruses, bacteria, fungi, and parasites. However, non-infectious substances are also capable of triggering the immune system, which might act against the body's own healthy cells and tissues in what is known as autoimmunity. There are two main lines of action against an infection: (i) a fast and broadly effective **innate immunity**, which also includes anatomical and physiological barriers, and (ii) a late and more specific **adaptive immunity** (**Figure 1**). However, these two types of immunity work together: innate immunity not only confers initial protection and a fast response to stop and delay the infection, but also prepares and influences adaptive immunity, which may also potentiate the protective mechanism of innate immunity (Abbas, Lichtman, & Pillai, 2012).

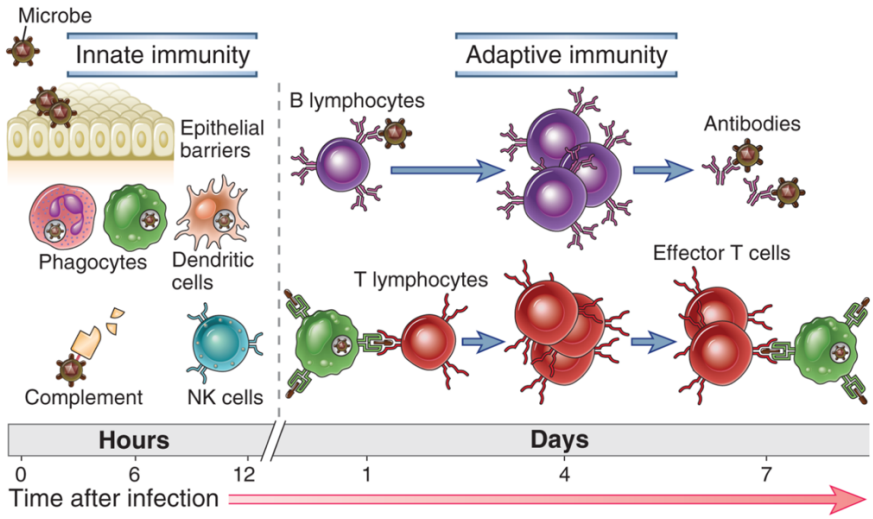

Figure 1: Integrated immune system. *The innate and adaptive immune components act sequentially after infection. Reproduced from Abbas et al., 2012.*

2.1.1 Innate immunity

Innate immunity is the first immune response against microbes; it stops, controls, and removes them from the host. It is comprised of anatomical and physiological barriers as well as cellular and humoral (macromolecules) components.

2.1.1.1 Anatomical and physiological barriers

The anatomical and physiological barriers are the first line of defence against pathogens. Epithelial surfaces are the initial physical barriers that pathogens encounter before entering into the host. Epithelial cells produce antimicrobial peptides and proteins (such as defensins); mucus; a low pH (stomach); and bacteriolytic lysozymes in tears, saliva, and other secretions that make the pathogens' entrance difficult. These barriers comprise skin, digestive, lung, and urogenital mucosal surfaces (Abbas, Lichtman, & Pillai, 2012).

The humoral and cellular components of innate immunity interact together and supplement the defence and protection offered by the

anatomical and physiological barriers. Innate immunity exists before the infection occurs and has a rapid response, within hours. It has a broad effect and is only capable of stopping a pathogen's entrance to a certain degree.

2.1.1.2 Cellular innate immunity

Cellular innate immunity involves cells that recognize pathogen-associated molecular patterns (PAMPs), which are molecular structures foreign to the self-organism; they have invariant characteristics among the microorganisms of a given class and also play essential roles in microbial physiology (Medzhitov, 2007). Some examples of PAMPs are nucleic acids (single-stranded RNA [ssRNA], double-stranded [dsRNA] from viruses, or unmethylated CpG motifs from bacteria), proteins from bacteria (flagellin or pilin), lipids from the cellular wall from gram-negative bacteria (lipopolysaccharide [LPS] and lipoteichoic acid), and carbohydrates from bacteria and fungi (mannan and dectin). Innate cells can also recognize endogenous molecules that are produced or released from damaged or apoptotic cells. These molecules, which are called damaged associated molecular patterns (DAMPs) include heat shock proteins (HSPs) located in exosomes, adenosine triphosphate (ATP), uric acid, and nuclear or cytoplasm proteins (HMGB1 and S100), among others (Schaefer, 2014). PAMPs and DAMPs are recognized by pattern recognition receptors (PRRs), such as cell surface or endosomal Toll-like receptors (TLRs) numbered from 1 to 9 in humans, depending on their cellular location and ligands. The main cell types that constitute innate immunity are **phagocytic cells**, **dendritic cells**, and **innate lymphoid cells**, whose functions and components are described next.

2.1.1.2.1 Phagocytic cells

Phagocytic cells have the capacity to internalize and degrade foreign particles, debris, or cells. They are the second line of defence against pathogens that break the anatomical and physiological barriers. These cells possess myeloid origins.

Neutrophils comprise the major population of leucocytes in the circulating blood (50%–70%) and are normally the first to be recruited to an inflammatory site. They act as phagocytic cells, releasing lytic enzymes from their granules and secretory vesicles and producing reactive oxygen intermediates with antimicrobial potential. Moreover, they can also eliminate extracellular pathogens by degranulation or by releasing neutrophil extracellular traps (NETs), which have the capacity to immobilize pathogens facilitating their phagocytosis. NETs are DNA elements where histones, proteins, and other enzymes are attached. Neutrophils are mainly actors in acute inflammation, but they can also contribute to adaptive immunity (Kolaczkowska & Kubes, 2013). Although neutrophils are the most abundant type of granulocytes, other types are included in this category: mast cells, eosinophils, and basophils. They participate in both innate and adaptive responses and are also central effector cells in allergic inflammation (K. D. Stone, Prussin, & Metcalfe, 2010).

Macrophages play several important roles in both innate and adaptive immunity. Their major role in innate immunity is host defence through their phagocytic activity and clearance of apoptotic cells; in addition, macrophages also secrete both proinflammatory and antimicrobial mediators and participate in tissue development, homeostasis, and repair (Okabe & Medzhitov, 2016). They can be derived from monocytes; however, the resident macrophages that are located in the tissues are known to be derived from embryonic precursors that seed the tissue before birth (Ginhoux & Jung, 2014).

2.1.1.2.2 Dendritic cells (DCs)

Dendritic cells (DCs) are professional antigen processing and presenting cells (APCs) that shape a crucial interface between the innate sensing of pathogens and the adaptive immunity activation. They can be derived from a common DC progenitor giving rise to both plasmacytoid dendritic cells (pDCs) and to myeloid/conventional DCs (cDC1 or cDC2) or can also be derived from monocytes, as previously stated for macrophages,

creating another subset called monocyte-derived DCs (moDCs). Each DC subset is developed under the regulation of different repertoire transcription factors and express different surface markers, **Figure 2** (Collin & Bigley, 2018; Collin, Bigley, Haniffa, & Hambleton, 2011; Guilliams et al., 2014). DCs are highly phagocytic sentinels that process pathogenic antigens in tissues and migrate to secondary lymphoid organs where they present them to T lymphocytes in order to stimulate their proliferation and differentiation, therefore DCs are key mediators between innate and adaptive response (Worbs, Hammerschmidt, & Förster, 2017).

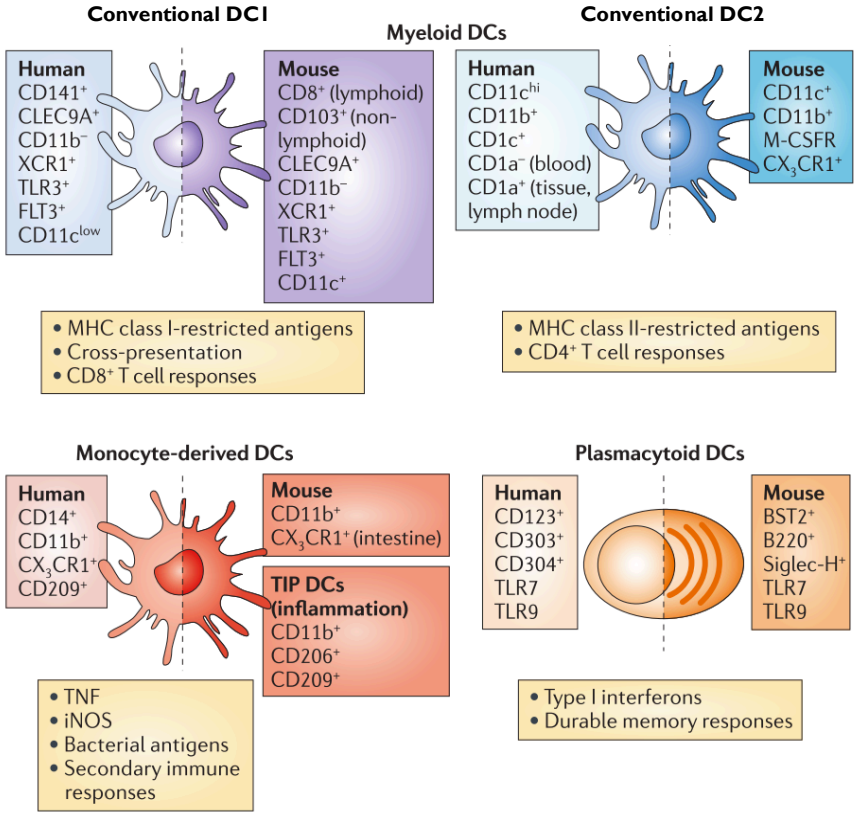

Figure 2: Types of dendritic cells (DCs). *Different subsets of dendritic cells in humans with their equivalent counterpart in mice. The surface markers that characterize each subset are indicated, and their main functions are indicated in the yellow boxes. Adapted from Collin et al., 2011.*

2.1.1.2.3 Innate lymphoid cells (ILCs)

Innate lymphoid cells (ILCs) are a new group of effector cells in innate immunity. Together with the adaptive B and T lymphocytes, ILCs are a family of hematopoietic cells derived from a common lymphoid progenitor cell, and they neither express antigen specific B- or T-cell receptors, nor possess myeloid or DC phenotypical markers. They can be subdivided into three groups based on their expression of lineage-defining transcription factors as well as on the cytokines – small proteins that participate in cell signalling, which they produce (**Figure 3**). The different patterns of cytokine production of these subpopulations mirror the cytokine-secreting profile of T helper cell subsets from adaptive immunity (Spits et al., 2013). Their preferential localization at epithelial barriers, as well as the absence of rearrangement of a specific antigenic receptor, allow these cells to rapidly produce a first wave of cytokines in response to a signal, suggesting that they have important effector functions during the early stages of immune response, tissue repair, and maintenance of epithelial integrity at barrier surfaces (Ebbo, Crinier, Vély, & Vivier, 2017; Spits et al., 2013).

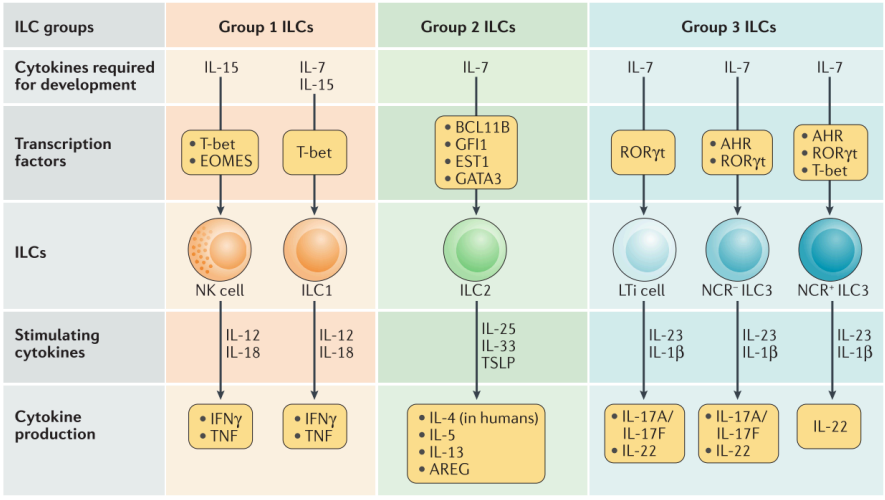

Figure 3: Types of innate lymphoid cells (ILCs). *The classification of the ILCs is based on the expression of key transcription factors as well as on the cytokines that they produce. Reproduced from Ebbo et al., 2017.*

Group 1 ILCs comprise natural killer (NK) cells and ILC1 cells. NK cells are capable of exerting a cytolytic function without differentiation or clonal expansion. They produce an array of cytokines with proinflammatory or immunosuppressive functions, along with chemokines. Although NK cells were recently and originally classified as effector lymphocytes from innate immunity, the findings in their biology have attributes of both innate and adaptive immunity (Vivier et al., 2011). ILC1 cells are comparable to T helper 1 (T_H1) cells; they mediate immunity against intracellular bacteria and parasites (Klose et al., 2014).

Group 2 ILCs comprise only ILC2 cells. They produce T_H2 cell-associated cytokines in response to stimulation (Spits et al., 2013). Moreover, they play a critical role in the differentiation of naïve T cells into T_H2 and also promote DC migration to the lymph node (Halim et al., 2014).

Group 3 ILCs comprise lymphoid tissue-inducer (LTi) cells and ILC3 cells. All members in this group produce IL-17 and/or IL-22. The classical cells in this group are LTi cells, which promote the formation of lymphoid tissue architecture during embryogenesis. ILC3s can be subdivided based on the natural cytotoxicity receptor (NCR) expression. They are involved in host defence against pathogens, tissue homeostasis, and repair after inflammation or damage (Montaldo, Juelke, & Romagnani, 2015).

2.1.1.3 Humoral innate immunity

Humoral innate immunity involves extracellular and blood proteins, along with other inflammatory intermediates such as complements, a contact system cascade, naturally occurring antibodies (NAbs), and pentraxins. First, the complement system consists of several plasmatic proteins that opsonize pathogens to promote and recruit phagocytes in the infected tissues. Second, the contact system is a plasma protease cascade that participates in coagulation and inflammation. Third, NAbs are antibodies that exist before an infection occurs; they recognize common molecular patterns of microbes, stress cells, or dying cells, and

they are potent initiators of the complement cascade. Finally, pentraxins are a group of pentameric proteins that are rapidly synthesized and serve as markers of infection, inflammation, and tissue damage. Similarly to NAbs and the contact system, pentraxins, after binding to the pathogen, can activate the complement cascade (Shishido, Varahan, Yuan, Li, & Fleming, 2012).

2.1.2 Adaptive immunity

In addition to innate immunity, there is another type of immune response that recognizes pathogens in a precise way. Moreover, the magnitude and capacity of its response augments with each successive exposure. Due to its capacity to respond and adapt to infection, it is called adaptive immunity. This response is capable of recognizing a vast number of different pathogens, remembering them producing memory cells, and responding to forthcoming challenges in an increasingly dependent manner (**Figure 4)**. Opposite to the innate response, where immune receptors are codified by the germinal line, the receptors of the cells in an adaptive response are generated by somatic recombination. The main components of this response are **T** (thymus-derived) and **B** (bursal or bone-marrow-derived) **lymphocytes** (Abbas et al., 2012).

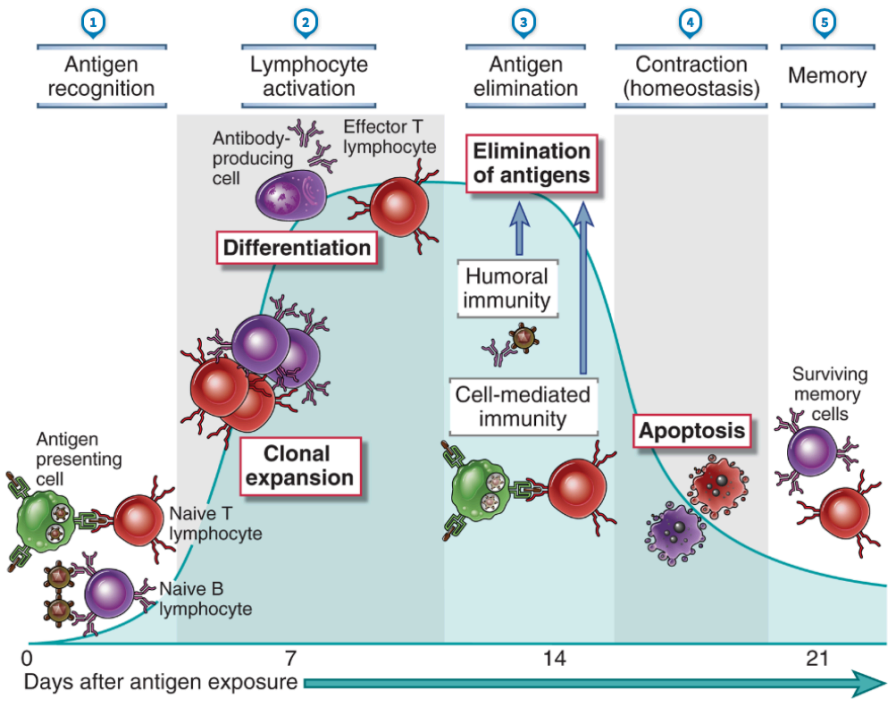

Figure 4: Phases of the adaptive immune response. *1) After the initial antigen recognition by antigen processing and presenting cells (APCs) of innate immunity, antigens are presented to naïve T lymphocytes; antigens can also be recognized by naïve B lymphocytes. 2) T and B lymphocytes are activated and then proliferate and differentiate into effector cells. 3) The humoral response itself, produced by the effector cells and their T cells, mediates the elimination of the antigens. 4) After antigen elimination, homeostasis is recovered. 5) Antigen-specific cells survive as memory cells that will produce a faster and larger response to the same antigen challenge. Reproduced from Abbas et al., 2012.*

2.1.2.1 T lymphocytes

T lymphocytes play important roles in immune responses either by secreting soluble mediators or through a cell-contact-mediated mechanism. They recognize pathogen antigens that must be presented by the major histocompatibility complex (MHC) on other cells such as APCs (macrophages or DCs) by their surface membrane T-cell receptors (TCRs). T cells can be divided into different subsets depending on their function and immunophenotyping markers, such as TCRs and cluster of designation (CD) surface signs.

2.1.2.1.1 αβ cells

T lymphocytes that possess αβ TCR can be divided into the following:

T helper (T_H) cells, which are $CD3^+$ and $CD4^+$, recognize MHC class II and participate in the B lymphocyte differentiation, macrophage activation, and the stimulation of inflammation. Depending on the specific cytokine and chemokine receptors that express on their surface, the transcription factors that mediate their response, and the effector molecules secreted, they can be subdivided into several subsets represented in

Table 1. After the activation of T_H lymphocytes, a small percentage (approximately 10%) remain quiescent, with an intermittent capacity for self-renewal and long-term survival in the absence of antigen presentation; they are called memory $CD4^+$cells (Pepper & Jenkins, 2011).

Cytotoxic T (T_C) cells, which are $CD3^+$ and $CD8^+$, recognize MHC class I and are known for their direct interaction with cellular targets (cells infected with a virus or bacteria) and their capacity to secrete cytolytic granules containing factors for apoptosis induction. T_C cells also have the ability to produce different subsets of cytokines similar to those mentioned in the $CD4^+$ T_H cells; therefore, T_C cells are named T_C1, T_C2, T_C9, T_C17, and T_C22 (Mittrücker, Visekruna, & Huber, 2014). As with T_H lymphocytes, the majority of effector T_C cells die after their response by apoptosis; however, a small fraction remains and becomes memory long-lived T_C cells, which will react with a strong proliferation and rapid reconversion into T_C effector cells upon antigen challenge (Kaech & Cui, 2012).

Table 1: Main T_H subsets characterized by their surface phenotypes, transcription factors and effector molecules. *Adapted from Chen Dong & Martinez, 2010; Raphael, Nalawade, Eagar, & Forsthuber, 2015.*

	T_H1 cell	**T_H2 cell**	**T_H9 cell**	**T_H17 cell**	**T_H22 cell**
Surface phenotype	αβ TCR, $CD3^+$ $CD4^+$ IL-12R, IFNγR, CXCR3	αβ TCR, $CD3^+$, $CD4^+$, IL-4R, IL-33R, IL-17RB CCR4, CRTH2	αβ TCR, $CD3^+$ $CD4^+$	αβ TCR, $CD3^+$ $CD4^+$, IL-23R, IL-1R, CCR6	αβ TCR, $CD3^+$ $CD4^+$, CCR10
Transcription factors	T-bet, STAT4, STAT1, STAT5	GATA3, STAT6, DEC2, MAF, IRF4	PU.1	RORγt, STAT3, RORα, BATF IκBζ, IRF4 and AHR	AHR
Effector molecules secreted	INFγ, IL-2, LTα, GM-CSF	IL-4, IL-5, IL-13, IL-9 and IL-10	Il-9 and IL-10	IL-17A, IL-17F, IL-21, IL-22, IL-25, IL-26 and CCL20	IL-22
Function	Induce macrophage activation; promote protective immunity against intracellular pathogens	Promote humoral response and host defence against multi-cellular parasites	Promote host defence against extracellular parasites, mainly nematodes	Promote protective immunity against extracellular bacteria and fungi, mainly at mucosal surfaces	Roles in protective immunity; promote tissue repair; involved in autoimmune diseases.

2.1.2.1.2 γδ cells

γδ cells are lymphocytes with γδ TCRs that are between the innate and adaptive response; they are $CD3^+$ $CD4^+$ and are activated in an MHC-independent manner. Their plasticity to rapidly act as innate-like responders, combined with their conventional adaptive potentials, places this population at the initiation phase of the immune response (Vantourout & Hayday, 2013).

2.1.2.1.3 Natural killer T (NKT) cells

Natural killer T (NKT) *cells* comprise a heterogeneous lymphoid population that also shares features from both innate and adaptive immunity. They recognize antigens presented by the class I MHC-like molecule DC1d and present semi-invariant αβ TCRs. Depending on the cytokines secreted, they can promote either inflammation or tolerance. There are two subsets in this group, namely, type I and type II NKT cells, with many further subgroups in each subset, depending on the tissue location, surface marker expression, specific TCR usage, and effector functions (F. C. Robertson, Berzofsky, & Terabe, 2014).

2.1.2.2 B lymphocytes

B lymphocytes possess several functions in adaptive immunity, among which the production of antibodies is perhaps their main feature. Moreover, they can regulate diverse immune responses, such as wound healing, transplanted tissue rejection, or tumour immunity and development, through cytokine production and other immune mediators. B cells can also act as antigen-presenting cells (Lebien & Tedder, 2008). There are mainly three types of B cells (**Figure 5**): **B1**, **follicular** (Fo), **and marginal zone** (MZ) **B cells**, classified according to their anatomic location and ontogeny. They express B-cell receptors (BCRs) on their surface, and these BCRs will interact with the antigens and generate their activation and further production of antibodies (Yam-Puc, Zhang, Zhang, & Toellner, 2018). *Fo B cells* circulate between the blood and spleen; they reside in the primary follicles where they may present T-dependent antigens to activated T cells, leading to the formation of germinal centres where class switching and somatic mutation of antibody genes occur. *MZ B cells* reside in the marginal sinus of the spleen and other lymphoid tissues; they can be induced by multivalent antigens, such as lipids, LPS, or nucleic acids, to differentiate in short-lived plasma cells in the absence of BCR ligation. Similarly to MZ B cells, *B1 B cells* also differentiate to short-lived plasma cells; however,

they reside in mucosal tissues and peritoneum. They produce the NAbs previously mentioned in the innate immunity section.

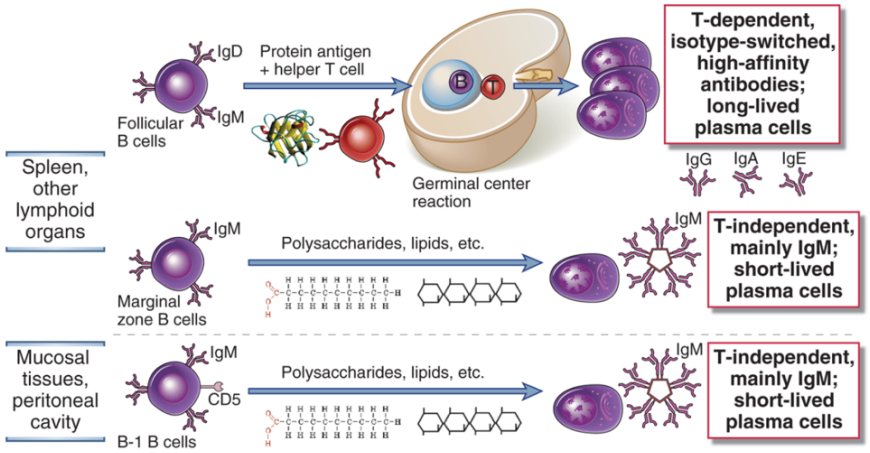

Figure 5: Types of B lymphocytes. *Different B cell subsets classified by their location. Follicular B cells. Reproduced from Abbas et al., 2012.*

2.1.3 Cytokines

Cytokines are small, secreted proteins produced by both innate and adaptive immune cells that regulate and coordinate the cellular activities of innate and adaptive immunity. Their production and release are highly regulated and temporally orchestrated. In response to pathogens, innate immune cells release proinflammatory cytokines to communicate with other cells and to shape the immune response (humoral and cell-based). The following are some of these intercellular messengers produced by innate immune cells: tumour necrosis factor (TNF), interferon gamma (INFγ), interleukin 1 (IL-1), IL-4, IL-6, IL-10, IL-12, IL-18, and transforming growth factor beta (TGFβ) (Lacy & Stow, 2018). Chemokines constitute an important group contained within the larger family of cytokines (i.e., chemoattractant cytokines that comprise a large family with ~50 members); they are released to control cell migration and cell positioning during development, homeostasis, and inflammation, and CCL4 and RANTES are chemokines produced by innate immune cells (Sokol & Luster, 2015).

2.2 IL-22 biology

The following section summarizes the biology of IL-22 and its receptors, with respect to the gene, protein properties, cellular production, molecular regulation and signalling.

2.2.1 IL-22, discovery

IL-22 was originally discovered by the Renauld group (Dumoutier, Louahed, & Renauld, 2000) in 2000 while looking for new messenger RNA (mRNA) transcripts that could be upregulated by IL-9 in mouse T cells and mast cells. Using the technique of representational difference analysis (Hubank & Schatz, 1994), they identified one transcript without a previous homology described in the literature; this new transcript was cloned and overexpressed, and the protein coded showed characteristic features of a cytokine: it had N-terminal signal peptide (SP); shared 22% of amino acid identity with IL-10; had potential N-glycosylation sites, and when secreted, was capable of triggering STAT3 and STAT5 phosphorylation in target cells. Due to the amino acid similarity to IL-10, they designated it as IL-10-related T-cell-derived inducible factor (IL-TIF). They also found upregulation of the gene under Con A stimulus in T cells, mast cells, the thymus, and the brain. In the same year, Xie et al. and Renauld's group (Dumoutier, Van Roost, Colau, & Renauld, 2000) again reported the identification of the human counterpart. The first group obtained the sequence based on a bioinformatic search in the human genome database; they termed it IL-22, based on cytokine convention nomenclature. Their study also focused on the identification of the receptor for IL-22. Given the homology of human IL-22 to IL-10 (23%), which binds and signals through the class II cytokine receptors, they searched for IL-22 receptors within this family. They found that IL-22 binds to the receptor complex CRF2-4 (which was also the receptor for IL-10) and a novel class II cytokine receptor (found in a protein database), which was then designated IL-22R. They also found that the interaction with both receptors caused STAT 1, 3, and 5 phosphorylation. The Renauld group obtained the human orthologue by peripheral blood

mononuclear cells' (PBMCs) stimulation with anti-CD3. They amplified the cDNA with murine primers, followed by an amplification of the human cDNA ends. They also reported that IL-22 was upregulated by anti-CD3 antibody or after LPS treatment *in vivo*. Furthermore, they demonstrated that IL-22 stimulated the production of acute phase reactants, such as serum amyloid, 1-antichymotrypsin, and haptoglobin, on HepG2 human hepatoma cells and also *in vivo* in mouse liver. IL-22 belongs to the IL-10 family and has been included in a subgroup called the IL-20 subfamily (IL-19, IL-20, IL-22, IL-24, and IL-26) due to the usage of common receptor subunits, cellular targets, and biological effects (Rutz, Wang, & Ouyang, 2014).

2.2.2 Gene

The human *IL22* gene is located on chromosome region 12q15 (**Figure 6**), close to the class II cytokines IL-26 and IFNγ (Dumoutier, Van Roost, Ameye, Michaux, & Renauld, 2000). It is positioned approximately 22 kbp and 89 kbp upstream from the *IL26* and *IFNG* loci, respectively, and 41 kbp downstream from the MDM1 locus. Since these are arranged in tandem and are transcribed in the same orientation, this region was suggested to correspond to a cytokine cluster (Dumoutier, Van Roost, Ameye, et al., 2000). An ortholog of the IL22 gene has also been found in teleost, with a syntenic conservation of this region suggesting that this cluster is well conserved during evolution (Igawa, Sakai, & Savan, 2006). In activated T cells, *IL22* and *IL26* are usually co-expressed (Walter, 2011).

The *IL22* gene is composed of six exons that are separated by five introns (**Figure 6**). As is typical of all of the IL-10-related genes, it has a 'phase 0' intron/exon boundary. Fifty-three base pairs (bp) of the exon1 encode for the 5'-untranslated region, containing a putative TATA box, and the last 541 bp of the exon 5 encodes for the 3'-untranslated region containing eight times the ATTTA motif, which is related to mRNA degradation. *IL22* codes for a protein of 179 amino acids.

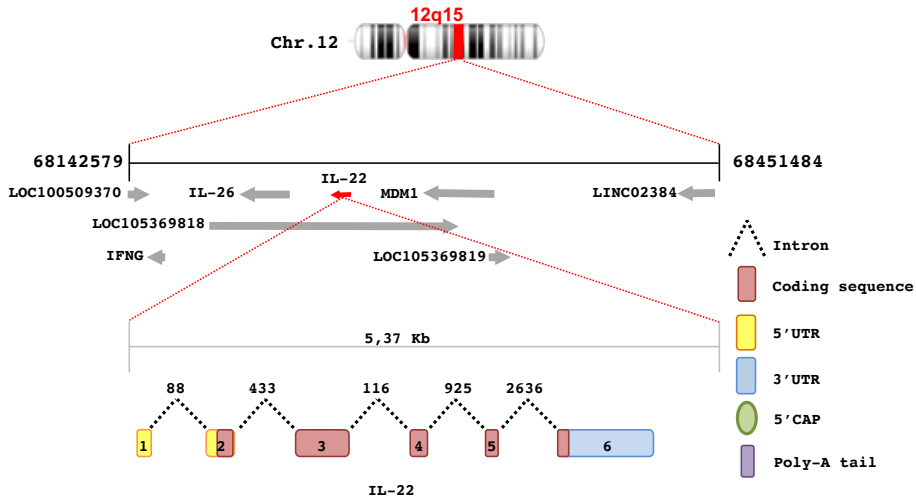

Figure 6: Chromosomal localization and gene structure of human IL22.

2.2.3 Protein structure

Human IL-22 possesses 179 amino acids, an SP in the N-terminal site, and three potential N-linked glycosylation sites (NetNglyc 1. Server). All three of them (Asn^{54}-Arg^{55}-Thr^{56}, Asn^{68}-Asn^{69}-Thr^{70}, and Asn^{97}-Phe-^{98}-Thr^{99}) are described to be N-glycosylated (Logsdon et al., 2004; T. Xu, Logsdon, & Walter, 2004). Its theoretical molecular weight is 16.7 kDa; however, it varies from 23 kDa to 30 kDa due to glycosylation (Kotenko et al., 2001b; Logsdon et al., 2004). Asn^{54} glycosylation has been deemed an important hotspot in IL-10R2 binding (Logsdon et al., 2004).

Furthermore, crystallographic structure studies in *E.coli* and *D. melanogaster* revealed that, as observed with the other members of the IL-10 family, the human IL-22 tertiary structure (**Figure 7**) possesses one domain composed of six α-helixes (labelled A-F) in anti-parallel conformation and also has two intracellular disulphide bonds Cys^{40}-Cys^{132} and Cys^{89}-Cys^{178} (Nagem et al., 2002; T. Xu, Logsdon, & Walter, 2005).

Although it can occur as a homodimer (**Figure 7**) composed of two monomers held together by intermolecular interactions, and despite IL-10 binding to its receptor as a dimer, IL-22 signals as a monomer at

physiological concentrations; the proposed binding site of human IL-22 with its receptor IL-22R was occluded when it dimerizes (Nagem et al., 2002). It has previously been seen that other cytokines at high protein concentrations can be found as dimers, although they are biologically active as monomers, such as IL-8 (Goger et al., 2002).

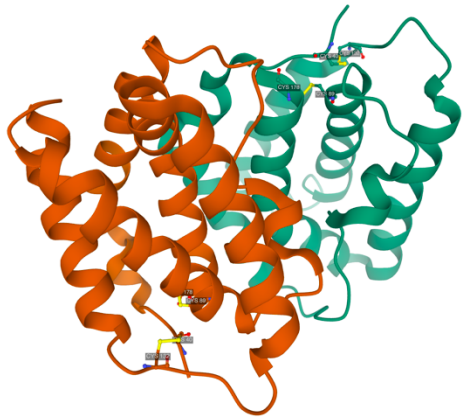

Figure 7: Three-dimensional (3D) structure of the human IL-22 homodimer. *The 3D crystal representation was created using Mol viewer from the accession code 1M4R located in the Protein Data Bank (Nagem et al., 2002). The residues of the disulphide bonds are shown in yellow.*

2.2.4 Cellular sources and tissue distribution

Il-22 production has been mainly described in cells with immune origin (both adaptive and innate immune responses); IL-22 was identified for the first time in mouse T cells and mast cells activated by IL-9 (Dumoutier, Louahed, et al., 2000). It was later suggested that IL-22 could be secreted by NK cells (Wolk, Kunz, Asadullah, & Sabat, 2002). IL-22 production mainly occurs in cells with a lymphoid lineage: $CD4^+$T cells, $CD8^+$T cells ($\alpha\beta$ T cells), $\gamma\delta$ T, NKT cells and group 3 innate lymphoid cells (ILC-3) (**Figure 8**) (Rutz, Eidenschenk, & Ouyang, 2013; Sabat, Ouyang, & Wolk, 2013).

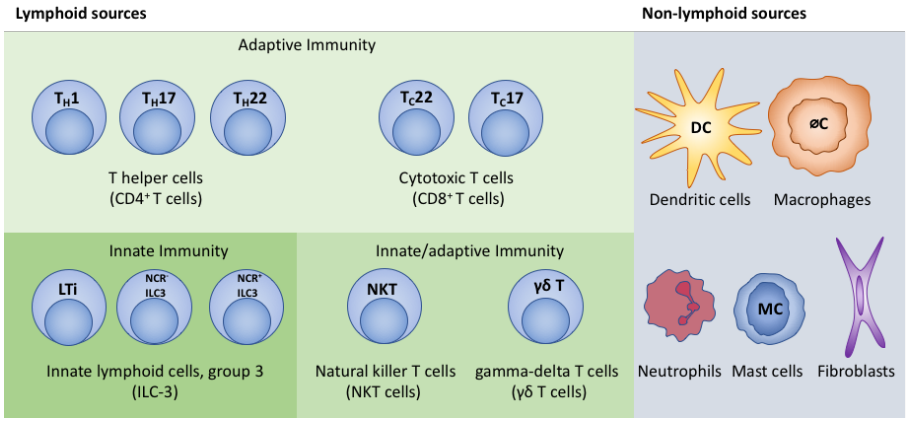

Figure 8: Cellular sources of IL-22.

Within the T cell subsets, **T_H1** (Wolk et al., 2002), **T_H17** (Chung et al., 2006; Spencer C. Liang et al., 2006; Volpe et al., 2008), and **T_H22** (Duhen, Geiger, Jarrossay, Lanzavecchia, & Sallusto, 2009; Trifari, Kaplan, Tran, Crellin, & Spits, 2009) cell types are capable of producing and releasing IL-22. In addition to $CD4^+$ T cells, two subsets of $CD8^+$ T cells have also been found to produce IL-22: **T_C17 cells** produce IL-22 together with IL-17 (Ciric, El-behi, Cabrera, Zhang, & Rostami, 2009; Hamada et al., 2009), and **T_C22 cells** only produce IL-22 under an IL-21 trigger (Y. Liu et al., 2011). Furthermore, murine invariant natural killer T cells (**iNKTs**) under IL-1β and IL-23 stimuli are capable of producing IL-22 during infection (Doisne et al., 2011; Paget et al., 2012). In humans, an NK cell subset located in mucosa-associated lymphoid tissues and referred as **NK-22** cells has been found to secrete IL-22 when triggered with IL-23 (Cella et al., 2009). In mice, conventional **NK cells** from trachea and lungs have been found to a) produce IL-22 in response to influenza infection and b) mediate epithelia regeneration and inflammation protection (P. Kumar, Thakar, Ouyang, & Malarkannan, 2013).

In addition to αβ T cells, murine **γδ T** cells, which are mostly found in the gut mucosa, have also been described as IL-22 producers in response to IL-1β and IL-23 in the absence of exposure to exogenous antigens (Sutton et al., 2009), and this production is mediated by AhR (B. Martin, Hirota, Cua, Stockinger, & Veldhoen, 2009).

In contrast to $CD4^+$ cells, in which IL-22 production is dependent on activation or stimulation through the binding of the TCR to its cognate antigen, ILC3, which lacks TCRs, can produce IL-22 during a steady state (Sanos et al., 2009; Savage, Liang, & Locksley, 2017). All subsets from the ILC3 group, LTi, and natural cytotoxicity-triggering receptor (**NCR^+ ILC3** and **NCR^- ILC3**) cells share RORγt expression and are capable of producing IL-22 (Buonocore et al., 2010; Spits et al., 2013; Spits & Cupedo, 2012) under different stimuli.

Although the lymphoid lineage has been described as the major IL-22 source, the production of this cytokine by myeloid and non-hematopoietic cells has also been reported. These non-lymphoid sources include macrophages, DCs, neutrophils, mast cells, and fibroblasts. Alveolar macrophages can produce and release IL-22 in the lung during an innate immune response (Hansson, Silverpil, Lindén, & Glader, 2013), and TLR4- and TLR9-activated DCs also produce IL-22 in an IL-23-independent manner (Fumagalli et al., 2016). In contrast, IL-22 is produced by colon-infiltrating neutrophils induced by IL-23 or TNFα (Chen et al., 2016; Zindl et al., 2013). IL-23, which induces IL-22 from γδ T and $CD8^+$ T cells, can also induce monocytes to produce IL-22 to a smaller extent (Zheng et al., 2007). Another IL-22-hematopoietic source has recently been described: skin mast cells from psoriatic plaques (Mashiko et al., 2015). Additionally, synovial fibroblasts and macrophages from patients with rheumatoid arthritis (RA) can also produce IL-22, thus indicating the possible promotion of inflammation through its activation (Ikeuchi et al., 2005), and cancer-associated fibroblasts are also capable of producing IL-22, suggesting the promotion of gastric cancer cell invasion (Fukui et al., 2014). **Figure 9** depicts *IL-22* RNA expression in different tissues and in different cell lines from the Human Protein Atlas (HPA) project (Uhlen et al., 2015), available from the web page www.proteinatlas.org.

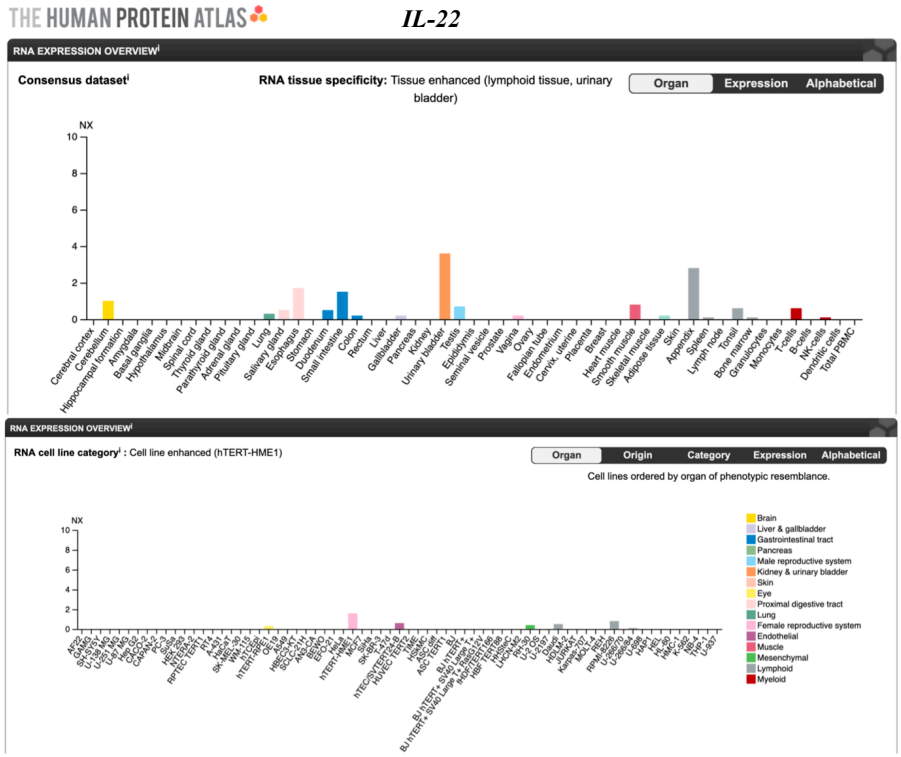

Figure 9: RNA-seq data of IL22 in different tissues and cell lines stored on the Human Protein Atlas (HPA) website. Data from cell lines came from the HPA project. *Data from tissues came from Consensus Normalized eXpression (NX) levels for 55 tissue types and six blood cell types, created by combining the data from the three transcriptomic datasets (the HPA project, the GTEx Genotype-Tissue Expression project, and the FANTOM5 project) using an internal normalization pipeline. From: https://www.proteinatlas.org/ENSG00000127318-IL22/tissue, or cell available from v20.0 at www.proteinatlas.org.*

2.2.5 IL-22 receptors

IL-22 acts via a transmembrane (TM) receptor complex that, contrary to the production of IL-22, only localizes in cells with non-hematopoietic origin, such as tissue cells from the skin, liver, and kidneys, and from organs of the respiratory and gastrointestinal systems. Moreover, IL-22 can also bind to a soluble receptor with stronger affinity that prevents its cellular effects. This section describes the TM receptor complex, its distribution, and its functions.

2.2.5.1 Membrane receptor

The IL-22 heterodimer receptor (IL-22R) is composed of two TM subunits, IL-22RA1 and IL-10Rβ (Dumoutier, Van Roost, Colau, et al., 2000; Kotenko et al., 2001b; Xie et al., 2000). The *IL22RA1* gene (NM_021258.3) is located on chromosome 1 in the region 1p36 close to the *IL28R*A locus, while *IL10RB* gene is located on chromosome 21q22, together with the *IFNRA1* and *IFNRA2* genes. *IL22RA1* and *IL10RB* produce only one variant each that encode for the proteins of 574 aa and 325 aa, respectively. Both genes encode members of the class II cytokine receptor family, which contain an extracellular moiety presenting two fibronectin type III domains positioned in tandem with conserved cysteine residues and do not contain the Trp-Ser-X-Trp-Ser signature motif of the class I cytokine receptor family (Bleicher et al., 2008; B. C. Jones, Logsdon, & Walter, 2008; Sabat et al., 2013; Yoon et al., 2010). IL-10 family receptors are usually heterodimers of class II cytokine receptors containing one subunit with a long cytoplasmic domain and another subunit with a short chain (Renauld, 2003). In the case of IL-22R, IL-22RA1 is the long one, and within its intracellular domain, it contains four Tyr-X-X-Gln motifs that are potential STAT3 docking sites (Kotenko et al., 2001b; Sabat et al., 2013). Several binding studies have demonstrated that IL-22 has a high affinity for IL-22RA1, but no affinity for IL-10Rβ (B. C. Jones et al., 2008; J. Li et al., 2004; Logsdon et al., 2004; Logsdon, Jones, Josephson, Cook, & Walter, 2002; Wolk et al., 2005; Yoon et al., 2010). In contrast, the IL-10Rβ subunit has a high affinity for the IL-22/IL-22RA1 complex. Accordingly, it has been proposed that the binding of IL-22 to IL-22RA1 induces conformational changes in IL-22, thus making it accessible for binding to IL-10Rβ (Bleicher et al., 2008); adjacent sites on the IL-22 surface are responsible for the temporal formation of IL-22/IL-22RA1 and IL-22/IL-22RA1/IL-10Rβ complexes (P. W. Wu et al., 2008). This stepwise process has also been described for IL-10.

2.2.5.2 Signal transduction

Figure 10 represents the downstream signalling events of IL-22 coupled to IL-22R.

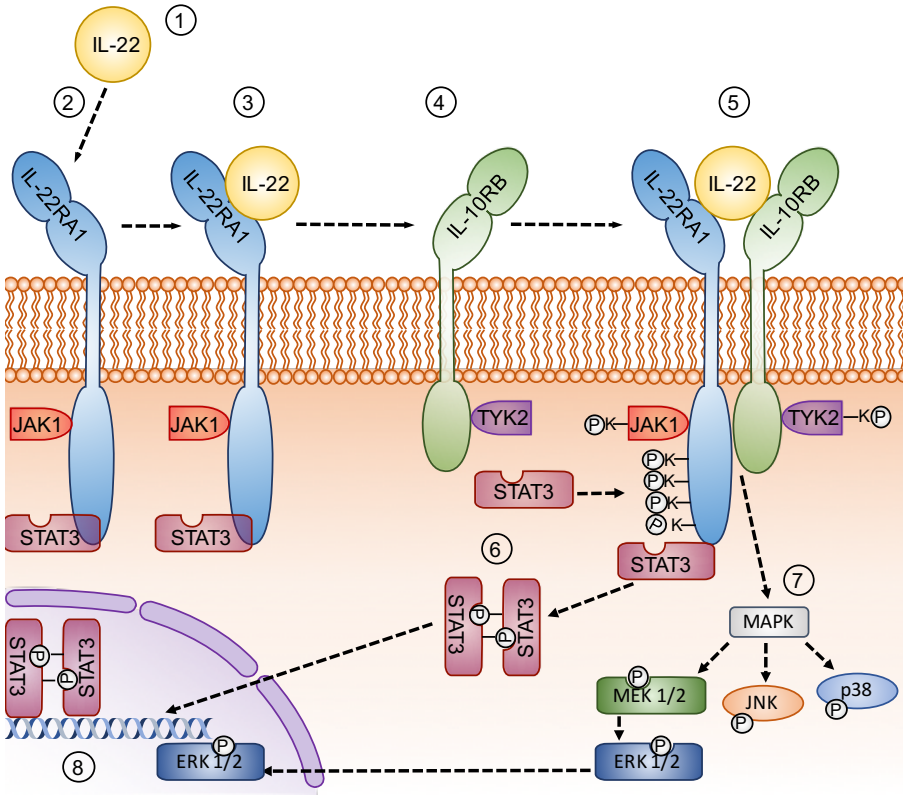

Figure 10: Signal transduction pathways activated upon IL-22 binding to the membrane receptor complex. *Soluble IL-22 (1) binds first to the transmembrane IL-22RA1 receptor (2). This binding makes conformational changes in IL-22 (3), thereby making it accessible to the IL-10RB subunit (4). The complex IL-22/IL-22RA1/IL-10RB (5) is phosphorylated and activated, leading to phosphorylation of STAT3 (6), activation of MAPK pathways (7), and translocation to the nucleus for transcription regulation of target genes (8).*

Once the complex of IL-22/IL-22RA1/IL-10Rβ is formed, the tyrosine kinases attached to the subunits of the receptors (Janus kinase JAK1 and tyrosine kinase TYK2 bound to IL-22RA1 and IL-10Rβ, respectively) are phosphorylated and activated, leading to phosphorylation of STAT (signal transducer and activator of transcription) factors (Lejeune et al.,

2002). Efficient STAT phosphorylation depends on the capacity of the STAT Src homology 2 (SH2) domain to bind to the phosphotyrosine residues of the cytoplasmic domain of the receptor. This is dictated by the residues surrounding the phosphotyrosine; for example, the consensus Tyr-X-X-Gln motif is well known to recruit STAT3. However, it STAT3 has also been found to interact with the C-terminal domain of IL-22RA1 by its coiled-coil domain and not through the SH2 domain (Dumoutier, de Meester, Tavernier, & Renauld, 2009). This dual STAT3 interaction could speed up and/or enhance the signalling. Apart from phosphorylation of the Tyr^{705} of STAT3, IL-22 leads to a serine phosphorylation of STAT3 on Ser^{727}. Signalling through STAT3 phosphorylation has been described as occurring for other cytokines of the IL-10 family; however, Ser^{727} phosphorylation is a characteristic of IL-22 signalling (Lejeune et al., 2002). Although the phosphorylation of STAT3 has been observed as the main IL-22 signalling mediator, STAT1 and STAT5 phosphorylation has also been recognized (Aggarwal, Xie, Maruoka, Foster, & Gurney, 2001; Dumoutier, Louahed, et al., 2000; Dumoutier, Van Roost, Colau, et al., 2000; Lejeune et al., 2002; Xie et al., 2000). The phosphorylation of STAT3 allows for its dimerization and its posterior translocation to the nucleus for transcription regulation of target genes. Other additional pathways have been described for IL-22, such as three of the major mitogen activation protein kinase (MAPK) pathways: ERK1/2, JNK, and p38 kinase (Andoh et al., 2005; Lejeune et al., 2002; Sekikawa et al., 2010).

Interestingly, IL-22RA1 has been described as a relatively short-lived protein ($t_{1/2}$ ~1.5 hours), degraded by the ubiquitin proteasome under normal unstimulated conditions, and the binding to IL-22 has been found to accelerate this degradation (Weathington et al., 2014). Moreover, FBXW12, which is an F-box family E3 ligase subunit, causes the depletion of overexpressed and endogenous IL-22RA1, leading to its ubiquitination and further degradation by the proteasome (Franz, Jerome, Lear, Gong, & Weathington, 2015). This negative regulation of the cytokine receptor by its degradation, via proteasome and/or lysosome is a common mechanism to 'turn off' signalling, and it is therefore critical for the

proliferation and survival of the cells in which these receptors are expressed (Javed, Richmond, & Barber, 2010).

2.2.5.3 Receptor expression

While IL-10Rβ is ubiquitously expressed in different cells of the human body, IL-22RA1 expression is much more restricted. This implies that the biological effects of IL-22 are confined to the expression of the latter. Surprisingly, in contrast to *IL22* expression, *IL22RA1* expression has not been observed in either activated or resting immune cells such as monocytes, macrophages, DCs, T cells, B cells, or NK cells (Nagalakshmi, Murphy, McClanahan, & de Waal Malefyt, 2004; Nagalakshmi, Rascle, Zurawski, Menon, & de Waal Malefyt, 2004; Wolk et al., 2004, 2002). Its expression is observed in cells that contribute to the outer body barriers, such as the skin and the gastrointestinal and respiratory systems, allowing for directional signalling from immune cells to tissues. *IL22RA1* expression has also been found in the liver, pancreas, and kidneys (Dudakov, Hanash, Brink, & van den Brink, 2015; Hernandez, Gronke, & Diefenbach, 2018; Sabat et al., 2013). However, a recent study of pneumococcal infected mice identified macrophages from lungs to express *IL22RA1* mRNA (Trevejo-Nunez et al., 2019). **Table 2** summarizes the main *IL22RA1* producer cells and (**Figure 12)** illustrates RNA expression in different tissues and in different cell lines from the HPA project (Uhlen et al., 2015), available from the web page www.proteinatlas.org.

Table 2: Cellular sources of IL22RA1

Organ	IL-22RA1 producer cells	Organism	Reference
Respiratory system	Alveolar epithelial cells	human	(Whittington, Armstrong, Uppington, & Millar, 2004)
	A549 Alveolar epithelial cell line	human	(Whittington et al., 2004) (Wolk et al., 2004)
	Bronchial epithelia cells	human	(Aujla et al., 2008)
	Airway smooth muscle cells	human	(Chang et al., 2012)
	Macrophages	mouse	(Trevejo-Nunez et al., 2019)
Gastrointestinal system	Colonic epithelial cells	human/mouse	(Zheng et al., 2008)(Sugimoto et al., 2008) (I. Adzhubei, Jordan, & Sunyaev, 2013)
	Colonic subepithelial myofibroblast	human	(Andoh et al., 2005)
Skin	Fibroblast	mouse	(Wolk et al., 2009)
	Keratinocytes	mouse/human	(Wolk et al., 2004) (Wolk et al., 2009)/(Sa et al., 2007)(Boniface et al., 2005) (B. Wang et al., 2020)
Liver	Hepatocytes	human/mouse	(Wolk et al., 2004)(Radaeva, Sun, Pan, Hong, & Gao, 2004)
	Hepatic stellate cells	human/mouse	(Kong et al., 2012)
Pancreas	Acinar cells	mouse	(Aggarwal et al., 2001)
	Langerhans islets	human	(Shioya, Andoh, Kakinoki, Nishida, & Fujiyama, 2008)
Kidney	Tubular epithelial cells	mouse	(Kulkarni et al., 2014)
Brain	Astrocytes	human	(Perriard et al., 2015)

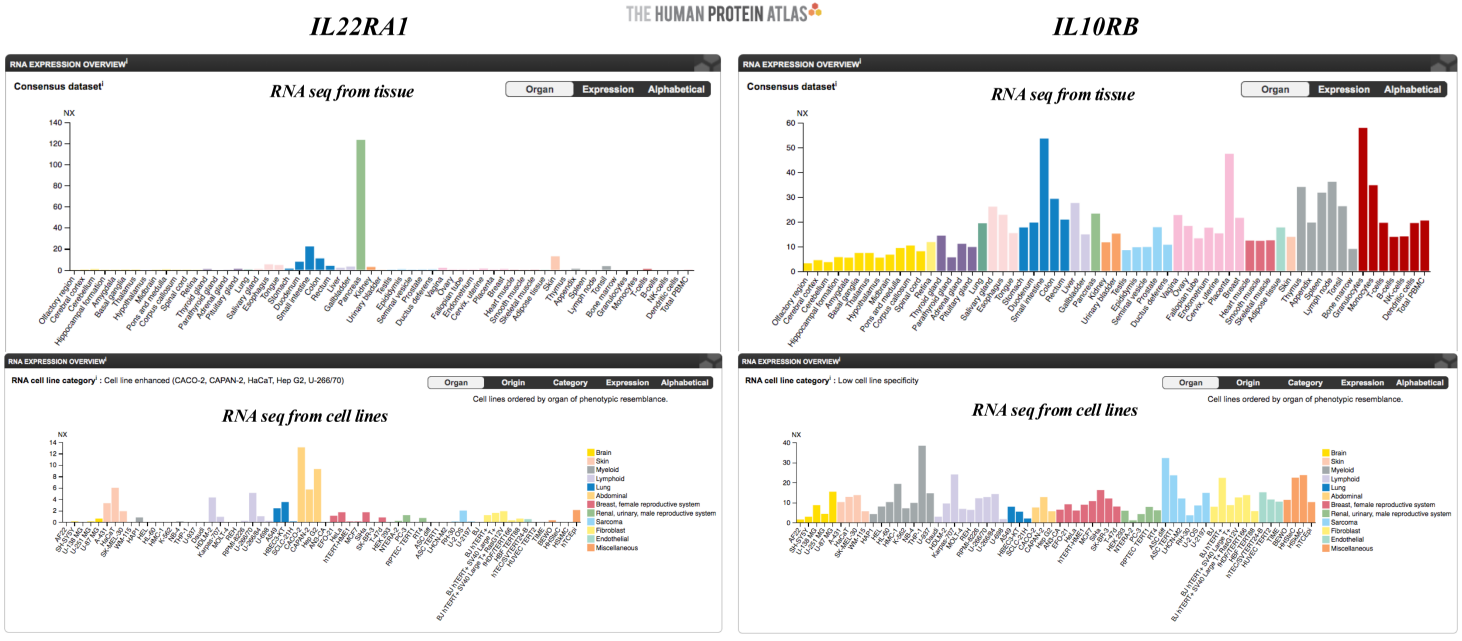

Figure 11: RNA-seq data of IL22RA1 and IL10RB in different tissues and cell lines stored on the HPA website. *Data from cell lines came from the HPA project. Data from tissues came from Consensus Normalized eXpression (NX) levels for 55 tissue types and six blood cell types, created by combining the data from the three transcriptomic datasets (the HPA project, the GTEx_Genotype-Tissue Expression project, and the FANTOM5 project) using an internal normalization pipeline. From: https://www.proteinatlas.org/ENSG00000243646-IL10RB/tissue and https://www.proteinatlas.org/ENSG00000142677-IL22RA1/tissue, or cell available from v19.3 at www.proteinatlas.org.*

2.2.6 IL-22 functions

The expression of *IL22RA1* – epithelial cells, pancreatic cells, hepatocytes, and fibroblasts, among others (**Table 2**) – determines the site of action of IL-22 **(Figure 12**) (Sabat et al., 2013). Given that IL-22 production occurs at sites of inflammation, it may be mediating a physiologic response to the local repair of tissues, or it may be contributing to pathophysiologic inflammation (Dudakov et al., 2015). Some of the genes upregulated by IL-22 signalling include mucins (mucus-associated proteins), which are necessary to create a protective layer between the epithelium and enteric contents (Sugimoto et al., 2008); antimicrobial peptides such as β-defensin 2, β-defensin 3, S100A7, S100A8, S100A9, and lipocalin 2 (Boniface et al., 2005; Wolk et al., 2004, 2006); antiapoptotic proteins such as Bcl-2 and Bcl-xL (W. Zhang et al., 2008); acute phase proteins, such as serum amyloid A, α-antichymotrypsin, and haptoglobin, that exert anti-inflammatory, antibacterial, and regenerative effects (Dumoutier, Van Roost, Colau, et al., 2000; S. C. Liang et al., 2010; Wolk et al., 2004); and proinflammatory molecules such as IL-1, IL-6, IL-8, IL-11, G-CSF, GM-CSF, and LPS binding protein (Andoh et al., 2005; Dudakov et al., 2015).

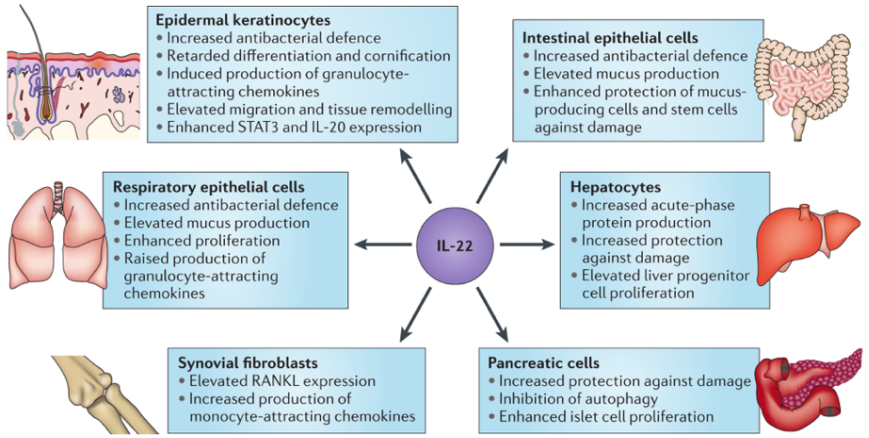

Figure 12: Target cells and physiological effects of IL-22. *IL22RA1 is mainly expressed in epidermal keratinocytes, intestinal and respiratory epithelial cells, hepatocytes, synovial fibroblasts, and pancreatic cells where IL-22 increases antibacterial defence, induces proliferation, and aids in host defence and barrier function. Reproduced from Sabat et al., 2013.*

Much attention has been paid to the IL-22 effects in the gastrointestinal tract, where this cytokine, produced by ILC3 cells, has been observed inducing epithelial fucosylation, which regulates the gut microenvironment (Goto et al., 2014). It also increases epithelial permeability by upregulating tight junctions (Y. Wang, Mumm, Herbst, Kolbeck, & Wang, 2017).

Altogether, protective and proinflammatory roles can be attributed to IL-22, depending on the context and location in which it is expressed. In a context of acute inflammation, IL-22 functions are suggested to be protective, and in more chronic settings, IL-22 roles are pathogenic (Zenewicz, 2018). Increasing epithelial cell survival and inducing both proliferation and antimicrobial defence may play a protective and regenerative role after injury, whereas chronic expression of IL-22 may lead to hyperproliferation, the production of proinflammatory mediators, and the subsequent recruitment of pathologic effector cells to the inflamed tissues (Dudakov et al., 2015). Understanding and elucidating the factors that make this cytokine protective versus proinflammatory is one of the actual gaps in IL-22-related knowledge. Moreover, the regulation of IL-22 production, its modulation by IL-22BP, and the way in which both are homeostatically or pathologically regulated, remain unknown in IL-22 biology (Zenewicz, 2018).

2.3 Object of study: IL-22 binding protein (IL-22BP)

Another level of regulation of IL-22 is by the IL-22 binding protein (IL-22BP) soluble receptor, a secreted protein with a high homology to the surface receptor IL-22R1 but with a higher affinity. This soluble receptor has the capacity to antagonize IL-22 function. The following section summarizes the biology of IL-22BP with respect to the gene, protein properties, cellular production, molecular regulation, signalling, and its role in health and disease.

2.3.1 Discovery

By 2001, while all the members and some receptors from the IL-10 family were already identified, the identification of other receptors, such as IL-19, IL-24, and IL-26 was still lacking. A common effort was consequently made to identify the remaining receptors, which led to the identification of a novel soluble receptor for IL-22 by four independent groups in the same year (Dumoutier, Lejeune, Colau, & Renauld, 2001; Gruenberg et al., 2001; Kotenko et al., 2001a; Wenfeng Xu et al., 2001). Dumoutier et al. (Dumoutier, Lejeune, et al., 2001) identified and cloned a soluble receptor for IL-22 in a DNA database following screening for sequences with homology to the extracellular domain of class II CRF, and functional analysis indicated that the protein coded by this gene specifically blocked IL-22-induced STAT3 activation on hepatocytes and intestinal epithelial cells. They proposed naming this IL-22 antagonist IL-22BP, and two splice variants for this gene (variants 1 and 2) were discovered in this study. At the same time, Kotenko et al. (2001a) published the identification and cloning of a soluble receptor capable of binding and blocking IL-22 activity using similar methods, which they initially designated CRF2-10, and apart from the two splice variants recognized by Dumoutier group, they identified an additional one (variant 3 [v3]). A different group, Xu and colleagues (Wenfeng Xu et al., 2001), identified the same soluble receptor gene when searching for conserved structural elements of the fibronectin domains of the class II CRF; they mainly detected two variants in the placenta and spleen from human origin (v1 and v2), and three in

the monocytic human cell line, U937. Finally, in the same year, a fourth group also published the identification of the *IL22RA2* gene; however, they only recognized two spliced forms (v1 and v2) (Gruenberg et al., 2001).

Two and three years later, orthologs only for the human variant 2 of *IL22RA2* (*IL22RA2v2)* were identified in mice and rats, respectively (C.-C. Wei, Ho, Liang, Chen, & Chang, 2003; Weiss et al., 2004).

2.3.2 Gene and evolution (variants and exonization)

The human *IL22RA2* gene (**Figure 13**), which encodes for IL-22BP, is located on chromosome 6q23.3 It is positioned at approximately 23 kbp downstream from the *IFNGR1* gene and 98 kbp upstream from the *IL20RA* gene (Dumoutier, Lejeune, et al., 2001; Gruenberg et al., 2001; Kotenko et al., 2001a; Wenfeng Xu et al., 2001), which are both transcribed in the same direction. The gene comprises seven exons and six introns spanning 29 kbp, and the exon-intron organization of *IL22RA2* is similar to that of its adjacent genes (*IL20RA* and *IFNGR1*), indicating that this region forms a cluster of class II cytokine receptors, which may be the result of gene duplication with subsequent divergence of function and regulation (Wenfeng Xu et al., 2001). It is interesting that the ligands for IFNGR1 and IL-22BP (IFNG and IL-22) are encoded by genes also located together, as mentioned before, within the same 12q15 chromosomal region and separated by ~ 90 kbp (Dumoutier, Van Roost, Colau, et al., 2000).

In humans, three variants are produced by alternative splicing: *IL22RA2v1*, *IL22RA2v2*, and *IL22RA2v3*, with each variant encoding a different protein isoform IL-22BPi1, IL-22BPi2, and IL-22BPi3, respectively (**Figure 13**). The 5'UTR region is located in the non-coding exon 1 and also involves 66 bp of exon 2; the rest of this exon codes for the SP. The 3'UTR occupies almost all of exon 7. Variant 1 (NM_052962.2), which is encoded by all the exons, has an open reading frame (ORF) of 792 nt and encodes a predicted 263-amino-acid protein (Dumoutier, Lejeune, Colau, & Renauld, 2001; Gruenberg et al., 2001; Kotenko et al.,

2001a;). Variant 2 (NM_181309.1) lacks the sequence encoded by exon 4; the ORF of this variant is comprised of 696 nt and encodes a predicted 231-amino-acid protein (Dumoutier, Lejeune, et al., 2001; Gruenberg et al., 2001; Kotenko et al., 2001a; Wenfeng Xu et al., 2001). Variant 3 (NM_181310.1), apart from lacking the sequence coded for by exon 4, additionally lacks the one from exon 6, resulting in an ORF of 393 nt. The absence of exons 4 and 6 generates a frame shift with a premature termination codon, thus producing a predicted 130-amino-acid protein (Kotenko et al., 2001a).

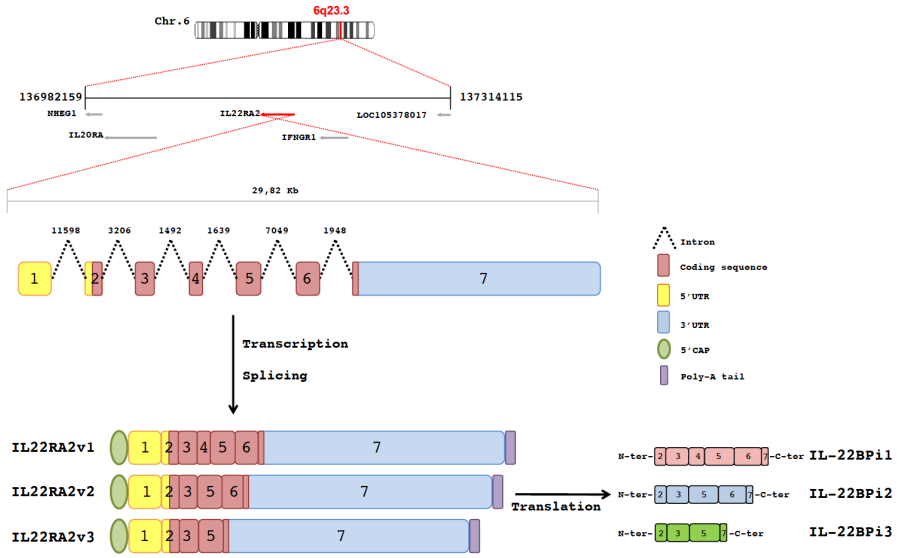

Figure 13: Chromosomal localization and gene structure of IL22RA2.

IL-22BP resembles the IL-22RA1 receptor of the IL-22R TM receptor, mentioned in the previous section. Soluble receptors typically emerge by two main mechanisms: either by alternative splicing of the preRNA (e.g., *IL6ST*, *IL7R* or *IL2RA*) or by proteolytic cleavage of the cell-surface receptor. However, there are also other mechanisms for generation of soluble receptors, such as the extracellular secretion of TM receptors associated with exosomes, virally expressed decoy receptors, or soluble receptors coded for by specific genes that do not express TM receptors, which is the case for *IL22RA2* and is the only such example in the IL-10

family biology (Felix & Savvides, 2017; Levine, 2008; Wenfeng Xu et al., 2001).

Variant 2 has been the most studied among the three, likely because it has been found to be the most strongly and widely expressed and also because of the absence of variants 1 and 3 in other species such as mice (C.-C. Wei et al., 2003; Weiss et al., 2004). Surprisingly, variant 3 has been found in rats, showing a 73% identity with human isoform 3 (J. C. Martin et al., 2014). Variant 1 has been described as having emerged during the divergence of orangutans and humans by an exonization process of a long terminal repeat insertion in the ape lineage (Piriyapongsa, Polavarapu, Borodovsky, & McDonald, 2007). This study also found that this exonization process conferred positive selection to the great apes compared to the Old World monkeys, which seemed to not have activated and expressed the exon.

2.3.3 Protein structure

The class II cytokine receptor family comprises TM glycoproteins with a single membrane spanning a region of 20–25 amino acid residues (Trivella, Ferreira-Júnior, Dumoutier, Renauld, & Polikarpov, 2010). IL-22BP lacks both typical TM and intracellular domains, but shares a 34%, 29%, and 30% amino acid homology with the extracellular domains of the IL-22R1, IL-10R1, and IL-20R1 receptors, respectively. Moreover, the 3D structure of IL-22BP is topologically similar to the extracellular structure of IL-22R1 (de Moura et al., 2009). The molecular mass of human IL-22BPi2 observed by Western blot had a higher molecular mass (35–45 kDa) than the predicted mass (26.98 kDa), suggesting that the protein must have post-translational modifications (PTMs); five potential N-linked glycosylation sites have been predicted for this protein (Kotenko et al., 2001a). However, a recent study predicted that isoforms 1 and 2 may have two glycosylation sites, while isoform 3 has only one. In this study, the three intracellular isoforms were subjected to enzymatic deglycosylation and revealed evidence for glycosylation (Lim, Hong, & Savan, 2016). Crystallographic studies of IL-22 bound to IL-22BPi2

resolved the structure of this complex and provided the molecular characteristic thereof (de Moura et al., 2009). IL-22BP contains two disulphide bridges in its structure: the first one between Cys^{78} and Cys^{86}, and the second disulphide bridge links Cys^{206} to Cys^{227} (de Moura et al., 2009).

The mature protein folds to acquire an L-shape consisting of two fibronectin III domains (FBN-III) in tandem, named D1 (N-terminal domain [NTD]) and D2 (C-terminal domain). Each FBN-III domain consists of a sandwich of two anti-parallel β-sheets formed from seven β-strands (A, B, E and C, C', F, G). The two fibronectin domains are connected by an interdomain of a small 3_{10} α-helix displaying an angle of 125°, which is similar to the one described for the extracellular domain of IL-22R1 (de Moura et al., 2009) (**Figure 14**).

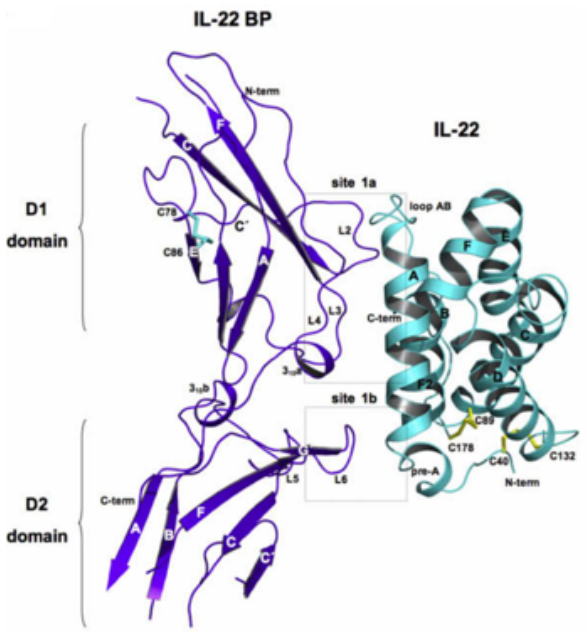

Figure 14: Representation of IL-22BP isoform 2 bound to IL-22. *There are two binding interfaces between IL-22BP and IL-22 (site 1a and site 1b). Adapted from de Moura et al., 2009.*

2.3.4 Physicochemical interactions with IL-22

Notwithstanding the high structural homology of IL-22BPi2 with the extracellular domains of IL-22RA1 and IL-20R, only IL-22 and no other IL-10 homolog, such as IL-10, IL-19, IL-20, IL-24, IL-26, or INFγ, has the capacity to bind IL-22BPi2 (Donnelly, Sheikh, Kotenko, & Dickensheets, 2004; Dumoutier, Leemans, Lejeune, Kotenko, & Renauld, 2001; Sheikh et al., 2004). Crystallographic studies have confirmed the structural similarities between IL-22BPi2 and IL-22RA1, which are higher in the D1 domain of both receptors (de Moura et al., 2009). Several studies have demonstrated that IL-22BPi2 neutralizes the biological activity of IL-22 via the formation of an exceptionally tight (Kd ≈ 1 pM) complex with IL-22 (Dumoutier, Lejeune, et al., 2001; B. C. Jones et al., 2008; Kotenko et al., 2001a; Lim et al., 2016; C.-C. Wei et al., 2003; Wolk et al., 2007; Wenfeng Xu et al., 2001). IL-22BPi3 has also shown inhibition of IL-22-induced STAT3 phosphorylation (Lim et al., 2016; C.-C. Wei et al., 2003). Surface plasmon resonance studies have revealed that the affinity of IL-22 to IL-22BPi2 is up to 1,000-fold higher than that of the IL-22RA1/IL-22 complex; compared to a soluble form of the cell-surface receptor sIL-22RA1, the dissociation half-time ($t_{½}$) values of the IL-22/IL-22BPi2 complex are strikingly larger (≈ 4.7 days for IL-22/IL-22BPi2 versus 7 minutes for IL-22/sIL-22RA1). Thus, IL-22BPi2 exhibits a much larger affinity for IL-22 than the cell-surface receptor (B. C. Jones et al., 2008). In that study, the authors also analysed the affinity of IL-22 to IL-22BPi3, which showed similar binding kinetics to those to IL-22RA1. The resolution of the crystal structure of IL-22BPi2/IL-22 complex (de Moura et al., 2009; Watanabe et al., 2009; PDB 3G9V) revealed the amino acids implicated in the interaction as well as the physicochemical basis of the high affinity. IL-22BPi2 contacts IL-22 through five binding loops (L2-6, **Figure 14**), which are also observed for the IL-22/IL-22RA1 complex. L2–L4 are positioned in the D1 domain (site 1a), forming 14 hydrogen bond / salt bridge interactions where Tyr67 dominates the molecular recognition of IL-22 by IL-22BPi2. Fewer electrostatic interactions occur in L5 and L6, which are located in the D2 domain (site 1b) (de Moura et al., 2009). They also compared IL-22BPi2/IL-22 X-ray structure with that of the IL-22/IL-

22RA1 complex – PDB 3DLQ, previously obtained by Bleicher et al. (2008). This comparison revealed four structural differences explaining the higher binding affinity of IL-22 for IL-22BPi2 compared to that of IL-22RA1: 1) the number of electrostatic interactions is higher for IL-22/IL-22BPi2 than for IL-22/IL-22RA1 complex; 2) some of these electrostatic interactions are shorter for IL-22/IL-22BPi2 complex, conferring a tighter binding; 3) there are more direct protein-protein interactions for IL-22/IL-22BPi2 complex, whereas IL-22/IL-22RA1complex has both direct and water-mediated interactions; and 4) there is a larger hydrophobic cluster in site1b of IL-22/IL-22BPi2 complex compared to the one in IL-22/IL-22RA1 complex that contributes to strengthening the interaction (de Moura et al., 2009).

The amino acid residues in IL-22 and IL-22BPi2, which are critical for their optimal binding, have been identified by mutagenesis studies. There are 12 and four specific amino acids of IL-22 that are key for optimal binding to IL-22RA1 or IL-22BP, respectively, and three of them (Asp^{67}, Arg^{73}, and Lys1^{62}, indicated in blue in **Figure 15** are identical (P. W. Wu et al., 2008). Another site-directed mutagenesis study of two key amino acid residues of IL-22BPi2, located at the complex interface of IL-22/IL-22BPi2 in site 1a (Tyr^{67} and Arg^{119}) or their IL-22RA1counterparts (Tyr^{60} and Arg^{112}), showed that their mutation completely abolished the interaction with IL-22 (de Moura et al., 2009).

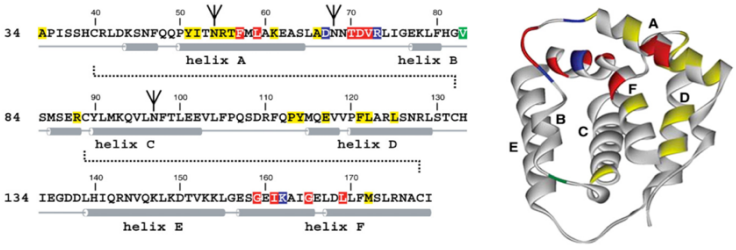

Figure 15: Amino acids in IL-22 critical for optimal binding to IL-22RA1, IL- 10Rβ, and IL-22BP. *The key amino acids implicated in the binding of IL-22 to the receptors are represented in red and blue for IL-22RA1, yellow and green for IL-10Rβ, and blue and green for IL-22BP. The 3D structure of IL-22 is represented on the right-hand side. Reproduced from P. W. Wu et al., 2008.*

2.3.5 Cellular sources and tissue distribution

The cellular source of IL-22BP has not been clearly defined; to date, the main recognized cellular sources of *IL22RA2* mRNA are immature DCs. In 2004, in an expression pattern analysis of IL-10 ligands and receptors, *IL22RA2* was found to be specifically expressed by moDCs, and LPS decreased its expression (Nagalakshmi, Murphy, et al., 2004). It was not until 2012 that human moDCs and colonic mouse DCs were described as major producers of *IL-22RA2* in steady-state conditions (Huber et al., 2012). The constitutive expression of *IL22RA2* in lymphoid and gut tissues results from a subset of cDCs in an immature state, and it is upregulated by retinoid acid (RA) (J. C. Martin et al., 2014). In human gut mucosa, three major subpopulations of the conventional $CD11c^+$ cell have been found; among them, $CD103^+$ $Sirp\alpha^+$ displayed the highest expression for *IL22RA2* (Watchmaker et al., 2014). Moreover, Perriard and colleagues found *IL22RA2* expression in human moDCs as well as in **monocytes** (Perriard et al., 2015). It has also been reported that within the intestine tract of mice, the highest expression of *Il22ra2* is in $CD11b^+CD8\alpha^-$ DCs located in the subepithelial dome region of Peyer's patches, where it blocks IL-22 signalling, thereby reducing the expression of mucin and antimicrobial peptides (Jinnohara et al., 2017). A recent study further reported its expression in human moDCs and in human psoriatic skin (Voglis et al., 2018). However, in the liver of mice, in addition to DCs, infiltrating $CD11b^+Ly6C^+$ monocytes exhibited the highest expression of *Il22ra2* under steady-state conditions compared to other hematopoietic cell populations, and monocytes also co-expressed *Il22* and *Il22ra2* after acute liver damage (Kleinschmidt et al., 2017). Aside from DCs, **eosinophils** in the human gut are also a substantial source of IL-22BP production (Kempski et al., 2020; J. C. Martin et al., 2016). In addition, *IL22RA2* expression has been found in both mouse and human pathogenic **$CD4^+$T cells** (Kempski et al., 2020; Kleinschmidt et al., 2017; Pelczar et al., 2016). Mouse **macrophages** ($Yet40^+$) recently appeared to constitute a major source of *Il22ra2*, more than DCs, in the solitary intestinal lymphoid tissue (SILT), a network of lymphoid tissues that are located in the small intestine (Savage et al., 2017). In another recent study

of mice, epidermal **keratinocytes** were the major *Il22ra2* source in the skin in the steady-state condition, (Fukaya et al., 2018). Finally, a new study conducted on mice demonstrates that NK and $CD45^-$ cells and macrophages are the main cellular sources of *Il22ra2* under naive conditions and that after influenza infection, these cellular sources decrease *Il22ra2* production, whereas production by DCs is upregulated (Hebert et al., 2020).

The precise role of and mechanisms by which L-22BP modulates the IL-22 biology is as yet a largely unresolved subject. The vast majority of studies regarding this soluble receptor have only reported mRNA expression rather than protein/isoform detection, in part because there are few commercially available reagents, and those that exist are difficult to authenticate (Zenewicz, 2018). Moreover, commercial polymerase chain reaction (PCR) primers mostly do not distinguish between the three isoforms. There is also no information on whether commercial antibodies are able to distinguish between isoforms or between free IL-22BP and complexed IL-22/IL-22BP. Thus far, only three studies have been published that provide variant-specific information; they have demonstrated that while the expression of variant 2 seems to be more abundant than the other two, variant 1 has been found to be more abundant and preferentially expressed in the placenta (Gruenberg et al., 2001; Lim et al., 2016; Wenfeng Xu et al., 2001). **Figure 16** illustrates RNA expression in different tissues and in different cell lines from the HPA project (Uhlen et al., 2015), available from the web page www.proteinatlas.org.

Figure 16: RNA-seq data of IL22RA2 in different tissues and cell lines stored on the Human Protein Atlas (HPA) website. *Data from cell lines came from the HPA project. Data from tissues came from Consensus Normalized eXpression (NX) levels for 55 tissue types and six blood cell types, created by combining the data from the three transcriptomic datasets (the HPA project, the GTEx_Genotype-Tissue Expression project, and the FANTOM5 project) using an internal normalization pipeline. From: https://www.proteinatlas.org/ENSG00000164485-IL22RA2/tissue, or cell available from v19.3 at www.proteinatlas.org.*

2.3.6 Regulation of IL-22BP expression

Huber et al. (Huber et al., 2012) explained that IL-18 downregulates *IL22RA2* in DCs in a time- and dose-dependent manner and that it is not regulated by the TLR-2, TLR-4, TLR-5, or IL-1 pathways. The authors demonstrated that knockout mice for NLRP3$^{-/-}$ and NLRP6$^{-/-}$ inflammasomes blocked that downregulation, which was mediated by IL-18. In the same period of time, it was observed that RA and the RA

receptor agonist, AM580, were strong upregulators of *IL22RA2* in moDC. Moreover, the presence of prostaglandin E_2 (PGE_2), which has been found to inhibit the dehydrogenases RALDH2 activity that metabolizes retinal into RA, also abolished the expression of *IL22RA2* (J. C. Martin et al., 2014). Different maturation stimuli, including LPS, LPS + INFγ, TLR3, and TLR 5 ligands, dramatically downregulate *IL22RA2* expression in moDC (J. C. Martin et al., 2014). It has also been described that among the different maturation stimuli of DCs (IL-6, IL-1β, PEG_2, and TNF-α), PGE_2 alone or in combination with other previously mentioned stimuli, acts as a potent downregulator of *IL22RA2* expression in moDC (Voglis et al., 2018). Interestingly, the authors also reported a significant upregulation of the mRNA levels of *IL22RA2* after IL-6 treatment. *IL22RA2* production in DCs has recently been described as being directly induced by lymphotoxin (LTα1β2) via the non-canonical NF-κB pathway (Kempski et al., 2020). However, different inflammatory environments may account for different regulations; while downregulation in the intestine may be mediated by the microbiome and inflammasome activation, *Il22ra2* expression in mice is not changed upon acute liver damage (Kleinschmidt et al., 2017).

2.3.7 Modulation of IL-22 activity by IL-22BP

Functional studies of IL-22BP have proposed that the administration of recombinant IL-22BP during bacterial sepsis to inhibit IL-22 can provide protection through an enhancement in the accumulation of neutrophils and mononuclear phagocytes, thereby reducing bacterial load at the site of infection (Weber et al., 2007). The limited presence of IL-22BP in epithermal alterations in psoriasis cannot cope with the deleterious actions of IL-22 in the skin (Fukaya et al., 2018; J. C. Martin et al., 2017; Voglis et al., 2018). Another protective role of IL-22BP has been proposed in acute liver damage: in *Il22ra2*-deficient mice, two models of acute liver injury, ischemia reperfusion, and N-acetyl-p-aminophenol intoxication showed an increase in liver injury due to IL-22 (Kleinschmidt et al., 2017). In contrast, detrimental roles have also been attributed to this protein: IL-22BP produced by $CD4^+$T cells plays an important role in the

development of IBD, both in humans and in mouse models (Pelczar et al., 2016). Furthermore, the expression of IL-22BP by eosinophils in the gut may inhibit the protective effects of IL-22 in intestinal inflammation (J. C. Martin et al., 2016). However, the absence or diminished inhibition of IL-22 functions could also lead to potentially dangerous long-lasting proliferative effects on intestinal epithelial cells during acute colitis (Huber et al., 2012; J. C. Martin et al., 2014) or even contribute to colorectal tumorigenesis (Kempski et al., 2020).

The dual function that IL-22 possesses is inversely mirrored by the inhibitory function of IL-22BP, at least for isoform 2. A tight and exquisite balance between both of them must exist to maintain homeostasis; as previously mentioned for IL-22, the environmental context of the inflammation may determine an imbalance between these two leading to protection vs. inflammation.

2.3.8 L22/IL-22BP axis: health and disease

As previously described, the restricted expression of IL-22R1 determines the site of action of IL-22. In this regard, IL-22 mainly acts on the epithelial cells of different organs (the skin or the digestive or respiratory systems), pancreatic cells, hepatocytes, and synovial fibroblasts. Il-22 induces the production of antibacterial proteins, protects its target cells against damage, inhibits their differentiation, or increases its proliferation; it also induces the expression of other molecules that generate a positive feedback loop, which amplifies its actions (Sabat et al., 2013).

The soluble receptor, IL-22BP, antagonizes the action of IL-22 by inhibiting its binding to the membrane receptor. In this regard, the balance between these two components must be tightly regulated. There are several disorders where the dysregulation in IL-22 and/or IL-22BP breaks the homeostasis of this axis. These disorders include auto-immune diseases; inflammatory bowel diseases; liver diseases; bacterial, fungal, and viral infections; and cancer.

This subsection discusses the most well-described disorders in which this axis participates, with a special focus on MS. As previously mentioned,

this focus stems from our group's identification of the SNP rs28385692, located in the *IL22RA2* gene, which was found to be significantly associated with this disease.

2.3.8.1 Multiple sclerosis (MS)

MS is a chronic inflammatory disease associated with central nervous system (CNS) inflammation, demyelination, and neurodegeneration mediated by an unregulated immune response of both innate and adaptive immune arms. It is a heterogeneous multifactorial disease that occurs in genetically predisposed individuals with favourable environmental triggers (Baecher-Allan, Kaskow, & Weiner, 2018).

The pathological features that characterize MS include immune cell infiltration across the blood brain barrier, multifocal inflammation, demyelination, oligodendrocyte loss, neuroaxonal degeneration, and gliosis, leading to disruption of neuronal signalling (Baecher-Allan et al., 2018; Dendrou, Fugger, & Friese, 2015).

The disease course and symptomatology of MS is heterogeneous; it can include sensory and visual disturbances, motor impairments, fatigue, pain, and cognitive deficits (Dendrou et al., 2015). Despite its heterogeneity, three major types of MS (**Figure 17**) have been agreed by neurologists based on disease activity (clinical relapse rate, inflammatory component / magnetic resonance imaging [MRI], and disease progression) (Lublin et al., 2014).

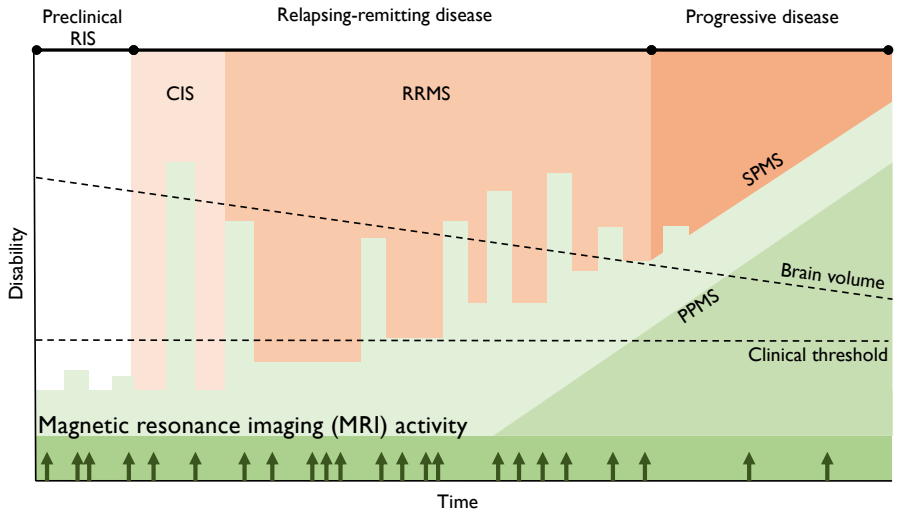

Figure 17: Multiple sclerosis (MS) disease stages and disease phenotypes*. Three major types of MS are described based on the disability, relapses, and magnetic resonance imaging (MRI), among others: a preclinical stage called radiologically isolated syndrome (RIS); a relapsing-remitting disease, which includes clinically isolated syndrome (CIS) and relapsing-remitting MS (RRMS); and a progressive disease that includes primary progressive MS (PPMS) and secondary progressive MS (SPMS). Vertical bars represent relapses. Vertical arrows represent MRI activity. Adapted from Baecher-Allan et al., 2018.*

Preclinical stage

A preclinical phase, called radiologically isolated syndrome (RIS), occurs in genetically predisposed individuals, combined with environmental and lifestyle risk factors. This classification is not included in the MS phenotype range; it occurs in a preclinical stage when incidental imaging findings suggest inflammatory demyelination in the absence of clinical signs or symptoms. It is under debate whether MRI-consistent features without MS clinical association can confirm the diagnosis for MS (Filippi et al., 2016).

Relapsing-remitting stage

-Clinically isolated syndrome (CIS): this is the first clinical neurologic symptom/episode caused by inflammation and demyelination in the CNS. It may manifest in MS, but has not yet fulfilled the criteria of

dissemination in time. It should be followed to determine the subsequent disease course.

-Relapsing-remitting MS (RRMS): this is the most common MS disease phenotype (85%). It is dominated by clearly defined attacks of new or increasing inflammatory events of the periphery and the CNS that can be fully or partially recovered. It can be further classified as active or not active within a specified time frame.

Progressive stage

-Primary progressive MS (PPMS): a small proportion of patients can directly enter into this stage after clinical onset. It is characterized by progressive and irreversible accumulation of neurological disabilities due to axonal injury and neuronal loss from onset.

-Secondary progressive MS (SPMS): this involves a progressive and irreversible accumulation of neurological disabilities after an initial RRMS course. The majority of RRMS patients will get the SPMS phenotype after years.

PPMS and SPMS can be further subclassified into the following: active and with progression, active without progression, not active and without progression, or not active and with progression.

Epidemiology

The epidemiology data from the Atlas of MS 2013 database indicated that MS is one of the world's most common neurological disorders. The estimated number of people with the disease is 33 per 100,000 individuals (accounting for 79% of the world population). The ratio of women to men is twice, and it is considerably higher in some regions, such as East Asia (reaching 3:1) or North America (2.6:1), and the average age of onset is 30 years (Msif, 2013).

The aetiology of MS is still obscure, but the experimental evidence supports that both genetic and environmental factors converge to determine the susceptibility. The initial evidence of the genetic

component in MS came from epidemiological analysis, which revealed that the disease clusters in families. Cross-sectional studies of MS patients with their families (Sadovnick & Baird, 1988; Sadovnick & Macleod, 1981) and twin studies (Sadovnick et al., 1993) further confirmed the genetic component in MS. The systematic reduction in relative risk with genetic distance was further reported (N. P. Robertson et al., 1996), and other analyses of adopted children (G. C. Ebers, Sadovnick, & Risch, 1995), stepsiblings (Dyment, Yee, Ebers, & Sadovnick, 2006), or conjugal pairs (G. C. Ebers, Yee, Sadovnick, & Duquette, 2000) corroborated that the familial disease aggregation can be partially attributable to the shared genetic factors. In contrast, the fact that in monozygotic twins, the concordance was not 100% (Willer, Dyment, Risch, Sadovnick, & Ebers, 2003) indicated that other factors participate in the disease contribution (Fagnani et al., 2015).

Epidemiological studies have also revealed differences in the geographical frequency distribution (Rosati, 2001). A positive association has been confirmed between MS prevalence and latitude globally, with some exceptions as a result of genetic and behavioural-cultural variations (Simpson, Blizzard, Otahal, Van Der Mei, & Taylor, 2011). While family clustering might mainly be determined by genetic factors, the heterogeneity in the geographical frequency may be due to a combination of both genetic and environmental factors (George C. Ebers, 2008).

Several studies have focused on the environmental components that have been found to contribute to the disease. Some of them are vitamin D deficiency, Epstein bar virus infection, adolescent obesity, smoking, and geographic latitude distribution influenced by sunlight exposure (O'Gorman, Lucas, & Taylor, 2012; Olsson, Barcellos, & Alfredsson, 2016). Less established environmental factors, such as organic solvent exposure and night shift work, have also been associated with MS risk. However, other factors, such as oral tobacco, cytomegalovirus infection, alcohol, and coffee consumption habits, are associated with decreased risk. Additional elements not well studied may also participate in MS, including diet and the type and distribution of gut microbiota (Olsson et al., 2016).

In addition to the previously stated genetic and environmental factors, epigenetic components have recently been included in the picture as a link between the two factors. Epigenetic modifications such as DNA methylation, histone modifications, and microRNA-mediated post-transcriptional gene silencing have been considered as other factors influencing MS (Olsson et al., 2016; Y. Zhou et al., 2014).

Initial attempts to identify genes associated with susceptibility to MS successfully found human leukocyte antigen (HLA) polymorphisms within the MHC to be associated with MS (Bertrams & Kuwert, 1972; Naito, 1972). Since then, many other studies have replicated the associations of HLA polymorphisms with MS risk and have also found variants from others genes in that region (Sawcer, 2008). However, the polygenic model of MS heritability, in which the risk is the result of the contributions of many variants common in the population, each one determining a moderate portion of the risk, provided the theoretical justification for genome-wide association studies (GWASs) to find variants linked with MS (Baranzini & Oksenberg, 2017). In the last decade, several GWASs have been realized thanks to major multicentre, worldwide collaborations (Bahlo et al., 2009; Baranzini et al., 2009; Beecham et al., 2013; Comabella et al., 2008; De Jager et al., 2009; Jakkula et al., 2010; Patsopoulos et al., 2017; Sawcer et al., 2011). To date, 200 autosomal susceptibility variants with independence to MHC, one chromosome X variant, and 32 independent associations within the extended MHC establish a reference map of the MS genetic architecture (**Figure 18)** (The International Multiple Sclerosis Genetics Consortium [IMSGC], 2019b). In this study, ~19.2% of the genetic predisposition to MS can be explained with the validated susceptibility genes (being the MHC region responsible for 4% of the overall heritability). Another important finding is that a significant enrichment for MS susceptibility loci was observed not only in the well-known T cells but also in B cells, NK cells, DCs, and microglia, thus highlighting the immune nature of MS genetics.

The genetic architecture underlying susceptibility to MS follows a complex polygenic model in which the risk may be determined by the so-called common disease, common variant (CD-CV) hypothesis, where the

genetic risk stems from either the cumulative effects of a large number of small-effect variants with high frequencies, or less frequent variants with moderate effects; these variants are identified by GWASs (Didonna & Oksenberg, 2015; Sawcer, Franklin, & Ban, 2014; The International Multiple Sclerosis Genetics Consortium [IMSGC], 2010). However, the MS loci identified in the GWASs only explains part of the heritability. Several hypotheses have been discussed for the 'missing heritability', such as the rare variant hypothesis, where low-frequency variants (MAF < 0.5%) with high ORs (>2) are responsible for that missing heritability and due to their low frequency are not identified in the GWASs (Lill, 2014; Visscher, Brown, McCarthy, & Yang, 2012). Linkage studies are required to identify rare variants. Another hypothesis for the missing heritability in MS may be attributable to previously mentioned epigenetic modifications. Moreover, the major environmental risks associated with MS are all known to exert epigenetic changes (Küçükali, Kürtüncü, Çoban, Çebi, & Tüzün, 2015). A recent study that focused on the investigation of rare disease-causing variants in multi-incident MS families identified 12 rare genetic variants (missense or nonsense) located in genes implicated in specific immunological pathways, which are largely responsible for the onset of MS in these families (Vilariño-Güell et al., 2019).

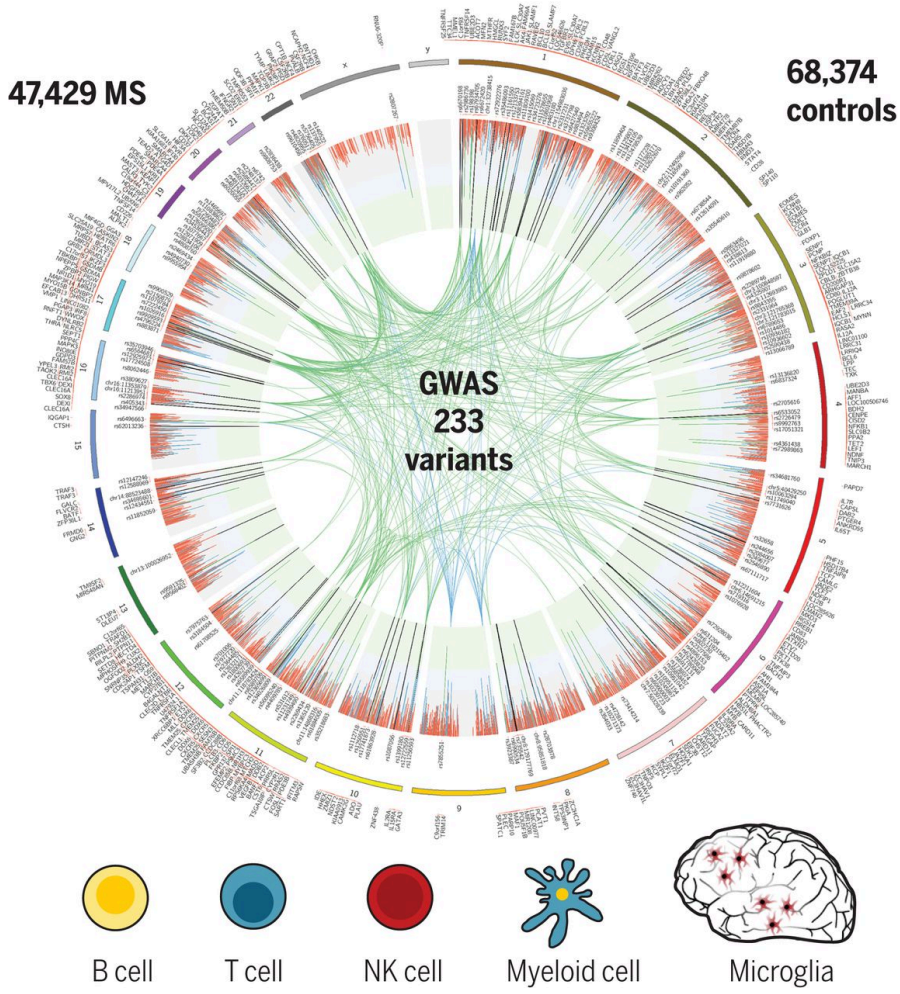

Figure 18: Genetic Atlas for multiple sclerosis. *The outermost track of the circos plot lists the 200 autosomal non-major histocompatibility complexes (MHCs) and one in chromosome X genome-wide effects are listed, and 551 prioritized genes are plotted on the outer surface. Reproduced from The International Multiple Sclerosis Genetics Consortium (IMSGC), 2019b.*

IL-22 and IL-22BP in MS

As previously mentioned, the advent of GWASs dramatically increased the number of associated MS risk genes, the majority of which are known as immune-related factors. One of these is the *IL22RA2* gene. Moreover, inflammation is known to play a major role in the onset and propagation of the disease, where proinflammatory cytokines, including IL-17, IL-22,

TNFα, IL-1, IL-12, and IFNγ, contribute to MS through several pathways (K. Wang et al., 2018). Although the role of IL-22 and IL-22BP in MS has not been fully understood, there are some lines of evidence at genetic, molecular, and cellular levels suggesting an important function of these axes in the disorder.

Several studies have described SNPs located in the *IL22RA2* gene to be associated with MS. The first time that *IL22RA2* was established as an MS risk gene was in a combined approach that included genetic and immunological investigation in an animal model with association studies of MS patients. In that study, Olson's group identified the SNP rs276474 located at the very end of *IL22RA2* as a candidate gene that was significantly associated with MS severity in a combined Swedish and Norwegian cohort (Beyeen et al., 2010).

The SNP rs17066096, which is intergenetically located near *IL22RA2*, was found to be significantly associated to MS susceptibility by the IMSGC (Sawcer et al., 2011). This association was further confirmed by independent datasets (Beecham et al., 2013; Lill et al., 2014). Furthermore, in vitro analyses of this variant have recently shown that the protective allele of rs17066096 is associated with lower mRNA expression of *IL22RA2* in moDCs (Lindahl, 2017); however, they did not find an association between the SNP and the protein levels of IL-22BP detected by ELISA in cerebrospinal fluid (CSF) and serum samples from MS patients (Lindahl et al., 2019). In addition, this group has recently found the presence of IL-22BP protein levels in the CSF of rats and humans, and transcript expression in mice microglia (Lindahl, 2017; Lindahl et al., 2019). The detection of this protein in the CSF of MS patients has also been previously reported by an independent group (Perriard et al., 2015).

Further evidence for the *IL22RA2* SNP's association with MS was found in a cytokine and cytokine receptor gene association screening performed by our group. Although the combined dataset analysis did not reveal a significant association, two independent datasets did for the intronic *IL22RA2* SNP, rs202573 (K. Vandenbroeck et al., 2012). In a fine mapping study performed by our group, another non-synonymous SNP located in

exon 2 of *IL22RA2*, namely, rs28385692, which leads to a missense mutation on the 16th residue located in the SP (L16P), has emerged as a rare SNP associated with MS, with a high odds ratio (Gómez-Fernández et al., 2020). The functional effect of this SNP will be further analysed in this thesis.

A recent study of the identification of causal disease genes at the MS-associated region, 6q23, using the Capture Hi-C method in human T- and B-cell lines, demonstrated that the 6q23 region presents numerous complex chromatin-looping interactions clustered in two regions. One of these regions contains the previously mentioned rs17066096 SNP, together with two other SNPs, namely, rs7769192 and rs67297943. In that study the found that these SNPs interact with each other and with several immune-related genes, such as *IL20RA*, *IL22RA2*, *IFNGR1*, and *TNFAIP3*, indicating that they may be involved in the inflammatory processes that typically occur in autoimmunity (P. Martin et al., 2016).

Apart from the genetic studies, other lines of research have found evidence for the role of IL-22/IL-22BP in MS. Two of the earliest events that have been described for MS are the dysregulation of the blood-brain barrier (BBB) and the transendothelial migration of activated leukocytes (Minagar & Alexander, 2003). In that regard, it has been shown that *IL-22R* and *IL17R* are expressed on the surface of BBB endothelial cells and that IL-22, together with IL-17 and cytolytic enzymes produced by T$_H$17 cells, contributes to the disruption of the BBB tight junctions in MS lesions, allowing T$_H$17 lymphocytes to transmigrate efficiently across the BBB and hence promoting CD4$^+$ recruitment and CNS inflammation (Kebir et al., 2007). Moreover, T$_H$22 cells have been found to play an important role in the pathogenesis of MS (Fard, Azizi, & Mirshafiey, 2016). The proportion of T$_H$22 cells as well as the serum levels of IL-22 are increased in MS patients, suggesting that IL-22 may participate in the pathogenesis of this disorder (Wen Xu et al., 2013). Further investigations revealed an increase in these cells and in the IL-22 protein levels in relapsing MS (Muls, Nasr, Dang, Sindic, & Van Pesch, 2017; Perriard et al., 2015; Rolla et al., 2014). Similarly, studies performed on experimental autoimmune encephalomyelitis (EAE) animal models – a widely used

tool to study neuroinflammatory disease mechanisms – have found that IL-22 is likely involved in the disease. In an analysis of the genetic expression of several MS candidate genes in an EAE rat model using a susceptible DA strain, IL-22 was also found to be increased during the initial disease induction and reactivation (Thessen Hedreul, Gillett, Olsson, Jagodic, & Harris, 2009). Additionally, in an acute EAE-induced rat model, IL-22 levels have been found to be elevated during the induction and peak phases of EAE, and they markedly decreased during the recovery phase (Almolda, Costa, Montoya, González, & Castellano, 2011). However, another study using an EAE model demonstrated that *Il22*$^{-/-}$ mice possess the same susceptibility to EAE as wild-type mice, suggesting an indirect role of IL-22 in the disease pathogenesis in the murine model (Kreymborg et al., 2007). In another EAE study, Olson's group described that *Il22ra2*-deficient mice exhibited a less severe disease course, less demyelination, and less infiltration of immune cells in the CNS than in controls, proposing that an absence in the IL-22 blockage may have a protective role in the inflammation of the EAE; however, the knockout mice displayed a slightly earlier onset (Laaksonen et al., 2014).

A dysregulation in the expression of IL-22 and IL-22BP has been found in MS patients. While IL-22 has been found to be significantly increased in the sera of MS patients, its antagonist, IL-22BP, does not increase (it should be mentioned that a trend can be observed). The same study showed that human astrocytes express both subunits of IL-22 membrane receptor and that MS patients exhibit higher expression of these receptors around blood vessels and in MS plaques than healthy controls. Furthermore, the study also found that IL-22 increases the survival of astrocytes (Perriard et al., 2015), which have been described as playing a central role in the pathogenesis of MS (Ponath, Park, & Pitt, 2018).

Although an emerging body of data exists on the matter, the pathogenic mechanism of the IL-22/Il-22BP axis in MS remains unresolved.

2.3.8.2 Systemic lupus erythematosus (SLE)

Systemic lupus erythematosus (SLE) is an autoimmune disease where the dysregulation of the immune system (innate and adaptive), triggered by genetic, environmental, viral, and hormonal factors, attacks and damages organs and tissues, including the skin, joints, CNS, and kidneys (Kaul et al., 2016). This damage is caused and characterized by an abundant production of autoantibodies, the activation of the complement, and immune-complex deposition (Pan, Ye, & Li, 2008). Although increased levels of cytokines produced by abnormal T helper cells have been found to be involved in the pathogenesis of SLE (Pan et al., 2008; Wong, Ho, Li, & Lam, 2000), the resulting levels of IL-22 in plasma and serum were decreased (F. Cheng, Guo, Xu, Yan, & Li, 2009; Pan et al., 2009). IL-22 has been described as contributing to renal repair, inducing renal progenitor cell proliferation, and ensuring recovery from kidney injury (S. Kumar, 2018). Moreover, increased urinary IL-22BP levels correlate with Lupus nephritis activity (Badr, Farag, Abdelshafy, & Riad, 2017; X. Yang et al., 2014), suggesting that a dysregulation in IL-22/IL-22BP may participate in the lupus nephritis pathology.

2.3.8.3 Rheumatoid arthritis (RA)

RA is a chronic inflammatory autoimmune disease that affects joints. It is characterized by the infiltration of inflammatory mononuclear cells, such macrophages and T cells, and the proliferation of synovial fibroblasts, and with the production of autoantibodies against immunoglobulin G (rheumatoid factor, RF) and citrullinated proteins. It occurs in genetically susceptible individuals and involves environmental factors (Smolen et al., 2018). Several proinflammatory cytokines, such as TNF-α, IL-6, and IL-1β, mainly produced by macrophage-like synoviocytes, are known to play central roles in the development of RA (Smolen et al., 2018). Although the pathophysiology role of IL-22 in the development of RA has not been studied, IL-22 produced by macrophages and fibroblasts in the synovial tissues has been found to promote inflammatory responses in RA by inducing synovial fibroblast proliferation and chemokine

production in the rheumatoid synovium, and *IL22RA1* has been found to be expressed in both the lining and sublining layers of RA synovial tissue (Ikeuchi et al., 2005). In addition, elevated plasma levels of IL-22 have been found to correlate with high levels of RF (da Rocha et al., 2012), disease severity (L. Zhang et al., 2011), and progression of bone erosion (Leipe et al., 2011). The dual role of IL-22, depending on the phase of the arthritis, has also been described as protective prior to the onset of the disease, and pathogenic after onset of arthritis (Justa, Zhou, & Sarkar, 2014). To date, there are few studies explaining the role of IL-22BP in the development of the disease. *IL22RA2* expression in the ankle synovia of mice has been found to concomitantly increase with the severity of the disease and correlate with the increase in IL-22, thus indicating the possibility of a local IL-22 modulator (Marijnissen et al., 2011). Some studies also show that IL-22 blocking with antibodies may be beneficial for RA therapy (Marijnissen et al., 2011; Zhong, Zhao, Liu, & Jiang, 2017).

2.3.8.4 Psoriasis

Psoriasis is a chronic and immune-mediated disorder of both the immune and adaptive immune systems, where DCs, keratinocytes, and T cells play key roles. The disease can be triggered by different factors, including infections and medications, in genetically susceptible individuals. Inflammatory myeloid DCs produce IL-12 and IL-23 to activate T_H17, T_H22, and T_H1 cells to produce abundant psoriatic cytokines, such as IL-17, INFγ, TNF, and IL-22; these cytokines induce hyperproliferation and impairment in the terminal differentiation of keratinocytes, thereby causing epidermal thickening, hypogranularity, and hyperkeratosis, which ultimately lead to skin alterations observed in psoriasis (**Figure 19**) (Greb et al., 2016; Lowes, Suárez-Fariñas, & Krueger, 2014; Sabat et al., 2013).

In 2004, psoriasis arose as the first disease associated with the dysregulation of IL-22 production and was in that study when the target of IL-22 was related to cells without hematopoietic origin, such as keratinocytes (Wolk et al., 2004). IL-22 expression is strongly upregulated

in lesioned psoriatic skin compared to non-lesioned skin or healthy skin, where it is almost absent (Boniface et al., 2005; J. C. Martin et al., 2017; Wolk et al., 2004, 2006). The main producer cells of IL-22 in psoriasis are $CD4^+$, mostly by T_H22 and T_H17 cells, and by T_H1 cells to a lesser extent (Nograles et al., 2009). In contrast to other cytokines upregulated in psoriasis, such as IL-1β or INFγ, which are barely detected in blood or plasma, the levels of IL-22 are increased in psoriasis and correlate with the disease severity (J. C. Martin et al., 2017; Wolk et al., 2006).

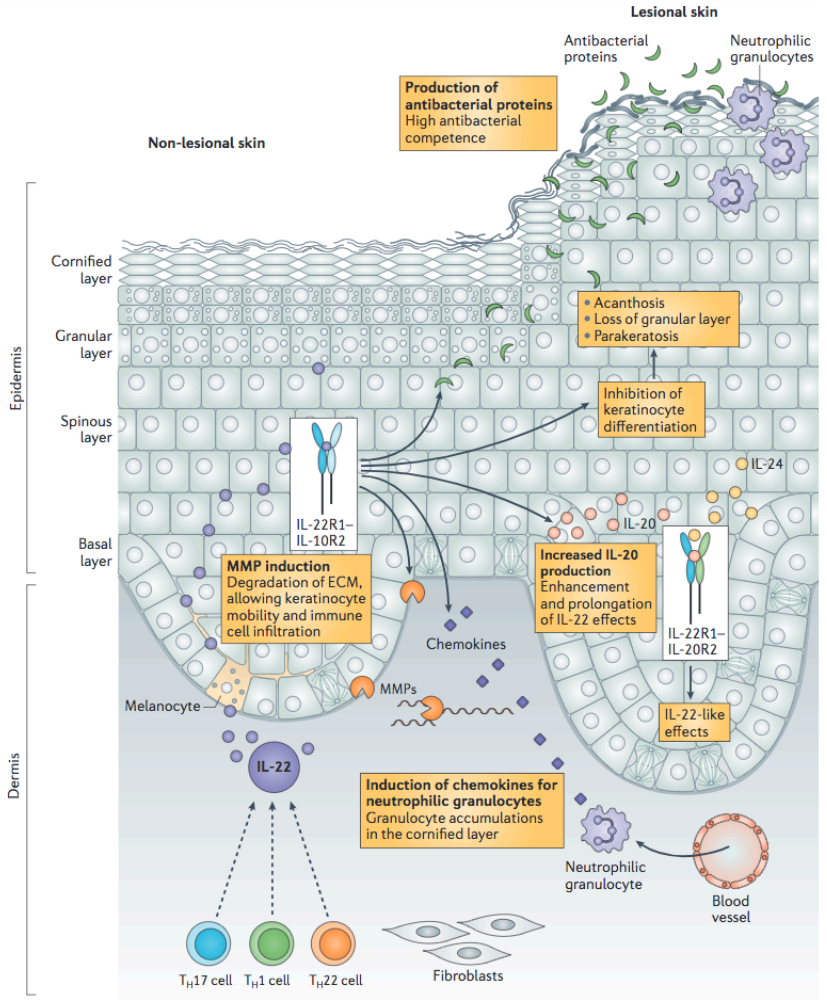

Figure 19: Function of the IL-22–IL-22R1 axis in psoriasis. *During a lesion of psoriasis, $CD4^+$ cells (Th22, Th17, and Th1 cells) migrate from the dermis to the epidermis where, after*

stimulation with IL-23, they release high levels of IL-22. Il-22 consequently induces five features in keratinocytes: (i) the inhibition of the keratinocyte differentiation and cornification, leading to a process of epidermal thickening (acanthosis), loss of granular layer, and retention of nuclei remnants in the cornified layer (parakeratosis); (ii) the production of antibacterial proteins; (iii) the production of extracellular matrix (ECM)-degrading enzymes (matrix metalloproteinase, MMP) that facilitate the immune cell infiltration and the epidermis restructuration; (iv) the accumulation of neutrophils by the IL-22-induced chemokine production by keratinocytes; and (v) the induction of IL-20, a cytokine that amplifies IL-22 actions. Reproduced from Sabat et al., 2013.

During psoriasis, the increased levels of IL-22 induces several features in keratinocytes. First, it inhibits its maturation and differentiation through the downregulation of keratinocyte differentiation-associated genes, including profilaggrin (FLG), keratin 1 and 10 (KRT1 and KRT10), keratinocyte differentiation-associated protein (KDAD), kallikrein 7 (KLK7), and calmodulin-like protein 5 (CALML5) (Wolk et al., 2006). Second, IL-22 increases the expression of anti-microbial peptides, including S100A7, S100A8, S100A9, β-defensin 2, β-defensin 3, and lipocalin 2, in keratinocytes (Boniface et al., 2005; Wolk et al., 2004, 2006). Third, IL-22 induces the expression of extracellular matrix (ECM)-degrading enzymes, such as matrix metalloproteinases MMP-1 and MMP-3, in keratinocytes (Boniface et al., 2005; Wolk et al., 2006). Fourth, it promotes the accumulation of neutrophils mediated by the production of neutrophil-attracting chemokines, such as CXC-chemokine ligand 1 (CXCL1), CXCL2, CXCL5, and CXCL8 (Boniface et al., 2005; Wolk et al., 2009). The main mechanisms of the physiopathology of IL-22 in psoriasis are represented in (**Figure 19**). Finally, IL-22 increases the expression of IL-20, a cytokine that has effects similar to those of IL-22 on keratinocytes, thereby promoting the amplification of IL-22 signalling (Wolk et al., 2009). The anti-apoptosis role of IL-22 on keratinocytes in psoriasis has recently been described as contributing to plaque formation (B. Wang et al., 2020). In this study, the authors showed that the apoptotic keratinocytes only increased in the stratum corneum layer, but not in the spinous and basal layers of psoriasis plaques, where the keratinocyte apoptosis was inhibited by the increased expression of IL-22. They also demonstrated that IL-22 had an anti-apoptotic effect on keratinocytes in

the spinous and basal layers by regulating the Bcl-xL/Bax anti-apoptosis gene/pro-apoptosis gene.

While lymphocytes are the main sources of IL-22 in the skin, evidence exists that mast cells are the main IL-22 sources during psoriasis and atopic dermatitis (Mashiko et al., 2015).

Apart from the upregulation of IL-22 in this disease, its antagonist, IL-22BP, has recently been found to be strongly downregulated in skin biopsies of psoriatic patients compared to healthy controls (Voglis et al., 2018), and the levels of IL-22BP in unaffected skin of psoriatic patients are lower than in the skin of controls (J. C. Martin et al., 2017). Moreover, the IL-22/IL-22BP serum protein ratio correlates positively with the disease severity (J. C. Martin et al., 2017). In a psoriasis-induced mouse model, Il-22BP-knockout mice exhibited aggravation of psoriasis with increased expression of IL-22-associated anti-microbial peptides; the injection of a neutralizing antibody of IL-22BP in the mouse model also reproduced the results (J. C. Martin et al., 2017). Altogether, these studies suggest that the limited presence of this IL-22 antagonist contributes to the development and maintenance of the disease. Epidermal keratinocytes in mice have recently been reported to be the major cellular sources of IL-22BP in the skin during the steady-state condition, and this transcriptional expression is said to be downregulated during psoriatic inflammation (Fukaya et al., 2018).

2.3.8.5 Sjögren's syndrome (SS)

Sjögren's syndrome (SS) is a chronic autoimmune disease characterized by the inflammation of exocrine glands, with salivary and lacrimal glands being the most affected. However, glands located in the nose, the upper-respiratory tract, the oropharynx, and even the vagina in women can also be affected. This inflammation leads to sicca symptoms, which are characterized by a dryness of those mucosal surfaces (Brito-Zerón et al., 2016). The IL-22/IL-22BP axis has been found to be imbalanced in this disease; IL-22, which is mainly produced by T_H17 and $NKp44^+$ NK cells in SS patients, is increased in the salivary glands (Francesco Ciccia et al.,

2012) and in the sera of patients (Lavoie, Stewart, Berg, Li, & Nguyen, 2011), and its membrane receptor, IL-22R1, has also been found to be over-expressed in SS. However, despite its soluble receptor, IL-22BP, which would block the IL-22 effect, being found to be over-expressed in SS patients (no description of which variant), isoform 2 was absent in the neoplastic tissue of the SS-associated lymphoma (F. Ciccia et al., 2015). There is a mutually exclusive tissue distribution of IL-18 and IL-22BP; this may be due to the fact that the upregulation of IL-18 negatively modulates the expression of IL-22BP, but positively increases the expression of IL-22R1 (F. Ciccia et al., 2015). IL-22 may therefore play a proinflammatory role in the pathogenesis of SS.

2.3.8.6 Inflammatory bowel disease (IBD)

Inflammatory bowel disease (IBD) is a chronic, relapsing, immune-mediated disorder of the intestine with a disruption of the epithelial barrier that is subdivided into two major forms: Crohn's disease (CD) and ulcerative colitis (UC). IBD is a multifactorial disorder whose course and severity are affected by the genetic susceptibility and environmental factors cross-related with an immune dysregulation status and the intestinal flora of the host (Kaser, Zeissig, & Blumberg, 2010). While CD is characterized by the inflammation of all layers of the intestinal wall and is often located in the terminal ileum and proximal colon, UC usually begins in the rectum and continuously spreads proximally, usually affecting the mucosa. Both diseases show increased IL-22-producing cells and increased levels of this cytokine in colonic tissues (Andoh et al., 2005). This increase promotes proinflammatory gene expression and intestinal epithelial cell migration, and it has also been demonstrated to be more pronounced in the inflamed lesions of CD patients than in UC (Andoh et al., 2005; Brand et al., 2006). Similarly, the levels of IL-22 in the blood of CD patients are increased compared to healthy controls, and the IL-22 levels in serum positively correlate with the disease activity (Schmechel et al., 2008; Wolk et al., 2007). Contrary to what occurs in psoriasis, evidence points to the protective role of IL-22 in IBD mouse models: IL-22 produced by $CD4^+$ T cells or NK cells protects mice from IBD

(Zenewicz et al., 2008); the ectopic expression of IL-22 ameliorates intestinal inflammation in a mouse model of UC (Sugimoto et al., 2008); IL-22 participates in the gut homeostasis, thus promoting mucosal wound healing by survival and proliferation of epithelial cells (Pickert et al., 2009); IL-22 produced by neutrophils enhances the antimicrobial peptide production from colonic epithelial cells and contributes to restoring the epithelium after the mucosal injury (Zindl et al., 2013); and AhR-induced signals increase IL-22 levels and inhibit inflammation in the gastrointestinal tract in a mouse colitis model (Monteleone et al., 2011). However, the role of IL-22 in IBD is controversial. It has also been reported that in some conditions, IL-22 could drive acute colitis and that the IL-22 actions depend on the origin source and microenvironmental factors (Eken, Singh, Treuting, & Oukka, 2014; Kamanaka et al., 2011).

Two groups have reported that in mouse models of dextran sulphate sodium (DSS)-induced acute colitis, the mRNA expression of *Il22ra2* decreased compared to controls, leading to an increase in the IL-22/IL-22BP ratio (Huber et al., 2012; Wolk et al., 2007). However, in recent studies, the opposite results have been presented: IL-22BP production has been reported to be enhanced during inflammation in CD and UC, indicating that the protective role of IL-22 would be blocked by this soluble receptor in experimental colitis models (J. C. Martin et al., 2016; Pelczar et al., 2016).

2.3.8.7 Liver diseases

In the liver, the main action of IL-22 occurs on hepatocytes through the IL-22 receptor by inducing the expression of mitogenic and antiapoptotic proteins supporting cellular proliferation and therefore liver regeneration (O. Park et al., 2011; Radaeva et al., 2004). However, as with other diseases, there are also studies suggesting that IL-22 might have pathogenic functions in chronic liver damage. Elevated serum levels of IL-22 correlate with a poorer prognosis in patients with hepatitis B virus (HBV) cirrhosis (Kronenberger et al., 2012; L.-Y. Wu et al., 2015). In contrast, limited and conflicting data are available regarding the role of

IL-22BP in liver diseases. Gene variants of IL-22BP associated with high IL-22BP expression are related to the development of severe fibrosis in schistosomiasis and hepatitis C (Sertorio et al., 2015), whereas IL-22BP knock-out mice are more susceptible to acute liver injury (Kleinschmidt et al., 2017). A recent study has suggested that IL-22BP is of decisive importance for the bioactivity of the IL-22 system and that the interleukin interplay with its binding protein and membrane receptor may be at least as important as the interleukin itself (Støy et al., 2020). In that study, the authors found that IL-22BP plasma levels were decreased in alcoholic hepatitis patients compared to controls and that those low IL-22BP levels were associated with high mortality. They also found an association for how IL-22 modulates IL-22RA1 expression.

2.3.8.8 Bacterial, fungal, and viral infections

IL-22 has been described as having anti-microbial functions and mediating tissue repair, protection, and wound healing responses from epithelial cells during infection and inflammation (Rutz et al., 2013).

It has been observed that mouse models deficient in *Il22 or Il22ra1* showed marked intestinal epithelial damage, systemic bacterial burden, and mortality compared to wild type after bacterial infections of *Citrobacter rodentium*, which is a bacterium that induces acute colitis in mice. Il-22 induces fucosylation, which promotes intestinal colonization resistance to opportunistic pathogens and the production of antimicrobial peptides by epithelial cells (Pham et al., 2014; Zheng et al., 2008) Moreover, IL-22 induces a systemic protective response inducing the production of hemopexin, which limits the availability of heme iron to microbes, leading to the suppression of bacterial systemic growth (Sakamoto et al., 2017). However, a potential pathological role of IL-22 during infection has also been reported; recombinant IL-22BP administration attenuated the bacterial load and organ failure during polymicrobial sepsis in a mouse model (Weber et al., 2007). In addition to controlling bacterial pathogens, deficient-*Il22* mice exhibited an alteration in the colonic microbiota,

indicating that IL-22 is important in shaping the homeostatic balance between immunity and colonic microbiota (Zenewicz et al., 2013).

It has also been found that Il-22 contributes to the immunoprotection of fungal infections such as *Candida albicans* (De Luca et al., 2010; Y. Liu et al., 2009), *Aspergillus fumigatus* (Gessner et al., 2012), and *Rhizomucor pusilluscan* (Bao et al., 2013). Il-22 targets epithelial cells to release antifungal peptides such as S100A8, S10A9, lipocalin2, or Dectin-1 (De Luca et al., 2010; Gessner et al., 2012).

Apart from bacterial and fungal protection, IL-22 has been found to participate in protection against viral infections by recruiting antiviral neutrophils, promoting tissue regeneration after infection, maintaining mucosal integrity, and decreasing microbial translocation, among other things. However, a paradoxical protective versus pathological function of IL-22 in viral infections has been found depending on the timing and context in which IL-22 is produced (Brias, Stack, Stacey, Redwood, & Humphreys, 2016). In a recent study, we demonstrated that shifting the balance of the IL-22/IL-22BP axis in favour of IL-22 promotes recovery during influenza infection by promoting tight junction formation (Hebert et al., 2020).

2.3.8.9 Cancer

Many studies have shown the association between IL-22 and different cancers, including colon, lung, gastric, liver, pancreatic, breast, bladder, thyroid, and brain cancer, as well as lymphoma (Hernandez et al., 2018). However, the role of this cytokine in cancer is complex and has been described as having both promoting and restraining functions. IL-22 may primarily constitute a barrier against cancer development, promoting tissue repair and anti-microbial peptides production; however, conversely, IL-22 overexpression caused by chronic inflammation could contribute to cancer progression.

Among the different types of tumours where IL-22 participates, the association between this cytokine and colon cancer has been described the best. IL-22 polymorphism (rs1179251, G variant) has been associated

with colorectal cancer (CRC) risk (Thompson, Plummer, Tucker, Casey, & Li, 2010). Kirchberger et al. (2013) found an increased number of IL-22-producing cells in human colon cancer samples. In their cancer model, they also found that IL-22 was the main activator of the STAT3 pathway, instead of IL-6 or IL-17, and that it might facilitate cancer perpetuation via the proliferative action of this cytokine in the epithelium. Moreover, the induction of the methyltransferase DOT1L via IL-22/STAT3 signalling has been associated with cancer stemness and the promotion of colon cancer tumorigenicity (Kryczek et al., 2013). Huber et al. (2012) described the importance of the IL-22/IL-22BP axis in the modulation of tumorigenesis in the colon (

Figure 20). In their colon cancer model, they showed that intestinal insults, such as bacteria or tissue damage, trigger the inflammasome, which leads to IL-18 activation. This cytokine downregulates IL-22BP expression, allowing IL-22 to exert its tissue repair function; finally, the homeostasis can be recovered, and the IL-22BP levels are restored. In their *IL22Ra2*$^{-/-}$ knockout mice, deficiency in IL-22BP caused prolonged IL-22 proliferative actions on colon epithelial cells, thus promoting colon tumorigenesis. However, in the same study, *IL22*$^{-/-}$ knockout mice did not have the capacity to restore the IL-22-mediated tissue repair, which also led to delayed wound healing and increased inflammation, thus promoting tumorigenesis in the colon. A recent study of CRC human tumours identified that IL-22BP levels were downregulated in CRC and associated with shorter survival times related to unregulated activity of IL-22 promoting tumorigenesis (Kempski et al., 2020).

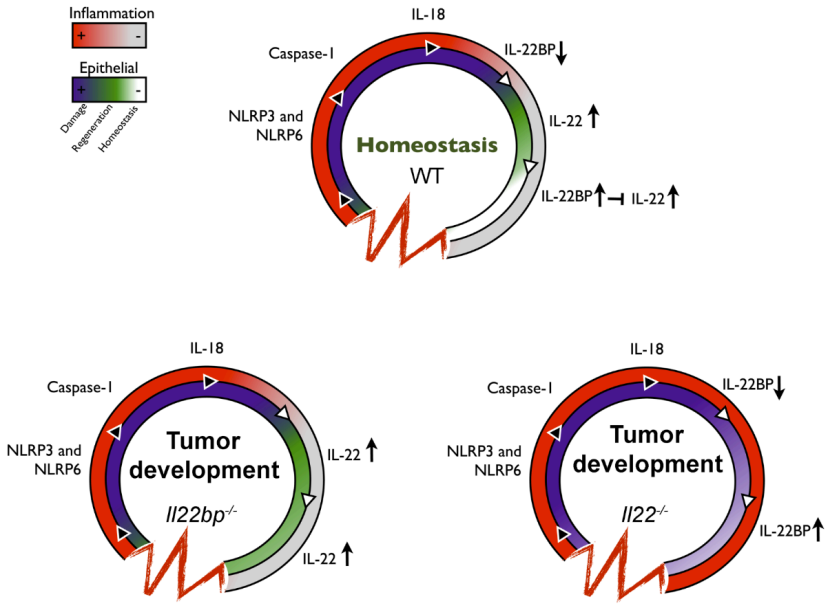

Figure 20: Role of IL-22/IL-22BP axis on intestine tumour development. *Under homeostatic conditions, after tissue damage and bacterial ligand, NLEP3/6 follows its activation, ultimately leading to IL-18 activation. IL-18 downregulates IL-22BP production by intestinal dendritic cells (DCs), thereby allowing IL-22 to exert its protective function during tissue repair. A dysregulation of the IL-22/IL-22BP axis caused by IL22 or IL-22BP deficiency promotes tumorigenesis in the colon. Reproduced from Huber et al., 2012.*

The delivery of IL-22BP for colon cancer therapy has also been proposed. An in vitro study, where the mRNA of *Il22ra2* was delivered into cationic micelles to a mouse colon cancer model, suggested that this approach inhibits cancer cell growth (Men et al., 2018).

2. Motivation and Aims

3 Motivation and Aims of the Thesis

3.1 Motivation

Our group's motivation to study IL-22BP isoforms began midway through 2013 when we found a non-synonymous SNP, rs28385692, which was located in the *IL22RA2* gene and was significantly associated with MS. At that time, the *IL22RA2* gene was then revealed as a new player in our quest to understand the polygenic basis of the risk of contracting MS. The scarcity of available data on the properties and biochemical characteristics of this protein and its associated isoforms attracted our interest and motivated us to develop this thesis.

3.2 Aims

The **overall aim** of this thesis is to understand the function and fate of IL-22BP by biochemically characterizing its isoforms.

The specifics aims are as follows:

1- to study *IL22RA2* transcript expression and link it to IL-22BP isoform secretion by biochemical characterization, as well as to identify the key factors involved in their folding and secretion and investigate their secretion and function within the cell;

2- to evaluate whether the pharmacological targeting of IL-22BP partners may have differential effects on the secretion of IL-22BP isoforms; and

3- to determine whether and to what extent the MS-risk variant, rs28385692, has functional effects on IL-22BP isoforms.

4. Materials and Methods

4 Materials and Methods

4.1 *In silico* protein post-translational modifications (PTMs) and structure prediction software

4.1.1 Multiple sequence alignment of IL-22BP isoforms

The amino acid protein sequences for each isoform of IL-22BP were obtained from the UniProt repository (https://www.uniprot.org/uniprot/Q969J5) for the following entry: Q969J5. The UniProt database is a collection of sequences and annotations for over 120 million proteins across all branches of life (The UniProt Consortium, 2019).

Multiple sequence alignment was performed using the Clustal Omega programme (https://www.ebi.ac.uk/Tools/msa/clustalo/). This software uses seeded guide trees and hidden Markov model (HMM) profile-profile techniques to generate alignments between three or more sequences (Sievers et al., 2011).

4.1.2 Signal peptide and transmembrane prediction

The bioinformatic prediction of the presence and location of SP cleavage sites in the amino acid sequences of the three IL-22BP isoforms was made running the SignalP 4.1 software (http://www.cbs.dtu.dk/services/SignalP-4.1/). This software is based on an artificial neural network (ANN) model and discriminates between SPs and TM regions (Petersen, Brunak, von Heijne, & Nielsen, 2011).

The prediction of potential ER resident proteins was made with the webserver ERPred (http://proteininformatics.org/mkumar/erpred/index.html). This is a support vector machine-based method that predicts ER resident proteins, even if the query protein does not contain specific ER-retention signals (R. Kumar, Kumari, & Kumar, 2017).

The TM helices prediction was made with the TMHMM server (http://www.cbs.dtu.dk/services/TMHMM/), which is a hidden Markov-based model for predicting TM helices in protein sequences (Krogh, Larsson, Von Heijne, & Sonnhammer, 2001).

4.1.3 Protein glycosylation prediction

The two most common types of glycosylation are N-glycosylation and O-glycosylation. Prediction of N-glycosylation sites was made with the NetNGlyc 1.0 server (http://www.cbs.dtu.dk/services/NetNGlyc/). The consensus sequence, Asn-Xaa-Ser/Thr (where Xaa is not proline), is known to be a prerequisite for the modification. However, not all of these sequons are modified, so, this consensus sequence does not discriminate between glycosylated and non-glycosylated asparagines. This software, which trained ANNs on the surrounding sequence context, discriminates between acceptor and non-acceptor sequons (Gupta, Jung, & Brunak, 2004). O-glycosylation prediction was performed by running the NetOGlyc 3.1 server (http://www.cbs.dtu.dk/services/NetOGlyc-3.1/). This software predicts protein modification by O-linked N-acetylglucosamine (O-GlcNAc) in mammalian proteins and was developed by training the ANNs through the sequence context of glycosylated and non-glycosylated serines and threonines (Julenius, Mølgaard, Gupta, & Brunak, 2005).

4.1.4 Disulphide bonds

The prediction of disulphide bonds for the three isoforms of IL-22BP was made with DIpro 2.0, a software that is based on a 2D recurrent neural network, a support vector machine, graph matching, and regression algorithms that predict whether a given sequence has disulphide bonds or not, estimates the number of disulphide bonds, and predicts the bonding state of each cysteine and the bonded pairs (J. Cheng, Saigo, & Baldi, 2005). This software is hosted in SCRATCH, which is a protein structure and structural feature prediction server (http://scratch.proteomics.ics.uci.edu).

4.1.5 Secondary and tertiary protein structure predictions of IL-22BP isoforms

The secondary protein structure prediction was performed by running three different bioinformatic prediction software programmes:

1. **POLYVIEW 2D-SABLE**. This is a predictor of the relative solvent accessibilities of amino acid residues in proteins and secondary structures (α-helix, β-strand, and coil). It uses evolutionary profiles and predicts the relative solvent accessibility of an amino acid residue as a fingerprint of the overall packing (Adamczak, Porollo, & Meller, 2004).
2. **JPRED4.** This is another similar secondary structure (α-helix, β-strand, and coil) and solvent accessibility predictor that uses a different algorithm, namely, JNet 2.3.1 (Drozdetskiy, Cole, Procter, & Barton, 2015).
3. **PSIPRED 4**. This is a web server based on the previous version, PSIPRED, with additional architectural modifications, a neural network architecture with two hidden layers instead of one, and rectifier rather than sigmoid activations (D. W. A. Buchan & Jones, 2019).

Tertiary structure prediction was performed by running the I-TASSER (Iterative Threading ASSEmbly Refinement) server (https://zhanglab.ccmb.med.umich.edu/I-TASSER/) for the three isoforms of IL-22BP. This bioinformatic tool models the 3D structure of protein molecules from amino acid sequences. It detects structure templates from the Protein Data Bank (PDB) via a technique called fold recognition (or threading). The full-length structure models are constructed by reassembling structural fragments from threading templates using replica exchange Monte Carlo simulations (Roy, Kucukural, & Zhang, 2010). The results obtained with I-TASSER were visualized and colour-edited with PyMOL 2.3 (https://pymol.org/2/).

4.1.6 Protein disorder prediction of IL-22BPi1 isoforms

Two different computational programmes for protein disorder prediction were run for the three IL-22BP isoforms:

1. **RaptorX Property**. This web server predicts the structure properties of a protein sequence without using any template information. It outperforms other servers, especially for proteins without close homologues in the PDB or with a sparse sequence profile. This server employs an emerging machine learning model called DeepCNF (Deep Convolutional Neural Fields) to predict disorder regions in a protein sequence (S. Wang, Li, Liu, & Xu, 2016).
2. **DISOPRED3**. This software is a new version of DISOPRED, a software originally trained on the evolutionarily conserved sequence features of intrinsically disordered sequences from missing residues in high-resolution X-ray structures. DISOPRED3 extends the previous architecture with two independent predictors of intrinsic disorder: one module that combines the intermediate results and one component that annotates protein-binding intrinsically disordered regions (IDRs) (D. T. Jones & Cozzetto, 2015).

4.1.7 Protein alignment of the 32-amino-acid sequence in IL-22BPi1

The Protein Basic Local Alignment Tool (BLAST) web server (https://blast.ncbi.nlm.nih.gov/Blast.cgi) was used to compare the 32-amino-acid sequence unique in the isoform 1 of IL-22BP to different sequence databases. This software was run with the selection of the BlastP algorithm (Johnson et al., 2008).

4.2 Molecular biology techniques

4.2.1 RNA extraction

RNA was extracted from living cells with TRI Reagent (Sigma, T9424) in accordance with the manufacturer's instructions. The extraction protocol was divided into the following steps:

1. **Sample preparation**. 5-10 x 10^6 cells were homogenized with 1 mL of TRI Reagent for at least 10 minutes at room temperature (RT) to allow for complete nucleoprotein dissociation. This volume was scaled down depending on the cell number.
2. **Homogenization and phase separation**. 1 mL of homogenate was mixed with 0.1 mL of 1-bromo-3-chloropropane and shaken vigorously for 15 seconds. The mix was then allowed to stand for 15 minutes at RT, followed by centrifugation at 12,000 × g for 15 minutes at 4°C. Centrifugation separates the mixture into three phases: a red organic phase (containing protein), a white interphase (containing DNA), and a colourless upper aqueous phase (containing RNA).
3. **RNA precipitation**. The aqueous phase was then transferred to a fresh tube, and 0.5 mL of 2-propanol per mL of TRI Reagent used in step 1 was added and mixed. The mix was allowed to stand for 10 minutes at RT prior to centrifugation at 12,000 × g for 10 minutes at 4°C. In this step, the RNA precipitated, forming a pellet on the side and bottom of the tube.
4. **RNA wash**. The supernatant was removed, and the RNA pellet was washed by adding 1 mL of 75% ethanol per 1 ml of TRI Reagent used in step 1. The sample was vortexed and centrifuged at 7,500 × g for 5 minutes at 4°C.
5. **RNA solubilization**. The RNA pellet was air-dried for approximately 10 minutes. The almost completely dried RNA was then solubilized in molecular-grade water and incubated at 55°C for 15 minutes.

The concentration of RNA was determined by using a Nanodrop 2000c spectrophotometer (Thermo Scientific) at 260 nm. Apart from the concentration, the A260/A280 ratio was also calculated for each sample. Samples with ratios smaller than 1.7 or greater than 2.1 were discarded. The integrity of the RNA was confirmed by visualization of the 28S and 18S ribosomal RNA sharp bands with a 2:1 ratio (28S:18S) on Tris acetate-EDTA 1.5% (w/v) agarose gels (Agarose: Sigma, A9539) using SYBR Safe staining (Thermo Fisher Scientific, S33102). Gels were visualized with the ChemiDoc Imaging System (Bio-rad), and RNA samples were stored at -80°C if they were not immediately processed.

4.2.2 cDNA synthesis

Five hundred nanograms of the extracted RNA were reverse-transcribed to cDNA according to the manufacturer's instructions (Thermo Scientific, 4368814) in a final volume of 20 µL (the volume and the concentration of each component are indicated in Table 3). Then, 500 ng of RNA were converted to cDNA under the programme conditions described in **Table 3** on a Veriti thermocycler (Applied Biosystems). The resulting cDNA was diluted to 12.5 ng/µL with nuclease-free water and stored at -20°C for further processing.

Table 3: Components, concentrations, and settings used for cDNA synthesis:

Component	Volume (µL)	Final concentration
10X RT Buffer	2	1X
25X dNTP Mix (100 mM each)	0.8	4 mM each
10X Random Primers	2	1X
MultiScribe Reverse Transcriptase 50 U/ µL	1	2.5 U/µL
RNase inhibitors (20 U/µL)	1	10 U/ µL
RNA (500 ng)	10	25 ng/ µL
Nuclease-free H2O	to 20 µL	-

Settings	Step 1	Step 2	Step 3	Step 4
Temperature (°C)	25	37	85	4
Time (minutes)	10	120	5	∞

4.2.3 Conventional polymerase chain reaction (PCR)

PCR was carried out on a Veriti thermocycler (Applied biosystems). All PCR reactions were performed using Taq DNA polymerase (Thermo Fisher Scientific, 10342020) in the presence of dNTPs (Thermo Fisher Scientific, 10297018). Ten microliters of each cDNA product were amplified with the components, concentrations, and thermal cycling conditions indicated in **Table 4**. All primers used in this thesis are listed with references and sequences in **Table 6**.

Table 4: Components, concentrations, and settings used for conventional polymerase chain reactions.

Component	Volume (µL)	Final concentration
10X PCR Buffer	2.5	1X
$MgCl_2$ (50 mM)	0.75	1.5 mM
dNTP Mix (10 mM each)	0.5	0.2 mM each
Forward Primer (10 µM)	1.25	0.5 µM
Reverse Primer (10 µM)	1.25	0.5 µM
Taq DNA polymerase (5 U/µL)	0.2	1 U/rxn
Template DNA (12.5 ng/µL)	8	100 ng
Nuclease-free H_2O	to 25	-

Thermocycling conditions

	1 cycle	30 cycles			1 cycle
	Initiation step	**Denaturation step**	**Annealing step**	**Extension step**	**Final extension step**
Temperature (°C)	94	94	Primer Tm	72	72
Time	3 min	45 secs	45 secs	90 secs/kb	10 min

PCR products were run on 2% agarose (w/v) gels (Agarose: Sigma, A9539) in Tris acetate-EDTA buffer with SYBR Safe (Thermo Fisher Scientific, S33102) to visualize the amplicons. Gels were visualized with the ChemiDoc Imaging System (Bio-rad).

4.2.4 Quantitative PCR (qPCR)

One microliter of cDNA (corresponding to 12.5 ng of cDNA) was amplified by qPCR using primers and SYBR Green (Thermo Scientific, 4385616) DNA-intercalating dye or Taqman probes on a 7500 Fast Real Time PCR System (Applied Biosystems). The qPCR thermocycling parameters used for quantitative PCR are indicated in **Table 5**, and the primers used are summarized in **Table 6**.

Table 5: Components, concentrations, and settings used for conventional quantitative polymerase chain reactions.

		SYBR Green		Taqman probes	
		Temperature (°C)	Time (seconds)	Temperature (°C)	Time (minutes)
Cycles	1	95	20	50	2
				95	10
	40	95	3	95	15 secs
		60	30	60	1
	1	95-60-95	0.15-1-0.15	-	-

The threshold for detection was set within the linear phase of the logarithmic amplification plot, and all targets were measured in technical duplicates or triplicates. Quality negative controls were included in all runs, and melting temperatures were analysed for SYBR Green qPCRs. Furthermore, qPCR product sizes were analysed by gel electrophoresis. The levels of expression of each gene were normalized to the housekeeping genes used, as indicated, and expressed as $2^{-\Delta\Delta Ct}$ relative to the average of the control group to obtain the expression fold change.

Table 6: Sequences and references of the primers used in this thesis.

Designed SYBR Green primers (purchased from IDT)

Isoform specific	Transcripts	Sequence (5'→3')
FW IL22RA2	3 *IL22RA2* variants	5′ TGCTTTCTAGGCTTCCTCATC 3′
RV IL22RA2		5′ TGAGCCCCTTCATAAACCTT 3′
FW 1q*	*IL22RA2v1*	5′ ATTTTGCAATGGCAGCCTG 3′
RV 1q*		5′ GCCTGGGAAGTTACAAGAAATG 3′
FW 2&3q*	*IL22RA2v2*	5′ GTGCAGTACAAAATATATGGACAGA 3′
RV 2q*		5′ GAGGATCTATTTTTGTTTCCCACC 3′
RV 3q*	*IL22RA2v3*	5′ CTTTTGCTCTTTCCCACCAG 3′

*Taken from Lim, Hong, & Savan, 2016.

Designed cloning primers (purchased from IDT)

Primer name	Sequence (5'→3')
FW IL22RA2v1 cloning Fragment 1	5′ GCCGCGATCGCCATGATGCCTAAACATTGCTTTCTAG 3′
RV IL22RA2v1 cloning Fragment 1	5′ GCGTCATGCTCCATTCTGAG 3′
FW IL22RA2v1 cloning Fragment 2	5′ CATGTTCTCATGCAGCATGAAAAGCTCTCACCAGA 3′
RV IL22RA2v1 cloning Fragment 2	5′ CGTACGCGTTGGAATTTCCACACATCTCTCTTCACTTC 3′
FW IL2 cloning	5′ CATCGCTCTAGAAATGTTCTCATGCAGCATG 3′
RV IL2 cloning	5′ GACGGCTCTAGACATTTAGCCAATGTTCTGCA 3′

Site-directed mutagenesis primers (purchased from IDT)

Primer name	Sequence (5'→3')
FW IL22RA2_L16P	5′ TCATCAGTTTCTTCCCTACTGGTGTAGCAGG 3′
RV IL22RA2_ L16P	5′ CCTGCTACACCAGTAGGGAAGAAACTGATGA 3′

Other primers (purchased from IDT)

Primer name	Sequence (5'→3')
FW GAPDH	5′ CACATCGCTCAGACACCAT 3′
RV GAPDH	5′ GCAACAATATCCACTTTACCAGAG 3′
FW XBP1	5′ TTACGAGAGAAAACTCATGGCC 3′
RV XBP1	5′ GGGTCCAAGTTGTCCAGAATGC 3′

Pre-designed SYBR Green primers (purchased from IDT)

Gene	Official name	Reference
HPRT1	HPRT1	Hs.PT.58v.45621572
IL22RA2 BC (3 *IL22RA2* variants)	IL22RA2	Hs.PT.58.40811
HERP	HERPUD1	Hs.PT.58.21409911
CHOP	DDIT3	Hs.PT.58.3400360
GRP78	HSPA5	Hs.PT.58.22715160
ERP44	ERP44	Hs.PT.58.4529248
PPIB	PPIB	Hs.PT.58.40291667

Pre-designed SYBR Green primers (purchased from Qiagen)

Gene	Official name	Reference
GRP94	HSP90	QT01848273
ERDj3	DNAJB11	QT00042560
GRP170	HYOU1	QT00046214

TaqMan primers (purchased from ThermoScientific)

Gene	Official name	Reference
IL22RA2 (3 *IL22RA2* variants)	IL22RA2	Hs00364814_m1
IL12B	IL12B	Hs01011519_m1
IL6	IL6	Hs00174131_m1
ACTB	ACTB	Hs99999903_m1

4.3 Vectors and cloning

4.3.1 Vectors

IL22RA2v2 myc-FLAG tag and *IL22RA2v3*-FLAG tag plasmids were purchased from OriGene (RC219095) and GenScript (Ohu00490), respectively.

Vectors expressing C-terminal Myc-FLAG-tagged IL22RA2v2, IL-2, IL-4, IL-10, IL-17, IL-22, IFN-γ, and GRP94 were also from OriGene.

The five truncated GRP94 constructs were kindly provided by Yair Argon. These plasmids were developed by their team to investigate the

interaction site of GRP94 with OS-9 (Dersh, Jones, Eletto, Christianson, & Argon, 2014).

pCDNA3, wild-type, and mutant (T37G) GRP78 constructs came from a previous study carried out by our lab (Koen Vandenbroeck, Martens, & Alloza, 2006). Those constructs were kindly provided by Linda Hendershot (Gaut & Hendershot, 1993; J. Wei, Gaut, & Hendershot, 1995).

4.3.2 Cloning of IL22RA2v1 into pCMV6-entry vector

The cDNA coding for *IL22RA2v1* (isoform-1) was initially amplified with *Pfu* polymerase (EP0501, ThermoScientific) from two overlapping fragments with primers including terminal MluI and SgfI restriction sites starting from retrotranscribed RNA extracted from immature moDCs.

The reaction components and concentrations, as well as the thermocycling conditions for the reactions performed with the *Pfu* enzyme, are indicated in **Table 7**.

Table 7: Components, concentrations, and settings used for Pfu polymerase chain reactions.

Component	Volume (µL)	Final concentration
10X Pfu Buffer with $MgSO_4$	5	1X
dNTP Mix (2 mM each)	5	0.2 mM each
Forward Primer (10 µM)	1	0.5 µM
Reverse Primer (10 µM)	1	0.5 µM
Pfu DNA polymerase (2.5 U/µL)	0.8	2 U/rxn
Template DNA (12.5 ng/µL)	5	-
Nuclease-free H_2O	to 50	-

	Thermocycling conditions				
	1 cycle	**35 cycles**			**1 cycle**
	Initiation step	**Denaturation step**	**Annealing step**	**Extension step**	**Final extension step**
Temperature (°C)	95	95	Tm-5	72	72
Time	3 min	30 secs	30 secs	2 min/kb	10 min

Overlapping fragments were run on 2% low-melting agarose gels, and the band corresponding to the desired DNA size was excised with a clean scalpel and extracted with the GeneJET gel extraction and a DNA Clean-up Micro kit (K0831, ThermoScientific) following the DNA extraction-from-gel protocol provided with the kit. DNA was quantified by using a Nanodrop 2000c spectrophotometer (Thermo Scientific). Equimolar isolated and clean overlapping fragments were overlapped and extended by overlap extension PCR. The annealing temperature was set at 65.9°C, and the PCR reaction was carried out for 25 cycles without primers because templates primed one another. The components are described in **Table 8**.

Table 8: Components, concentrations, and settings used for overlap extension polymerase chain reactions.

Component	Volume (µL)	Final concentration
10X Pfu Buffer with $MgSO_4$	1.5	1X
dNTP Mix (2 mM each)	1.5	0.2 mM each
FRAGMENT 1 601 bp (100 ng)	1	0.16 ng/bp
FRAGMENT 2 418 bp (69.55 ng)	1	0.16 ng/bp
Pfu DNA polymerase (2.5 U/µL)	0.8	2 U/rxn
Nuclease-free H_2O	to 15	-

Thermocycling conditions					
	1 cycle	**25 cycles**			**1 cycle**
	Initiation step	**Denaturation step**	**Annealing step**	**Extension step**	**Final extension step**
Temperature (°C)	95	95	65.9	72	72
Time	3 min	30 secs	30 secs	2 min/kb	10 min

The whole PCR product was then amplified with primers that annealed at the beginning and end of the overlapped product. The concentrations and the PCR conditions are indicated in **Table 9**. The concentrations of the dNTPs and Buffer already present in the template were considered for the reaction final concentrations.

Table 9: Components, concentrations and settings used for amplification of the overlapping PCR product.

Component	**Volume (µL)**	**Final concentration**
10X Pfu Buffer with $MgSO_4$	3.5	1X
dNTP Mix (2 mM each)	3.5	0.2 mM each
Primer FW 1 (10 µM)	1	0.5 µM
Primer RV 2 (10 µM)	1	0.5 µM
Template (overlapped fragment)	15	-
Pfu DNA polymerase (2.5 U/µL)	0.5	2 U/rxn
Nuclease-free H_2O	to 50	-

Thermocycling conditions					
	1 cycle	**20 cycles**			**1 cycle**
	Initiation step	**Denaturation step**	**Annealing step**	**Extension step**	**Final extension step**
Temperature (°C)	95	95	60	72	72
Time	3 min	30 secs	30 secs	2 min/kb	10 min

The PCR product was run on low-melting agarose gel (2%), and the corresponding band was excised and purified with GeneJET gel extraction and a DNA Clean-up Micro kit (K0831, ThermoScientific). Purified DNA was quantified by using a Nanodrop 2000c spectrophotometer (Thermo Scientific), and purified fragments were sent for sequencing to StabVida laboratories (https://www.stabvida.com/sanger-sequencing-service) with their corresponding primers. Sequenced results were analysed with CLUSTAL O (1.2.2) multiple sequence alignment (https://www.ebi.ac.uk/Tools/msa/clustalo/) to check homology with the desired sequence. Only 100% correct products were used.

Products with correct sequences and pCMV6-entry vector (PS100001, OriGene) were double digested with MluI (R0198S, New England Biolabs) and SgfI (R0630S, New England Biolabs) restriction enzymes following the concentrations listed in **Table 10** for 15 minutes at 37°C. A small portion of digested and non-digested products was run on agarose gels to check the enzymatic digestion, and the rest was purified with a GeneJET gel DNA Clean-up Micro kit (K0831, ThermoScientific) following the protocol provided with the kit.

Table 10: Components and concentrations used for plasmid and insert enzymatic digestions.

Component	Volume (µL)	Final concentration
Buffer 3.1 10X	5	1X
MluI (10,000 U/mL)	1	10 U/rxn
SgfI (10,000 U/mL)	1	10 U/rxn
Insert or Plasmid	x	500 ng for insert or 1 µg for plasmid
Nuclease-free H_2O	To 50	-

Finally, different double-digested plasmid:insert molar ratios (1:0, 1:3, 1:6, and 1:9) were ligated with T4 DNA ligase (M0202S, New England Biolabs) and left o/n at 16°C following the manufacturer's instructions.

Ligation products were transformed into DH5α cells as described in Section 0. The resulting construct was sequenced to confirm the cloning of *IL22RA2v1*.

4.3.3 Subcloning of *IL22RA2v2* into TET-express system.

The multiple cloning site of pTRE3G-BI-mCherry vector (Clontech, 631333) was modified by including the following sequence via overlapping oligo PCR: BamHI-MluI-BspEI-FLAG-Stop-Stop-EaglI. Overlapping conditions were similar to those described in section 4.3,2 p.98. The *IL22RA2v2* sequence was amplified from the original PCMV6-entry vector (OriGene RC219095) with *Pfu* polymerase, digested with BglII and MluI, and cloned into the modified pTRE3G vector. The reaction components and concentrations, as well as the thermocycling conditions for the reactions performed with the *Pfu* enzyme, are indicated in **Table 7**.

4.3.4 Site-directed mutagenesis

The L16P mutants of IL-22BPi1, 2, and 3 were generated using the GENEART® site-directed mutagenesis system (A13282, Invitrogen) from the *IL22RA2v1*, 2, and 3 expression plasmids following the manufacturer's instructions. This protocol is based on an initial methylation of plasmid DNA, followed by an amplification of the plasmid with two complementary mutagenic oligonucleotide predesigned primers (**Table 6**) with centrally located L16P mutation sites; the DNA methylation and amplification steps were combined in a single reaction. The PCR components and thermocycling conditions used are presented in **Table 11**. The PCR product was then *in vitro* recombined to boost the mutagenesis efficiency and increase the colony yield; the recombination reaction components used are indicated in **Table 12**. The recombination reaction was mixed and incubated at RT for 10 minutes, and the reaction was then stopped by the addition of 1 µL of 0.5 M EDTA.

Table 11: Components, concentrations, and conditions used for methylation and amplification steps.

Component	Volume (µL)	Final concentration
10X Pfu Buffer	5	1X
10X Enhancer	5	1x
Primer FW (10 µM)	1.5	0.3 µM
Primer RV (10 µM)	1.5	0.3 µM
Plasmid DNA (20 ng/µL)	2	40 ng
DNA Methylase (4 U/µL)	1	4 units
25X SAM	2	1X
Pfu DNA pol. (2.5 U/µL)	0.4	1 U/rxn
Nuclease-free H_2O	to 50	

Thermocycling conditions

	1 cycle		**18 cycles**			**1 cycle**
	Methylation and initiation steps		**Denaturation step**	**Annealing step**	**Extension step**	**Final extension step**
Temperature (°C)	37	94	94	57	72	72
Time	**20 min**	**45 secs**	**45 secs**	**45 secs**	**6 min**	10 min

Table 12: Components, concentrations, and conditions used for methylation and amplification steps.

Component	Volume (µL)	Final concentration
5X Reaction Buffer	4	1X
PCR sample	4	
10X Enzyme mix	2	1X
Nuclease-free H_2O	to 20	

Ligation products were transformed into DH5α-T1 cells as described in the following section (0). This strain circularizes the linear mutated DNA, and the *Mcr*BC endonuclease in the host cell digests the methylated template DNA, leaving only unmethylated mutated product. The resulting constructs were sequenced to confirm the point mutations of *IL22RA2* variant constructs.

4.3.5 Bacterial transformation

The chemically competent DH5α cells (18263-012, Invitrogen) or DH5α-T1 cells (supplied with the GENEART Site-Directed Mutagenesis kit) were used to amplify the plasmid DNA for subsequent extraction and purification. Bacterial transformation for site-directed mutagenesis products was done following the manufacturer's instructions and are indicated in brackets in the following general transformation protocol. For the rest of the transformations, 100 µL [50 µL] of competent cells were thawed on ice and mixed with 1 µL of plasmid DNA containing 1-10 ng [2 µL] of site-directed mutagenesis product. Tubes were swirled gently and incubated on ice for 30 minutes [12 minutes]. After incubation, cells were heat-shocked in a 42°C thermo-block for 45 seconds [30 seconds] and then immediately transferred to ice for 2 minutes. Then, 900 µL [250 µL] of the S.O.C. medium was added to the cells and incubated at 37°C for 1 hour with shaking at 225 rpm. Thereafter, 100–200 µL [20 µL of the transformation mixture + 80 µL S.O.C.] of the transformation mixtures were plated on LB agar plates containing the appropriate antibiotic and incubated inverted overnight at 37°C. The culture plates were examined the next day for colony formation.

4.3.6 Plasmid preparations

4.3.6.1 Growth of transformants for plasmid mini preparations to select clones

To check for successful ligations by sequencing and enzyme digestion, a GeneJET Plasmid Miniprep kit (K0502, ThermoScientific) was used.

Single colonies were picked from freshly streaked selective plates to inoculate 1–5 mL of LB medium supplemented with the appropriate selection antibiotic. Inoculums were incubated for 12–16 hours at 37°C while shaking at 300 rpm. After that time, an aliquot of 500 µL of the bacteria culture was mixed with 500 µL of 50% glycerol and gently mixed. Bacterial glycerol stocks were frozen at -80°C for long-term storage of plasmids and for higher plasmid preparations. The rest of the bacterial culture was harvested by centrifugation at 6,800 x g for 2 minutes at RT. Supernatants were discarded, and 250 µL of Resuspension Solution were added and vortexed. Then, 250 µL of Lysis Solution were added, and the tube was thoroughly mixed by inverting the tube six times. The lysis was stopped by mixing after the addition of 350 µL of the Neutralization Solution. Chromosomal DNA and cell debris were pelleted by centrifugation at 12,000 x g for 5 minutes. Supernatants were transferred to spin columns and centrifuged for 1 minute at 12,000 x g. Columns were washed twice with 500 µL of the Wash Solution. Finally, 50 µL of Elution Buffer were added to the column and centrifuged for 2 minutes at 12,000 x g to elute the Purified DNA. The concentration of the DNA was determined using a Nanodrop 2000c spectrophotometer (Thermo Scientific). Sanger sequencing was performed by StabVida laboratories (https://www.stabvida.com/sanger-sequencing-service). Moreover, digestion with BamHI (R3136, New England Biolabs) and Xho (R0146S, New England Biolabs) enzymes was done to verify the *IL22RA2* variant 1 insertion into pCMV6 vector. Selected clones were then used for plasmid maxi preparations.

4.3.6.2 Growth of transformants for plasmid maxi preparations

Plasmid preparations for cell transfection were done using the Qiagen plasmid Maxiprep kit (12162, Qiagen) following the manufacturer's instructions. The principle was similar to that described before for the miniprep, the difference being that the plasmid DNA was eluted in a high-salt buffer and then concentrated and desalted by 2-propanol precipitation. For plasmid maxipreps, single colonies were obtained from freshly streaked agar plates from glycerol stocks. Colonies were

inoculated to a starter culture of 2–5 mL LB medium supplemented with the appropriate selection antibiotic. Inoculums were incubated for 8 hours at 37°C while shaking at 300 rpm. After that time, the starter culture was diluted 1/1,000 (final volume 250 mL) into selective LB medium and incubated for a further 12–16 hours at 37°C while shaking at 300 rpm. Bacterial cells were harvested by centrifugation at 6,800 x g for 15 minutes at 4°C. Pellets were then resuspended in 10 mL of resuspension Buffer. Thereafter, 10 mL of lysis buffer were added, and the tube was thoroughly mixed by inverting it six times following an incubation at RT for 5 minutes. The lysis was stopped by mixing after the addition of 10 mL of chilled neutralization buffer. To remove chromosomal DNA and cell debris, the mixture was poured into a Qiagen cartridge and incubated at RT for 10 minutes before filtration. Then, 2.5 mL of ER buffer were added to the filtrated lysate and mixed by inverting the tube 10 times, followed by an incubation on ice for 30 minutes. This mixture was then applied to QIAGEN-tip 500 and allowed to drain, and two washes with 30 mL of washing buffer were performed before DNA elution with 15 mL of elution buffer. This eluted fraction was precipitated with the addition and mix of 10.5 mL of 2-propanol, immediately followed by centrifugation at 15,000 x g for 30 minutes at 4°C. DNA pellets were carefully washed with 5 mL of endotoxin-free 70% ethanol and centrifuged at 15,000 x g for 10 minutes. Supernatants were discarded, and DNA pellets were air-dried for 10 minutes. The DNA plasmids were redissolved in 1 mL of endotoxin-free buffer TE, and dNA concentration was determined using a Nanodrop 2000c spectrophotometer (Thermo Scientific) at 260 nm. Moreover, plasmid digestion with restriction enzymes and analysis on agarose gels was also performed. The DNA plasmids were aliquoted and stored at -20°C.

4.4 Cell culture techniques

4.4.1 Cell maintenance

All cell lines were cultured in their corresponding cell culture media supplemented with 10% foetal bovine serum (FBS) and 2 mM L-glutamine (G7513, Sigma). **Table 13** provides information about the media and supplements used for each cell line. Cells were routinely checked under the microscope on a daily basis to ensure that they were healthy and growing, and the culture media were changed every 2 days. Cell passage (split) for adherent cells was done when they reached approximately 80% confluence (80% of the surface of the flask was covered by the cell monolayer). The density of cells grown in suspension was maintained between 1 x 10^5 and 2 x 10^6 viable cells/mL.

Table 13: Culture media, supplements and conditions employed for the cell lines used.

Cell line	Media	Supplements	Subculture
HEK293	DMEM	10% FBS 2 mM L-glutamine	Cell density was maintained between 6 x 10^4 and 7 x 10^4 cells/cm^2
HeLa	DMEM	10% FBS 2 mM L-glutamine	Cell density was maintained between 6 x 10^4 and 7 x 10^4 cells/cm^2
U937	RPMI	0.05 mM β-mercaptoethanol, 10% FBS and 2 mM L-glutamine	Cell density was maintained between 1 x 10^5 and 2 x 10^6 viable cells/mL.

4.4.2 Cell cryopreservation and thawing

All cell lines were permanently stored in liquid nitrogen to keep the cell line at early passages. To freeze them, adherent cells from one confluent T-75 flask at early passages were washed twice with PBS and trypsinized to detach them. Trypsinization was stopped with media containing 10% FBS, and the cell suspension was spun down at 300 x g for 5 minutes at RT. Supernatant medium was removed, and cells were resuspended in 2 mL of freezing medium – 10% (v/v) DMSO plus 10% FBS in culture medium – and aliquoted into two polypropylene cryovials (1 mL each).

These cryovials were immediately placed in a freezing vessel primed with 250 ml of 2-propanol and stored at -80°C overnight, where they were slowly frozen at a rate of 1°C min^{-1}. Finally, the cryovials were transferred to the gas phase of a liquid nitrogen vessel (-180°C) for permanent storage.

To thaw frozen cells, the cryovials of cells stored in liquid nitrogen were immediately placed in a 37°C water bath and quickly shaken until roughly 80% was thawed. The vials were then removed from the water bath, and the cells were transferred into a 15-mL tube containing 10 mL of complete culture medium and centrifuged at 300 x g for 5 minutes. Supernatant was discarded, and the cell pellet was resuspended in complete medium. The cell suspension was seeded in a T-75 flask, and after 24 hours, the culture media were changed. Cells were cultured at least one week after thawing prior to any experiment.

4.4.3 Monocyte-derived dendritic cells (moDCs)

Buffy coats were obtained from healthy donors from the Basque Biobank (http://www.biobancovasco.org/en/) with the approval of the Ethics Committee of Clinical Investigation of the Basque Country (CEIC-E) based on the provision of a detailed study protocol. PBMCs were separated through Ficoll-Paque (GE Healthcare) gradient centrifugation. Monocytes were isolated from PBMCs by CD14 positive selection using MACS CD14 microbeads (Miltentyi, 130- 050-201). To differentiate isolated monocytes into immature moDCs, monocytes were cultured at 1×10^6 cells/ml density in Mo-DC medium, which is a commercially available (Miltenyi, 130-094-812), moDC differentiation medium (DM) is based on RPMI 1640 medium containing FBS, L-glutamine, IL-4, and granulocyte-macrophage colony-stimulating factor (GM-CSF) for 6 days or as indicated, and an equal volume of fresh Mo-DC medium was added on day 3. Maturation of moDCs was induced by adding IFN-γ (Peprotech, AF-300-02; 500 pg/ ml) for overnight priming (16 hours), followed by late addition of LPS for 6 hours (Sigma, L6143; 2 μg/ml) to the culture or, alternatively, by the addition of CpG (Miltenyi, 130-100-

243; 1 μg/ml) or LPS/Poly(I:C) (Sigma, P1530; 1 μg/ml) for 6 hours. HEK293, HeLa, and A549 were cultured in DMEM supplemented with 10% FBS and 2 mM L-glutamine.

4.5 Protein overexpression and detection

4.5.1 Transient transfection

Plasmid DNA transient transfection of cells was performed with MACSfectin Reagent (Miltenyi, 130-098-411). This reagent is based on cationic lipopolyamines that optimize nucleic acid condensation and cellular uptake. Cells were plated 24 hours before transfection in an appropriate cell culture vessel in complete medium, including serum and supplements. Cells were >60% confluent on the day of transfection. The amount of Plasmid DNA transfected was calculated according to the vessel used (**Table 14**).

Table 14: Proportions of DNA and transfection reagent used for cell transfection.

Culture vessel	DNA (μg)	Final volume of DNA diluted in SFM medium (μL)	MACSfectin Reagent (μL)	Final volume of diluted MACSfectin Reagent in SFM medium (μL)	Cell culture volume (mL)
24-well plate	1	50	2	50	0.5
12-well plate	2	50	4	50	1
6-well plate	3	100	6	100	2
T75 flask	20	350	40	350	10

The steps followed for transfection are listed below:

-The corresponding volume of MACSfectin reagent was added to one tube containing serum-free medium (SFM) and supplements to a specific final volume depending on the culture vessel.

-The corresponding DNA quantity was added to another tube containing a medium without serum and supplements to a specific final volume depending on the culture vessel.

-An equal volume of the diluted DNA solution was added to the diluted MACSfectin Reagent solution and mixed by pipetting up and down 3–5 times. This mix was incubated for exactly 20 minutes at RT to allow for transfection complex formation.

-Cells were collected from the incubator and placed in the laminar flow cabinet. The mix was dropwise added to the cells and mixed by rocking the plate gently side to side to ensure uniform distribution. Cells were immediately returned to standard culture conditions and left untouched for at least 24 hours.

In the experiments where two plasmids were co-expressed, the transfection protocol was exactly the same as described above, with the exception that half of the total DNA quantity indicated in **Table 14** as used for each construct.

4.5.2 Drug treatment

All drugs were added to the cell cultures 24 hours after transfection. Cyclosporine A (CsA; 30024, Sigma) was added at 10 μg/mL, and 17-allylamino-17-demethoxygeldanamycin (17-AAG), 17-dimethylaminoethylamino-17-demethoxygeldanamyin (17-DMAG), and geldanamycin (GA) (ant-agl-5, ant-dgl-5 and ant-gl, Invivogen, San Diego, CA, USA) were added at either 1 or 5 μM in complete culture medium for 4 hours. The medium was then removed, and cells were carefully washed five times with complete culture medium to remove any remaining secreted IL-22BP isoforms produced prior to drug treatment. Thereafter, the new, complete culture medium containing CsA, 17-AAG, 17-DMAG, or GA was added, and cells were incubated for the indicated times.

4.5.3 Protein extraction from cells and conditioned media (CMs) collection

Cultured cells were collected at the indicated times in their conditioned media (CMs). Cells were centrifuged at 300 x g for 5 minutes at RT, and supernatants (CMs) were further processed or stored in the presence of a protease inhibitors cocktail (11697498001, Roche) at -20°C. Cells were then washed three times with cold PBS before the addition of lysis buffer (300 mM NaCl, 50 Mm NaH_2PO_4 pH 8, 1% Triton X-100) or RIPA buffer (25 mM Tris/HCl 150 mM NaCl, pH 7.6, 1% NP - 40, 1% sodium deoxycholate, 0.1% SDS) as indicated, both containing the protease inhibitors cocktail. Cell lysis was done for 30 minutes on ice, followed by centrifugation at 21,000 × g at 4°C. Protein fraction was then collected from the supernatants and immediately processed or stored at −80°C for further analysis.

4.5.4 Cell fractionation

Cell fractionation was carried out according to the protocol developed by Holden and Horton (Holden & Horton, 2009). This procedure sequentially extracts proteins from cultured mammalian cells in fractions enriched for cytosolic, membrane-bound organellar, nuclear, and insoluble proteins. Each subcellular fraction was obtained after sequential exposure to buffers of increasing stringency. The composition of buffers, the incubation times, and the centrifugation conditions are listed in **Table 15**. The subcellular fractions corresponded to the supernatant fraction after each centrifugation step. The pellets obtained after each centrifugation step were washed twice with PBS before the next fractionation step.

Table 15: Cell fractionation components and conditions.

Fraction	Buffer	Composition	Incubation conditions	Centrifugation
Cytosolic	Digitonin Buffer	150 mM NaCl 50 mM HEPES pH 7.4 25 μg/ml digitonin (SIGMA #D141)	On ice 10 min	2,000 x g 10 min
Membranous Organelles	NP40 Buffer	150 mM NaCl 50 mM HEPES pH 7.4 1% NP40	On ice 30 min	7,000 x g 10 min
Nuclear Membrane	RIPA Buffer	50 mM NaCl 50 mM HEPES pH 7.4 0.5% Sodium Deoxycholate 0.1% Sodium Dodecyl Sulphate (SDS) Benzonase (SIGMA# E1014) (1 U/ml) added just before use	On ice 1 h	7,000 x g 10 min
Insoluble Proteins	E-RIPA Extraction Buffer	150 mM NaCl 50 mM HEPES pH 7.4 0.5% Sodium Deoxycholate 1% Sodium Dodecyl Sulphate (SDS) 100 mM Dithiothreitol (DTT)	Vortex 30 secs Boil 15 min	12,000 x g 10 min

4.5.5 Protein quantification

Protein concentrations were determined using Bradford (Bio-Rad, 5000006) or BCA (Bio- Rad, 23225) colorimetric assays following the manufacturer's instructions. In all cases, dilution series from a known protein concentration were included to perform standard curves, and absorbance was measured with Varioskan Flash (Thermo Fisher Scientific) at 562 nm.

4.5.6 Acetone precipitation of secreted fractions

For acetone precipitation of CMs, cells were carefully washed five times with prewarmed SFM (12-764Q, Lonza, Basel, Switzerland) to remove abundant serum proteins, and fresh SFM containing L-glutamine (G5792, Sigma) was added for a further 4 hours prior to acetone precipitation and harvesting of cells for lysis. CMs were acetone-precipitated with four volumes of ice-cold acetone and incubated on ice for 10 minutes, followed

by centrifugation at 21,000 x g at 4°C. Pellets were resuspended in deglycosylation or SDS-PAGE reducing loading buffer.

4.5.7 Protein deglycosylation

Deglycosylations were performed using Endoglycosidase H (Endo H; New England Biolabs, P0702s) and Peptide:N-glycosidase F (PNGaseF; New England Biolabs, P0704s) enzymes. Equal protein concentrations of both cell lysates (CL) and acetone precipitates (APs) were subjected to enzymatic deglycosylation following the manufacturer's instructions under both denaturing and non-denaturing conditions.

4.5.8 Protein immuno-/affinity purification

Three different purification resins were used depending on the protein of interest. Anti-FLAG resin (GenScript, L00432), anti-c-Myc resin (Sigma, E6654), and S-protein agarose (Millipore, 69704) were used following the manufacturer's instructions. All purifications were performed overnight at 4°C on a rotating wheel. After incubation, resin was washed six times with washing buffer containing 50 mM Tris-HCl and 150 mM NaCl, with the pH adjusted to 7.4 and supplemented with 0.1% Tween 20. IL-22BP isoform complexes were eluted using acidic elution buffer (0.1 M glycine, 0.15 M NaCl, and 0.5% SDS pH 2). Elution buffer was then added to the resin, and samples were incubated for 5 minutes at RT with gentle mixing. The resins were then centrifuged at 300 × g for 2 minutes, and supernatants were carefully collected, avoiding the resin absorption, and the pH was adjusted by adding 1:10 of 1 M Tris pH 10.

4.5.9 IL-22BP isoforms interactome analysis

Isoform interactome analysis was done in collaboration with the CIC BioGUNE proteomics platform headed by Dr. Felix Elortza. Protein interactomes of IL-22BP isoforms were purified by anti-FLAG affinity chromatography as described above, and eluted fractions were resolved on 10% precast SDS-PAGE gels (Bio- Rad, 4561034). Gels were silver stained following the manufacturer's protocol (Thermo Fisher Scientific,

24612) and washed, and the gel bands were sliced. Each band was digested with trypsin following a standard in-gel digestion protocol based on Shevchenko et al. (Shevchenko, Wilm, Vorm, & Mann, 1996) with minor modifications. The resulting peptides were resuspended in 0.1% formic acid, separated using online NanoLC, and analysed using electrospray tandem mass spectrometry. Peptide separation was performed on a nanoACQUITY UPLC system connected to a SYNAPT G2-Si spectrometer (Waters, Milford, MA, USA). Samples were loaded onto a Symmetry 300 C18 UPLC Trap column of 5, 180 μm × 20 mm (Waters, Milford, MA, USA), connected to a BEH130 C18 column of 1.7, 75 μm × 200 mm (Waters, Milford, MA, USA). The column was equilibrated in 3% acetonitrile and 0.1% FA. Peptides were eluted at 300 nL min^{-1} using a 60-minute linear gradient of 3–50% acetonitrile. A SYNAPT G2-Si ESI Q-Mobility-TOF spectrometer (Waters, Milford, MA, USA) equipped with an ion-mobility chamber (T-Wave-IMS) for high-definition data acquisition analyses was used for the analysis of the peptides. All analyses were performed using electrospray ionization in a positive ion mode. Data were post-acquisition lock-mass corrected using the double-charged monoisotopic ion of [Glu1]-fibrinopeptide B. Accurate LC-MS data were collected in HDDA mode, which enhances signal intensities using the ion mobility separation. Mascot searching engine (MatrixScience) against Uniprot/SwissProt human database was performed.

4.5.10 Western blot

Equal quantities of CLs, volumes of eluted fractions, or CMs were loaded on SDS-PAGE gels (10% or 12%) and transferred to PVDF membranes for immunoblotting. Blots were blocked with 2% casein o/n at 4°C and subsequently incubated with primary antibodies o/n at 4°C. Blots were then washed with TBST buffer three times for 10 minutes each, and HRP-conjugated secondary antibodies were incubated for 1 hour. Immunoreactivity was assessed using a chemiluminescence substrate (Bio-Rad, 1705061) and measured using a ChemiDoc Imaging System

(Bio-Rad). Densitometry values were normalized to a control-loading protein or to the Ponceau staining using Image Lab Software (Bio-Rad).

4.5.11 ELISA

An in-house ELISA was developed for sensitive IL-22BP detection. High binding ELISA plates (Sarstedt, 82.1581.200) were coated with 100 µl of 0.5 µg/ml antigen-purified goat polyclonal IL-22BP antibody (R&D systems, AF1087; the immunogen used was recombinant human IL-22BP Thr22- Pro231 coinciding with mature IL-22BPi2) in coating solution (50 mM Tris/HCl, 150 mM NaCl, pH 8.5) and incubated o/n at 4°C. The next day, the coating mix was removed, followed by three washings steps with 200 µl of washing solution (50 mM Tris/HCl, 150 mM NaCl, 0.05% Tween 20, pH 7,4) each; 200 µl of blocking solution (50 mM Tris/HCl, 150 mM NaCl, 0.1% casein, pH 7,4) was added to the wells and incubated o/n at 4°C. Thereafter, the blocking solution was removed, followed by three washings with 200 µl of washing solution each. Semilog dilutions of biosamples were added to the plate (100 µl each) prediluted 1:10 in assay buffer (50 mM Tris/HCl, 150 mM NaCl, 0.1% casein, 0.05% Tween 20, pH 7,4), with recombinant IL-22BP human protein-His tag (Sino biologicals, 11025-H08H) used as standard. The samples and standard were incubated for 2 hours at 37°C. Samples were then removed, and the wells were washed six times with 200 µl of washing solution each. Antigen-purified goat polyclonal IL-22BP biotinylated antibody (R&D Systems, BAF1087) was added to each well in assay buffer at 0.5 µg/ml dilution and incubated for 1 hour at 37°C, followed by six washings. Biotinylated detection was performed with streptavidin conjugated to horseradish peroxidase (R&D systems, DY998) diluted in assay buffer 1:200 for a 1-hour incubation time at 37°C. Streptavidin-HRP mixture was then removed, and the plates were washed six times. ELISA was developed with 95 µl of TMB substrate solution (Thermo Scientific, 34028) in a 30-minute incubation period. The reaction was stopped with 95 µl of 2 M H2SO4, and absorbance was read at 450 nm using Varioskan Flash (Thermo Scientific). Preliminary experiments demonstrated that the

AF1087 or BAF1087 antibodies detected each of the three IL-22BP isoforms in Western blot in the CMs of individually transfected cells.

4.5.12 Flow cytometry

HEK293 cells were transfected with the indicated expression vectors 24 hours prior to collection. At that time, cells were washed twice with flow cytometry buffer (FC Buffer; PBS, 0.5% BSA, and 2 mM EDTA, pH 7.2) before immunostaining. Single cell suspensions were fixed with 4% paraformaldehyde for 10 minutes at RT, followed by permeabilization with 90% of ice-cold methanol for 30 minutes at 4C°. Cells were blocked with 1% BSA for 15 minutes at RT, incubated with anti-IL-22BP primary antibody (1:250; 66190, Proteintech) for 30 minutes at RT, and followed by another 30-minute incubation period with anti-mouse-FITC conjugated secondary antibody (1:500; AMI4608, ThermoFisher) protected from light. Two washes were performed after each step with FC buffer. A centrifugation at 300 x g for 5 minutes at RT was performed after each single step, including washes. Immunostained cells were analysed using a MACSQuant Analyzer (Miltenyi).

Antibodies used for Western blotting, ELISA, and flow cytometry

The primary antibodies were anti-FLAG (Rb, Proteintech; 20543-1-AP; 1:1,000, & Ms, Sigma; F1804; 1:1,000), anti-GRP94 (Rt, Enzo; ADI-SPA-850; 1:1,000), anti-IL-22BP(**1**) (Ms, Proteintech; 66190; 1:1,000), anti-IL-22BP(**2**) (Rb, Abcam; ab133965; 1:1,000), anti-IL-22BP(**3**) (Ms, Abcam; ab90937; 1:1,000), anti-IL-22BP(**4**) (Gt, R&D Systems; AF1087 and BAF1087; 1:1,000 each), anti-pSTAT3 (Rb, R&D Systems; AF4607; 1:1,000), anti-actin (Rb, Sigma-Aldrich; A2066; 1:100), anti-tubulin (Ms, GenScript; A01490; 1:1,000), anti-GAPDH (Ms, Millipore; ABS16; 1:2,000), anti-GRP78 (Gt, R&D Systems; AF4846; 1:1,000), anti-GRP170 (Ms, IBL; 10301; 1:100), anti-CNX (Rb, Enzo; ADI-SPA-860; 1:1,000), anti-ERdj3 (Rb, Proteintech; 15484-1-AP; 1:1,000), anti- KDEL (Ms, Enzo; ADI-SPA-827; 1:1,000), anti-histone H3 (Rb, Cell Signalling; 4499; 1:2,000), and anti-PPIB (Rb, Abcam; 16045; 1:500). All HRP-conjugated secondary antibodies were purchased from Jackson ImmunoResearch.

4.6 IL-22 bioassay

IL22BPi1, IL22BPi2, and IL-22 were independently transfected into HEK293 as previously mentioned. After 24 hours, secreted fractions of IL22BPi1 and IL22BPi2 were quantified by ELISA. Different dilutions and exposure times of IL-22 contained in the CMs were assessed to A549 to establish the optimal time and dose response of STAT3 phosphorylation, which was measured by Western blot via detection of the pSTAT3 form. IL-22 CMs were aliquoted and stored frozen at -80°C to always use the same batch. Equal amounts of IL22BPi1 or IL22BPi2 were mixed with the selected volume of IL-22 and filled to the same final volume with CMs. The mixture was incubated at 37°C for 1 hour prior to being added to A549. After the exposure time, the A549 protein fraction was extracted and analysed by immunoblotting.

4.7 *In silico* analysis of the effect of the Leu-to-Pro transition coded by rs28385692

To functionally estimate the neutral or deleterious functional effect of L16P mutation (rs28385692) in the SP of IL-22BP isoforms, three different consensus tools, based on the integration of various tools, were used. They were the **PredictSNP** web server (https://loschmidt.chemi.muni.cz/predictsnp1/) (Bendl et al., 2014), **Meta-SNP** (http://snps.biofold.org/meta-snp/) (Emidio Capriotti, Altman, & Bromberg, 2013), and the **Ensembl VEP tool** (http://www.ensembl.org/Homo_sapiens/Variation/Mappings?db=core;r=6:137161203-137162203;v=rs28385692;vdb=variation;vf=104559210#ENST00000296980_104559210_G_tablePanel) (Cunningham et al., 2019; McLaren et al., 2016).

Additionally, eight other predictors were run to predict structural modifications in the SP (cleavage site) introduced by the L16P mutation. These tools were as follows:

1. **SignalP 3.0**. This server predicts the presence and location of SP cleavage sites in amino acid sequences. The method incorporates a prediction of cleavage sites and an SP / non-SP prediction based on a combination of several ANNs and HMMs (http://www.cbs.dtu.dk/services/SignalP-3.0/, Bendtsen, Nielsen, von Heijne, & Brunak, 2004).

2. **Phobius**. This is an HMM that combines TM topology and SP predictions. The method makes an optimal choice between TM segments and SPs, and it allows for constrained and homology-enriched predictions (http://phobius.sbc.su.se/instructions.html, Kall, Krogh, & Sonnhammer, 2007).

3. **PsiPred v 3.3**. This method normalizes the sequence profile generated by PSI-BLAST (Position-Specific Iterated BLAST). Then, by using neural networking, the initial secondary structure is predicted (http://bioinf.cs.ucl.ac.uk/psipred.html, D. W. A. A. Buchan, Minneci, Nugent, Bryson, & Jones, 2013).

4. **SignalP 5.0**. This is a deep neural network-based method combined with conditional random field classification and optimized transfer learning (http://www.cbs.dtu.dk/services/SignalP/, Almagro Armenteros et al., 2019).

5. **PrediSi**. This method is based on a position weight matrix approach improved by a frequency correction that takes into consideration the amino acid bias present in proteins. The software was trained using sequences extracted from the most recent version of the SwissProt database (http://www.predisi.de/, Hiller, Grote, Scheer, Munch, & Jahn, 2004).

6. **Signal-3Lv2.0**. This is an SP predictor that uses a hierarchical mixture model based on three layers: (1) discrimination of SP and TMH proteins from the other globular proteins, (2) recognition of SP proteins from TMH proteins, and (3) identification of the cleavage sites of SP proteins

(http://www.csbio.sjtu.edu.cn/bioinf/Signal-3Lv1/, Zhang & Shen, 2017).

7. **RaptorX Property**. This was previously described in Section 4.1.6 (S. Wang et al., 2016).
8. **POLYVIEW 2D-SABLE**. This was previously described in Section 4.1.5, p. 90 (Adamczak et al., 2004).

4. Results

5 Results

5.1 *In silico* protein sequence analysis of IL-22BP isoforms

By alternative splicing, the human *IL22RA2* gene can produce three transcript variants (*IL22RA2v1*, *IL22RA2v2*, and *IL22RA2v3*), which encode three protein isoforms (IL-22BPi1, IL-22BPi2, and IL-22BPi3) (Dumoutier, Lejeune, et al., 2001; Kotenko et al., 2001a; Wenfeng Xu et al., 2001). Only two of these – IL-22BPi2 and IL-22BPi3 – have been described as being capable of neutralizing the biological activity of IL-22 (Dumoutier, Lejeune, et al., 2001; Kotenko et al., 2001a; Lim et al., 2016; C.-C. Wei et al., 2003; Weiss et al., 2004; Wenfeng Xu et al., 2001). The function of IL-22BPi1, which differs from IL-22BPi2 through an in-frame 32-amino-acid insertion at position 67 (**Figure 21**) provided by an alternatively spliced exon, remains unknown.

```
CLUSTAL O(1.2.4) multiple sequence alignment

SP|Q969J5|I22RA2i1_HUMAN      MMPKHCFLGFLISFFLTGVAGTQSTHESLKPQRVQFQSRNFHNILQWQPGRALTGNSSVY 60
SP|Q969J5-2|I22RA2i2_HUMAN    MMPKHCFLGFLISFFLTGVAGTQSTHESLKPQRVQFQSRNFHNILQWQPGRALTGNSSVY 60
SP|Q969J5-3|I22RA2i3_HUMAN    MMPKHCFLGFLISFFLTGVAGTQSTHESLKPQRVQFQSRNFHNILQWQPGRALTGNSSVY 60
                              ************************************************************

SP|Q969J5|I22RA2v1_HUMAN      FVQYKIMFSCSMKSSHQKPSGCWQHISCNFPGCRTLAKYGQRQWKNKEDCWGTQELSCDL 120
SP|Q969J5-2|I22RA2i2_HUMAN    FVQYKI---------------------------------YGQRQWKNKEDCWGTQELSCDL 88
SP|Q969J5-3|I22RA2i3_HUMAN    FVQYKI---------------------------------YGQRQWKNKEDCWGTQELSCDL 88
                              ******                                   ********************

SP|Q969J5|I22RA2v1_HUMAN      TSETSDIQEPYYGRVRAASAGSYSEWSMTPRFTPWWETKIDPPVMNITQVNGSLLVILHA 180
SP|Q969J5-2|I22RA2v2_HUMAN    TSETSDIQEPYYGRVRAASAGSYSEWSMTPRFTPWWETKIDPPVMNITQVNGSLLVILHA 148
SP|Q969J5-3|I22RA2v3_HUMAN    TSETSDIQEPYYGRVRAASAGSYSEWSMTPRFTPWWERAKGL------------------ 130
                              ************************************    .

SP|Q969J5|I22RA2v1_HUMAN      PNLPYRYQKEKNVSIEDYYELLYRVFIINNSLEKEQKVYEGAHRAVEIEALTPHSSYCVV 240
SP|Q969J5-2|I22RA2v2_HUMAN    PNLPYRYQKEKNVSIEDYYELLYRVFIINNSLEKEQKVYEGAHRAVEIEALTPHSSYCVV 208
SP|Q969J5-3|I22RA2v3_HUMAN    ------------------------------------------------------------

SP|Q969J5|I22RA2v1_HUMAN      AEIYQPMLDRRSQRSEERCVEIP 263
SP|Q969J5-2|I22RA2v2_HUMAN    AEIYQPMLDRRSQRSEERCVEIP 231
SP|Q969J5-3|I22RA2v3_HUMAN    -----------------------
```

Figure 21: Multiple sequence alignment of IL-22BP isoforms. *Sequence alignment done with Clustal Omega (https://www.ebi.ac.uk/Tools/msa/clustalo/) from the UniProt database (https://www.uniprot.org/uniprot/Q969J5). Potential N-glycosylation sites (Asn-Xaa-Ser/Thr sequons) in the sequences are highlighted in blue, and asparagines (N) predicted to be N-glycosylated are highlighted in red. The prediction was made by the NetNGlyc 1.0 server (http://www.cbs.dtu.dk/services/NetCGlyc/). Cysteine (C) residues are highlighted in yellow. Unique residues corresponding to IL-22BPi are highlighted in grey.*

Among the three IL-22BP isoforms, only the crystal structure of isoform 2 has been resolved (de Moura et al., 2009; Watanabe et al., 2009), and just a single study has focused on IL-22BP isoforms from a biochemical and molecular perspective; it was published during the completion of this thesis (Lim et al., 2016). To date, the structure, features, and function that this insertion confers to isoform 1 have not been described, and the biochemical characterization of all IL-22BP isoforms are understudied. In that regard, and prior to any *in vitro* study, an *in silico* analysis was performed to study the potential PTMs and structural differences that these isoforms could have to obtain information that might contextualize their cell localization, their interaction with other proteins, and the potential distinctions among them beyond those dictated by their shared sequences. For that purpose, several predictive software tools were used and are described next.

5.1.1 SP and TM prediction

Proteins that undergo secretion usually contain an SP sequence in their N-terminal part; this structure guides them to the secretory pathway. However, it is important to highlight that the sole presence of an SP does not mean that a protein will be secreted into the extracellular milieu; it only indicates that it will enter the secretory pathway. Sometimes, other factors may influence their fate; for example, if a protein possess TM domains downstream of the SP, then it could be retained in the membrane, or it could also contain other retention or transport signals that might keep it in one of the compartments of the secretory pathway, such as the ER, Golgi apparatus, or lysosome/vacuole, or even anchored to the outer face of the cytoplasmic membrane (Harter & Wieland, 1996). The SP will initially target the sequence to the ER membrane where it will be co-translationally translocated into this organelle. The SP is usually cut off during translocation by a signal peptidase complex (Kihara, 2017).

Bioinformatic prediction of the amino acid sequence of the three isoforms of IL-22BP using the SignalP 4.1 ANN software (http://www.cbs.dtu.dk/services/SignalP-4.1/) anticipated that all of them

contained identical SP sequences comprising the first 21 amino acids of the translated protein, and it predicted that the cleavage site would be between positions 21 and 22: VAG-TQ (**Figure 22**). Moreover, none of the isoforms possess TM helices or recognized ER-retention signals (**Figure 23A** and **B**). This information suggests that the fate of the three isoforms should initially be the same: the secretory pathway – first, the ER, and ultimately, the extracellular milieu. The prediction of potential ER resident proteins was made with the webserver ERPred, (http://proteininformatics.org/mkumar/erpred/index.html), which is a support vector machine-based method that predicts ER resident proteins, even if the query protein does not contain specific ER-retention signals (R. Kumar et al., 2017). The TM helices prediction was made with the TMHMM server (http://www.cbs.dtu.dk/services/TMHMM/), which is an HMM for predicting TM helices in protein sequences (Krogh et al., 2001).

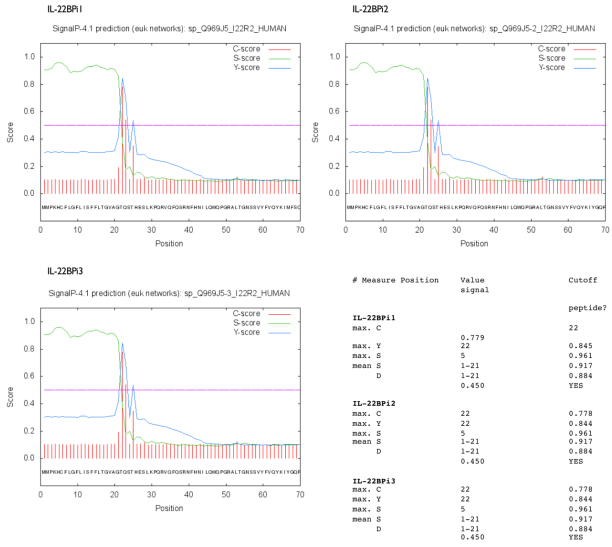

Figure 22: IL-22BP isoforms have identical signal peptides. *Output from the SignalP 4.1 web server for the sequences of human IL-22BP isoforms (http://www.cbs.dtu.dk/services/SignalP-4.1/). 'C-score' is the predicted cleavage site value; 'S-score' is the predicted signal peptide value; and 'Y-score' is a combination of C- and S-scores. The predicted cleavage site is between positions 21 and 22 for the three isoforms with the local sequence context 'VAG-TQ'. The calculated D-score = 0.884 for the three isoforms, and the D-cutoff = 0.450.*

A

IL-22BPi1

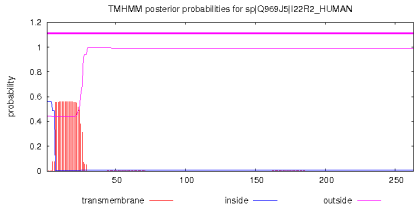


```
# sp|Q969J5|I22R2_HUMAN Length: 263
# sp|Q969J5|I22R2_HUMAN Number of predicted TMHs: 0
# sp|Q969J5|I22R2_HUMAN Exp number of AAs in TMHs: 11.00273
# sp|Q969J5|I22R2_HUMAN Exp number, first 60 AAs: 10.97345
# sp|Q969J5|I22R2_HUMAN Total prob of N-in: 0.55887
# sp|Q969J5|I22R2_HUMAN POSSIBLE N-term signal sequence
sp|Q969J5|I22R2_HUMAN TMHMM2.0 outside 1 263
```

IL-22BPi2

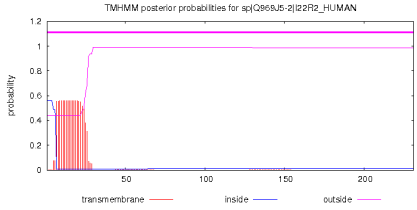


```
# sp|Q969J5-2|I22R2_HUMAN Length: 231
# sp|Q969J5-2|I22R2_HUMAN Number of predicted TMHs: 0
# sp|Q969J5-2|I22R2_HUMAN Exp number of AAs in TMHs: 11.06373
# sp|Q969J5-2|I22R2_HUMAN Exp number, first 60 AAs: 11.00464
# sp|Q969J5-2|I22R2_HUMAN Total prob of N-in: 0.56040
# sp|Q969J5-2|I22R2_HUMAN POSSIBLE N-term signal sequence
sp|Q969J5-2|I22R2_HUMAN TMHMM2.0 outside 1 231
```

IL-22BPi3

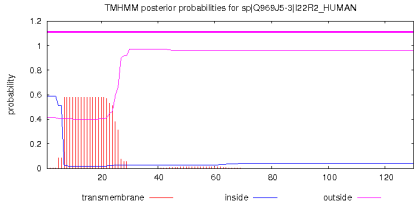


```
# sp|Q969J5-3|I22R2_HUMAN Length: 130
# sp|Q969J5-3|I22R2_HUMAN Number of predicted TMHs: 0
# sp|Q969J5-3|I22R2_HUMAN Exp number of AAs in TMHs: 11.57217
# sp|Q969J5-3|I22R2_HUMAN Exp number, first 60 AAs: 11.52558
# sp|Q969J5-3|I22R2_HUMAN Total prob of N-in: 0.58782
# sp|Q969J5-3|I22R2_HUMAN POSSIBLE N-term signal sequence
sp|Q969J5-3|I22R2_HUMAN TMHMM2.0 outside 1 130
```

B

ERPred Prediction Result	
Protein ID	**Prediction**
IL-22BPi1 sp|Q969J5	**Non-ER**
IL-22BPi2 sp|Q969J5-2	**Non-ER**
IL-22BPi3 sp|Q969J5-3	**Non-ER**
Job number **7106**	

Figure 23: IL-22BP isoforms do not contain transmembrane (TM) helices or endoplasmic reticulum-retention signals. *(A) Output from the TM helix prediction model TMHMM v.2.0 for the sequences of the human IL-22BP isoforms (http://www.cbs.dtu.dk/services/TMHMM/). None of the three sequences contain TM helices. Predicted TM segments in the N-terminal region, in this case, turn out to be the signal peptides. (B) Results of the prediction of endoplasmic reticulum (ER) retention signals for the three human IL-22BP isoforms done with the webserver ERPred (http://proteininformatics.org/mkumar/erpred/index.html).*

5.1.2 Glycosylation

Once the translocated nascent protein enters the luminal side of the ER, it encounters not only the signal peptidase, which cuts off the SP, but also an oligosaccharyltransferase, which might transfer high mannose oligosaccharides onto the nitrogen of the side chain of asparagine (Asn), located in potential acceptor sites within an Asn-Xaa-Ser/Thr consensus motif – being Xaa any amino acid except proline (Pro), Ser-denoting serine, and Thr threonine. This modification is termed N-glycosylation and occurs in unfolded proteins to aid in their folding and to increase their solubility and stability against proteolysis (Shental-Bechor & Levy, 2008).

IL-22BPi1 and IL-22BPi2 contain five Asn-Xaa-Ser/Thr sequons; however, the NetNGlyc 1.0 server (http://www.cbs.dtu.dk/services/NetNGlyc/) predicted that only three Asn residues of these sequons were N-glycosylated (**Figure 24)**. This server predicts N-glycosylation sites in human proteins using ANNs that examine the sequence context of Asn-Xaa-Ser/Thr sequons. IL-22BPi3, which only contains one potential N-glycosylation site corresponding to the shared sequence with isoforms 1 and 2, was predicted to be N-glycosylated in that shared residue (**Figure 24)**.

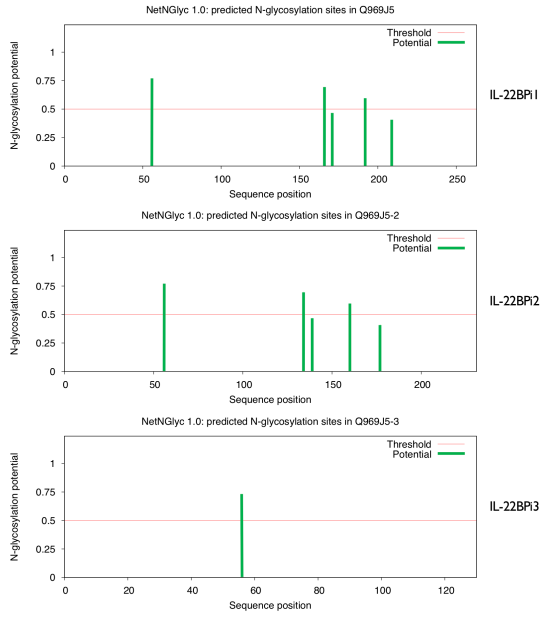

Figure 24: Predicted N-glycosylation sites across the IL-22BP isoforms. *Prediction was made by the NetNGlyc 1.0 server (http://www.cbs.dtu.dk/services/NetNGlyc/). Potential glycosylation sites are represented as vertical bars (green bars). Barsthat cross the threshold (horizontal line at 0.5) are predicted to be glycosylated.*

Another possible glycosylation event within the secretory pathway is O-glycosylation – the attachment of a sugar molecule to the oxygen atom of serine or threonine residues. This PTM takes place in the cis-Golgi compartment after N-glycosylation and folding of the protein. It has no such defined sequence as happens to N-glycosylation, but proline and β-sheet conformation around the glycosylation sites is present. The prediction of this type of PTM modification for IL-22BP isoforms, made by the NetOGlyc 4.0 Server (http://www.cbs.dtu.dk/services/NetOGlyc-3.1/), was that only Ser residue at position 28 on isoform 2 has the potential to be O-glycosylated.

5.1.3 Disulphide bonds

The structural changes generated by the disulphide bond formation constitute another common PTM during and after biosynthesis. These changes form an important feature of protein folding and structure that

promotes resistance to proteases and contributes to the protein thermodynamic stability. Moreover, disulphide bonds can be involved in the regulation of protein activity (Fass, 2012). Cysteine (Cys) is usually a rare and conserved residue that participates in the formation of disulphide bridges. The event of disulphide bond formation usually occurs during the folding of proteins that enter the secretory pathway in the oxidizing environment of the ER (Bulleid, 2012).

IL-22BPi1 contains nine cysteines (Cys^{6}, Cys^{70}, Cys^{82}, Cys^{88}, Cys^{93}, Cys^{110}, Cys^{118}, Cys^{238}, and Cys^{259}); IL-22BPi2 contains five (Cys^{6}, Cys^{78}, Cys^{86}, Cys^{206}, and Cys^{227}); and IL-22BPi3 contains three (Cys^{6}, Cys^{78}, and Cys^{86}) (**Figure 21** and **Figure 25**). The crystal structure of IL-22BPi2 contains two disulphide bridges: the first one between Cys^{78} and Cys^{86}, and the second one between Cys^{206} and Cys^{227} (de Moura et al., 2009). According to that structure, isoform 3 must contain only one disulphide bridge between Cys^{78} and Cys^{86} (**Figure 25**), and IL-22BPi1 must contain at least two. The prediction of disulphide bonds for all isoforms was made with DIpro 2.0, software based on a 2D recurrent neural network, support vector machine, graph matching, and regression algorithms that can predict whether a given sequence has disulphide bonds or not, estimate the number of disulphide bonds, and predict the bonding state of each cysteine and the bonded pairs. This software is hosted in SCRATCH, which is a protein structure and structural feature prediction server (http://scratch.proteomics.ics.uci.edu). The disulphide bond prediction for the sequence of IL-22BPi3 corroborates the formation of one disulphide bond (Cys^{78} and Cys^{86}). For IL-22BPi1, the additional 32-amino-acid sequence that it possesses, contributes with four cysteine residues in addition to the IL-22BPi2 shared sequence, resulting in nine cysteine residues. However, the DIpro predicted that six, not eight, cysteines would form disulphide bonds, excluding the cysteine within the SP. These cysteines, predicted to participate in the formation of three disulphide bonds, are as follows: the first disulphide bridge between Cys^{70} and Cys^{82}, unique among the three isoforms; the second bridge between Cys110 and Cys118, which is shared with isoforms 2 and 3; and

the third between Cys[238] and Cys[259], shared only with isoform 2 (**Figure 25**).

Figure 25: Cysteines and disulphide bridges predicted to occur in IL-22BP isoforms. *Cysteines (Cs) present in the sequence and not involved in any disulphide bond are highlighted in yellow. Cs that form disulphide bridges are bolded in orange, and their corresponding bridge is indicated with an orange line. Prediction performed with DIpro (http://scratch.proteomics.ics.uci.edu).*

5.1.4 Secondary and tertiary structure of IL-22BP isoforms

As mentioned above, only the crystal for IL-22BPi2 has been resolved to date (de Moura et al., 2009). Two fibronectin-III domains positioned in an L-shape conformed the structure of IL-22BPi2; both are connected by a small α-helix, and each fibronectin domain (β-sandwich domain) consists of two anti-parallel β-sheets formed from seven β-strands. Concerning IL-22BPi1 and IL-22BPi3, no information about their crystal structure or secondary structure has been described so far. Therefore, we aimed to assess *in silico* the secondary structure of the three isoforms as well as their 3D structure. The secondary structure prediction was performed by running different bioinformatic prediction programmes: POLYVIEW 2D-SABLE, JPRED4, and PSIPRED (D. W. A. A. Buchan et al., 2013; Drozdetskiy et al., 2015; Porollo, Adamczak, & Meller, 2004). **Figure 26**, **Figure 27**, and **Figure 28** depict the results obtained with each of the three

programmes, respectively. There is almost complete similarity among the common regions of the three isoforms, adopting β-strand conformations along the protein. However, the 32-amino-acid insertion, unique in isoform 1, was predicted to have neither an α-helix nor β-strand conformation by any of the software used (**Figure 26**, **Figure 27**, and **Figure 28**). Moreover, this insertion did not interrupt any of the β-strands conformations.

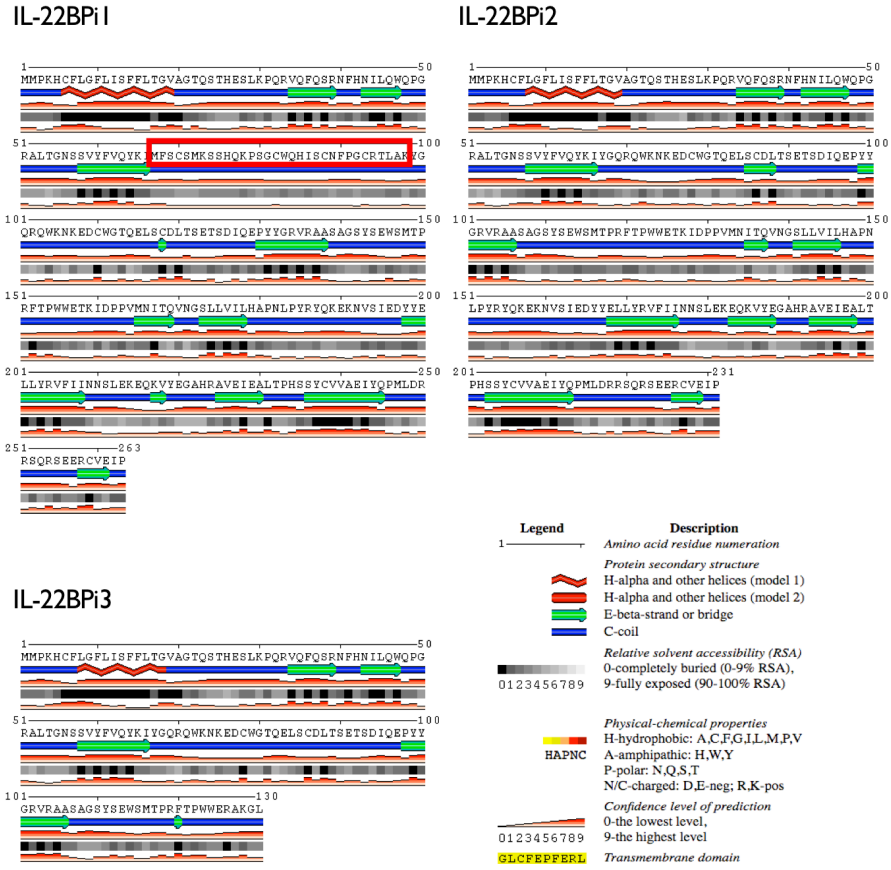

Figure 26: Secondary structure prediction of the three IL-22BP isoforms generated by PolyView 2D-SABLE. *Green and red colours represent β-strand and α-helix structures, respectively, while the blue line represents a random coil. The orange columns show the confidence of prediction for each position. The red-lined box indicates the 32-amino-acid insertion unique in IL-22BPi1.*

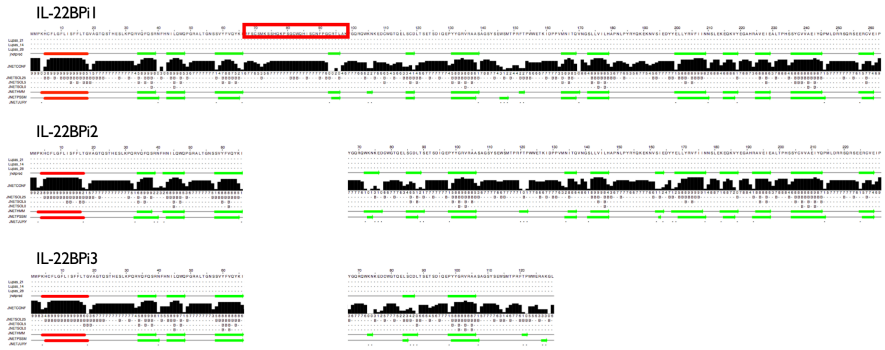

Figure 27: Secondary structure prediction of the three IL-22BP isoforms generated by JPRED4. *Green and red colours represent β-strand and α-helix structures, respectively. Black columns represent the confidence of prediction for each position. The red-lined box indicates the 32-amino-acid insertion unique in IL-22BPi1.*

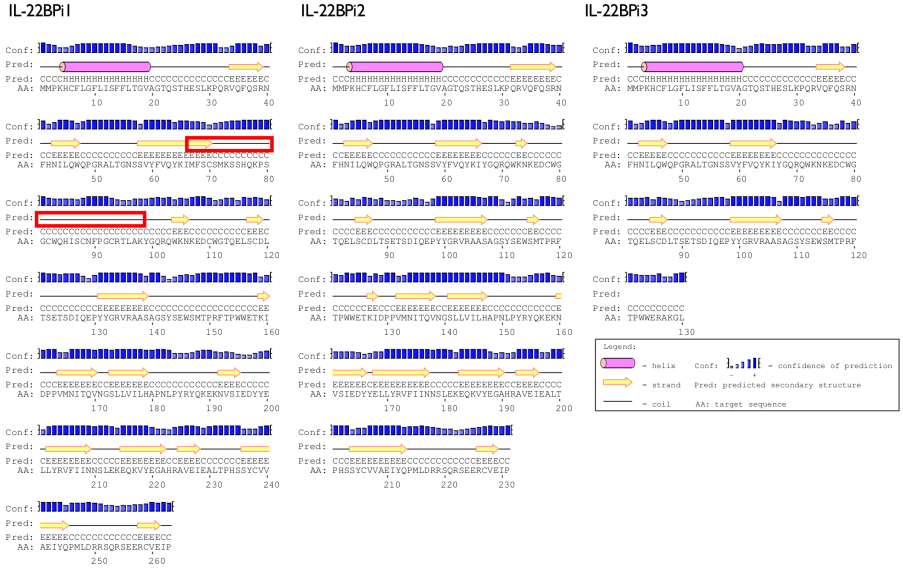

Figure 28: Secondary structure prediction of the three IL-22BP isoforms by PSIPRED. *Alpha helices are marked as pink cylinders, while beta strands are denoted by yellow arrows, and the confidence level of the prediction for each residue is provided by the blue bar. The red-lined box indicates the 32-amino-acid insertion unique in IL-22BPi1.*

It has been suggested that during exonization processes, such as those that occur in IL-22BPi1 (Piriyapongsa et al., 2007), the domains gained by the extension of existing exons contain the highest degree of disordered regions (Buljan, Frankish, & Bateman, 2010), suggesting that these processes are important mechanisms for the addition of disordered segments to proteins (R. van der Lee et al., 2014). IDRs are polypeptide sequences that do not contain sufficient hydrophobic amino acids to mediate co-operative folding; they are dynamic and lack a unique 3D structure, and they were traditionally thought to be passive segments in proteins that linked structured domains. It is now well established that IDRs participate in diverse functions mediated by proteins, contradicting the sequence-structure-function paradigm (Dyson & Wright, 2005). Several advantages have been attributed to proteins that contain IDRs that make them well suited to perform signalling and regulatory functions, some of these are as follows: they have the capacity to expose linear motifs that can mediate peptide interactions; they can facilitate the regulation of proteins via diverse PTMs of residues within the IDR; they can also regulate the protein half-life by efficiently engaging proteins that have been targeted for degradation by the proteasome; and finally, they have the capacity to adopt different conformations when binding to different partners (Babu, 2016). In this regard, and due to the lack of secondary structure prediction obtained with the previous secondary structure prediction software, two different computational programmes for protein disorder prediction – RaptorX (S. Wang et al., 2016) and DISOPRED3 (D. T. Jones & Cozzetto, 2015) – were run for the three IL-22BP isoforms. The results revealed that, apart from the SP sequence in all isoforms, only the 32-amino-acid sequence encoded by exon 4 in IL-22BPi1 was highly predisposed towards being disordered (**Figure 29**).

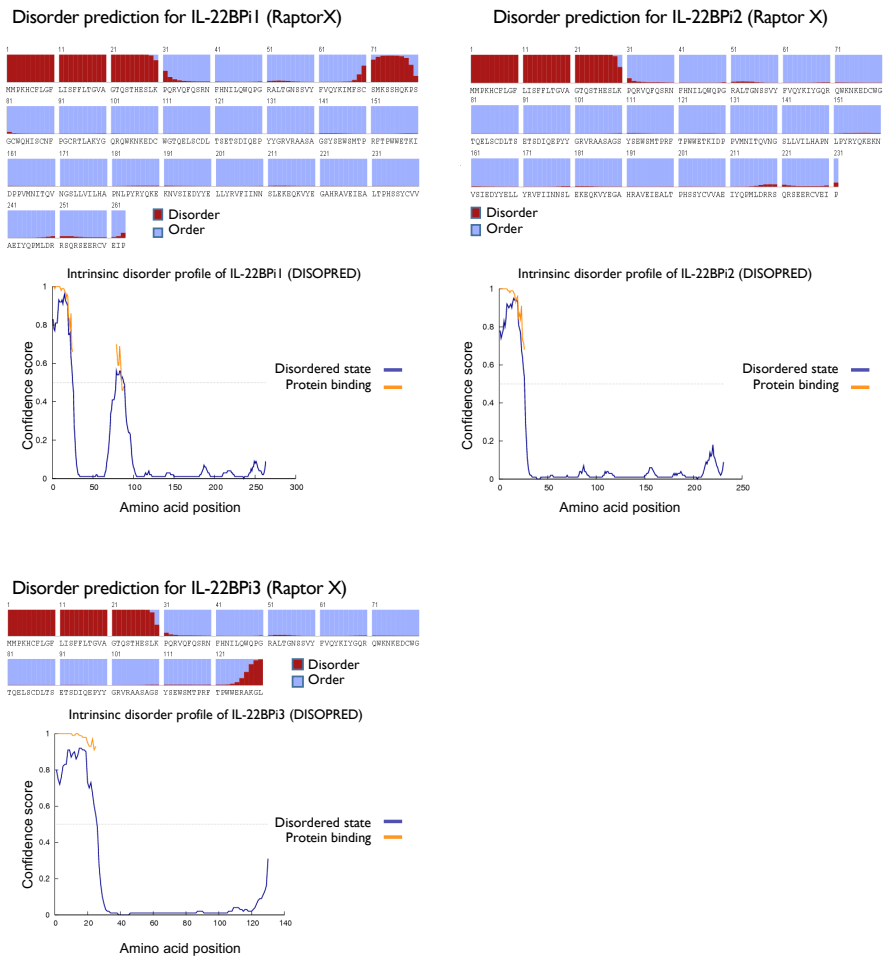

Figure 29: Protein disorder prediction of the three human IL-22BP isoforms by RaptorX and DISOPRED3 computational software. *For each residue, Raptor X provides a bar indicating the relative likelihood of a given residue being ordered or disordered. The DISOPRED plot shows the disorder confidence level against the sequence positions as a solid blue line. The grey dashed horizontal line marks the threshold above which amino acids are regarded as disordered. The orange line indicates the confidence of disordered residues being involved in protein-protein interactions.*

Tertiary structure prediction was run for the three isoforms with the I-TASSER server (https://zhanglab.ccmb.med.umich.edu/I-TASSER/). This bioinformatic tool models the 3D structure of protein molecules from amino acid sequences; it detects structure templates from the PDB by a technique called fold recognition (or threading). The full-length structure

models are constructed by reassembling structural fragments from threading templates using replica exchange Monte Carlo simulations (Roy et al., 2010). Results obtained with I-TASSER were visualized and colour-edited with PyMOL 2.3 (https://pymol.org/2/), and they are represented in **Figure 30**. The results indicate that the 3D model of IL-22BPi2, as expected, coincides with the one generated by de Moura (de Moura et al., 2009), which is hosted in the PDB as 3G9V (**Figure 31**). However, for the other isoforms, the prediction was done by the software-based algorithms. I-TASSER generates five models with the highest confidence scores; among them, the top one for each isoform was selected and is represented in **Figure 30**. The predicted overall 3D structure of isoform 1 was quite similar to isoform 2, except for the extra sequence unique in isoform 1 (**Figure 30**, coloured in cyan); this sequence failed to adopt any secondary structure in any of the five models generated.

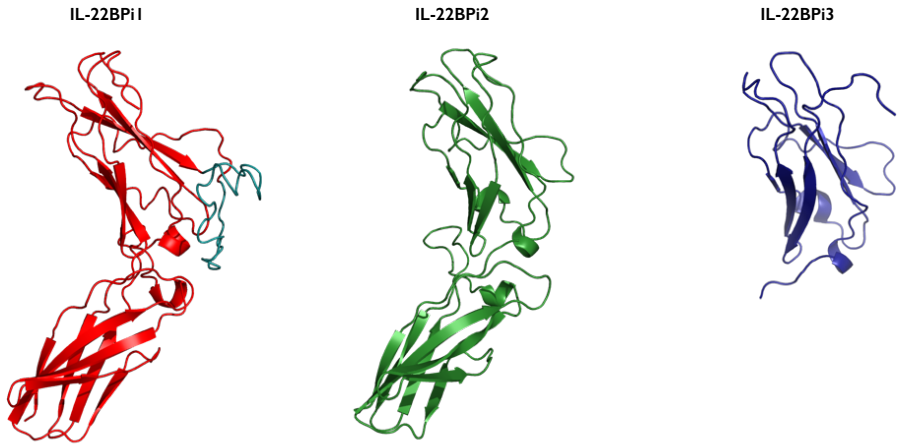

Figure 30: 3D structure model of human IL-22BP isoforms predicted with I-TASSER and visualized with PyMOL 2.3. *Red, green, and deep-blue colours correspond to IL-22BPi1, IL-22BPi2, and IL-22BPi3, respectively. The sequence coloured in cyan in isoform 1 corresponds to the 32-amino-acid sequence encoded by exon 4 and unique among the three.*

We further explore in detail the resolved crystal structure of IL-22BPi2 bound to IL-22 (**Figure 31**). IL-22BPi2 has been reported to contact IL-22

using five binding loops (named L2–L6); Tyr[67], located in L2, dominates the molecular recognition of IL-22 by IL-22BPi2 by making five direct contacts and one water-mediated interaction with IL-22 residues. Moreover, its hydroxyl group inserts in the swallow cavity formed in IL-22; this tyrosine residue has also been described as being critical for IL-22 binding, and its mutation has been found to completely abolish the interaction with IL-22 (de Moura et al., 2009). L2 is the site where more residues are participating in the interaction with IL-22 – not only Tyr[67], but also Lys[65], Gly[68], Gln[69], and Arg[70]. This site contributes with 11 out of the total 20 hydrogen bond and salt bridge interactions found at the IL-22/IL-22BP interface (de Moura et al., 2009). Considering these interactions, when looking at the amino acid sequence of IL-22BPi1 (**Figure 21**), we observed that its additional 32-amino-acid sequence is inserted between Ile[66] and Tyr[67] residues of IL-22BPi2. Taking into account that this sequence was not predicted to adopt any secondary conformation and that it is inserted within the L2 of IL-22BPi2 and may also generate steric hindrances in L3 and L4 (**Figure 30**), it can be speculated that this insertion may, to some extent, interfere in the binding of IL-22BPi1 to IL-22 because it is introduced in a critical binding region, as mentioned above.

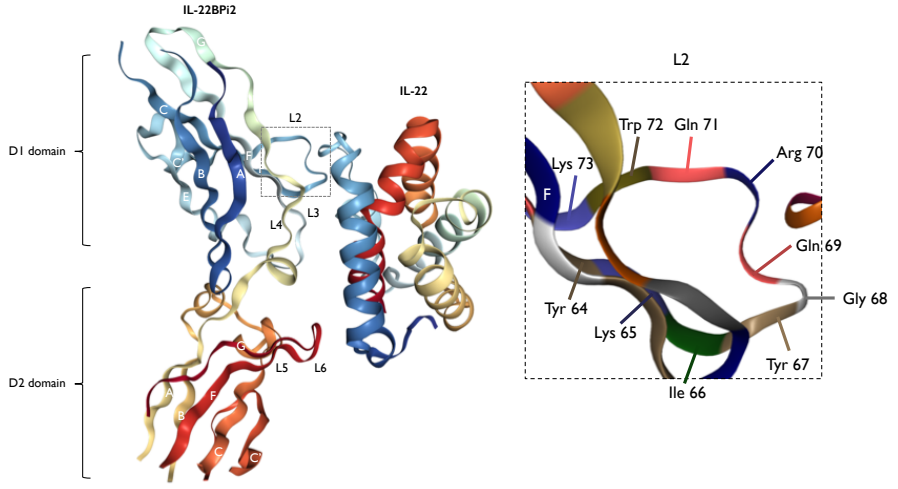

Figure 31: Crystal structure of human IL-22BP isoform 2 bound to interleukin-22. *The two fibronectin-III domains are labelled D1 and D2, and the β-sheets are indicated with capital*

letters. Five binding loops in IL-22BPi2 (labelled L2–L6) contact IL-22 by 20 hydrogen bond and salt bridge interactions. On the right-hand side, a magnification of the L2 site is displayed, where 11 out of the 20-hydrogen bond and salt bridge interactions with IL-22 occur. Residues Lys65, Tyr67, Gly68, Gln69, and Arg70 are responsible for such binding, with Tyr67 being the residue that dominates the molecular recognition of IL-22 by Il-22BPi2 with 5 out of the 11 interactions. Modified from PDB ID: 3G9V (de Moura et al., 2009) and visualized with the NGL viewer software (Rose et al., 2018).

5.1.5 Protein alignment of the 32-amino-acid sequence in IL-22BPi1

Finally, to extract more information about the amino acid sequence encoded by the extra exon of IL-22BPi1, the 32-amino-acid sequence was compared with different protein databases (listed in **Table 16**) using BLAST to look for a sequence match or sequence identity via the BlastP algorithm. BLAST (Johnson et al., 2008) is a suite of programmes provided by NCBI for aligning query sequences against those present in a selected target database (https://blast.ncbi.nlm.nih.gov/Blast.cgi).

In an initial search with protein BLAST in the non-redundant protein database, the results generated alignment with sequences related to IL-22BP in different species from homo, pan, gorilla, and macaca genera, among other primates. We then excluded taxonomic order primates (taxid:9443) from the search and obtained no sequence alignment at all. Similar results were obtained from reference proteins and model organism databases. When the search was performed with the UniProtKB/SwissProt databases, the following alignment was obtained (**Figure 32**): some similarity was found with 2,3-bisphosphoglycerate-independent phosphoglycerate mutase from *Wolbachia endosymbiont*, isoleucyl-tRNA synthetase from *Saccharophagus degradans*, and protein LIC_10976 from *Leptospira interrogans* serovar Copenhageni str. Fiocruz L1-130, apart from the match with IL-22BPi1 from humans.

Table 16: Databases used in the Protein Basic Local Alignment Tool (BLAST).

Database	Title	Description	Update date	# sequences
Non-redundant protein sequences (nr)	All non-redundant GenBank CDS translations + PDB + SwissProt + PIR + PRF excluding environmental samples from WGS projects	All non-redundant GenBank CDS translations + PDB + SwissProt + PIR + PRF excluding environmental samples from WGS projects	22/3/19	216048067
Reference proteins (refseq_protein)	NCBI protein reference sequences	Protein sequences from NCBI Reference Sequence Project	7/4/19	137318344
Model organism (landmark)	Landmark database for SmartBLAST	The landmark database includes proteomes from 27 genomes spanning a wide taxonomic range	12/3/19	422853
UniProtKB/Swiss (SwissProt)	Non-redundant UniProtKB/SwissProt sequences	Non-redundant UniProtKB/SwissProt sequences	7/4/19	470929
Patented protein sequences	Protein sequences derived from the patent division of GenBank	Protein sequences derived from the patent division of GenBank	22/3/19	2405013
Protein Data Bank proteins (pdb)	PDB protein database	Protein sequences from the 3D structure records from the PDB	7/4/19	106963
Metagenomic proteins (env_nr)	Proteins from WGS metagenomic projects (env_nr).	Protein sequences translated from the CDS annotation of metagenomic nucleotide sequences.	20/11/18	9184938
Transcriptome Shotgun Assembly proteins (tsa_nr)	Transcriptome Shotgun Assembly (TSA) sequences	Protein sequences translated from CDSs annotated on transcriptome shotgun assemblies	20/11/18	3071937

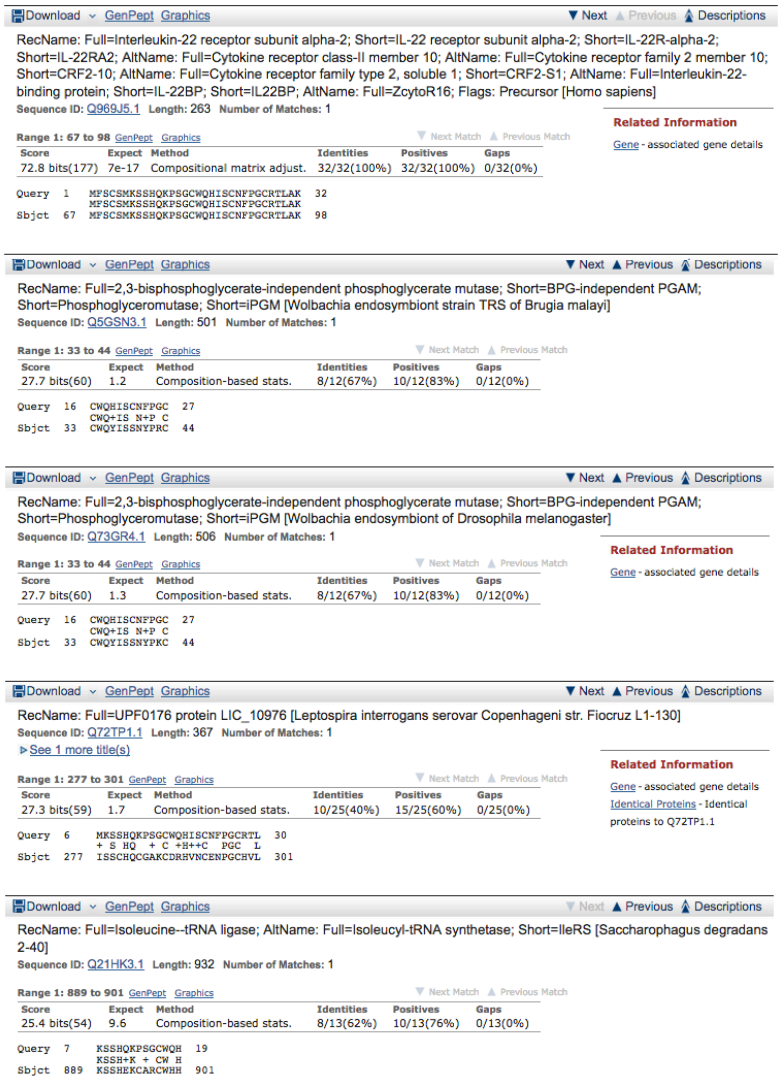

Figure 32: Output generated with protein BLAST using the non-redundant UniProtKB/SwissProt sequences for the 32-amino-acid sequence encoded by exon 4 in IL-22BPi1.

This search logically leads to the question of whether there is any domain homology between the enzymes found and their functions. First, the function of phosphoglycerate mutase enzyme is to catalyse the critical isomerization of 3-phosphoglycerate and 2-phosphoglycerate in glycolytic and gluconeogenic metabolic pathways. The homologous

sequence found in BLAST does not match any conserved regions or catalytical residues for this enzyme (Z. Li, Galvin, Raverdy, & Carlow, 2011). Second, the function of isoleucyl-tRNA synthetase is to catalyse the aminoacylation reaction by covalent linking of isoleucine to its cognate tRNA in the first step of protein translation. Again, the homologous region found with the 32-amino-acid sequence encoded by exon 4 in IL-22BPi1 does not comprise any of the key functional or conserved domains or residues of this enzyme (Rajendran, Kalita, Shukla, Kumar, & Tripathi, 2018).

The search in the GenBank patent database produced several hits, most of which were related to the IL-22BPi1 sequence; however, three of them were related to patented sequences (12942, 19753 and 24232) from the Monsanto Company corresponding to sequences to phosphoglycerate mutase from different *Wolbatchia* strains, already found in the previous search. These patented sequences from Monsanto correspond to the following patents: 'genes and uses for plant improvement' and 'genes encoding glutamine synthetase and uses for plant improvement' (**Figure 33**).

The PDB database search returned a single hit: adenylyl-sulphate reductase from *Desulfovibrio Gigas* (**Figure 34**). The 3D structure of this enzyme (3GYX_B) adopts a β-sheet from methionine 36 to glutamine 41, and an alpha-helix turn from 42 to 46; residues 38, 40, and 46 participate in the binding to the iron/sulphur cluster among other residues in the protein. The sequence of amino acids 36 to 67 is classified as 4Fe-4S ferredoxin-type 2 domain. Metagenomic and transcriptome Shotgun Assembly protein databases did not yield any results.

We also ran the smartBLAST tool, which searches a protein query against the landmark database using a combination of optimized BLAST searches and a multiple sequence alignment to produce its results. Apart from all the results related to IL-22BP orthologous, in the additional matches section, hypothetical protein VO64_3897 – from *Pseudomonas synxantha* with a 45-nucleotide length and with unknown function – was found (**Figure 35)**.

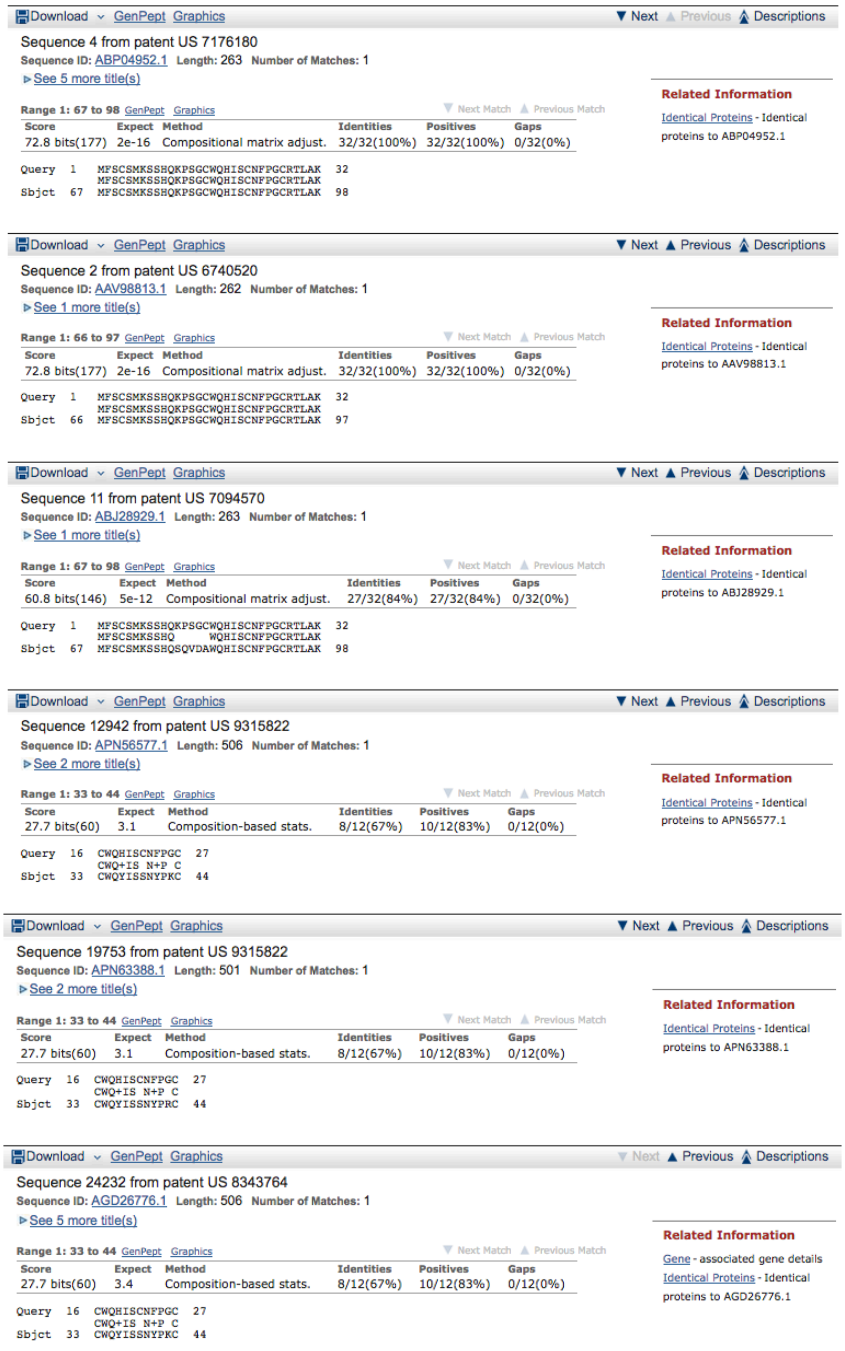

Figure 33 : Output generated with protein BLAST using the GenBank patent division database for the 32-amino-acid sequence encoded by exon 4 in IL-22BPi1.

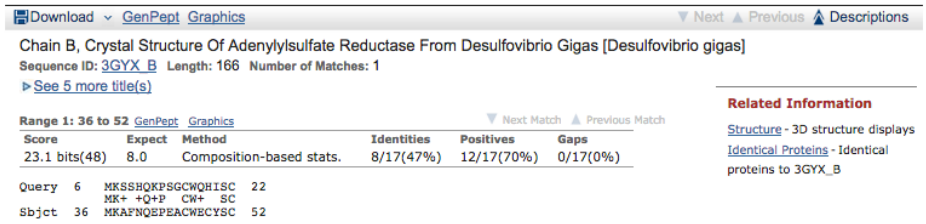

Figure 34: Output generated with protein BLAST using the PDB database for the 32-amino-acid sequence encoded by exon 4 in IL-22BPi1.

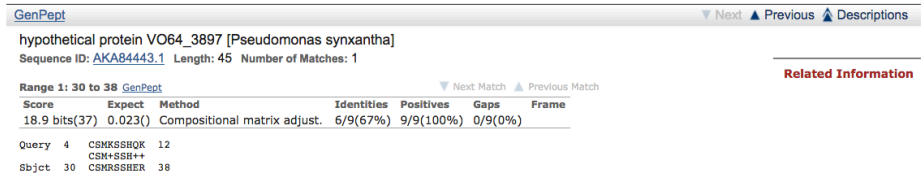

Figure 35: Output generated with smartBLAST for the 32-amino-acid sequence encoded by exon 4 in IL-22BPi1.

Searches of the different protein databases using BLAST revealed no additional structural or functional information for the 32-amino-acid sequence encoded by the extra exon 4 only present in the long isoform, IL-22BP1.

5.2 IL22BP protein levels reflect *IL22RA2* mRNA levels produced by U937DCs and moDCs

5.2.1 Expression of *IL22RA2* variants in U937DCs and moDCs

We aimed to investigate the protein expression of these isoforms in the natural producer cells; for that, we selected moDCs, a model that has been documented several times in the literature to be the major source of *IL22RA2v2* (Huber et al., 2012; Jinnohara et al., 2017; J. C. Martin et al., 2014; Voglis et al., 2018). The three *IL22RA2* mRNA variants were detected in immature moDCs (primary human monocytes cultivated for 6 days in DM containing GM-CSF and IL-4) by RT-PCR using both best coverage (primers designed to detect the three isoforms by annealing to shared regions in the expressed products) and variant-3-specific primers (**Figure 36**). Previous work by the Josien R. group (J. C. Martin et al., 2014) showed that under the stimulus of an agonist of retinoic acid receptor, AM580, the expression of *IL22RA2v1* and *IL22RA2v2* in moDCs was upregulated. We sought to reproduce those finding as well as investigate whether variant 3 followed the same trend. We found that the three variants were, to a similar extent, increased in cells cultivated in the presence of AM580 (**Figure 36**). In our hands, the maturation microbial-product stimulus LPS, which has been described as decreasing *IL22RA2* levels regardless of the isoform (J. C. Martin et al., 2014), decreased the expression of *IL22RA2v2* and *IL22RA2v3* in moDCs (**Figure 36)**. In contrast, the expression of the three variants in PBMCs was not detected, probably because the expression of these variants is restricted to a minoritarian cell type. Surprisingly, the expression of *IL22RA2v2* appeared after stimulation with LPS for 24 hours (**Figure 36**). This induction has also been reported after a 4-hour period of LPS stimulation in U937, HepG2 cell lines, and mouse monocytes (C.-C. Wei et al., 2003).

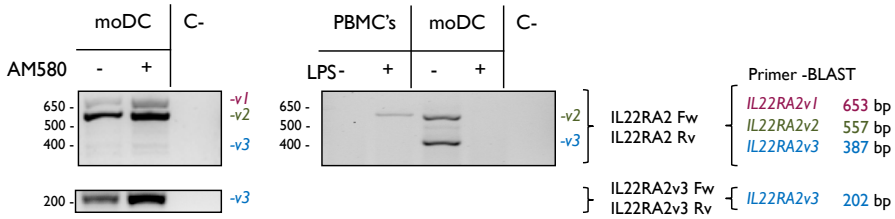

Figure 36: Expression of IL22RA2v1, v2, and v3 in monocyte-derived dendritic cells (moDCs) after 6 days of culture in differentiation medium ± AM580 or ± LPS and in peripheral blood mononuclear cells (PBMCs) ± lipopolysaccharide (LPS) by RT-PCR. *The IL22RA2 gene expression was analysed by RT-PCR using primers allowing for amplification of the three variants (IL22RA2 Fw and IL22RA2 Rv) and specifically of variant 3 (IL22RA2v3 Fw and IL22RA2v3 Rv). The expected products for each pair of primers run with Primer-BLAST are indicated on the right.*

We also analysed the expression of *IL22RA2* in different human cell lines from different origins in steady-state conditions. Among the different cell lines tested, U937 displayed the highest expression for *IL22RA2* (**Figure 37A**). We then analysed the expression of the *IL22RA2* variants in the human monocytic cell line that U937 differentiated to an immature dendritic phenotype following the same procedure as was done for human monocytes. The U937 cell line has been previously reported to express the three transcripts for *IL22RA2*; however, data related to isoform expression have not been shown (C.-C. Wei et al., 2003; Wenfeng Xu et al., 2001). U937DCs expressed the three variants in a similar fashion to human moDCs, with variant 2 being the most strongly expressed among the three (**Figure 37B**). These results indicate that U937 could be a useful cell line to study *IL22RA2*.

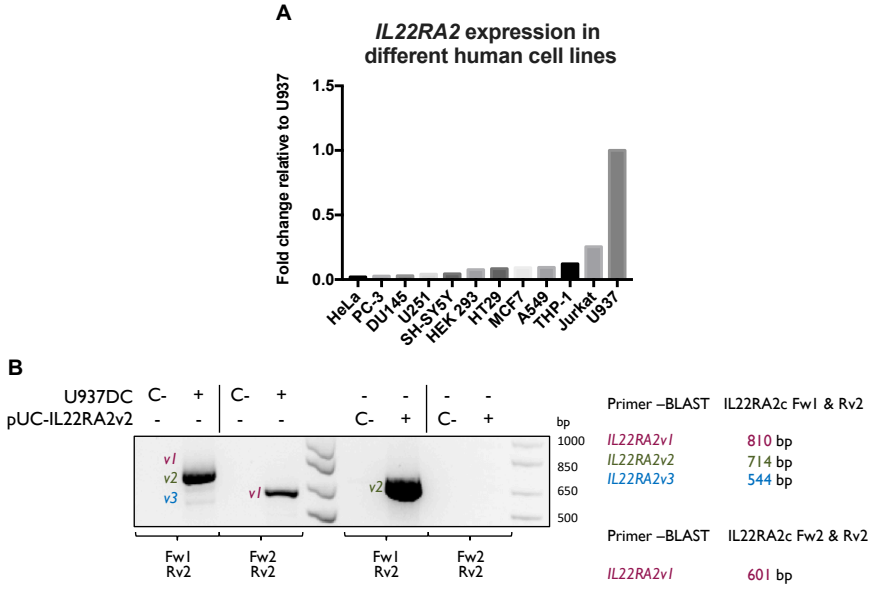

Figure 37: Expression of IL22RA2 in human cell lines. (A) Expression of IL22RA2 in different human cell lines. *IL22RA2 mRNA expression relative to the mean of the housekeeping gene GAPDH was measured by RT-qPCR using pre-designed SYBR Green primers. (B) Expression of IL22RA2v1, v2, and v3 in U937DCs after 6 days of culture in differentiation medium by RT-PCR. The IL22RA2 gene expression was analysed by RT-PCR using primers allowing for amplification of the three variants (IL22RA2c Fw1 and IL22RA2c Rv2) and specifically of variant 1 (IL22RA2c Fw2 and IL22RA2c Rv2). The expected products for each pair of primers run with Primer-BLAST are indicated on the right. C- represents PCR negative controls. pUC-IL22RA2, plasmid containing variant 2 was included as a positive control.*

5.2.2 Protein expression of IL-22BP in U937DCs and moDCs

Given that the three isoforms share the same functional SP and should therefore be secreted (**Figure 22**), and that secretion of IL-22BP by primary monocyte-derived cultures or monocytic cell lines has not been reported in the literature, we set out to demonstrate IL22BP immunoreactivity in both $CD14^+$ moDC and U937DC lysates and culture media by means of an in-house-developed antigen-purified goat polyclonal ELISA (see Materials and Methods, p.114) capable of detecting 30 pg/ml recombinant IL22BP and Western blot.

In immature moDCs, strongly increasing levels of *IL22RA2* mRNA were observed by qPCR over the cultivation period until day 10 (**Figure 38A**), but corresponding IL-22BP levels in the culture medium of these moDCs as measured by ELISA increased modestly over time (**Figure 38B**). Furthermore, flow cytometric analysis of *in-vitro*-generated moDCs verified their phenotype by the presence of the DC-sign molecule, CD-209, (Geijtenbeek et al., 2000; Vliet et al., 2000) (**Figure 38C**). Upon stimulation, moDCs undergo a number of phenotypical and morphological changes, such as an increase in the expression surface cell marker, CD83 (L. J. Zhou & Tedder, 1996). This expression was analysed by flow cytometry, and its increase indicated that the DC population was matured in the presence of the LPS stimulus (**Figure 38C**). Moreover, the expression of the CD209 marker also decreased after maturation, coinciding with what has been previously described in the literature (Relloso et al., 2002). Morphological observable changes were also detected after maturation stimulus, from a round shape with several dendrites to a more elongated shape (**Figure 38E).** In Western blot, intracellular IL-22BP immunoreactive protein bands were detected with molecular masses extending from around 38 kDa to 50 kDa and increasing over the cultivation period (**Figure 38D**). The expression of IL-12 (p40), a cytokine known to be strongly induced by LPS in moDC (Snijders, Kalinski, Hilkens, & Kapsenberg, 1998), confirmed maturation by LPS. However, after LPS stimulation, the relative intensity of IL-22BP reactive bands did not follow the trend observed in the mRNA levels. Only the band close to 34 kDa exhibited a decreased signal (**Figure 38A**). Apart from the morphological changes observed during the differentiation process of monocytes to immature or mature moDCs, the composition of the machinery in the ER also displayed a simultaneous change; it can be speculated that the ER of immature and mature DCs must be prepared to cope with a high protein processing and secretion demand. In this regard, we observed a change in the expression of the peptidyl-prolyl cis-trans isomerases (PPI) family. A distinct pattern of reactive bands was detected with the anti-PPIC antibody along the differentiation process from monocytes to moDCs; this antibody is

capable of detecting PPIB and PPIA apart from PPIC (Stocki, Chapman, Beach, & Williams, 2014).

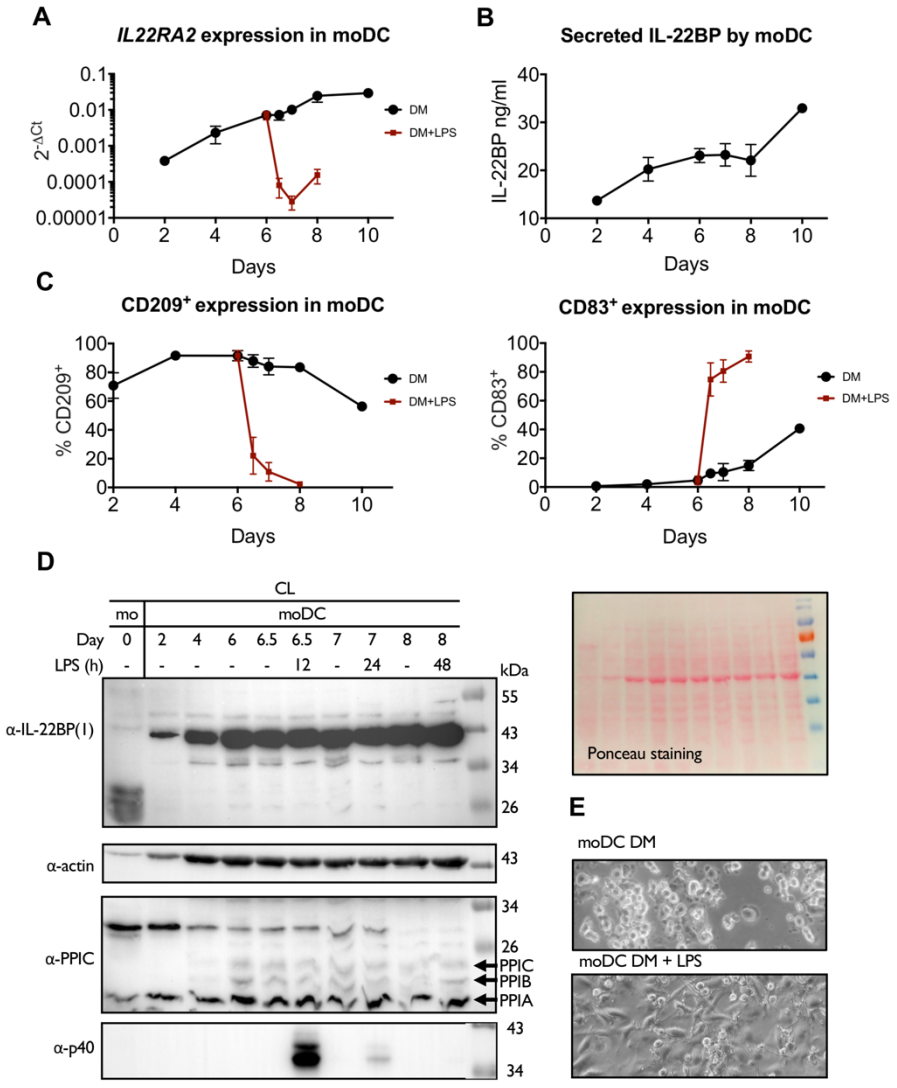

Figure 38: IL22BP protein levels reflect IL22RA2 mRNA levels produced by monocyte-derived dendritic cells (moDCs). *CD14⁺ monocytes were isolated from peripheral blood mononuclear cells (PBMCs) and differentiated into immature moDCs for 6 days. Cells were harvested at the indicated times following cultivation in differentiation medium (DM) supplemented (or not) with lipopolysaccharide (LPS) on day 6. (A) IL22RA2 mRNA expression levels analysed by RT-qPCR using Taqman probes (IL22RA2 and ACTB probes) (mean ± SEM, n = 2). Levels correspond to (B) IL-22BP protein levels, and both increase over*

the cultivation period (mean ± SEM, n = 2). (C) Surface marker (CD209 and CD83) expression characteristic from moDCs and maturation status were measured by flow cytometry (mean ± SEM, n = 2). (D) moDCs were harvested during the cultivation period and immunoblotted for detection of IL-22BP (IL-22BP antibody 1), PPIC, and p40, using actin and Ponceau staining as loading controls. (E) Morphology of immature moDC for 7 days in DM or stimulated with LPS for 12 hours showed elongated morphology and adherence. Cells were photographed using a digital camera assembled on a bright field inverted microscope. Original magnification was 40×.

We aimed to detect the isoforms in the cellular secreted fraction by Western blot means. However, individual secreted IL-22BP isoforms could not be resolved in the culture medium of moDCs (**Figure 39A**) or following a concentration of medium with acetone (AP) (**Figure 39B**). We also noticed that the signal detected for IL-22BP in the CLs (**Figure 39**) presented similar patterns of bands to those found in **Figure 38D**: two bands close to 34 kDa plus an additional, more intense band close to 43 kDa. It is of note that a certain degree of heterogenicity was found in the amount of IL-22BP in the AP among donors; the bands observed in the AP fractions in **Figure 39** exhibited different intensities, while the bands of IL-22BP in donor N6, but not N5, displayed a band at around 50 kDa, reduced under LPS stimulus, that could correspond to IL-22BPi2.

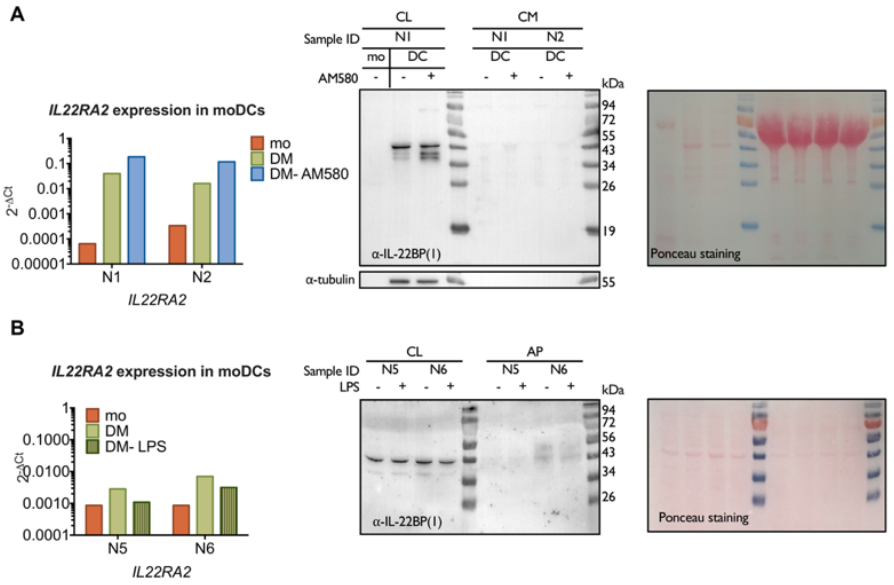

Figure 39: IL22BP isoforms are not detected in the cultured medium of monocyte-derived dendritic cells (moDCs) by immunoblotting. *(A) moDCs and conditioned media (CMs) were harvested after 6 days in DM ± AM580 from two healthy controls (N1 and N2) and immunoblotted for detection of IL-22BP using tubulin and Ponceau staining as loading controls. IL-22RA2 mRNA expression was measured by RT-qPCR from the same cells and normalized to the housekeeping gene ACTB. Cell lysates (CLs) reflect the mRNA expression levels; however, there is no signal in the CM. Ponceau staining served as a loading control. (B) moDCs from two healthy controls (N5 and N6) and their CMs were harvested after 6 days in DM ± LPS. On the day of collection, cells were carefully washed five times with prewarmed serum-free medium (SFM) to remove abundant serum proteins, and fresh SFM containing L-glutamine was added for a further 4 hours prior to acetone precipitation and recovery of CLs. Acetone precipitates (APs) and CLs were immunoblotted for detection of IL-22BP using Ponceau staining as a loading control. IL-22RA2 mRNA expression was measured by RT-qPCR from the same cells. CLs reflect the mRNA expression levels; however, there is no signal in the APs.*

We also removed N-linked glycans by enzymatic deglycosylation, as the presence of this moieties can sometimes interfere with antibody detection and sensitivity. However, the CMs' deglycosylation with peptide N-glycosidase F (PNGase F) did not result in any differential reactive band in any of the three donors relative to the negative control for any of the three antibodies used (**Figure 40**, u*pper three blots).* The Ponceau staining included in **Figure 40** (lower blots) for each Western blot membrane

revealed successful PNGase F activity, as relatively lower bands appeared. Moreover, this unspecific protein staining also revealed a high number of proteins around 34–56 kDa in all conditions, which likely correspond to the 10% FBS included in the basal culture media and which bind to secondary HRP-conjugated antibodies (middle horizontal blots), thus generating a high background and unspecificity. Therefore, secreted levels of IL-22BP by moDCs seem to be low or under the detectable limits by Western blot.

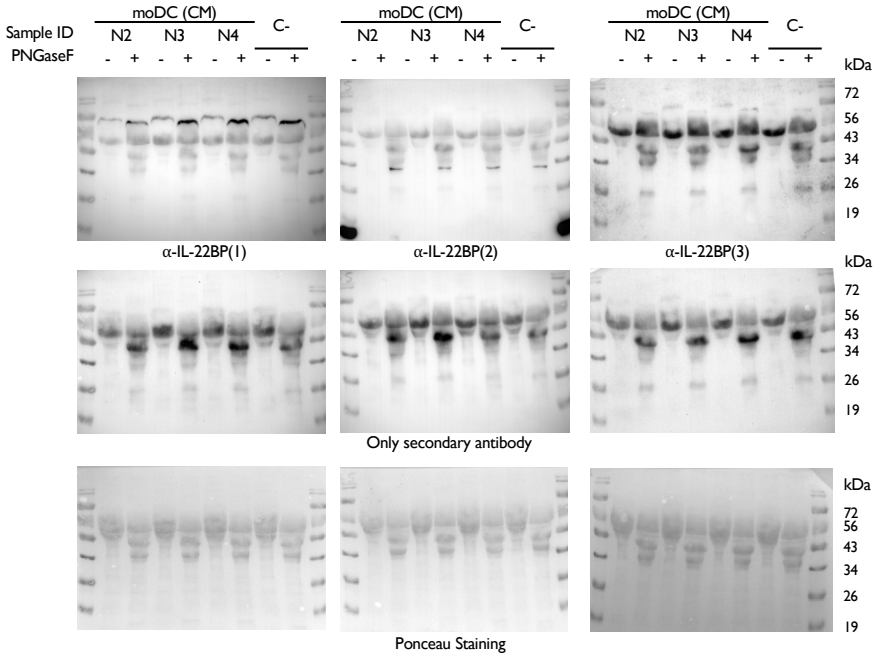

Figure 40: IL-22BP is not detected in the cultured medium of monocyte-derived dendritic cells (moDCs) by immunoblotting. *moDC conditioned media (CMs) from three different healthy donors (N2, N3, and N4) was collected after 6 days in differentiation media (DMs). Then, 20 µl of each or culture media without cell contact (C-) were subjected to PNGase F treatment to enhance detectability of secreted IL-22BP proteins and immunoblotted for detection of IL-22BP with three different anti-IL-22BP antibodies. Before primary antibody incubation, membranes were immunoblotted with the corresponding secondary-HRP conjugated antibody. Notice the high antibody reactivity with the serum that is present in the CM. Ponceau staining indicates equal loading volumes. We did not detect specific proteins in the CM of moDC reactive with any of the three antibodies used.*

We also wondered whether the immortalized monocytic U937 cell line, which also produced the three *IL22RA2* transcripts (**Figure 37**), cultivated in DM also produced increased levels of *IL22RA2* mRNA and IL-22BP protein levels as those in moDCs. To evaluate that, we analysed the *IL22RA2* mRNA expression using best coverage primers as well as the expression of the IL-22BP protein levels in the CLs and in the medium by ELISA and flow cytometry means (**Figure 41**). U937 cells cultivated in DM produced higher levels of IL22BP immunoreactivity in both CLs and culture medium than those cultivated in RPMI medium in accordance with mRNA levels (**Figure 41A**). Measured by flow cytometry using a mouse monoclonal Ab, the IL-22BP-positive fluorescence intensity of U937 cells was 71.5% in DM versus 17.4% in RPMI (**Figure 41A**). Comparable to its effect on *IL22RA2* mRNA levels, AM580 augmented IL-22BP detection by ELISA in U937 CLs, while maturation with LPS, which inhibits *IL22RA2* gene expression, reduced these levels (**Figure 41B**). Similar to moDCs (**Figure 38A**), gradually increasing levels of *IL22RA2* mRNA were observed in U937 cells by qPCR over the cultivation period (**Figure 41B**). Additional experiments were conducted to detect IL-22BP in the monocytic U937 cell line by Western blot using distinct anti-IL-22BP antibodies. In this regard, moDCs and non-derived DCs were subjected to glycan removal with PNGase F or Endo H. Reactive bands corresponding to the molecular weight of isoform 2 were only observed in the CLs of monocyte-derived U937 cells (**Figure 41C**).

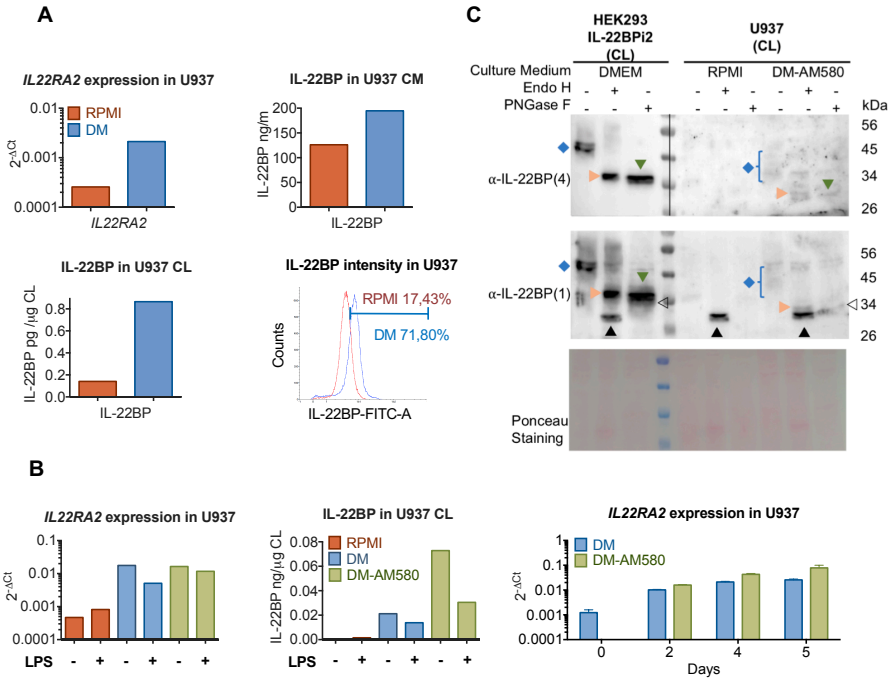

Figure 41: IL22BP protein levels reflect IL22RA2 mRNA levels produced by monocyte-derived U937 cells. *(A) Experiment showing correlation between IL22RA2 mRNA expression and IL-22BP protein levels in U937 cells grown in RPMI or differentiation media (DMs) for 6 days. (Left) IL22RA2 mRNA expression measured by RT-qPCR normalized to ACTB, (second) IL-22BP protein levels in the conditioned medium (CM) and cell lysates (CLs) (third) measured by ELISA, and IL-22BP intracellular fluorescence measured by flow cytometry (right). (B) Experiment showing effect of LPS on IL22RA2 mRNA normalized to ACTB (left) and IL-22BP levels in U937 CLs cultured for 6 days ± AM580 (middle). (Right) IL22RA2 expression, measured by RT-qPCR in U937 and normalized to GAPDH housekeeping gene, increases over the cultivation time in DM ± AM580 (mean ± SEM; n = 2). (D) U937 cells were harvested after 6 days of culture in RPMI or DM supplemented with AM580. HEK293 cells were transfected as in (A). CLs were treated with or without PNGase F or Endo H and immunoblotted for detection of IL-22BP with different antibodies. Ponceau staining indicates equal loading quantity. Glycosylated IL-22BPi2, Endo H, and PNGase F products are denoted by a blue diamond, an orange arrowhead, and a green inverted triangle, respectively. Black triangles and open arrowheads indicate the reactivity of the antibody α-IL-22BP (1) for Endo H and PNGase F enzymes, respectively. Anti-IL-22BP immunoreactive bands have a higher Mr in HEK293 compared to U937 cells due to the added myc-FLAG affinity tag. The vertical line separates parts of the same membrane under different exposures (left part, short; right part, long).*

Thus, changes in *IL22RA2* gene expression levels in $CD14^+$ monocytes or the U937 cell line through cultivation in DM, the addition of AM580, and/or TLR maturation signals are associated with equivalent changes in IL-22BP levels in naturally producing cells. The absence of detection of reactive bands in the CM by WB may be due to the low levels of secreted IL-22BP, as detected by ELISA. Therefore, in the next section, we used recombinant expression vectors transfected into HEK293 cells to gain further insight into the mechanism governing the secretion of IL-22BPi1, IL-22BPi2, and IL-22BPi3.

5.3 *In vitro* characterization of IL-22BP isoforms

Due to the low levels of protein detection and the difficulty to discriminate among isoforms in the natural producer cells, we decided to characterize them by means of recombinant systems in order to better understand their production and secretion. Vectors expressing IL-22BPi2 and IL-22BPi3 were commercially available, and an expression vector for IL-22BPi1 was constructed from moDCs mRNA.

5.3.1 Cloning of IL22RA2v1 into pCMV6-entry vector

The cDNA coding for *IL22RA2v1* was amplified from retrotranscribed RNA extracted from immature moDCs and cloned into pCMV6-entry vector following the strategy indicated in **Figure 42**. Two overlapping fragments were produced with primers including terminal MluI and SgfI restriction sites. The overlapped final fragment and pCMV6-entry empty vector were digested with MluI and SgfI restriction enzymes and ligated. The results from the cloning steps are presented in **Figure 43**.

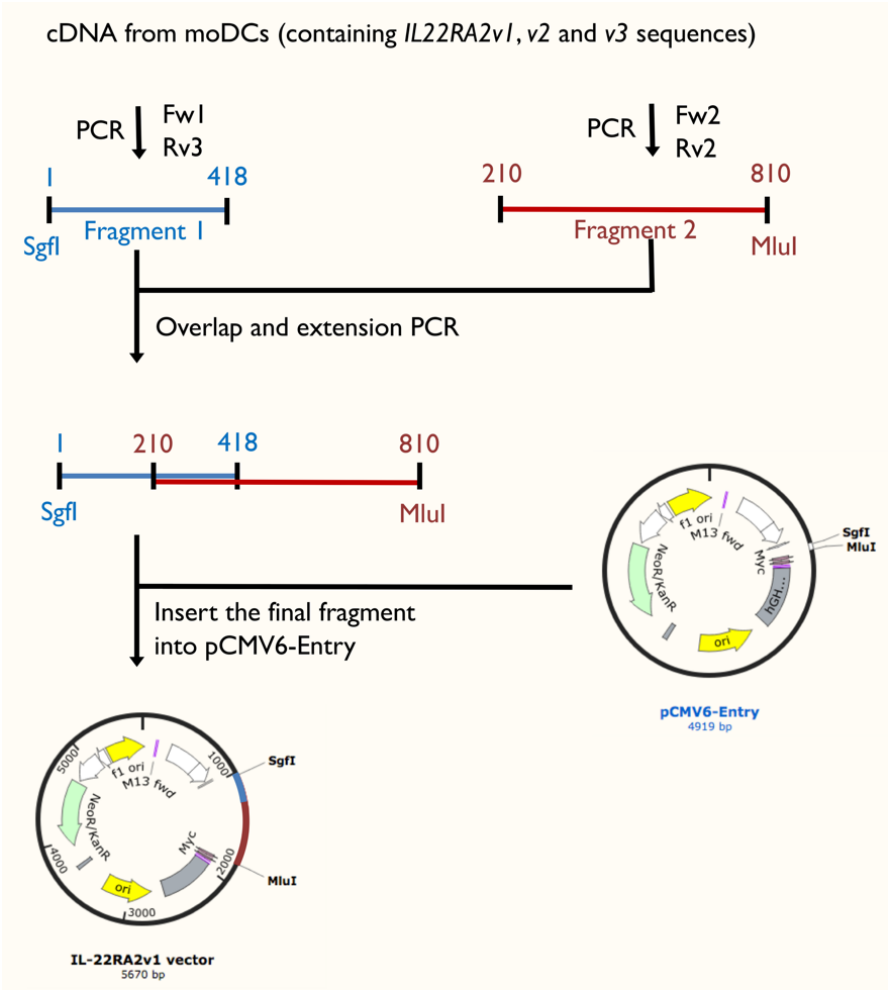

Figure 42: Cloning strategy of IL22RA2v1 into pCMV6-entry vector.

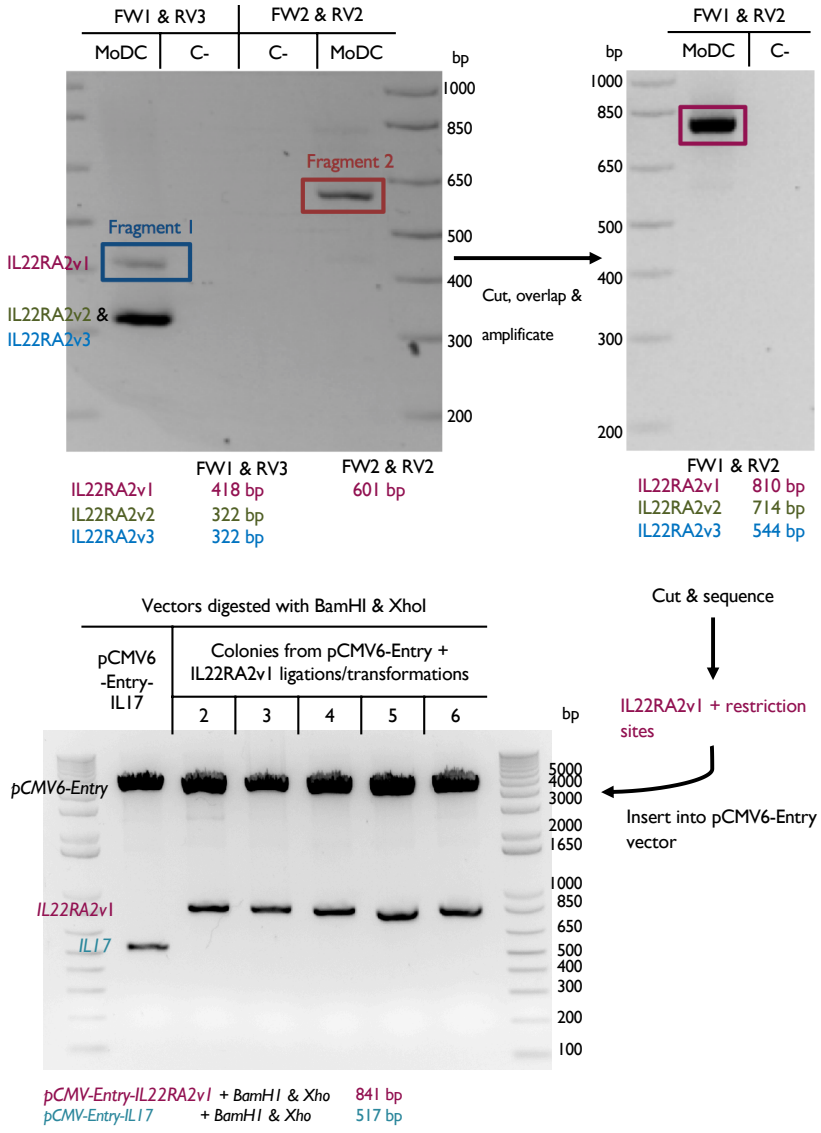

Figure 43: Cloning IL22RA2v1 sequence into pCMV6-entry vector. *The cDNA coding for IL22RA2v1 was initially amplified with Pfu polymerase from two overlapping fragments with primers including terminal MluI and SgfI restriction sites, starting from retrotranscribed RNA extracted from immature monocyte-derived dendritic cells (moDCs). The polymerase chain reaction (PCR) product and pCMV6-entry vector were digested with MluI and SgfI restriction enzymes and ligated. The ligation product was verified by enzymatic digestion with BamH1 and XhoI restriction enzymes, and IL17pCMV6-entry vector served as the negative control.*

5.3.2 IL-22BP isoform expression in transfected HEK293 cells

C-terminally myc-FLAG-tagged *IL22RA2v1*, *IL22RA2v2*, and *IL22RA2*v3 expression plasmids were individually transfected into HEK293 cells. *IL22RA2* mRNA expression and secreted IL-22BP levels were subsequently measured by RT-PCR and ELISA, respectively, and intracellular expression was determined by densitometry of immunoblotted CLs (**Figure 44**). While high levels of IL-22BPi2 were observed in the culture medium (**Figure 44C**), those of both IL-22BPi1 and IL-22BPi3 were much lower, even if transfection efficiencies, measured by RT-qPCR through quantification of mRNA levels, were similar (**Figure 44A).** Conversely, intracellular levels of IL-22BPi1, but not of the other two isoforms, continuously increased over time after transfection (**Figure 44B**), suggesting that the former's poor secretion was related to preferential intracellular accumulation.

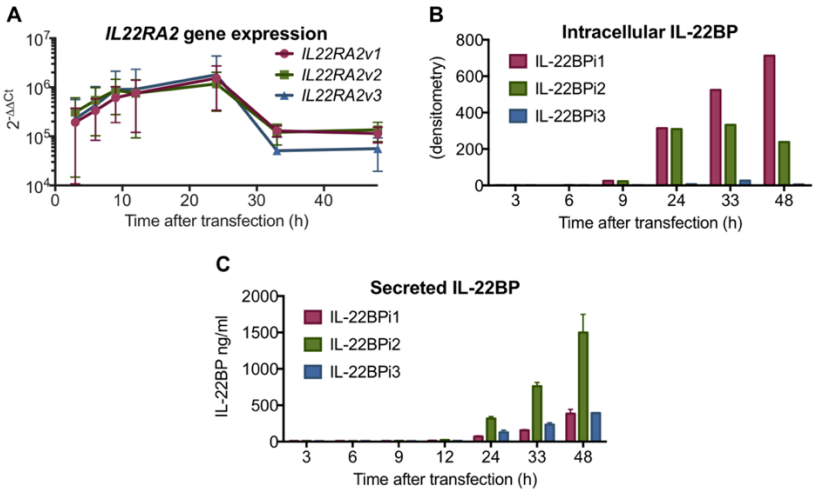

Figure 44: Differential secretion of IL-22BP isoforms. *HEK293 cells were transiently transfected with expression vectors encoding IL-22BPi1, IL-22BPi2, IL-22BPi3, or empty vector as a negative control for 24 hours (A) Transfection efficiency was measured by IL22RA2 RT-qPCR relative to the housekeeping gene GAPDH (mean ± SEM; n = 3). (B) Intracellular IL-22BP isoforms were resolved by immunoblotting with FLAG antibody, IL-22BP immunoreactive bands were scanned and the arbitrary units corresponding to their densitometry scanning are represented, representative experiment out of three performed. (C) Secreted IL-22BP isoforms were measured by ELISA (mean ± SEM; n = 2).*

5.3.3 Secreted and intracellular IL-22BP detection by Western blot means

5.3.3.1 IL-22BPi2 is difficulty detected in CMs by WB means

Next, we compared the detection of secreted IL-22BPi2 with a series of human recombinant secreted cytokines that were, like IL-22BPi2, expressed with C-terminal myc-FLAG tags. In contrast to these cytokines, IL-22BPi2 was not detected in the cell culture medium by Western blotting using an anti-FLAG antibody; however, the intensity of the detection signal of this protein in the CLs was comparable to the other cytokines that were secreted (**Figure 45)**.

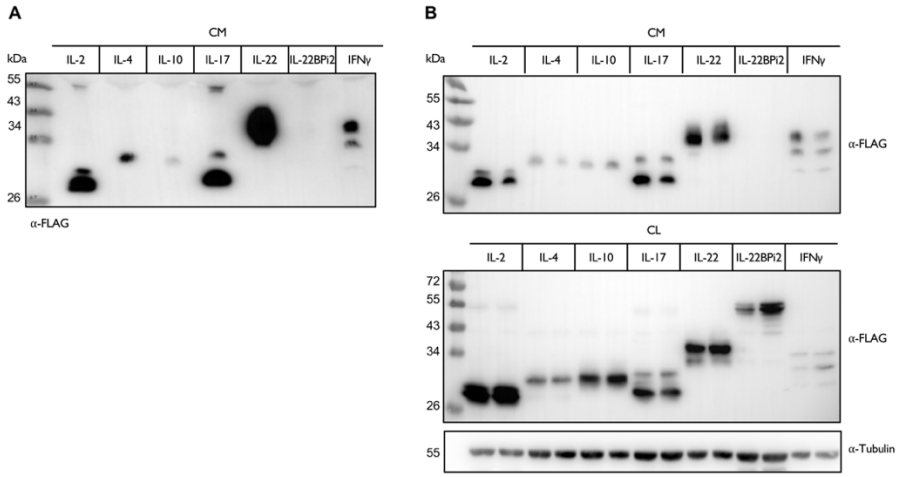

Figure 45: Secreted recombinant IL-22BPi2 is not detected by Western blot in unconcentrated conditioned media (CMs). *(A) Single experiment where various cytokine expression vectors containing Myc-FLAG-tags, as indicated, were transiently transfected into HEK293 cells; after 24 hours, equal volumes of CMs were immunoblotted for FLAG. (B) Single experiment where various cytokine expression vectors containing Myc-FLAG-tags, as indicated, were transiently transfected into HEK293 cells; after 24 hours, CMs and cell lysates (CLs) were immunoblotted for FLAG and tubulin as loading controls; adjacent lanes are biological replicates.*

Finally, the secreted IL-22BPi2 signal was detected with different anti-IL-22BP antibodies after concentration of culture medium with acetone

(**Figure 46**). We also found that deglycosylation of the acetone-precipitated, secreted fraction with peptide N-glycosidase F (PNGase F, an enzyme that cleaves all N-linked glycans) enhanced the detection in all cases (**Figure 46**). Moreover, it was also noticed that in the absence of a reducing agent (e.g., β mercapthoethanol, βME), IL-22BPi2 reactive bands were detected at higher molecular mass values (around 72 kDa under PNGase F) in the case of antibodies with higher sensitivity – α-IL-22BP (1) and α-FLAG – thus suggesting that IL-22BPi2 could be forming homodimers and/or interacts with other proteins through disulphide bonds (**Figure 46**, *asterisk*). On the other hand, the lower mobility of IL-22BPi2 in the presence of βME is compatible with a reduction of disulphide bonds converting the protein to a more extended form with seemingly higher Mr.

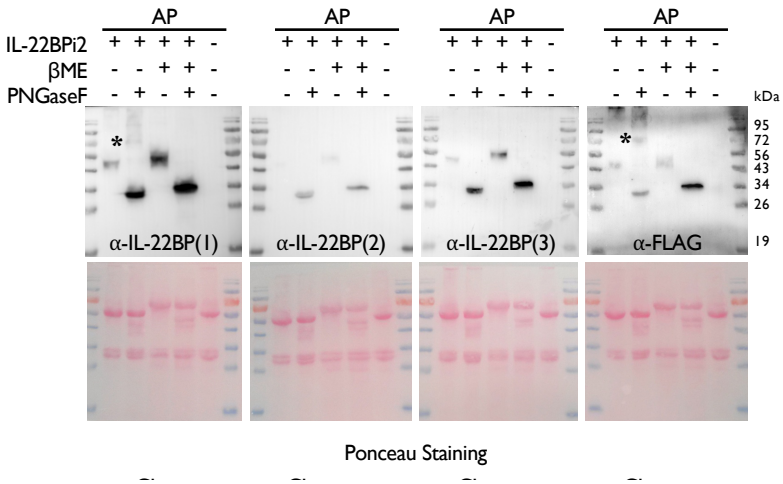

Figure 46: Secreted IL-22BPi2 detection by Western blot is enhanced upon deglycosylation. *HEK293 cells were transiently transfected with the expression vector encoding IL-22BPi2 or left untransfected. Twenty hours after transfection, cells were carefully washed five times with prewarmed serum-free medium (SFM) to remove abundant serum proteins, and fresh SFM containing L-glutamine was added for a further 4 hours prior to acetone precipitation. Then, 300 μL of conditioned medium (CM) was acetone-precipitated, treated with or without PNGaseF, and immunoblotted for IL-22BP with different antibodies under non- or reducing conditions (in the presence of β-mercaptoethanol, βME). Ponceau staining indicates equal loading volumes. Asterisks indicate IL-22BPi2 reactive bands detected around 72 kDa under non-reducing conditions and in the presence of PNGase.*

5.3.3.2 Detection of IL-22BPi2:IL-22 complex by Western blot means

We further explored the possibility of detecting IL-22BPi2 bound to IL-22 by Western blot means. We hypothesized that the presence of IL-22, which is the natural ligand for IL-22BPi2 in the extracellular space, may stabilize IL-22BP's lifetime or may interfere with the antibody detection, thereby masking its presence. We mixed and incubated equal volumes of CM from independently transfected HEK293 cells with IL-22BPi2 or IL-22 expression vectors. Mixed CMs and single ones (each condition contained the same amount of IL-22 or IL-22BPi2) were further acetone-precipitated and either treated or not treated with PNGase F. The presence of a reducing agent (i.e., βME) in the sample preparation was also considered as another condition. All conditions were immunoblotted against IL-22BP or IL-22 antibodies (**Figure 47**). No stabilization (increased signal) was observed in the immunoblots; however, we noticed that when they occurred together, IL-22BPi2, and not IL-22, was resistant to PNGase F deglycosylation (**Figure 47,** *purple arrowheads*). This may be due to the inaccessibility of IL-22BPi2 N-glycosylated sites to the enzyme when the complex is formed, and it therefore indicates that physical interaction between both has taken place. Nevertheless, this did not occur with IL-22, where all N-glycosylation sites appear accessible when bound to IL-22BPi2 (**Figure 47**). Moreover, apart from the interference in IL-22BP deglycosylation, IL-22 presence also decreased IL-22BPi2 detection levels under non-reducing conditions (**Figure 47**, *compare green arrowheads*). A decrease in detectability but not in the prevention from deglycosylation also occurred for IL-22; the presence of both proteins together reduced IL-22 detectability levels under non-reducing conditions (**Figure 47**, *compare blue arrowheads*). Furthermore, we did not find any band corresponding to the complex (which should be expected to be around 90 kDa); it is probable that the SDS present in the buffers and gel may have interfered and disrupted the complex.

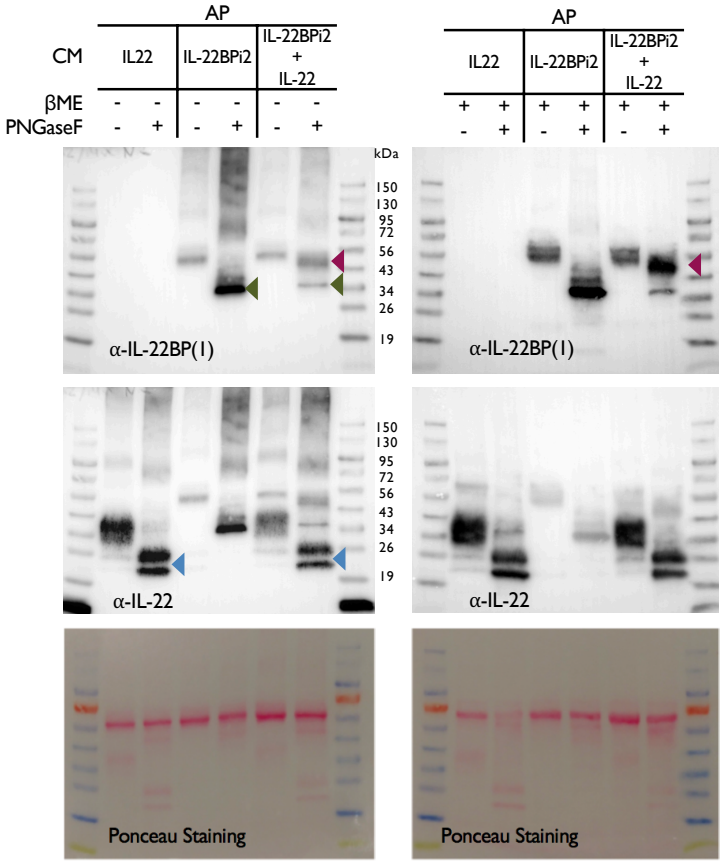

Figure 47: Secreted IL-22BPi2 is resistant to PNGaseF when complexed to IL-22. *HEK293 cells were transiently transfected with IL-22 or IL-22BPi2 expression plasmids. After 20 hours, cells were carefully washed five times with prewarmed serum-free medium (SFM) to remove abundant serum proteins, and fresh SFM containing L-glutamine was added for a further 4 hours prior to media collection and acetone precipitation. Conditioned media (CMs) were collected, and equal volumes were incubated for 1 hour at 37 ℃. After that time, different volumes of CM containing equal amounts of IL22BP or IL-22 and IL-22BP + IL-22 were acetone-precipitated (AP), treated ± PNGase F, and then resolved by SDS-PAGE under reducing or non-reducing conditions (± β-mercapthoethanol; ± βME) and immunoblotted against IL-22BP (upper blots). The same membranes were sequentially reproved with IL-22 antibody without regeneration of the membrane; that is why IL-22BP reactive bands are still present. Ponceau staining indicates equal loading volumes. Purple arrowheads indicate that IL-22 makes IL-22BP resistant to PNGase F deglycosylation. Green arrowheads point out evidence that the presence of IL-22 also decreased IL-22BPi2 detection levels under non-reducing conditions. Blue arrowheads indicate that the presence of both proteins together reduced IL-22 detectability levels under non-reducing conditions.*

5.3.3.3 IL-22 and IL-22BPi2 detection with binding proteins

We also evaluated the possibility of detecting IL-22 or IL-22BPi2 in CLs and in CMs by far-Western blotting. In brief, we resolved CLs and CMs from HEK293 cells independently transfected with IL-22 or IL-22BPi2 expression vectors under the presence or absence of a reducing agent (i.e., βME). We further incubated the membranes with IL-22- or IL-22BPi2-containing CMs to allow for direct protein-protein binding, followed by incubation with IL-22 or IL-22BP antibodies in order to detect the complex. The results (**Figure 48**) indicate that we were capable of detecting IL-22BPi2 in the CMs through IL-22 but not in the cytosol, and this detection was favoured under non-reducing conditions. However, the detection of IL-22 through IL-22BPi2 was not possible (**Figure 48**). This could be because after protein-protein interaction, the epitope from IL-22BP recognized by the antibody is no longer accessible, or because IL-22 and IL-22BPi2 do not interact in this specific setting.

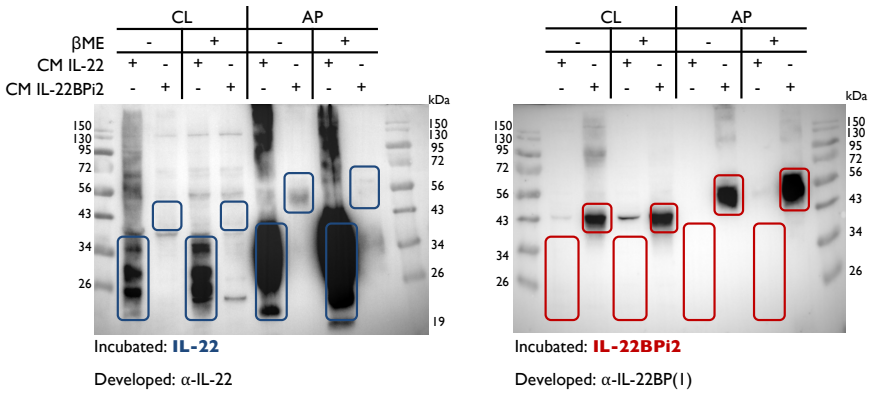

Figure 48: IL-22BPi2 and IL-22 detection by far-Western blotting. *HEK293 cells were transiently transfected with IL-22 or IL-22BPi2 expression plasmids. Twenty hours later, conditioned media (CMs) were removed and stored; cells were carefully washed five times with prewarmed serum-free medium (SFM) to remove abundant serum proteins; and fresh SFM containing L-glutamine was added for a further 4 hours prior to acetone precipitation and recovery of cell lysates (CLs). Acetone precipitates (APs) and CLs were resolved by SDS-PAGE under reducing or non-reducing conditions (± β-mercapthoethanol; ± βME). Membranes were incubated with IL-22 or IL-22BP CM for 2 hours at 37 ℃, as indicated. Membranes were further immunoblotted against IL-22BP or IL-22 with the corresponding antibodies. Elongated and square blue boxes indicate the direct detection of IL-22 and the*

indirect detection of IL-22BP, respectively, by IL-22 ab. Elongated and square red boxes indicate the indirect detection of IL-22 and the direct detection of IL-22BP, respectively, by IL-22BP ab.

Similar to this approach, we also investigated whether the interaction between IL-22 and IL-22BPi2 might decrease the interaction with the detection antibody due to steric hindrance or competition for the binding site. For this purpose, immobilized IL-22 or IL-22BPi2 in PVDF membranes were incubated with their corresponding ligand (IL-22BPi2 or IL-22, respectively, **Figure 49**). We were only able to detect interaction when IL-22BPi2 was incubated with the immobilized IL-22; the other way around did not result in any interference in the detecting signal (**Figure 49**, blue-lined and dashed squares). This may be related to size, since IL-22 is smaller than and shielded by the larger IL-22BPi2.

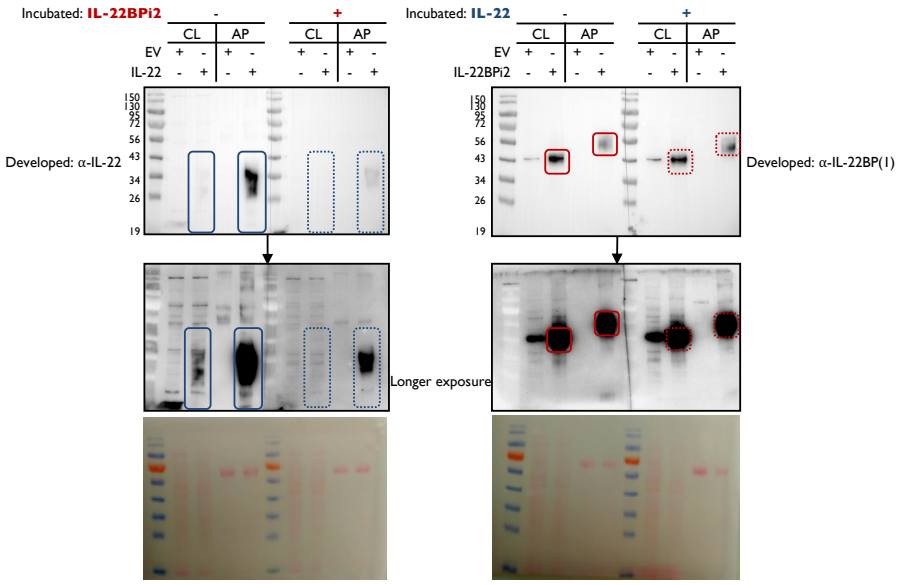

Figure 49: IL-22BPi2 and IL-22 detection by a decrease in the signal of Western blot. *HEK293 cells were transiently transfected with empty vector (EV), IL-22, or IL-22BPi2 expression plasmids. Twenty hours later, conditioned media (CMs) were removed and stored. Cells were carefully washed five times with prewarmed serum-free medium (SFM) to remove abundant serum proteins, and fresh SFM containing L-glutamine was added for a further 4 hours prior to acetone precipitation and recovery of cell lysates (CLs). Acetone precipitates (APs) and CLs were resolved by SDS-PAGE under reducing conditions. Membranes were*

incubated with IL-22 or IL-22BP CM for 2 hours at 37ºC, as indicated. Membranes were immunoblotted against IL-22BP or IL-22, as indicated. Elongated solid- and dotted-lined blue boxes indicate the direct detection of IL-22 in the absence and presence of IL-22BP protein, respectively, by IL-22 ab. Square solid- and dotted-lined red boxes indicate the direct detection of IL-22BPi2 in the absence and presence of IL-22 protein, respectively, by IL-22BP ab.

Thus, the three approaches – IL-22:IL-22BP complex deglycosylation, far-Western blotting, and incubation with binding proteins – revealed that recombinant IL-22 and IL-22BPi2 were capable of undergoing interaction together and that this interaction, *albeit* with the mentioned limitations, could be detected by Western blot means.

5.3.3.4 Secreted recombinant IL-22BPi2 is not efficiently purified by FLAG immunoprecipitation

Finally, to increase the detection of the secreted signal of recombinant IL-22BPi2, we purified the secreted fraction of transiently transfected HeLa cells with IL-22 or IL-22BP expression plasmids with FLAG agaroses. However, we observed (**Figure 50**) that the purification of the secreted fraction for the first 24 hours after transfection (where the secretion is the highest, as shown in **Figure 44**) was not as efficient as the acetone precipitation, even if this was from the secreted fraction corresponding from 24 hours after transfection to 48 hours. Moreover, we observed that FLAG agaroses purified IL-22 more efficiently than IL-22BPi2, suggesting that the FLAG tag in the IL-22BPi2 mature protein may somehow not be easily accessible to the antibody.

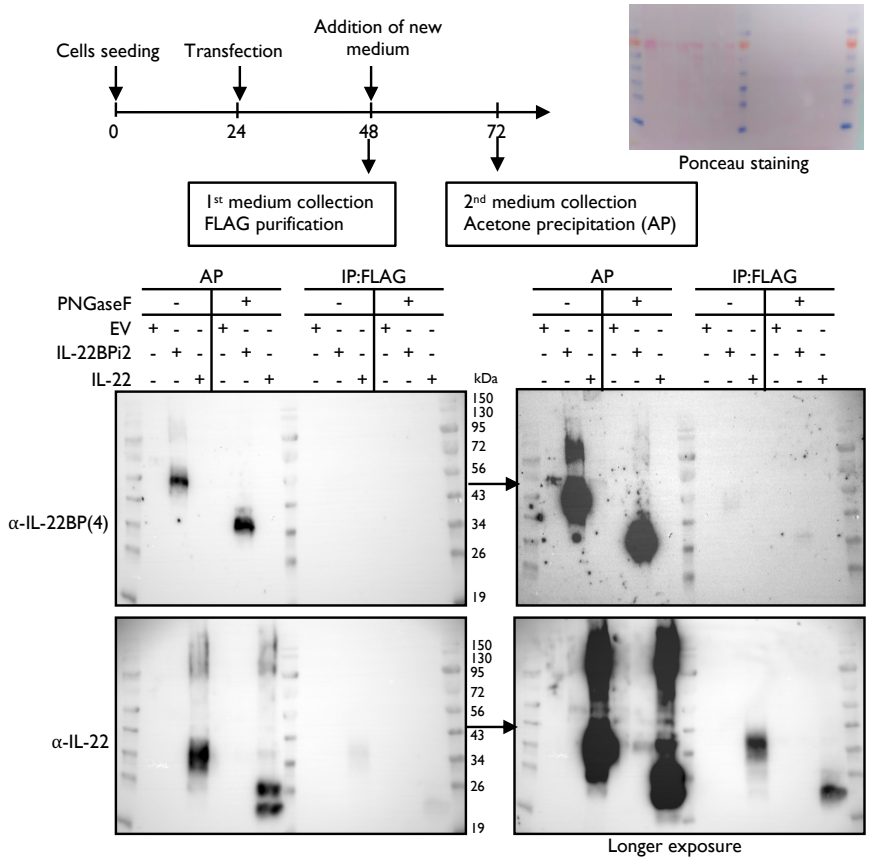

Figure 50: Conditioned medium (CM) containing IL-22BPi2 is not efficiently purified. *HeLa cells were individually transfected with expression plasmids for IL-22BPi2, IL-22, or empty vector (EV); 24 hours after transfection, CMs were collected, co-immunoprecipitated (IP) with FLAG agaroses, and eluted (IP-FLAG fractions). Cells were carefully and sequentially washed five times with prewarmed serum-free medium (SFM) to remove abundant serum proteins, and fresh SFM containing L-glutamine was added for a further 24 hours prior to acetone precipitation. Acetone precipitates (APs) and immune-purified FLAG CM were treated ± PNGase F and resolved by SDS-PAGE under reducing conditions. Membrane was incubated with IL-22 or IL-22BP antibodies. Membrane was subjected to longer exposure times for low signals.*

5.3.4 Detection of IL-22BPi2, IL-22, and IL-22BPi2:IL-22 complex by ELISA

During the completion of this research, the number of validated antibodies and ELISAs available for IL-22BP detection was limited.

Indeed, a recent claim is that one of the reasons that IL-22BP is a vastly understudied aspect of IL-22 biology is in part because there are few commercially available reagents, and those that do exist are difficult to authenticate (Zenewicz, 2018).

Therefore, we developed and evaluated three in-house sandwich ELISAs for the detection of secreted IL-22, IL-22BPi2, and IL-22:IL-22BP complex. To validate them, we used the CMs produced by HEK293 cells transiently transfected with IL-22 or IL-22BPi2 expression plasmids. For the complex, a 2-hour incubation period of equal volumes of independently secreted media was held. The conditions were the same as those presented in **Figure 47**, including PNGase F treatment. For IL-22 detection, we used two antibodies: a rabbit and a goat polyclonal; for IL-22BP detection, we also used two antibodies: a rabbit polyclonal and a mouse monoclonal. We went through all possible pair set combinations and evaluated them with the same CMs. The results obtained are illustrated in **Figure 51**. The ELISA for IL-22 composed of α-IL-22 (goat) coating Ab/α-IL-22 (rabbit) detection Ab showed the same signal for IL-22 regardless of the presence or absence of IL-22BPi2, suggesting that the binding to IL-22BPi2 does not interfere with the detection (**Figure 50A,** *left*). It was noticeable that the detection signal increased after deglycosylation. The ELISA composed of the same antibodies but in a different order – α-IL-22 (rabbit) coating Ab/α-IL-22 (goat) detection Ab – displayed similar trends; however, it was less sensitive (**Figure 50A,** *right*). The ELISA for IL-22BP, the α-IL-22BP (mouse) coating Ab/α-IL-22BP (rabbit) detection Ab pair set, exhibited a strong detection capacity for IL-22BP that increased after the deglycosylation, in line with what was previously observed by Western blotting (**Figure 46**). When IL-22 is present in the sample, the amount of IL-22BP detected decreased (**Figure 50B,** *left*); this was also observed in previous experiments by Western blotting (**Figure 47**, *upper left*). The ELISA composed of the same antibodies but the other way around – α-IL-22BP (rabbit) coating Ab/α-IL-22BP (mouse) detection Ab – exhibited similar trends, but it was less sensitive (**Figure 50B,** *right*). Finally, in the ELISA developed for IL-22:IL-22BP complex, two of the three antibody pairs sets gave no signal (α-IL -22BP [mouse] coating Ab/ α-IL -22 [goat]

detection Ab and α-IL -22BP [rabbit] coating Ab/ α-IL -22 [goat] detection Ab) (**Figure 50C**, *left and right*); this was in line with the previous results suggesting that α-IL-22 (goat) antibody was not sensitive enough as a detection antibody (**Figure 50A,** *right*). The combination of α-IL-22BP (mouse) coating Ab/α-IL-22 (rabbit) detection Ab yielded the highest detection levels, although with high background noise; there was an increase in the detection when the complex was deglycosylated, but there was also a relatively high signal when IL-22 was present alone; this could be due to an incomplete blocking step or contamination with IL-22BP (**Figure 50C**, *middle*).

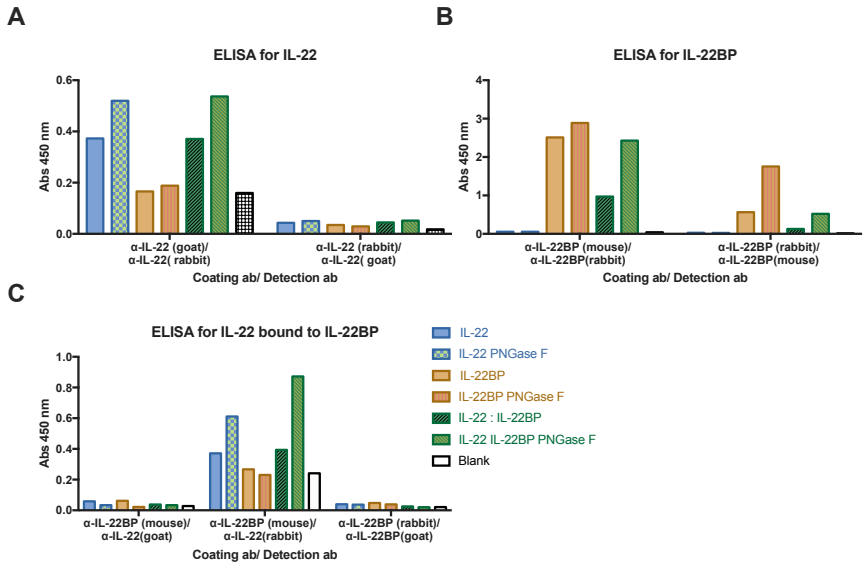

Figure 51: Detection of secreted IL-22, IL-22BP, and IL-22:IL-22BP complex by ELISA. *HEK293 cells were transiently transfected with IL-22 or IL-22BPi2 expression plasmids. After 20 hours, cells were carefully washed five times with prewarmed serum-free medium (SFM) to remove abundant serum proteins, and fresh SFM containing L-glutamine was added for a further 4 hours prior to media collection and acetone precipitation. Conditioned media (CMs) were collected, and equal volumes were incubated for 1 hour at 37℃. After that time, CMs were acetone-precipitated, treated ± PNGase F, and reconstituted in PBS. All samples were analysed by a different combination of antibodies indicated in the x-axes of each sandwich ELISA. A, B, and C represent the absorbance values measured at 450 nm for IL-22, IL-22BP, and IL-22:IL-22BP complex detection, respectively.*

We continued developing an ELISA for the detection of both intracellular and secreted IL-22BPi2. As such, a comparison of a commercial ELISA (from CUSABIO) with two developed in-house sandwich ELISAs was done. The first in-house ELISA was the one that gave the highest signal in **Figure 50B** *left*, (α-IL-22BP [mouse] coating Ab/α-IL-22BP [rabbit] detection Ab), and the other one was made using the same antigen-affinity-purified goat polyclonal antibody for both capture and detection; the difference between them was that the detection Ab was biotinylated, whereas the capture Ab was not. The comparison of the three ELISAs (**Figure 52**) demonstrated that the commercial one did not work with the samples analysed, and the one developed with the goat polyclonal pair sets was the most sensitive of the three for both intracellular and secreted IL-22BPi2. The sensitivity of the standard curve reached the standard of 30 pg/ml of recombinant protein. We used this ELISA for all analyses in this thesis.

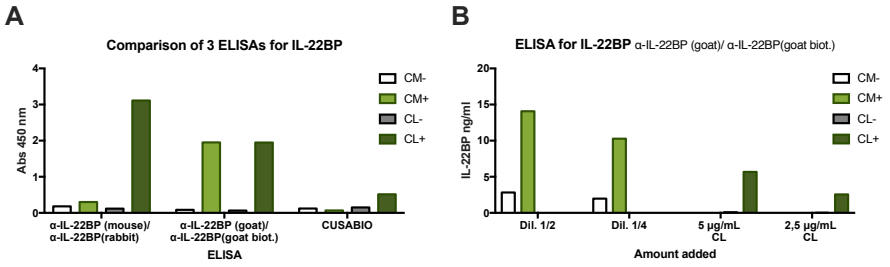

Figure 52: Detection of secreted and intracelularIL-22BPi2 by ELISA. *HEK293 cells were transiently transfected with IL-22BPi2 or empty expression plasmids as negative controls. After 24 hours, conditioned media (CMs) were collected, and cell lysis was performed. (A) All samples, CMs, and cell lysates (CLs) were analysed by a different combination of antibodies indicated in the x-axis of each sandwich ELISA. Bars represent the absorbance values measured at 450 nm. (B) Different dilutions of CMs and amounts of total CLs were measured in the ELISA that gave the best results in A (middle).*

5.3.5 IL-22BPi1 is not efficiently secreted

Similar to secreted IL-22BPi2, IL-22BPi3 was detected with anti-FLAG after concentration of the culture medium with acetone, while IL-22BPi1 was not detected (**Figure 53A**). We also found that secreted IL-22BPi2 was

resistant to endoglycosidase H (Endo H, which cleaves within the chitobiose core of high-mannose but not complex glycans) but not to peptide N-glycosidase F (PNGase F), and compared to the cell-associated protein, secreted IL-22BPi2 gained around 8 kDa in molecular mass (56 kDa versus 48 kDa). All of this reflected the sole presence of complex *N*-glycans and thus transit via Golgi (**Figure 53A,** *rightmost panel*). Treatment of CLs with PNGase F or Endo H revealed that the three intracellular isoforms contain high-mannose-type *N*-glycans (**Figure 53**) compatible with the three predicted *N*-glycosylation sites for IL-22BPi1 and IL-22BPi2, and one for IL-22BPi3 (NetNGlyc 1.0 server; **Figure 24**), and that the majority of the three intracellular IL-22BP isoforms detected correspond to the non-mature forms.

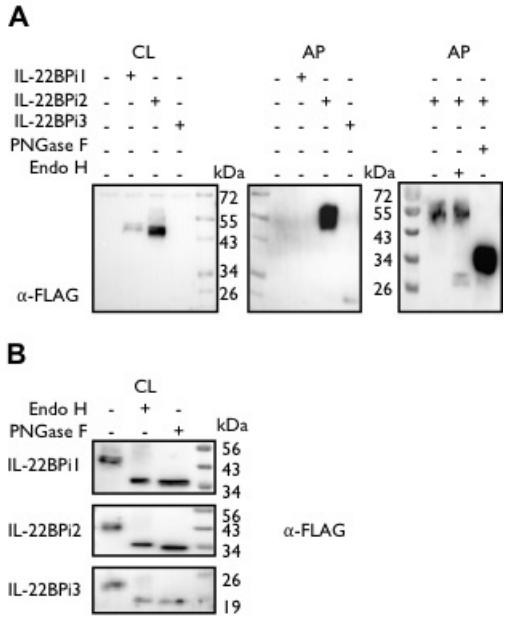

Figure 53: IL-22BPi1 is not efficiently secreted. *HEK 293 cells were transiently transfected for 24 hours with the indicated IL-22BP isoform expression plasmids. Twenty hours later, conditioned media (CMs) were removed; cells were carefully washed five times with prewarmed serum-free medium (SFM) to remove abundant serum proteins, and fresh SFM containing L-glutamine was added for a further 4 hours prior to acetone precipitation and recovery of cell lysates (CLs). Acetone precipitates (AP) and CLs treated ± PNGase or EndoH were resolved by SDS-PAGE under reducing conditions. (A) Detection of IL-22BP isoforms in CLs and APs by FLAG Ab. (B) Detection of intracellular IL-22BP isoforms by FLAG Ab.*

5.3.6 Intracellular IL-22BP isoforms are located in the membranous organelles (MOs)

To exclude the possibility that the absence of IL-22BPi1 secretion could be due to insoluble aggregation and to identify the cellular location in which the IL-22BP isoforms were occurring, we performed sequential subcellular fractionations. We generated separate cytosolic, membranous organelle (MO), nuclear, and insoluble fractions (named 1, 2, 3, and 4, respectively), followed by immunoblotting. The cell fractionation revealed that the three IL-22BP isoforms were detectable in the MO fraction and that none of these proteins sedimented in the insoluble fraction as aggregates (**Figure 54**).

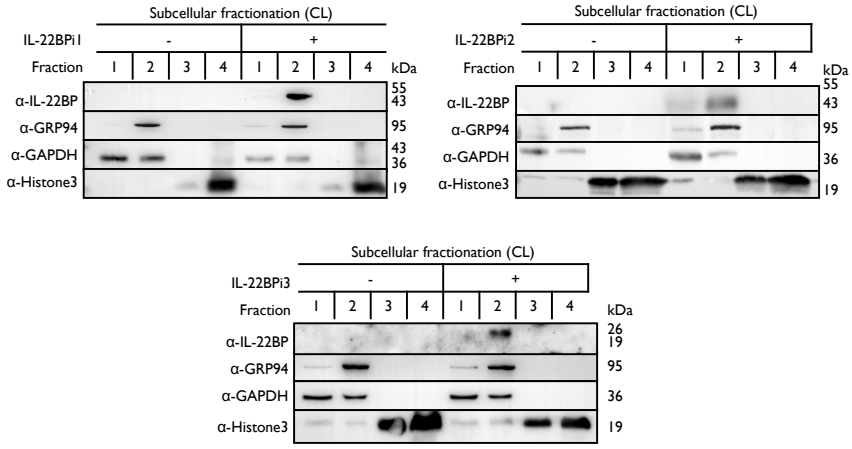

Figure 54: IL-22BP isoforms are located in the membranous organelles fraction. *HEK293 cells were transiently transfected with the indicated expression plasmids, and after 24 hours, cells were collected and fractionated following Holden and Horton's protocol (Holden & Horton, 2009). Equal amounts of protein per fraction were immunoblotted for GRP94, GAPDH, IL-22BP, and Histone 3. Fractions 1, 2, 3 and 4 represent cytosol, membranous organelles, nucleus and insoluble cell lysate (CL) fractions respectively.*

5.3.7 IL-22BPi1 and IL-22BPi2 are degraded by the proteasome

Moreover, we asked whether the poor secretion of IL-22BPi1 could be due to a high intrinsic tendency to misfold. Misfolded proteins are known to

be intercepted by the ER quality control system (ERQC) and delivered for ER-associated degradation (ERAD) by the proteasome (Smith, Ploegh, & Weissman, 2011). Thus, increased intracellular protein levels upon pharmacological inhibition of the proteasome point to misfolding reactions taking place. **Figure 55** illustrates increased levels of IL-22BPi1 and, noteworthy, also of IL-22BPi2 upon treatment of transfected cells with proteasome inhibitors, while IL-22BPi3 appeared not to be affected.

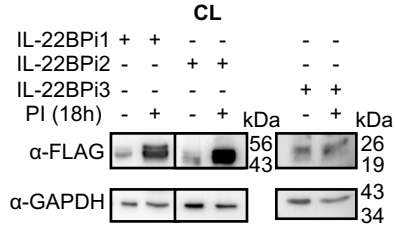

Figure 55: IL-22BPi1 and IL-22BPi2 are degraded by the proteasome. *HEK293 cells were transiently transfected with the indicated expression plasmids. After 24 hours, cells were treated with a mix of proteasome inhibitors (PI) (5 μM lactacystin, 5 μM MG132, and 1 mM epoxomicin). Eighteen hours later, cells were lysed and cell lysates (CL) immunoblotted for FLAG using GAPDH as a loading control.*

5.4 IL-22 'chaperones' the secretion of IL-22BPi2 and IL-22BPi3 but not that of IL-22BPi1

We tested the capacity of IL-22BPi1 to interact with IL-22 and also to neutralize its biological activity in both a bioassay and a co-folding assay. The first downstream signalling protein in the IL-22 cascade is the phosphorylation of STAT3. The bioassay was thus based on the capacity of IL-22BP to inhibit IL-22-induced STAT3 phosphorylation in the A549 adenocarcinomic human alveolar basal epithelial cell line – a cell line that has both heterodimers of the IL-22 surface receptor and does not express *IL22* or *IL22RA2* (Whittington et al., 2004). First, we transfected HEK293 cells with IL-22 expression vector; second, we determined the largest dilution of CM from transfected IL-22-HEK still able to induce maximal phosphorylation of STAT3 on Tyr705 residue in A549 cells; and third, we

determined the time point after the addition of IL-22 at which STAT3 phosphorylation was most pronounced (i.e., dilution 1/512 and 20 minutes, respectively [**Figure 56]**).

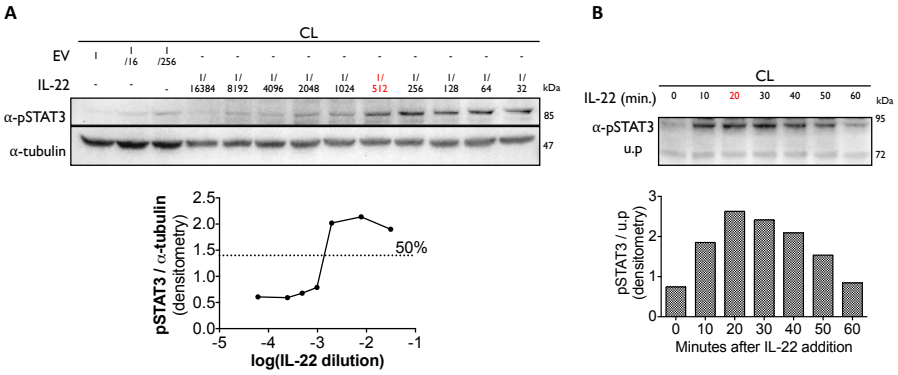

Figure 56: IL-22 induces STAT3 phosphorylation. *(A) A549 cells were exposed for 30 minutes to dilutions of IL-22-containing culture medium (CM) previously produced by IL22-transfected HEK293 cells. A549 cell lysates (CLs) were immunoblotted for pSTAT3 and tubulin as the loading control. The relative densitometry of pSTAT3 normalized to that of tubulin is also depicted. (B) A549 cells were treated with the optimum IL-22 dilution from A (1/512) for different periods of time, lysed, and immunoblotted for pSTAT3(Tyr^{705}). An unspecific protein band (u.p.) was used as the loading control.*

Next, we assayed the capacity of IL-22BPi1, IL-22BPi2, or IL-22BPi3 to inhibit the phosphorylation of Y705 in STAT3 induced by IL-22. Hence, we transfected HEK293 cells with IL-22BPi1, BPi2, or BPi3, and by ELISA, we determined the concentrations of IL-22BP in the CM. We then incubated different quantities of IL-22BPi1, IL-22BPi2, or IL-22BPi3 with the previously selected dilution of IL-22 (**Figure 56**) for 1 hour to allow for protein binding. Inhibition of STAT3 phosphorylation by IL-22BPi2 was consistently observed, while equal quantities of IL-22BPi1 did not impair IL-22-mediated STAT3 phosphorylation (**Figure 57A**); IL-22BPi3 inhibited STAT3 phosphorylation to a lesser extent than IL-22BPi2 (**Figure 57B**). Under the conditions of this assay, IL-22BPi1 therefore does not seem to neutralize the biological activity of IL-22.

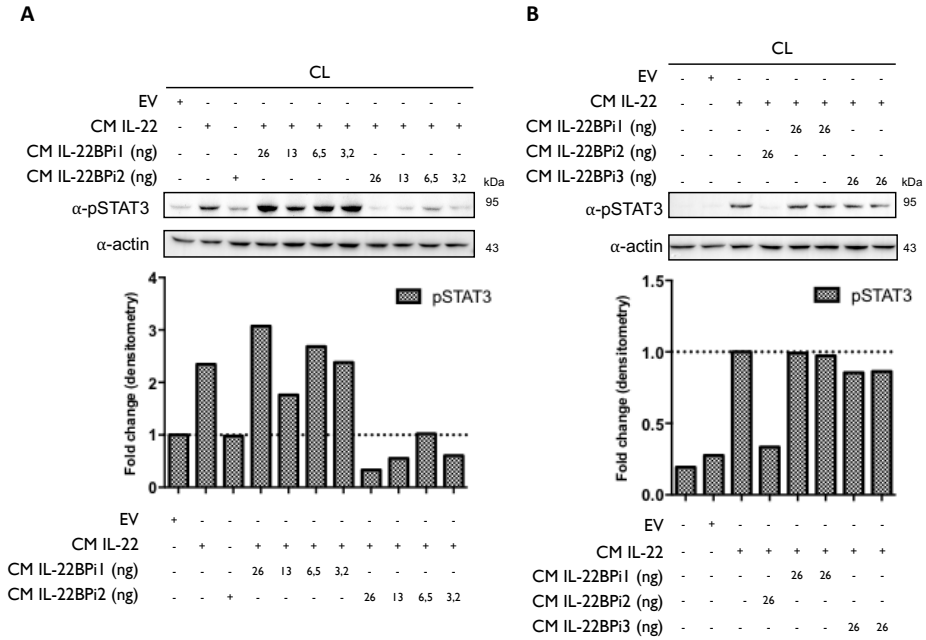

Figure 57: IL-22BPi1 does not inhibit pSTAT induced by IL-22. *(A and B) IL-22BP concentration in conditioned medium (CM) of transfected HEK293 cells was measured by ELISA, and the indicated amounts in nanograms (ng) of IL-22BPi1 or IL-22BPi2 were pre-incubated for 1 hour at 37°C with the selected IL-22 concentration from Figure 36. A549 cells were exposed to the pre-incubated combinations for 20 minutes. An excess of IL-22BPi2 was used as the phosphorylation blocking control (lane 3). After that time, cells were lysed and cell lysates (CL) were immunoblotted for pSTAT3 and actin as the loading control.*

For implementation of the co-folding assay, we found inspiration in earlier work done on IL-15 and IL-15R. In NK cells, the α-chain of the IL-15 receptor acts as a chaperone to stabilize IL-15 within the secretory tract against proteasome degradation and to export it in a complex to the membrane in its bioactive conformation (Bergamaschi et al., 2009; Mortier, Woo, Advincula, Gozalo, & Ma, 2008). It has recently been described that IL-22BP can be produced by a $CD4^+$ subset of tissue-infiltrating T lymphocytes from immune bowel disease (Pelczar et al., 2016). However, another study of immune cell subsets in IBD discarded T cells and confirmed myeloid cells as unique sources of *IL22RA2* mRNA in IBD (Fantou et al., 2019). Given that various subsets of lymphocytic cells (T and ILT) are known producers of IL-22 (Jia & Wu, 2014; Plank et

al., 2017), the theoretical possibility exists that IL-22BP and IL-22 may occur co-expressed in specific, yet-to-be-determined, natural circumstances. We thus asked whether, in the foldase- and chaperone-rich, folding-permissive environment of the ER, a cytokine-receptor co-assembly interaction may take place between IL-22 and IL-22BPi1, contingent upon the unstable partner in this case being the receptor and not the cytokine ligand, which indeed is efficiently secreted (**Figure 45A**). As demonstrated for IL-15/IL-15RA, these interactions can be reproduced in transfected human cell lines (Bergamaschi et al., 2009). We co-transfected the three isoforms of IL-22BP each with IL-22, or as negative control IL-17, which is a cytokine reported not to bind any IL-22BP isoform (Lim et al., 2016). Co-expression of IL-22BPi2 and IL-22 strongly decreased the intracellular level and increased the secreted level of the former in Western blot, suggestive of productive interactions taking place, thus enhancing the folding and/or transit of IL-22BPi2 (**Figure 58**). Increased secretion in the presence of IL-22 was not seen for IL-22BPi1. Furthermore, in ELISA, co-expression of IL-22 significantly enhanced the secretion of IL-22BPi2 and IL-22BPi3 but not that of IL-22BPi1 (**Figure 58C**). Co-expression of IL-17 did not have any effect on IL-22BP isoform levels (**Figure 58C**).

In light of these findings, the exon-4-encoded sequence in IL-22BPi1 appears to have disrupted this isoform's capacity for interaction with IL-22, in line with the previous hypothesis raised after the evaluation of the 3D-structure prediction and the site of insertion of this extra sequence in IL-22BPi2 (Section 5.1.4; p.129).

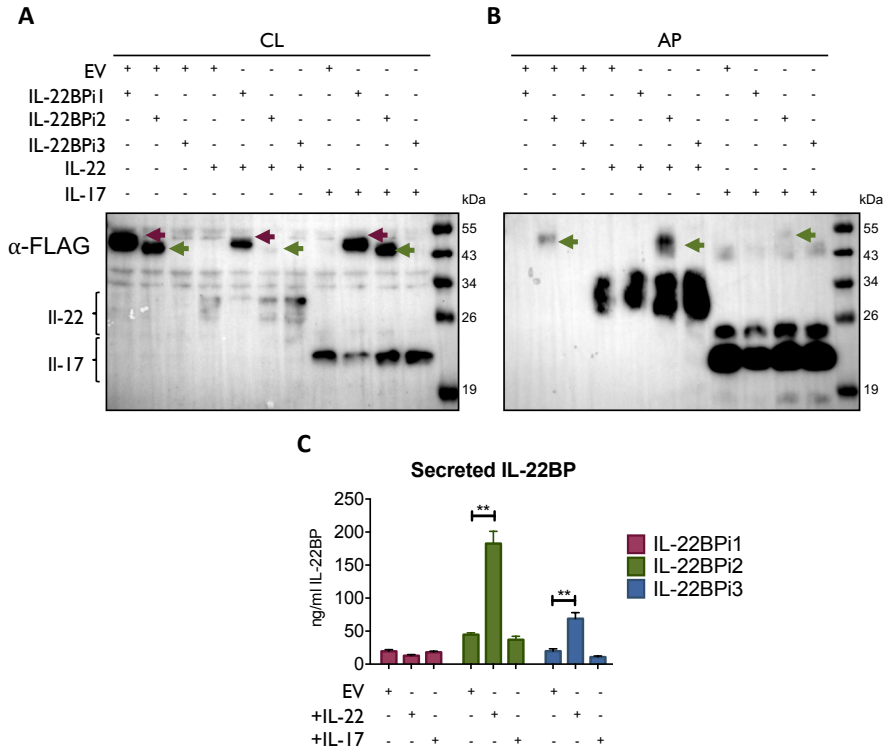

Figure 58: IL-22 enhances IL-22BP secretion when produced together. *HeLa cells were co-transfected with the indicated expression plasmids (EV corresponds to empty vector), and 20 hours later, conditioned media (CMs) were removed. Cells were carefully washed five times with prewarmed serum-free medium (SFM) to remove abundant serum proteins, and fresh SFM containing L-glutamine was added for a further 4 hours prior to acetone precipitation and recovery of cell lysates (CLs). CLs (A) and acetone precipitates (APs) (B) were immunoblotted for FLAG. Intracellular IL-22BPi1 is indicated with dark purple arrows, while intracellular and secreted IL-22BPi2 is indicated with green arrows, and co-expressed IL-22 and IL-17 are also indicated. (C) CMs from three independent experiments, similar to the one represented in A and B, were analysed by ELISA for IL-22BP (mean ± SEM; n = 3; ** $p < 0.01$ by unpaired t-test).*

Given the predominant ER localization of IL-22BPi1 (**Figure 54**), its inability to bind to IL-22 (**Figure 57**), and its co-production with IL-22BPi2 in natural producer cells (**Figure 36**), we investigated whether IL-22BPi1 had the capacity to physically interact with IL-22BPi2. We co-expressed myc-FLAG-tagged IL-22BPi1 with FLAG-tag-only IL-22BPi2 in HEK293 cells. Purification with anti-Myc resin only recovered IL-22BPi1, while

further purification via anti-FLAG resin recovered IL-22BPi2 from the flow-through fraction, suggesting that both isoforms do not interact (**Figure 59**).

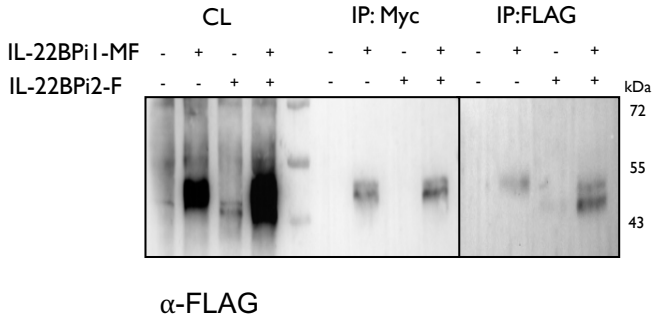

Figure 59: IL-22BPi1 does not interact with IL-22BPi2. *IL-22BPi1-MF expression plasmid containing Myc and FLAG tags was co-transfected with an inducible pTRE3G-based vector expressing IL-22BPi2 with only a FLAG tag. After 24 hours, cells were induced for IL-22BPi2 production by adding Tet-Express activator to the medium for a further 24 hours. Cells were lysed and immunoprecipitated with anti-Myc agarose, and the flow-through fractions were then further subjected to FLAG immunoprecipitation. Cell lysates (CLs) and eluted fractions were immunoblotted for FLAG.*

5.5 IL-22BPi1 and IL-22BPi2, but not IL-22BPi3, are clients of GRP78 and GRP94, among other ER resident proteins

To identify proteins that may be responsible for the intracellular retention and degradation of IL-22BPi1, we analysed the interactomes of the three IL-22BP isoforms purified from HeLa and HEK293 cells by nLC MS/MS. A 75-kDa band was co-purified from HEK293 cells, both with IL-22BPi1 and IL-22BPi2, but not IL-22BPi3, which was identified as GRP78. We observed that upon densitometric analysis of silver stained gels, the relative amount of GRP78 co-purified with IL-22BPi1 was more than four times higher than that associated with IL-22BPi2 (**Figure 60A**). Via mass spectrometry, in HeLa or HEK293 cells, we reproducibly identified four partners for IL-22BPi2 (i.e., GRP78, calnexin, GRP94, and GRP170), all of which are ER-localized chaperone-type proteins (**Figure 60A**, **B,** and *inset*). GRP78 was not co-purified with IL-22 (**Figure 60B**).

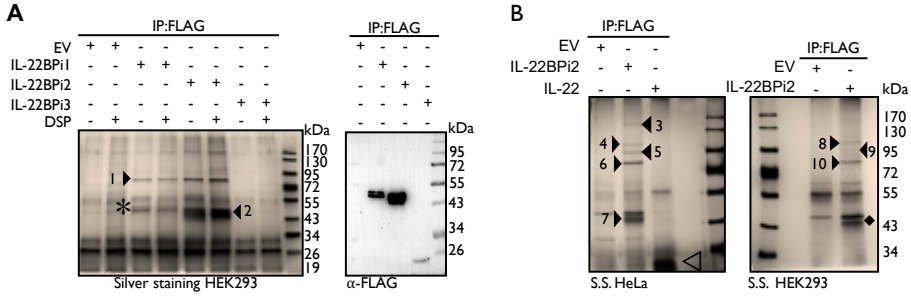

Band #	Description	Score	Coverage (%)	# Unique Peptides	# Peptides	# PSMs
3	GRP170	122,98	1,6	1	1	2
4	GRP94	319,74	9,22	7	7	9
8		86,14	2,99	2	2	2
5	Calnexin	29,18	1,52	1	1	1
9		234,66	13,18	6	6	6
1	GRP78	574,38	28,29	14	14	14
6		745,97	33,79	18	18	23
10		503,39	19,57	10	10	13
2	IL-22BPi2	469,75	20,53	6	6	11
7		165,5	15,21	4	4	5

Figure 60: IL-22BPi1 and IL-22BPi2, but not IL-22BPi3, interact with GRP78. *(A and B) Identification of GRP78, GRP94, GRP170, and calnexin in interactomes of IL-22BPi1 and IL-22BPi2. Silver-stained (S.S) gels of proteins (co-)immunoprecipitated (IP) with FLAG resins from HEK293 or HeLa cells transiently transfected with the indicated expression plasmids or control empty vector (EV) are shown. Numbered arrowheads indicate proteins*

identified by mass spectrometry included in the inset summary table. Co-immunoprecipitated proteins without DSP treatment were immunoblotted for detection by FLAG. Asterisk, IL-22BPi1; empty arrowhead, IL-22; solid rhombus, IL-22BPi2; Summary table with the mass spectrometry results from protein identification. # Unique peptides, # Peptides, and # PSMs are the number of peptide sequences unique to a protein group, the number of distinct peptide sequences in the protein group, and the total number of identified peptide sequences (peptide spectrum matches) for the protein, respectively.

5.5.1 IL-22BPi1 and IL-22BPi2 are natural clients of GRP78

We then further validated the interaction found in the previous identifications by immunoblot. Interaction of IL-22BPi1 and IL-22BPi2 with GRP78, GRP94, GRP170, and calnexin, as well as with additional ER residential proteins, was confirmed (**Figure 61A**). Next, to assess the role of GRP78 in protein folding in vitro, we characterized its interactions with IL-22BP isoforms. We co-transfected the three IL-22BP isoforms with wild-type (*wt*) GRP78 or a mutant form of GRP78, in which the substitution of Thr-37 with Gly (T37G) inhibits ATPase activity and blocks the ATP-mediated release of cargo from GRP78 (Gaut & Hendershot, 1993). *Wt* but not GRP78^{T37G} significantly increased secreted levels of IL-22BPi1 and IL-22BPi2, while it did not affect the secretion of IL-22BPi3 (**Figure 61B**). This was mirrored by a tendency towards increased intracellular levels of IL-22BP isoforms in the presence of *wt*GRP78 (**Figure 61A)**. Thus, the binding of IL-22BPi1 and IL-22BPi2 to GRP78 as well as their enhanced secretion upon overexpression with *wt* but not ATPase-deficient GRP78 suggests that both isoforms are natural client proteins of GRP78.

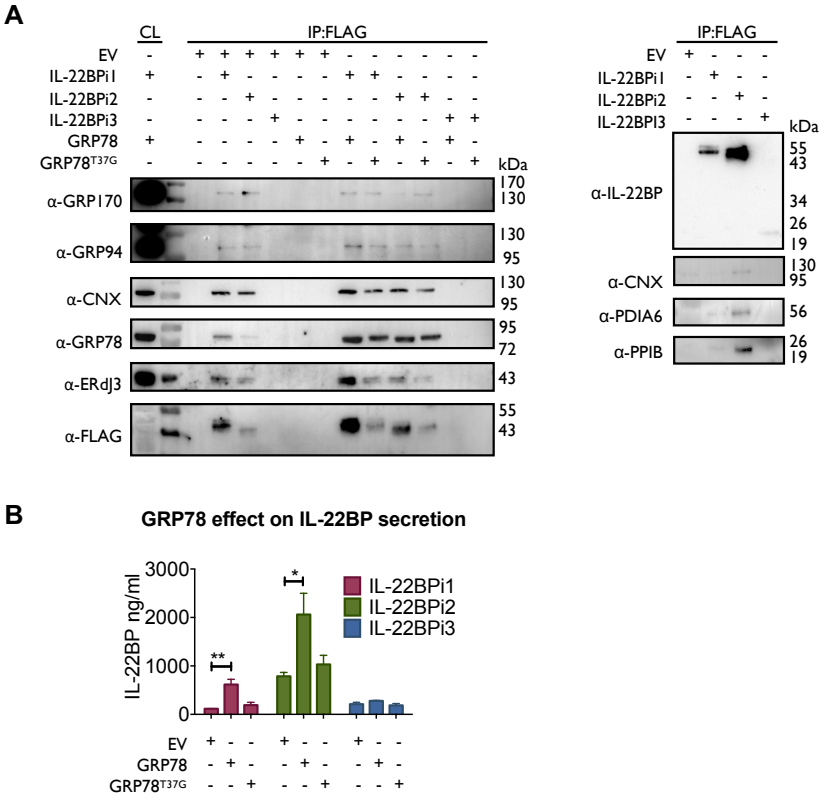

Figure 61: GRP94, GRP78, PPIB, PDIA6, ERdj3, calnexin, and GRP170 are partners of IL-22BPi1 and IL-22BPi2. (A) *HEK293 cells were individually transfected with expression plasmids for the three IL-22BP isoforms together with either GRP78 or GRP78T37G expression vectors or empty vector (EV). After 24 hours, cell lysates (CLs) were co-immunoprecipitated with FLAG agaroses. Co-immunoprecipitated proteins (IPs) were immunoblotted for GRP170, GRP94, calnexin (CNX), GRP78, ERdj3, cyclophilin (PPIB), PDIA6, IL-22BP (Ab 4), and FLAG. (B) HEK293 cells were individually transfected with expression plasmids for the three IL-22BP isoforms together with either GRP78 or GRP78T37G expression vectors empty vector EV. Then, 24 hours later, secreted protein was measured by ELISA for IL-22BP (mean ± SEM; n = 3; *p < 0.05, **p < 0.01 by unpaired t-test).*

5.5.2 IL-22BPi1 and IL-22BPi2 interact with the C-terminal half (amino acids 455-577) of the middle domain (MD) of GRP94

As shown above, both IL-22BPi1 and IL-22BPi2 interact with GRP94. Like GRP78, GRP94 is an ER luminal chaperone, but unlike GRP78, it has a

highly selective client base of proteins, including specific Toll-like receptors and integrins, which, apart from exhibiting disulphide bonds, share no further apparent structural features (Marzec, Eletto, & Argon, 2012; S. Wu et al., 2012). The amount of GRP94 co-IPed via anti-FLAG purification of IL-22BP isoforms from HEK293 cells transfected with identical quantities of cytokine vectors was relatively higher for IL-22BPi1 than for IL-22BPi2; GRP94 was borderline detectable in IL-22BPi2 IP (**Figure 62A**, *left panel*). Upon reverse IP using S-tagged GRP94, IL-22BPi1 but neither IL-22BPi2 nor BPi3 were found in complex with GRP94 (**Figure 62A**, *right panel*). To identify the region(s) in GRP94 responsible for binding to IL-22BPi1 or IL-22BPi2, we probed the interaction of both isoforms with a series of GRP94 truncation and deletion mutants. This selection of constructs was based on well-defined GRP94 regions (Marzec et al., 2012) that constitute the modular fold of GRP94, and it was previously used to investigate the interaction site of GRP94 with OS-9 (Dersh et al., 2014) (**Figure 62B**). IL-22BPi1 and IL-22BPi2 were purified from CLs by means of their myc-tag. Although all GRP94 constructs contained both N-terminal FLAG-tag and C-terminal native KDEL sequences, their individual detectability in Western blot varied according to the antibody used; mouse anti-FLAG Ab detected the GRP94 middle domain (MD) mutant better than did rabbit anti-FLAG Ab, and mouse anti-KDEL Ab was only successful in detecting the GRP94 C-terminal domain (CTD) and ΔA-GRP94 mutants (**Figure 62C**). CTD and NTD GRP94 mutants were not found in complex with either isoform, while the MD-GRP94 and ΔA-GRP94 MD variants interacted strongly with IL-22BPi1 and IL-22BPi2 (**Figure 62C)**. Thus, while the middle subdomain of GRP94 shared by MD- and ΔA-GRP94 (amino acids 455-577) emerges as critical region for binding both IL-22BPi1 and IL-22BPi2, this client-binding site differs from that used by the ERAD component OS-9 (i.e., amino acids 356–456 of the GRP94 MD; Dersh et al., 2014) or by GRP94 client proteins such as TLRs and integrins (i.e., amino acids 635–656 of the GRP94 CTD; S. Wu et al., 2012). Co-expression of either GRP94 MD or ΔA mutants with IL-22BPi1 or BPi2 isoforms significantly decreased their secretion, suggesting that the interaction between these IL-22BP isoforms

and these GRP94 mutants sequesters them from the productive folding/secretory pathway (**Figure 62C,** *bottom graphs*). Truncated regions absent in MD and ΔA-GRP94 therefore seem to be responsible for a proper GRP94–IL-22BP interaction cycle. While the GRP94 NTD mutant did not affect secretion, the GRP94 CTD mutant appeared to decrease the secretion of IL-22BPi1 but not that of IL-22BPi2, and this possibly reflects additional weak interactions of IL-22BPi1 with this domain that did not survive the IP procedure efficiently.

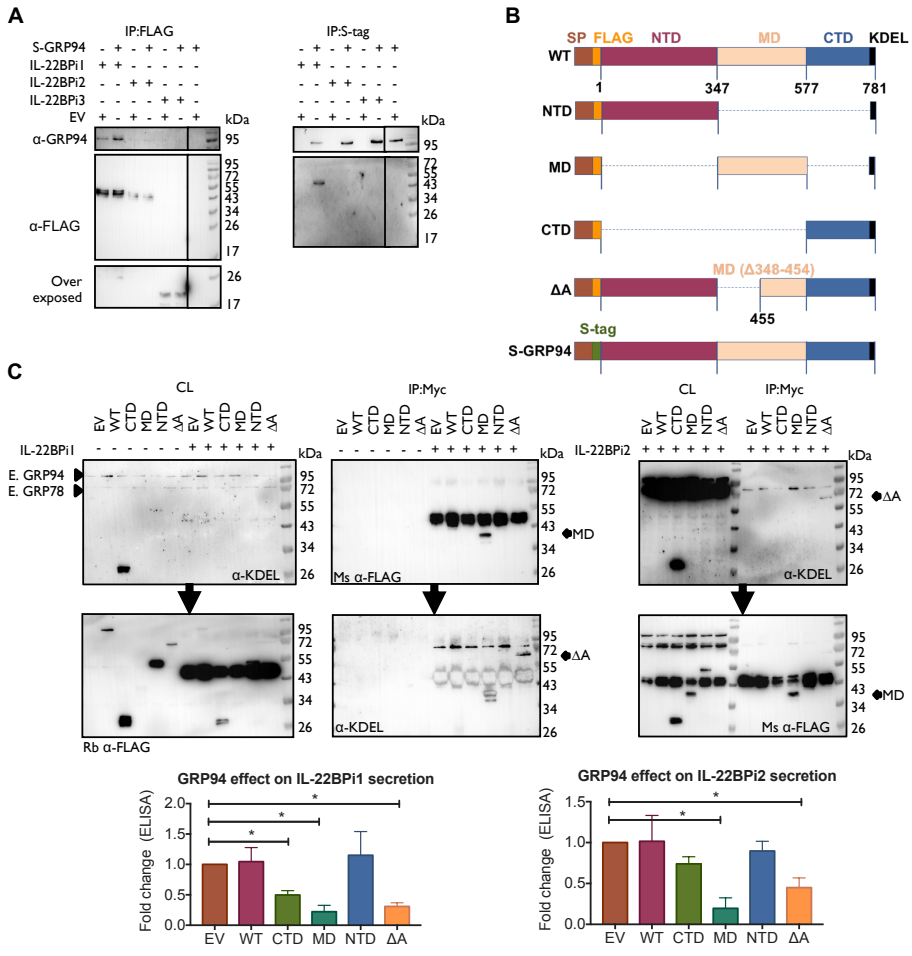

Figure 62: Both IL-22BPi1 and IL-22BPi2 interact with the middle domain of GRP94. ***(A)*** *HEK293 cells were transiently co-transfected with the indicated expression plasmids, and 24 hours later, cell lysates (CLs) were immunoprecipitated with FLAG resin to*

*immuoprecipitate IL-22BP isoforms or with S-tag agarose to immuoprecipitate GRP94. Co-immunoprecipitated proteins (IPs) were immunoblotted for GRP94 and FLAG. (B) A schematic diagram of full-length (WT) and structural mutants of GRP94 used. (C) (Western blot images) HEK293 cells were transiently co-transfected with the indicated expression plasmids, and 24 hours later, CLs were co-immunoprecipitated with Myc agarose. Membranes with CLs and IPs were sequentially exposed for detection by KDEL and mouse (Ms) or rabbit (Rb) FLAG Abs, or vice versa. MD-GRP94 or 1A-GRP94 co-immunoprecipitated with IL-22BPi1 or IL-22BPi2 are indicated with black arrows. (Lower) Expression vectors for IL-22BP isoform-1 and -2 were individually transfected into HEK293 cells together with either GRP94 wild-type (WT) or GRP94 mutant vectors (CTD, MD, NTD, or deltaA) or empty vector (EV). Twenty-four hours after transfection, secreted IL-22BP was quantified by ELISA, analysed by paired t-test on original data, and represented as a fold change relative to EV condition (mean ± SEM; n = 3; *p < 0.05 by paired t-test).*

Co-expression of GFP-tagged *wt*GRP94 as well as the ATPase-negative mutant GRP94^{E82A} (Marzec et al., 2016) with IL-22BP isoforms revealed that compared to *wt*GRP94, GRP94^{E82A} significantly reduced the secretion levels of IL-22BPi1 and IL-22BPi2, but not that of IL-22BPi3 (**Figure 63**). Together, these experiments provide evidence that GRP94 interacts with both the former isoforms and that the secretion of both isoforms is proportional to intact GRP94 activity.

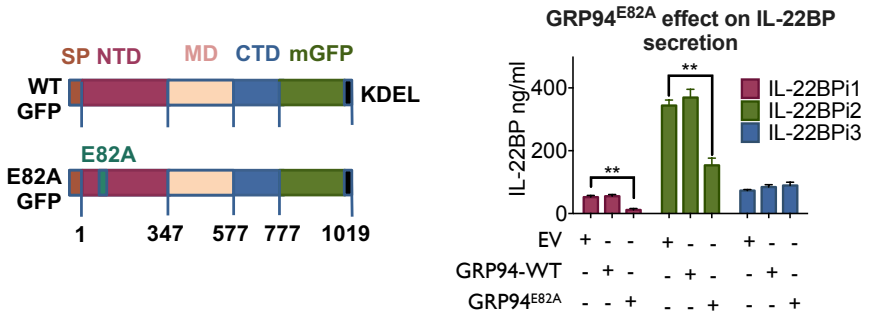

Figure 63: GRP94 ATPase activity is important for IL-22BPi1 and IL-22BPi2 secretion. *HEK293 cells were transiently co-transfected with IL-22BP isoforms together with the indicated GFP-GRP94 fusion constructs (depicted on the left); secreted IL-22BP was measured by ELISA in the conditioned media (CMs) 24 hours after transfection (mean ± SEM; n = 4; **p < 0.01 by unpaired t-test).*

5.6 Pharmacological targeting of the ER resident chaperones GRP94 and cyclophilin B induces secretion of IL-22BPi1

IL-22 targeting is emerging as an attractive approach to prevent pathologies associated with conditions in which IL-22 is known to drive inflammatory processes. Neutralizing IL-22 antibodies or recombinant IL-22BP are under investigation as promising therapeutic tools (https://clinicaltrials.gov/ct2/home). In this regard, the possibility to modulate IL-22BP levels by direct interference with its folding or secretion has not yet been studied. The ER machinery has been widely scrutinized as a therapeutic target for the treatment of diseases in which dysregulation of the unfolded protein response (UPR) is involved, including neurodegenerative, autoimmune, and cardiovascular diseases, as well as for the prevention of acute rejection and cancer treatment (M. Liu, Chen, & Chen, 2016; S. W. Park & Ozcan, 2013; Rivas, Vidal, & Hetz, 2015). As described in the previous section, the secretion of both IL-22BPi1 and IL-22BPi2, but not IL-22BPi3, is dependent on the functionally intact luminal ER chaperones GRP78 and GRP94. Moreover, cyclophilin B, which is an ER peptidyl-prolyl isomerase, was also detected in the IL-22BPi1 and IL-22BPi2 interactomes by immunoblot (**Figure 61**). Another interesting observation is that during the differentiation of $CD14^+$ monocytes to moDCs, the expression of cyclophilin B and its counterparts, cyclophilin C and A, was increased similarly to that of IL-22BP (**Figure 38**). A similar increase has also been described for GRP94 from monocytes to moDCs (Wolfram et al., 2013).

We considered whether interference with these factors could modulate the secretion of IL-22BP isoforms. The disruption of GRP78 may be off limits due to its central role in UPR and the dependency of numerous secretory and membrane proteins on its activity (McLaughlin & Vandenbroeck, 2011); however, GRP94 has a highly selective client base of proteins, and the prospect of selectively blocking its activity in protein folding by pharmacological agents constitutes an area of active investigation (Eletto, Dersh, & Argon, 2010; McLaughlin & Vandenbroeck, 2011). While paralog-specific inhibitors of HSP90-type

chaperones are in development (Duerfeldt et al., 2012; Gewirth, 2016), GA, which is a 1,4-benzoquinone ansamycin, is known to inhibit various homologues of HSP90, including GRP94, by binding to the characteristic ADP/ATP pocket, and it is therefore useful to test proof-of-concept (McLaughlin & Vandenbroeck, 2011; Randow & Seed, 2001). Cyclophilin B displays the ability to bind the immunosuppressive drug cyclosporine A (CsA) (J. Liu et al., 1991). CsA induces the secretion of cyclophilin B into the culture medium, but not that of other ER chaperones, which *de facto* depletes the former's ER levels (Price et al., 1994) and facilitates scrutiny of its net effect on IL-22BP secretion.

In this section, we investigate the effect of GRP94 and cyclophilin B targeting drugs on the secretion of IL-22BP isoforms.

5.6.1 GRP94 inhibitors enhance IL-22BP1 secretion

We analysed the effect of GA and its more stable and water-soluble analogues 17-allylamino-17-demethoxygeldanamycin (17-AAG) and 17-dimethylaminoethylamino-17-demethoxygeldanamycin (17-DMAG), respectively, on the secretion of IL-22BPi1 and IL-22BPi2 from transiently transfected HEK293 cells. As measured using ELISA, all three GA analogues significantly increased the secretion of IL-22BPi1 but not that of IL-22BPi2, and the inhibitory effect was maximal at drug concentrations of 1 μM (**Figure 64A**). As demonstrated before **(Figure 53A**) and here (**Figure 64B**), IL-22BPi1 is not detectable by Western blot in the APs of the medium of transfected cells. Interestingly, GA and its analogues enhanced the secretion of IL-22BPi1 to the point where it became visible in Western blots of AP as a series of 50 kDa to 56 kDa bands (**Figure 64B**). Moreover, the intracellular levels of IL-22BPi1 were higher in the presence of GA analogues. No such effects were seen for IL-22BPi2. We asked whether the multiple secreted IL-22BPi1 bands corresponded to distinct glycoforms. Intracellular IL-22BPi1, similarly to IL-22BPi2 and IL-22BPi3, contains only high-mannose-type N-glycans (**Figure 53B**). However, the secreted form of IL-22BPi2 contains exclusively complex-type sugar chains, and this corroborates its secretory

transit via the Golgi apparatus, which is known to contain the necessary glycosyltransferases for complex glycan attachment. As depicted in **Figure 64C**, IL-22BPi1 secreted in the presence of GA was sensitive to both Endo H (which cleaves only mannose-rich glycan chains) and PNGase F deglycosylation (which cleaves all high-mannose, hybrid, and complex glycan chains) and was compatible with high-mannose-type N-glycans (**Figure 64C**). However, PNGase F treatment generated a more intense signal than Endo H, suggesting that part of IL-22BPi1 withstands Endo H treatment and is secreted as a heterogeneous complex-type N-glycosylated protein that is borderline-visible as an Endo H-resistant smear extending upward from around 50 kDa (**Figure 64C**). The higher sensitivity of deglycosylated IL-22BPi1 to detection in immunoblot also revealed the presence of secreted protein in the APs of untreated cells. This demonstrated that both in the absence and presence of GA, IL-22BPi1 is secreted as a mixture of high-mannose and complex-type glycoforms, with both glycoform types increased in the presence of GA. IL-22BPi2, secreted at much higher levels than IL-22BPi1, was largely resistant to Endo H digestion, confirming its secretion as a complex-type glycoprotein. In a separate experiment, we compared the secreted fraction of the three isoforms treated with PNGase F in the presence or absence of GA. Secretion of neither IL-22BPi3 nor IL-22BPi2 increased under GA treatment, in contrast to IL-22BPi1 (**Figure 64D**).

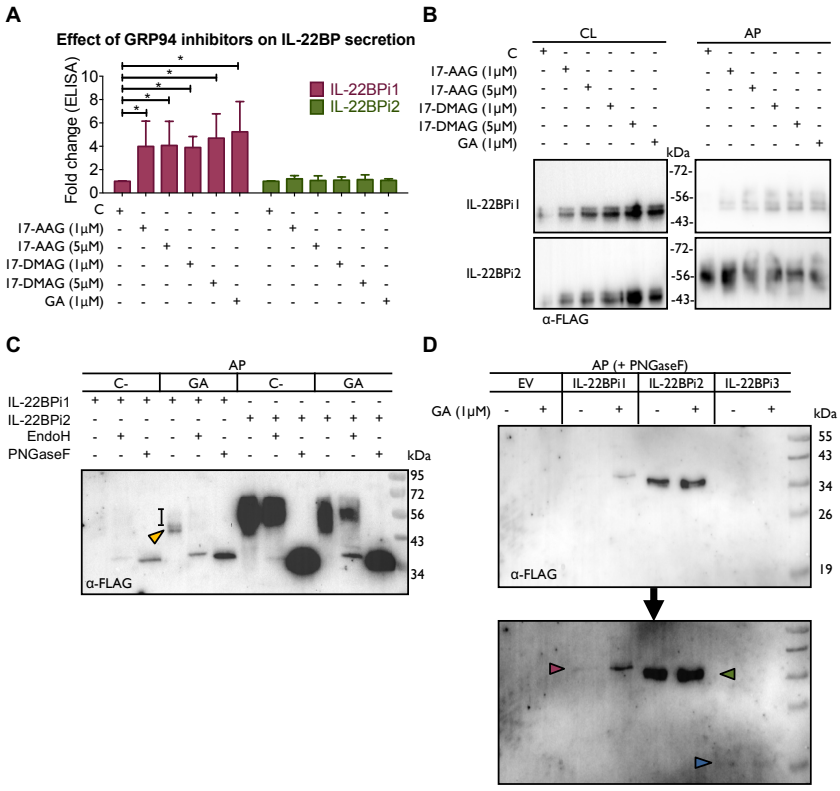

Figure 64: GRP94 inhibitors enhance IL-22BPi1 secretion. (A) *HEK293 cells were transiently transfected with equal quantities of the indicated expression plasmids; 24 hours later, cells were pretreated with the indicated concentrations of 17-dimethylaminoethylamino-17-demethoxygeldanamyin (17-DMAG), 17-allylamino-17-demethoxygeldanamycin (17-AAG), or geldanamycin (GA) for 4 hours, or they were left untreated, and cell monolayers were then carefully washed five times with complete culture medium. Fresh complete culture medium was added, containing the same compounds at the same concentrations. IL-22BP protein levels were measured in the conditioned medium (CM) after 20 hours, using ELISA (mean ± SEM; n = 5; * p < 0.05 by paired t-test). (B) As in (A), with the exception that CM was removed 16 hours after transfection, cells were carefully washed five times with prewarmed serum-free medium (SFM) to remove abundant serum proteins, and fresh SFM containing L-glutamine was added for a further 4 hours prior to acetone precipitation and recovery of cell lysates (CLs). Acetone precipitates (APs) and CLs were analysed by immunoblot against FLAG Ab, which detects the C-terminal FLAG-tag on the IL-22BP isoforms. (C) HEK293 cells were transiently transfected with identical quantities of the indicated expression plasmids. Experimental procedures were as described in (B). AP was incubated with either PNGase F or Endo H, or left untreated. Proteins were immunoblotted and detected with anti-IL-22BP Ab. The orange arrowhead indicates the main Endo-H-*

sensitive high-mannose-type glycoform of IL-22BPi1, while the Endo-H-resistant smear is indicated with a vertical black line. (C) Negative control. (D) HEK293 cells were transiently transfected with identical quantities of the indicated IL-22BP expression plasmids. Experimental procedures as in (B). APs were treated with PNGase F. Proteins were immunoblotted and detected with FLAG Ab. Since IL-22BPi3 is difficult to detect, even in APs, the membrane was overexposed for visualization. Red, green, and blue arrowheads indicate IL-22BPi1, IL-22BPi2, and IL-22BPi3, respectively.

5.6.2 CsA increases IL-22BPi1 secretion

We evaluated the effect of CsA on the secretion of IL-22BP isoforms by transiently transfected HEK293 cells. CsA caused depletion of intracellular cyclophilin B by inducing its secretion, as previously reported (Fearon et al., 2011; Price et al., 1994), but it did not appreciably alter the intracellular levels of IL-22BPi1, and those of IL-22BPi2 were also unaffected (**Figure 65A**). However, while secretion of IL-22BPi2 and IL-22BPi3 appeared to be unaffected or suppressed, IL-22BPi1 secretion was significantly increased (**Figure 65A**). We also compared the effect of CsA with that of 17-DMAG on the comparative secretion of the three IL-22BP isoforms as measured by ELISA. 17-DMAG and CsA increased the secreted fraction of IL-22BPi1; however, CsA decreased the secretion of IL-22BPi2 and IL-22BPi3, while 17-DMAG did not seem to exert any effect (**Figure 65B**). Used in combination, CsA and 17-AAG also increased the secretion of IL-22BPi1; however, this increase was not higher than that induced by the individual treatments (**Figure 65C**).

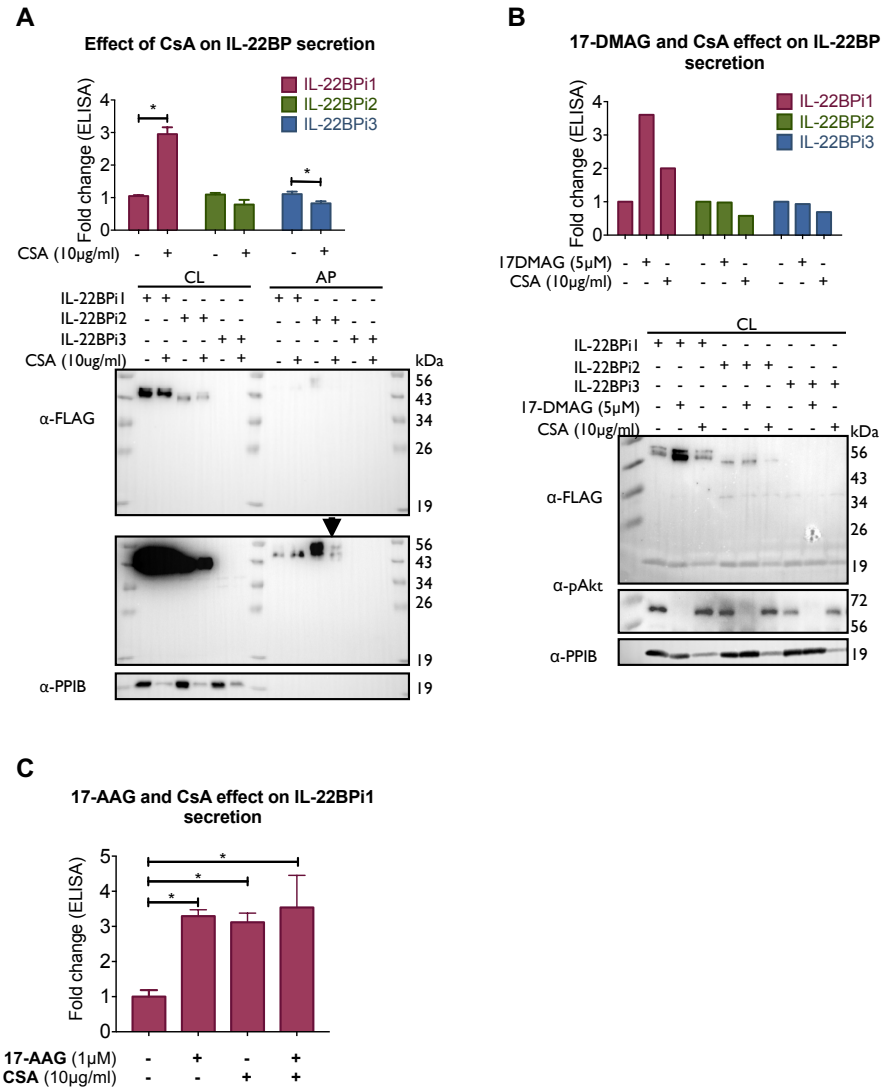

Figure 65: Cyclosporin A (CsA) enhances IL-22BPi1 secretion. *(A) HEK293 cells were transiently transfected with the indicated expression plasmids. Twenty-four hours later, cells were pretreated with cyclosporin A (CsA; 10 µg/mL) for 4 hours or left untreated. The medium was then removed; cell monolayers were washed five times with complete culture medium; and new complete culture medium containing CsA was added, whereby cells were incubated for a further 12 hours, and the CM collected. Secreted IL-22BP was measured by ELISA in the CM (mean ± SEM; n = 3; * p < 0.05 by paired t-test). Next, the cell monolayers were carefully washed five times with prewarmed serum-free medium (SFM) to remove serum components, and fresh SFM containing L-glutamine was added for a further 4 hours prior to acetone*

*precipitation, at which point the cells were lysed. Cell lysates (CLs) and acetone precipitates (APs) were immunoblotted for FLAG and cyclophilin B (PPIB). IL-22BPi3 was detected in ELISA but not in Western blots, as previously shown. (B) A representative experiment comparing the effect of 17-dimethylaminoethylamino-17-demethoxygeldanamyin (17-DMAG) and CsA on the intracellular and secreted levels of IL-22BP isoforms. HEK293 cells were transiently transfected with the indicated expression plasmids, and 24 hours later, cells were pretreated, or not, with CsA (10 μg/mL) or 17-DMAG (5 μM) for 4 hours. Then, the medium was removed; cells were washed five times; a new complete culture medium containing CsA or 17-DMAG was added; and cells were incubated for a further 12 hours. CM was collected, and cells were lysed. Secreted IL-22BP was measured by ELISA in the CM. CLs were immunoblotted for FLAG, pAkt, and PPIB. 17-DMAG blocks Akt phosphorylation, validating its biological activity. (C) The effect of co-treatment with 1 μM 17-allylamino-17-demethoxygeldanamycin (17-AAG) and 10 μg/mL CsA on the secretion of IL-22BPi1, as measured by ELISA. Cells were treated as in (a); mean ± SEM; n = 4; * p < 0.005 by paired t-test.*

5.7 IL22RA2 alternatively spliced exon-coded sequence confers ability to induce the unfolded protein response (UPR) programme

The results obtained in the previous sections offer evidence for IL-22BPi1 being an IL-22 non-binding protein (**Figure 57)** with stronger intrinsic propensity to misfold than IL-22BPi2 (**Figure 29**). Rather than changing the specificity of intracellular protein interactions based on interactome analysis, the alternatively spliced exon-encoded sequence appears to compromise the folding and secretion of its recipient protein. Thus, both IL-22BPi2 and IL-22BPi1 are client proteins of, and interact with identical domains of, GRP78 and GRP94. However, IL-22BPi1 binds more strongly to each of these than IL-22BPi2, is less efficiently secreted, accumulates intracellularly, and is apparently confined to the luminal ER seen via immunofluorescence co-localization with GRP94 and ERp72 coupled to less protein accumulation in the Golgi apparatus than that seen for IL-22BPi2 and BPi3 (results generated by our group but not included in this study). We tested whether expression of IL-22BPi1 activates the UPR, which is a resolutive transcriptional programme to maintain ER homeostasis (Hetz, 2012) that is activated in response to an accumulation of misfolded proteins in the ER. **Figure 66A** shows that transfection of HEK293 cells with IL-22BPi1 induces expression of typical UPR genes, including GRP78, GRP94, CHOP, and HERP, peaking at around 36 hours after transfection. In contrast, IL-22BPi2, BPi3, or IL-2 had much less or no effect on the induction of these UPR genes. We also assayed whether UPR activation compromised cell viability in this experiment, but this was not the case (**Figure 66B**).

Moreover, an analysis of CLs in Western blot revealed that the appearance of IL-22BPi1 at 24 hours after transfection is associated with increased protein levels of GRP94 and GRP78 (**Figure 66C**). No such effects were found with IL-22BPi2, IL-22BPi3, or IL-2. Activation of the UPR was confirmed by enhanced splicing of XBP1 in cells expressing IL-22BPi1 (**Figure 66D**). Given the observation that ectopic GRP78 enhanced the secretion of both IL-22BPi2 and BPi1 (**Figure 61B**), we analysed

whether co-transfection of IL-22BPi2 with IL-22BPi1 may, similarly, enhance IL-22BP secretion secondary to UPR induction of GRP78 by IL-22BPi1. **Figure 66E** illustrates that at a BPi1:BPi2 1:1 transfection ratio, a reduced secretion of IL-22BP measured in ELISA was observed, while at smaller ratios approaching those seen in natural producer cells (**Figure 36**), a non-significant trend, at best, towards enhanced secretion of immunoreactive protein was observed (the same effect was observed when IL-22BPi2 was co-transfected with IL-2 rather than IL-22BPi1 [**Figure 67**]).

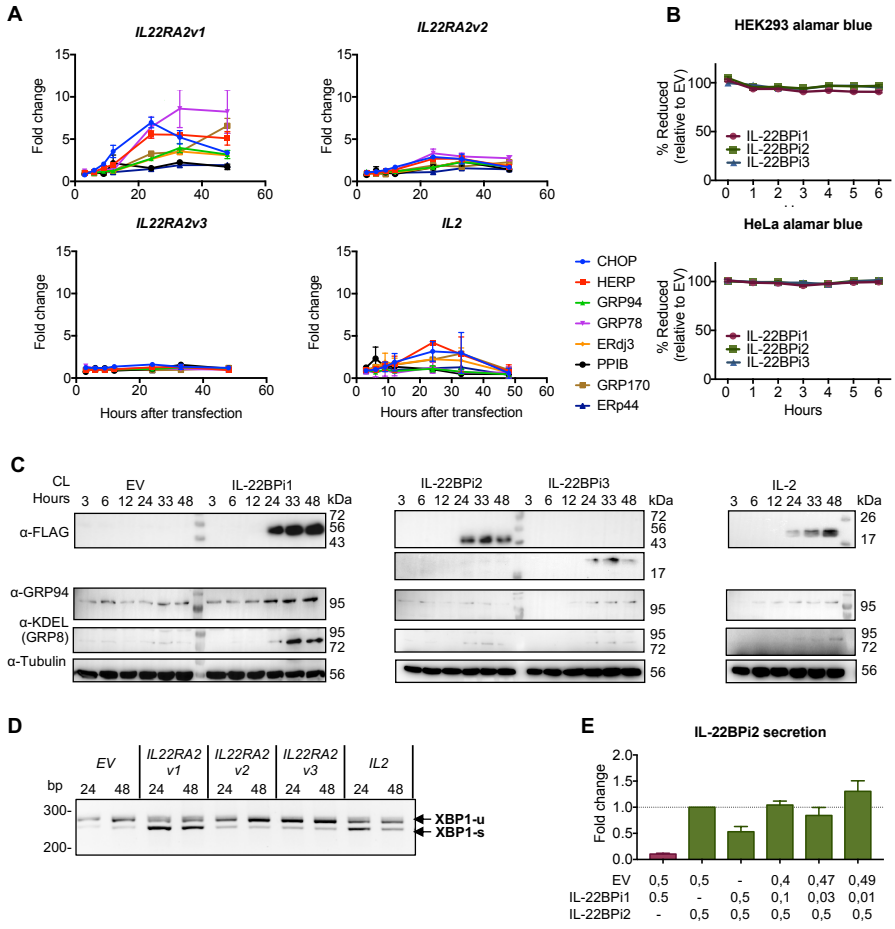

Figure 66: IL-22BPi1 induces unfolded protein response (UPR) genes. *HEK293 cells were transiently transfected with IL-22BPi1, IL-22BPi2, IL-22BPi3, IL-2, or empty vector*

(EV) as a control. Cells were collected at the indicated hours after transfection. (A) Expression of different genes related to endoplasmic reticulum (ER) function or UPR were analysed by RT-qPCR. Each gene expression value is represented as a fold change relative to the same time-point expression value of the EV condition and relative to the housekeeping gene GAPDH. Mean ± SEM of three independent experiments. (B) Cell viability measured with alamarBlue was not compromised by any of the conditions in two different cell lines. The reduction of alamarBlue was measured after 48 hours of transfection and assayed for the indicated times and cell lines. Values are represented as percentages of reduction in each condition relative to EV (mean ± SEM; n = 3). (C) GRP78 and GRP94 protein levels correlate with mRNA levels observed in (A). Cell lysates (CLs) were immunoblotted for FLAG, GRP94, KDEL, and tubulin as the loading control. (D) IL-22BPi1 causes XPB1 splicing. XBP1 splicing was detected with conventional PCR for the indicated conditions and times. Un-spliced and spliced XBP1 are indicated as XBP1-u or XBP-1s respectively. (E) IL-22BPi2 secretion was not increased when co-expressed with different ratios of IL-22BPi1. HEK293 cells were co-expressed with different ratios of EV:IL-22BPi1:IL-22BPi2 expression plasmids. Forty-eight hours later, secreted IL-22BP in conditioned media (CMs) was quantified by ELISA (mean ± SEM; n = 3).

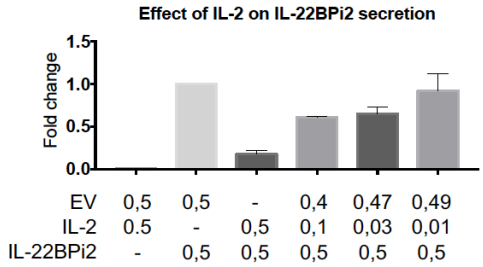

Figure 67: IL-22BPi2 secretion is not increased in the presence of IL-2. *HEK293 cells were co-expressed with different ratios of EV:IL-2:IL-22BPi2 expression plasmids. After 48 hours, IL-22BP secretion was measured by ELISA in conditioned medium. Error bars represent ± SEM of three independent experiments.*

5.8 The rs28385692 SNP, located in the *IL22RA2* gene, is associated with MS and decreases the secretion levels of IL-22BP

The human *IL22RA2* gene locus contains SNPs that have been found to be associated with cancer remission (Wade et al., 2011) and risk of contracting MS (Beyeen et al., 2010; Lill et al., 2014; Patsopoulos et al., 2017; Sawcer et al., 2011; The International Multiple Sclerosis Genetics Consortium [IMSGC], 2019; Vandenbroeck et al., 2012). The first evidence of an association between MS and the *IL22RA2* locus was found by Beyeen and colleagues (Beyeen et al., 2010). In a high-resolution linkage analysis, they initially found *Il22ra2* as a susceptibility locus for EAE disease, among others, in the EAE rat model. Then, they validated whether that finding correlated with the human *IL22RA2* gene with MS. Twenty-nine SNPs located across *IL22RA2* and its neighbouring gene, *IFNGR1,* were tested for an association with MS in a Swedish cohort. Three of these SNPs (i.e., *rs276474, rs72761*, and *rs13217897*) emerged as nominally significant ($p < 0.05$). The SNP with the strongest association, *rs276474,* which was located at the very end of *IL22RA2,* was also validated as an MS risk gene in a Norwegian cohort.

The association between *IL22RA2* and MS was subsequently clearly defined when GWASs identified the SNP *rs17066096* significantly associated with MS (Sawcer et al., 2011).

At that time, our group identified another SNP in *IL22RA2*, namely, *rs202573*, associated with MS in two different Spanish cohorts (Basque Country and Andalucía) in a cytokine and cytokine receptor gene screening for association with MS. However, none of the remaining or combined datasets yielded significant results (Vandenbroeck et al., 2012).

A new approach called a multivariate functional unit (FU)-wide association study (DeepWAS) has recently been developed. This approach fuses classical and functional GWASs. Instead of the classical approach analysing single SNPs individually, before filtering them in a separate follow-up step for regulatory information, SNPs are first

annotated for their regulatory potential (i.e., their affinity with an FU) and called deepSNPs, which are a combination of a specific chromatin feature, cell type, and treatment, before subjecting sets of SNPs with related functionality jointly to association tests by using regularized regression models (Arloth et al., 2020). In this new approach, the deepSNP (rs62420820), located in the intergenic region of *IL20RA-IL22RA2*, showed allele-specific transcription factor binding differences for MafF and MafK in the leukemia cell line K562, with gene regulatory capacity and a joint contribution to MS disease risk (Arloth et al., 2020).

It is quite common that after GWASs identify SNPs associated with a trait, fine-mapping studies follow them to determine the genetic variant (or variants) responsible for such an association (Schaid, Chen, & Larson, 2018). In that regard, our group conducted a fine-mapping study where 15 SNPs 123 kbp around the *IL22RA2* locus were analysed in the cohort of Bilbao, Basque Country (**Table 17**).

Four SNPs emerged with nominal significance ($p < 0.05$) (**Table 17**, highlighted in yellow) that were located in intronic regions. Among them, the original index SNP rs202573 showed the most significant association. However, the bioinformatic prediction of this SNP, which is located in a non-coding region, did not anticipate any functional role. Moreover, there was a lack of association in the validation cohorts (Gómez-Fernández et al., 2020), suggesting that this SNP is not likely to be of general relevance in MS. Contrary to what was previously identified in the GWASs, the SNP rs17066096 did not exhibit an association in the Bilbao cohort but was found to be significantly associated in the validation cohorts (Gómez-Fernández et al., 2020).

Table 17: Association values of SNPs included in the fine-mapping analysis. *SNP: single nucleotide polymorphism. Chr6: chromosome 6. RAF: risk allele frequency. P: p-value. OR: odds ratio. CI: confidence interval. SNPs with p < 0.05 are depicted in yellow, and those with p = 0.05 are shown in blue.*

SNP	*Position in Chr 6*	*Risk allele*	*RAF cases*	*RAF controls*	*Other allele*	*P*	*OR (95% CI)*
rs4896239	137490566	C	0.52	0.50	T	0.21	1.111 (0.942–1.31)
rs17066096	137494601	G	0.29	0.27	A	0.29	1.105 (0.92–1.328)
rs12194034	137499955	A	0.23	0.22	T	0.67	1.044 (0.89–1.271)
rs1543509	137507349	C	0.15	0.14	T	0.92	1.012 (0.80–1.279)
rs28366	137507780	C	0.24	0.23	T	0.54	1.063 (0.88–1.291)
rs276466	137508307	A	0.78	0.78	G	0.99	1.001 (0.80–1.248)
rs10484798	137512449	A	0.76	0.72	G	0.04	1.24 (1.0–1.526)
rs13217897	137513020	G	0.83	0.79	A	0.02	1.298 (1.0–1.602)
rs202573	137515365	A	0.33	0.28	G	0.01	1.26 (1.059–1.5)
rs2064501	137519516	T	0.50	0.49	C	0.70	1.033 (0.88–1.219)
rs11154914	137522104	G	0.19	0.16	A	0.07	1.223 (0.98–1.516)
rs28385692	137524533	C	0.02	0.01	T	0.05	1.947 (0.98–3.882)
rs13197049	137532904	A	0.83	0.80	T	0.03	1.264 (1.02–1.563)
rs6570136	137536315	A	0.46	0.45	G	0.85	1.018 (0.85–1.222)
rs7745487	137538365	A	0.18	0.15	G	0.11	1.197 (0.96–1.494)

More interesting was the case of the SNP rs28385692, which was included because of its potential functional effect given its location in a coding region. This nonsynonymous SNP is located in exon 2 of *IL22RA2*, in the 47th position of the coding sequence, and it results in an amino acid change from leucine to proline at position 16 (L16P) in the SP of the three isoforms of IL-22BP.

Although it was at the limit of significance in the Bilbao cohort ($p = 0.05$) (**Table 17**, highlighted in blue), it showed a confirmed association in the other Spanish and European cohorts analysed (Gómez-Fernández et al., 2020). The SNP was associated with MS in these cohorts comprising 8,960 MS patients and 7,613 controls ($p = 3.6 \times 10^{-4}$, OR = 1.262, 95% CI = 1.11–

1.434). This variant corresponds to a rare SNP, of which the minor allele frequency (MAF) corresponding to the risk allele in the Bilbao or European cohort was 0.015. The frequencies obtained in the 1,000 Genomes Project are similar for alleles A and G, exhibiting frequencies of 98.2% and 1.8%, respectively (**Figure 68**). As expected, due to the low frequency of the G allele, the frequency of the homozygous genotype for allele G is almost null (**Figure 68**).

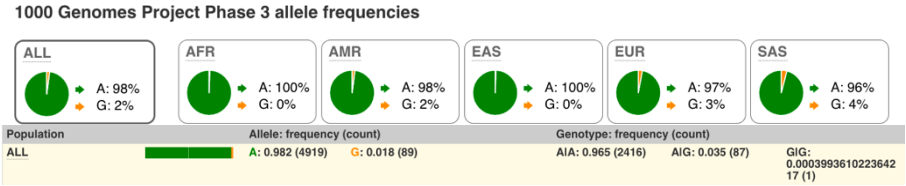

Figure 68: rs28385692 allele frequencies obtained from the 1,000 Genomes Project phase 3. *Pie charts depict the distribution of the alleles in a 1,000-genomes population for rs28385692. Data are separated into five super-populations: African (AFR), admixed American (AMR), East Asian (EAS), European (EUR), and South Asian (SAS). ALL stands for all 1,000 genomes' data, not separated by population. Allele and genotype frequencies for the combined populations are also represented.*

Thereafter, we attempted to better understand the possible functional effect of this missense mutation on IL-22BP isoforms. For that, different *in silico* and *in vitro* analyses were performed and are described next.

5.8.1 *In silico* analysis of rs28385692

We evaluated *in silico* whether the rs28385692 variant is functionally neutral or deleterious by using the following computational tools based on different approaches (Hassan et al., 2018): PredictSNP (Bendl et al., 2014), Meta-SNP (Emidio Capriotti et al., 2013), and Ensembl (Cunningham et al., 2019). A summary of the features for each tool used in this study are represented in **Table 18**. These tools are designed to predict whether a particular variation results in a neutral or deleterious substitution based on numerous parameters derived from the evolutionary, physicochemical, or structural characteristics by using different computational methods (Chengliang Dong et al., 2015;

Kulshreshtha, Chaudhary, Goswami, & Mathur, 2016). PredictSNP is a consensus classifier tool that includes a prediction of the SNP effect in distinct genomic regions by several established prediction tools: MAPP (E. A. Stone & Sidow, 2005), PANTHER (Thomas & Kejariwal, 2004), PhD-SNP (E. Capriotti, Calabrese, & Casadio, 2006), PolyPhen-1 (Ramensky, 2002), PolyPhen-2 (I. A. Adzhubei et al., 2010), SIFT (Prateek Kumar, Henikoff, & Ng, 2009), and SNAP (Bromberg & Rost, 2007). PredictSNP provides a calculated prediction based on the integrated results of the six best-performing tools (Bendl et al., 2014) by transforming the individual confidence scores to percentages to allow for comparison of the different tools. This analysis indicated that the overall result of the L16P transition was deleterious for the three isoforms; however, the outcome of the other seven tools was variable (**Figure 69A**). Meta-SNP (Emidio Capriotti et al., 2013), which integrates four existing strategies – PANTHER (Thomas & Kejariwal, 2004), PhD-SNP (E. Capriotti et al., 2006), SIFT (Prateek Kumar et al., 2009), and SNAP (Bromberg & Rost, 2007) – plus the Meta-SNP algorithm (combination of the previous ones), anticipated a neutral effect for the L16P point mutation in all IL-22BP isoforms (**Figure 69B**). Finally, Ensemble, which, similarly to the other tools, predicts the impact that a given SNP may have by the evaluation of several individual and ensemble predictors – CADD (Rentzsch, Witten, Cooper, Shendure, & Kircher, 2019), MetaLR (Chengliang Dong et al., 2015), Mutation Assessor (Reva, Antipin, & Sander, 2011), and REVEL (Ioannidis et al., 2016) – alongside SIFT (Prateek Kumar et al., 2009) and PolyPhen-2 (I. A. Adzhubei et al., 2010), predicted the substitution not to be deleterious except for Mutation Assessor, which gave a medium level of functional impact (**Figure 69C**). The overall results obtained with these computational tools were not robust enough to unequivocally assign a pathogenic effect to the L16P mutation.

A **PredictSNP**

RESULTS — neutral — deleterious — XX % expected accuracy

Annotation	Mutation	PredictSNP	MAPP	PhD-SNP	PolyPhen-1	PolyPhen-2	SIFT	SNAP	PANTHER
IL-22BPi1	L16P	55 %	75 %	59 %	67 %	-	70 %	89 %	68 %
IL-22BPi2	L16P	61 %	76 %	61 %	59 %	63 %	68 %	89 %	68 %
IL-22BPi3	L16P	51 %	76 %	61 %	59 %	63 %	74 %	55 %	68 %

B **Meta-SNP**

	Mutation	PANTHER	PhD-SNP	SIFT	SNAP	Meta-SNP	RI
IL-22BPi1	L16P	Neutral 0.283	Disease 0.672	Neutral 0.090	Disease 0.750	Neutral 0.432	1
IL-22BPi2	L16P	Neutral 0.283	Disease 0.696	Neutral 0.290	Disease 0.650	Neutral 0.493	0
IL-22BPi3	L16P	Neutral 0.283	Disease 0.686	Neutral 0.240	Disease 0.700	Neutral 0.466	1

Prediction:
Neutral: Neutral variants
Disease: Disease causing variants

Outputs: Value reported under each prediction
PANTHER: Between 0 and 1. (If >0.5 mutation is predicted Disease)
PhD-SNP: Between 0 and 1. (If >0.5 mutation is predicted Disease)
SIFT: Positive Value (If >0.05 mutation is predicted Neutral)
SNAP: Output normalized between 0 and 1 (If >0.5 mutation is predicted Disease)
Meta-SNP: Between 0 and 1. (If >0.5 mutation is predicted Disease)

RI: Reliability Index between 0 and 10.

C **Ensemble**

rs28385692

	Variant ID	Chr: bp	Alleles	Global MAF	Conseq. Type	AA	AA coord	SIFT	PolyPhen	CADD	REVEL	MetaLR	Mutation Assessor	Transcript
IL-22BPi1	rs28385692	6:137161703	A/G	0.018 (G)	missense variant	L/P	16	0.11	0.376	16	0.467	0.339	0.659	ENST00000296980.6
IL-22BPi2	rs28385692	6:137161703	A/G	0.018 (G)	missense variant	L/P	16	0.08	0.037	16	0.467	0.339	0.659	ENST00000339602.3
IL-22BPi3	rs28385692	6:137161703	A/G	0.018 (G)	missense variant	L/P	16	0.1	0.097	16	0.467	0.339	0.659	ENST00000349184.8

Figure 69: The pathogenicity prediction for rs28385692 variation. *The prediction of the pathogenicity was made using (A) PredictSNP, (B) Meta-SNP, and (C) Ensemble web servers. The results indicate the predictive severity of rs28385692 for each of the three IL-22BP isoforms.*

Table 18: Features of the individual and consensus computational tools used in this study. *Adapted from (Hassan et al., 2018).*

ID Server Name	Individual or consensus tool	Website	Machine learning techniques that based on	Input parameters	Deleterious threshold and outputs	Reference
Polyphen-2	Individual	http://genetics.bwh.harvard.edu/pph2/	Empirical rules	Protein, SNP identifier, or Protein sequence in FASTA format and positions of the substitution	Probably damaging or Benign, or Possibly damaging, Sensitivity, Specificity, Multiple sequence alignment, and 3D Visualization	(Adzhubei et al., 2010)
PhD-SNPg	Individual	http://snps.biofold.org/phd-snpg/method.htm	Gradient boosting algorithm	Chromosome position and Protein variation (position, and First amino acid, and second amino acid variant)	If the probability is >0.5, then the SNV is predicted to be Pathogenic, otherwise Benign	(E. Capriotti et al., 2006)
PANTHER	Individual	http://www.pantherdb.org/about.jsp	Alignment scores HMM	Protein sequence and substitution	All GO annotations and Phylogenetic annotation	(Thomas & Kejariwal, 2004)
SNAP2	Individual	https://rostlab.org/services/snap2web/	ANN	Protein sequence	Non-neutral and neutral, Score and accuracy	(Bromberg & Rost, 2007)
SIFT	Individual	http://sift.jcvi.org/www/SIFT_help.html#S	Alignment scores	The original amino acid, the position of the substitution, and the new amino acid	Score (0–1). The predicted is damaging if the score is <=0.05 and tolerated if the score is >0.05.	(Kumar et al., 2009)
Mutation Assessor	Individual	http://mutationassessor.org/r3/	Conservation method	Genome build, chromosome position, reference allele, and substituted allele or Protein ID and variant	(V/C) Variant conservation score and (VS) Variant specificity score. Level of functional impact (high, medium, low, neutral)	(Reva et al., 2011)
MAPP	Individual	http://mendel.stanford.edu/SidowLab/downloads/	Physicochemical properties and alignment score	The original amino acid, the position of the substitution, and the new amino acid	Score (0–1). The predicted is damaging if the score is <=0.05 and tolerated if the score is >0.05.	(Stone & Sidow, 2005)
CADD	Individual	http://cadd.gs.washington.edu/score	A linear kernel support vector machine (SVM)	SNVs	Functional, deleterious, and pathogenic variants	(Rentzsch et al., 2019)
REVEL	Consensus	https://omictools.com/revel-tool	RF	A score of MutPred, FATHMM, VEST, Poly-Phen, SIFT, PROVEAN, Mutation Assessor, Mutation Taster, LRT, GERP, SiPhy, phyloP, and phastCons	Disease variants or rare neutral variants	(Ioannidis et al., 2016)
PredictSNP	Consensus	https://loschmidt.chemi.muni.cz/predictsnp/	Weighted majority vote consensus	A score of PolyPhen-1, PolyPhen-2, SIFT, MAPP, PhD-SNP, and SNAP	Confidence scores and neutral or deleterious	(Bendl et al., 2014)
Meta-SNP	Consensus	http://snps.biofold.org/meta-snp/	RF	A score of PANTHER, PhD-SNP, SIFT, and SNAP	Disease related or Polymorphic non-synonymous SNVs.	(Emidio Capriotti et al., 2013)
Meta RL & Meta SVM	Consensus	https://omictools.com/functional-forecasts-	MMAF, linear kernel, radial kernel and polynomial	A score of SIFT, PolyPhen-2, GERPpp, Mutation Taster, Mutation Assessor, FATHMM, LRT, SiPhy, and PhyloP	D (Deleterious), N (Neutral), and U (Unknown)	(Dong et al., 2015b)

Because this point mutation occurs in the SP of IL-22BP protein, its potential effect on structural aspects was assessed in more detail by further *in silico* methods. SPs usually comprise a typical structure that consists of 25–30 residues with three well-defined regions: (i) the N-region (positively charged domain), which confers an orientation favouring or preventing translocation, usually with a more positive charge than the C-region to allow the former to be more accessible to the signal peptidase; (ii) the H-region (hydrophobic core with tendency to adopt alpha-helix), which determines the conformation of the SP and its orientation towards the cell membrane, the cleavage, and the rate and efficiency of protein translocation; and (iii) the C-region (the cleavage site), which typically contains helix-breaking proline and glycine residues and small, uncharged residues at positions -1 and -3 of the cleavage site. Coding SNPs in SPs may alter translocation efficiency, cleavage sites, and even post-cleavage events (Owji, Nezafat, Negahdaripour, Hajiebrahimi, & Ghasemi, 2018). A classical representation of these regions is presented in **Figure 70**.

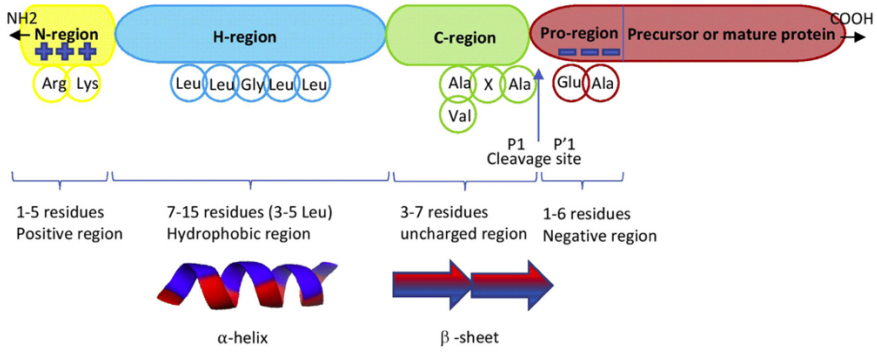

Figure 70: Classic structure of a signal peptide. *It comprises three structurally different regions; the N-region (usually characterized by the presence of positive residues); the H-region (a long hydrophobic core that adopts an α-helix structure – leucine residues predominate in this region); and the C-terminal segment (which contains helix-breaking proline and glycine residues and small, uncharged residues at positions -1 and -3 of the cleavage site, and it usually forms a β-sheet). Cleavage usually occurs after AXA or VXA motifs. Reproduced from Owji et al., 2018.*

We analysed the charge, the hydrophobicity, and the helix-breaker amino acid residues in the SP of IL-22PB, as well as the modifications that the L16P mutation may introduce (**Figure 71**). This mutation eliminates one of the three leucines present in the H-region and introduces a helix-breaker neutral residue that has no free hydrogen to contribute to helix stability. Results obtained with the SP cleavage site and secondary structure prediction tools (the SignalP-3.0, Phobius, and PSIPRED v3.3 tools) are illustrated in **Figure 71A**. While SignalP and PSIPRED did not predict any change in the cleavage site, Phobius predicted the L16P polymorphism to shift the SP cleavage site from residue 21 to 20. The three software applications coincided in predicting a shortening of the hydrophobic core of the SP. The results suggest that the change of leucine to proline, which has a cyclic structure sidechain that confers restricted conformational flexibility, will disrupt the alpha helix of the H-region of the SP and will also decrease the hydrophobicity of this region, ultimately affecting the cleavage site. Other prediction tools were run, and they predicted similar structural effects (**Figure 72**).

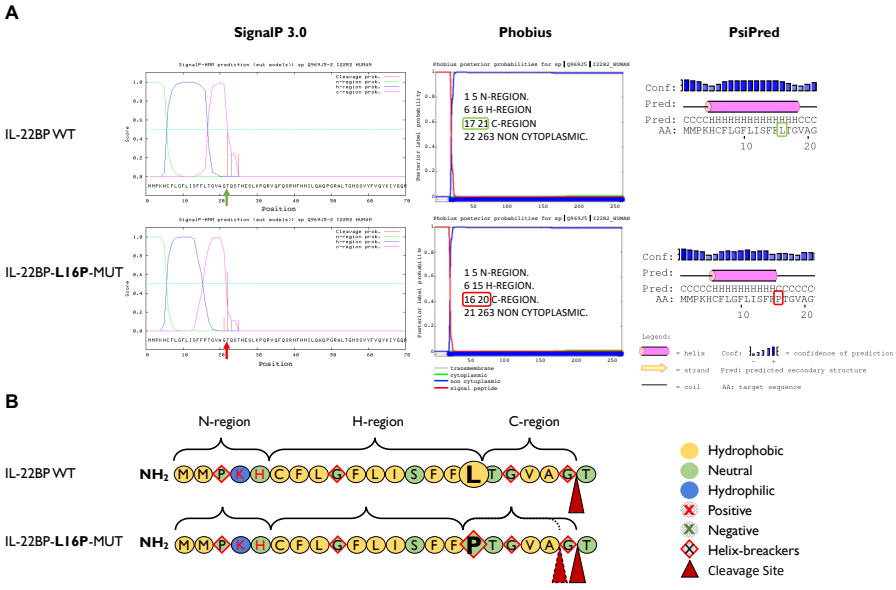

Figure 71: Prediction of the effect of Leu16Pro amino acid change on the signal peptide structure and cleavage site of IL-22BP. *(A) The signal peptide cleavage site was predicted*

using SignalP 5.0 (not represented in the figure), Phobius, and PsiPred software. These three tools' predictions of the cleavage site for the canonical sequence were between positions 21 and 22. According to Phobius, the amino acid change (L16P) shows a shift in the predicted cleavage site between positions 20 and 21; however, SignalP 5.0 and PsiPred predicted cleave sites identical to the canonical sequence. All software coincided that the hydrophobic region was decreased in the mutant form. (B) Representation of the composition, hydrophobicity, and charge of the amino acids that comprise the signal peptide of IL-22BP. The likely positioning of the typical three-domain structure of the signal peptide – (N-region) the hydrophilic, positively charged N-terminus region; (H-region) the hydrophobic core region; and (C-region) the uncharged polar C-terminal (cleavage site) region recognized by signal peptidase – is also represented based on the overall results obtained in A.

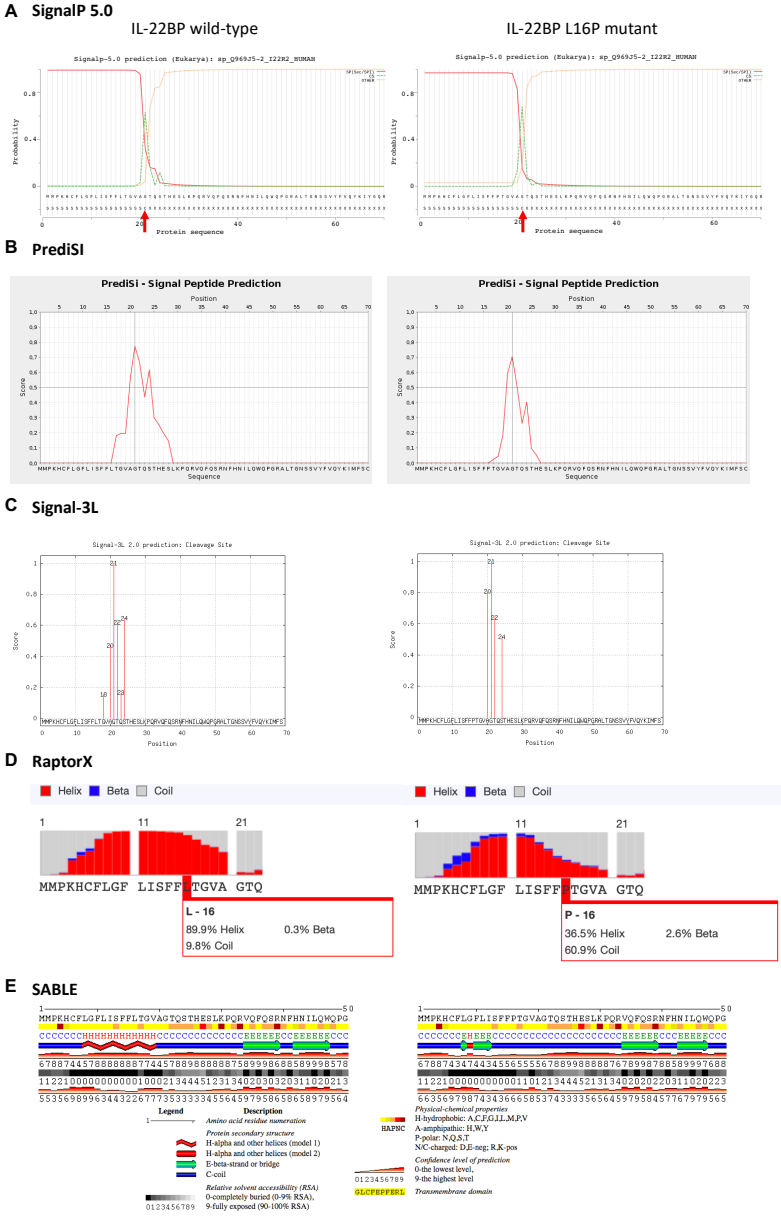

Figure 72: Signal peptide prediction in the wild-type and mutant L16P IL-22BP proteins. *SignalP 5.0, PrediSi, and Signal-3L predicted that the cleavage site for both wild-type and L16P mutant is the residue 21st of the signal peptide. Panels A, B, and C show cleavage sites from SignalP 5.0, PrediSi, and Signal-3L, respectively. D and E represent the secondary structure predictor from RaptorX and SABLE, respectively.*

5.8.2 *In vitro* analysis of rs28385692

We then sought to determine by *in vitro* studies whether and to what extent the non-synonymous SNP in this gene affects its protein product. To this end, site-directed mutagenesis (described in M&M) was performed in the three Myc-FLAG tagged constructs previously used in Section **5.3 above**. HEK293 cells were individually transfected with these vectors, and both intracellular and secreted levels of IL-22BPi1, IL-22BPi2, and IL-22BPi3 were measured by ELISA. We found that Pro16 strongly decreased the secreted levels of each isoform (**Figure 73A**). This was mirrored by non-significant trends towards decreased intracellular levels of IL-22BPi1 and IL-22BPi2 (**Figure 73B)**. The mRNA levels of *IL22RA2v2* wild-type and mutant were also analysed to exclude further differences associated with mRNA expression levels (**Figure 73C)**. These observations are compatible with the notion that the Pro16 variant renders the importing of the precursor IL-22BP isoforms into the ER less efficient, in agreement with effects predicted by the aforementioned in silico analysis. Flow cytometry analysis also revealed a decrease of 41% to 33% in IL-22BP positive cells following transfection of HEK293 with wild-type and mutant vectors, respectively, encoding IL-22BPi2 (**Figure 74**).

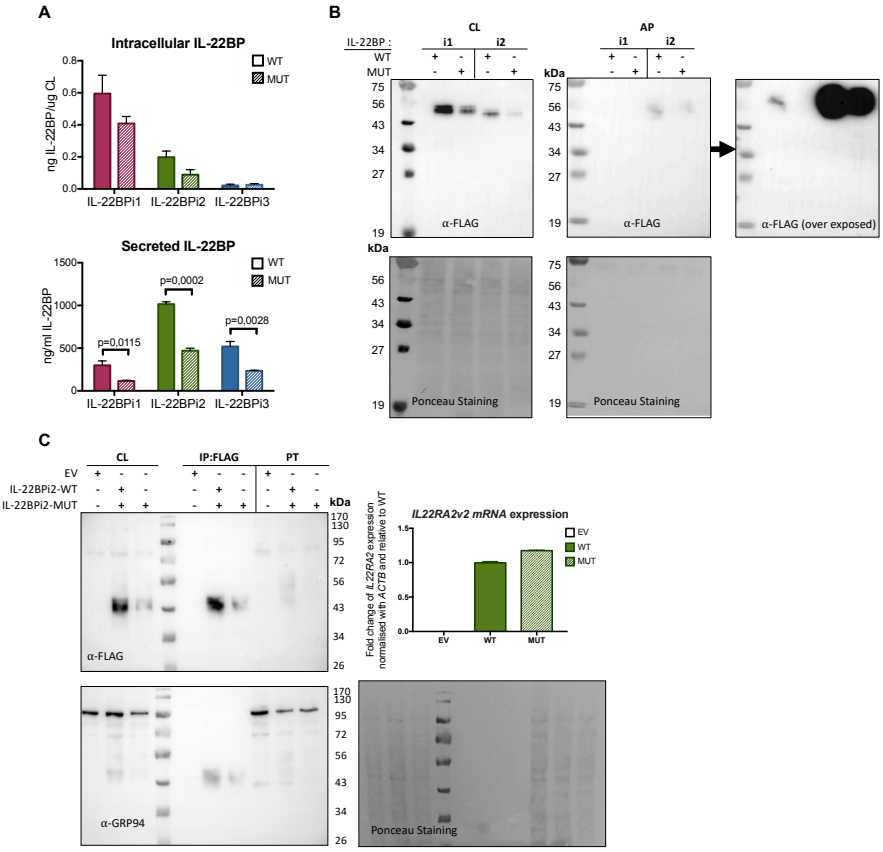

Figure 73: Leu16 to Pro mutation in the signal peptide of the three IL-22BP isoforms decreases their secretion. *(A) HEK293 cells were transfected with the indicated expression plasmids; 24 hours later, cells were lysed, and the conditioned medium was collected. Intracellular and secreted IL-22BP isoform protein levels were measured by ELISA (mean ± SEM; n = 3; p-values by unpaired t-test). (B) HEK293 cells were transfected with the indicated expression plasmids; 24 hours later, cells were lysed, and the conditioned medium was subjected to acetone precipitation. Both cell lysates (CLs) and acetone precipitates (APs) were resolved by SDS-PAGE under non-reducing conditions and immunoblotted against FLAG. For APs, the immunoblot membrane was subjected to longer exposure times. Ponceau staining served as the loading control. (C) HEK293 cells were transfected with the indicated expression plasmids; 24 hours later, cells were washed, and RNA was purified. Expression of IL22RA2 gene was analysed by RT-qPCR. The expression value is represented as a fold change relative to WT and relative to the housekeeping gene ACTB. Mean ± SEM of three technical replicates.*

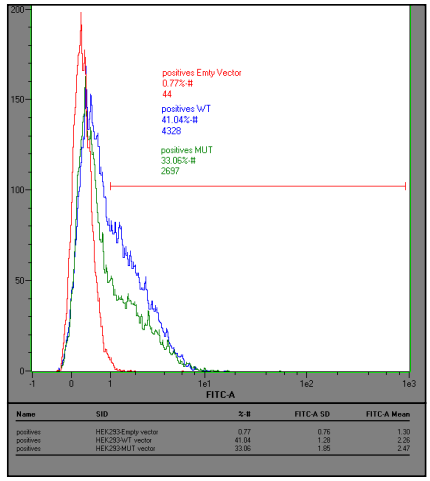

Figure 74: Leu16 to Pro mutation in the signal peptide of tIL-22BP isoform2 decreases its intracellular levels. *HEK293 cells were transfected with the IL22RA2 wild-type (WT), mutant (MUT), or empty vector (EV) expression plasmids; 24 hours later, cells were fixed, permeabilized, and immunostained with anti-IL22BP antibody and detected with a secondary antibody conjugated to FITC. Immunostained cells were analysed by flow cytometry. The graph represents the number of events (y-axis) and the intensity of the detection antibody for IL-22BP (x-axis).*

6. Discussion

6 Discussion

The focus of this thesis was on both the biological and genetic characterization of the *IL-22RA2* gene products IL-22BPi1, BPi2, and BPi3. At the start of this thesis, *IL22RA2* had emerged as a risk gene for MS in various studies (Beyeen et al., 2010; Sawcer et al., 2011, and Vandenbroeck et al., 2012). However, little information was available in the literature regarding the three IL-22BP isoforms encoded by this gene. Specifically, even though IL-22BPi2 and BPi3 had been characterized as secreted antagonists of the cytokine IL-22, the function of IL-22BPi1, the longest isoform, was unknown. In our lab, the identification of an non-synonymous SNP in the SP, strongly associated with MS in Europe, urged us to investigate in more detail how this variant affected the secretion of these isoforms.

In this study, we discovered that IL-22BPi1 displays the hallmarks of a poorly secreted, misfolded protein incapable of binding IL-22 in biological or co-folding assays. We also demonstrated that both IL-22BPi1 and IL-22BPi2 are found in a complex with a series of ER chaperones, including GRP78, GRP94, calnexin, GRP170, PDIA6, cyclophilin B, and ERdj3. Structure–function and ensuing analyses revealed that the secretion of both IL-22BPi1 and IL-22BPi2, but not IL-22BPi3, is dependent on functionally intact GRP78 and GRP94, and that IL-22BPi1 co-immunoprecipitates higher quantities of GRP94 than IL-22BPi2. We found that IL-22BPi1, but not IL-22BPi2 or IL-22BPi3, induces a UPR response resulting in higher GRP78 and GRP94 protein levels. We also analysed whether pharmacological targeting of GRP94 or cyclophilin B by GA analogues or cyclosporin A, respectively, can be translationally applied to modulate the secretion of IL-22BP isoforms. Finally, we found that the MS-associated infrequent SNP, rs28385692, has immediate functional effects by reducing secreted IL-22BP levels in the HEK293 cell line. This thesis demonstrates the importance of the characterization of protein isoforms by a) describing a new intracellular function of IL-22BPi1 unrelated to the neutralization of IL-22 and b) shedding light on

the properties of unique human IL-22BP isoforms that are not reflected in murine models due to their absence in expression.

We began by analysing the sequence and modelling the 3D structure of each isoform. All isoforms shared the same SP and were predicted to be efficiently secreted. In the analysis of the bioinformatic predictions of their PTMs (glycosylation and disulphide bond formation), they were all expected to be N-glycosylated – three N-linked glycosylations for IL-22BPi1 and IL-22BPi2, and only one for IL-22BPi3. In addition, Ser^{28} only on IL-22BPi2 was also predicted to be O-glycosylated. Several disulphide bridges were expected to participate in the structure of IL-22BP isoforms – three in IL-22BPi1, two in IL-22BPi2, and one in IL-22BPi3. Modelling the secondary and tertiary structures of the three isoforms with the additional observation of the IL-22/IL-22BPi2 binding sites previously described (de Moura et al., 2009), we anticipated that the additional 32-amino-acid sequence in IL-22BPi1 is an IDR that lacks a fixed secondary structure and may therefore interfere with the binding of IL-22 to IL-22BPi1.

We continued by investigating the gene expression of the three mRNA variants and corresponding proteins in natural producer cells. We selected human, immature moDCs, as these have been identified as the main cellular sources of *IL22RA2* (Huber et al., 2012; Jinnohara et al., 2017; Lim et al., 2016; Martin et al., 2014; Voglis et al., 2018). In line with previous observations (Lim et al., 2016; J. C. Martin et al., 2014), we found that the human gene co-expresses mRNAs for three protein isoforms and that the treatment of moDCs with retinoic acid receptor agonist AM580 or maturation with IFN-γ and LPS strongly increases or suppresses, respectively, all three *IL22RA2* isoform mRNA levels. Similarly, we found that U937DCs also co-expresses the three variants and that the LPS maturation stimulus and AM580 show comparable effects on *IL22RA2* expression, similar to human moDCs, serving as a model for future research. Moreover, we were also the first to detect IL-22BP at a protein level in the secreted fraction of human moDCs by an ELISA developed within this thesis. However, we were not able to detect secreted IL-22BP

by moDCs in CMs or APs via Western blot. A likely reason for this is that the protein levels are below the limit of detection.

Due to these low amounts of IL-22BP protein levels and the difficulties in discriminating between isoforms in the natural system, we switched to a recombinant system to determine the biochemical characteristics, cellular localization, and interacting partners for each isoform. Therefore, we used the widely employed HEK293 cell line by transfecting it with individual expression vectors for IL-22BPi1, IL-22BPi2, or IL- 22BPi3. We found that all isoforms were located in the MOs after sequential cell fractionation, and that all of them contained high mannose glycans compatible with the N-glycosylation sites bioinformatically predicted. Similar to what was published during the completion of this thesis by Lim and colleagues (Lim et al., 2016), we were unable to detect IL-22BPi1 in both (un-)concentrated culture media of transfected cells by Western blot means, though we could discern small amounts of secreted protein by ELISA. The work done by Lim also demonstrated that the subcloning of the alternatively spliced exon from IL-22BPi1 into IL-22BPi3 arrested the latter's secretion. Comparable results were obtained by others in our research group[1] and showed that the insertion of this exon into the reading frame of IL-2, which is an abundantly secreted cytokine, was sufficient to block its secretion. In that study, we also found that IL-22BPi2 and IL-22BPi3, but not IL-22BPi1, co-localize with a trans-Golgi protein marker observed by immunofluorescence confocal microscopy. Moreover, the diffuse perinuclear staining pattern of IL-22BPi1, in contrast, resembled that of the luminal ER protein ERP72, suggesting that the extra sequence acts as a powerful ER retention signal limiting the transit towards the Golgi apparatus (Gómez-Fernández et al., 2018).

We set out to determine the factors that cause intracellular retention of IL-22BPi1by performing an interactome analysis of the affinity-tagged IL-22BP isoforms purified from total CLs. We identified GRP78, which is a

[1] *Not included in this thesis*

crucial luminal ER chaperone involved in translocation, folding, and retrograde transport of newly synthesized proteins via direct interaction with the polypeptide backbone (Otero, Lizák, & Hendershot, 2010) as the main interacting partner of IL- 22BPi1 and IL-22BP2. These isoforms, but not IL-22BPi3, were found to interact with the substrate-binding domain of GRP78. Co-transfection with wtGRP78, but not the ATPase-negative T37G GRP78mutant (Gaut & Hendershot, 1993) significantly increased the secretion of IL-22BPi1 and IL-22BPi2, but not that of IL-22BPi3, as measured in ELISA. Thus, both IL-22BPi1 and IL-22BPi2 appear to behave as bona fide secretory client proteins of GRP78, and the extra exon sequence does not appear to change the site of interaction with GRP78. Interactomes of IL-22BPi2 purified from either HEK293 or HeLa cells reproducibly contained, apart from GRP78, also calnexin, GRP170, and GRP94, suggesting extensive ER quality control scrutiny of its folding. These chaperones, as well as ERdj3, cyclophilin B, and PDIA6 were found to interact with both IL-22BPi2 and IL-22BPi1 in Western blot analysis. The C-terminal half (amino acids 455–577) of the MD of GRP94 was identified as a critical client-binding region of both IL-22BPi1 and IL-22BPi2. This region differs from that identified for the GRP94 clients OS-9 or TLRs and integrins (Dersh et al., 2014; S. Wu et al., 2012), but the implications are still difficult to interpret given the scarcity of information on the mechanisms defining the interaction of client proteins with GRP94. The ATPase-negative GRP94 MD and ΔA mutants that show strong interaction with both isoforms also reduced their secretion, which is indicative of competition with a productive 'pro-secretion' role of GRP94 in IL-22BPi1 or IL-22BPi2 folding, dependent on functionally intact GRP94. Additional studies conducted by our group but not included in this thesis found a virtually perfect co-localization of IL-22BPi1 and a mutant form of IL-2 containing the extra *IL22RA2v1* exon with GRP94, identifying this chaperone as crucially associated with their arrest of transit to Golgi. Calnexin is part of the ER quality control system that acts to retain unfolded N-linked glycoproteins (Williams, 2006), compatible with mono-glucosylation of the high-mannose type N-glycans we identified on intracellular IL- 22BP isoforms. GRP170, which is an HSP70-

type chaperone, and ERdj3, which is a DnaJ-family GRP78 co-factor, recognize distinct sets of peptide sequences in unfolded proteins; interestingly, while GRP78 and ERdj3 can interact with many diverse client peptide sequences, GRP170 was recently shown to interact specifically with rarer, aggregation-prone regions that, if continuously exposed, may trigger disposal of the protein by ERAD given the toxicity of protein aggregates to cell survival (Behnke, Mann, Scruggs, Feige, & Hendershot, 2016). This potential link to ERAD is substantiated by the observation that both IL22-BPi1 and IL-22BPi2, but not IL-22BPi3, appear to be partially degraded by the proteasome.

As the secretion of both IL-22BPi1 and IL-22BPi2, but not IL-22BPi3, is dependent on the functionally intact luminal ER chaperones GRP94 and GRP78, and since other ER resident proteins have also been identified as their partners, we further analysed whether pharmacological targeting of IL-22BP ER-associated partners (GRP94 or cyclophilin B) could modulate their secretion. Interestingly, both intracellular and secreted levels of IL-22BPi1 were strongly increased by GA or its analogues (all GRP94 inhibitors). The secretion of IL-22BPi1 was also enhanced by cyclosporin A (CsA, a molecule that empties the cell from cyclophilin B and C). CsA did not seem to bind to IL-22BP in a bioinformatic study in which more than 100 putative CsA partners were identified (Hu et al., 2014). IL-22BPi2 and IL-22BPi3 were not affected by GA or its analogues, while their secretion appeared to decrease in the presence of CsA (summarized in **Figure 75**). Our results suggest that the source of extra secreted IL-22BPi1 protein is to be found in the fraction of IL-22BPi1 retained intracellularly and likely destined for degradation by the proteasome. This, in turn, indicates that both intact GRP94 and cyclophilin B are instrumental in the ER retention and ERAD of IL-22BPi1 and that unperturbed ATPase activity of GRP94 – despite the demonstrated need for intact GRP94 for the secretion of both IL-22BPi1 and IL-22BPi2 – is ultimately less crucial in facilitating the secretion of both isoforms than it is for the ERAD of IL-22BPi1. Pertinent to this finding, the extra exon in IL-22BPi1 is a strong determinant of the interaction with GRP94; when cloned into the reading frame of the unrelated GRP94-non-binding cytokine IL-2, the resulting

protein fails to be secreted and gains strong reactivity for GRP94 (Gómez-Fernández et al., 2018). The existence of multimeric complexes in which cyclophilin B associates with other ER resident proteins, such as GRP94, GRP78, and calreticulin, has been described (Jansen et al., 2012; Meunier, Usherwood, Chung, & Hendershot, 2002; J. Zhang & Herscovitz, 2003). The enzymatic activity of cyclophilin B has been found to play crucial roles in ERAD and ER redox homeostasis (Bernasconi et al., 2010; Kim et al., 2008; Stocki et al., 2014).

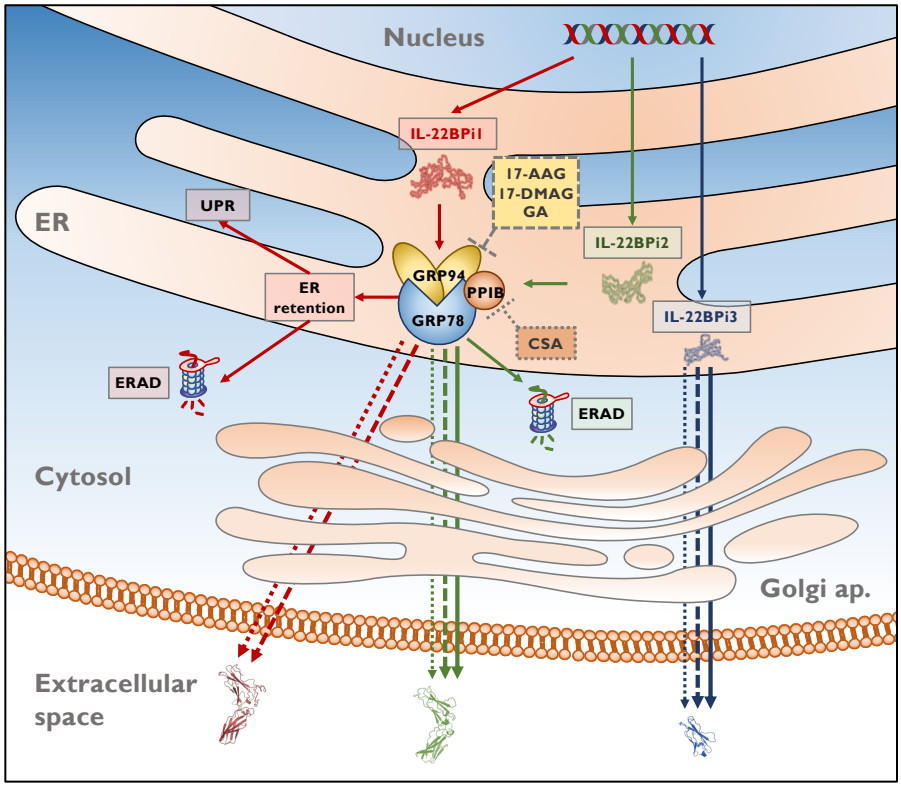

Figure 75: Pathways governing secretion and/or endoplasmic-reticulum-associated degradation (ERAD) of IL-22BP isoforms. *The diagram depicts the fates of IL-22BPi1, IL-22BPi2, and IL-22BPi3 in untreated transfected cells and following pharmacological targeting of the endoplasmic-reticulum (ER) resident chaperones GRP94 or cyclophilin B. IL-22BPi1 (red symbols and arrows), IL-22BPi2 (green symbols and arrows), and IL-22BPi3 (blue symbols and arrows) are produced through alternative splicing of primary IL22RA2 transcripts. The three isoforms are directed to the ER through their shared signal peptide. IL-22BPi1 and IL-22BPi2 interact in the ER with GRP78, GRP94, and cyclophilin B (PPIB), among other ER resident chaperones and foldases, while IL-22BPi3 does not appear to exhibit*

these interactions. IL-22BPi1 is retained in the ER, delivered for degradation by the proteasome, and is capable of activating the unfolded protein response (UPR). IL-22BPi2 and IL-22BPi3 are more efficiently secreted; however, part of IL-22BPi2 was also found to be subject to proteasomal degradation. Cyclosporin A (CsA) causes depletion of intracellular cyclophilin B (dotted grey line) and geldanamycin (GA), and its analogues 17-dimethylaminoethylamino-17-demethoxygeldanamyin (17-DMAG) and 17-allylamino-17-demethoxygeldanamycin (17-AAG) bind to GRP94 in the ATP-binding site, inhibiting its ATPase activity (dashed grey line). In the presence of CsA or GRP94 inhibitors, IL-22BPi1 is mobilized to be secreted into the extracellular space. GA and analogues do not alter IL-22BPi2 and IL-22BPi3 secretion, but CsA decreases the secretion of both.

As previously mentioned – apart from IL-22BPi1 – IL-22BPi2 but not IL-22BPi3 was found to be partially targeted for degradation by the proteasome. However, while IL-22BPi2 is efficiently secreted, isoform 1 is not, suggesting that the rate of ERAD for the long isoform must be much higher than for the canonical isoform. GRP94 is also thought to be an essential player in ERAD (Christianson, Shaler, Tyler, & Kopito, 2008; Di et al., 2016; Eletto et al., 2010). In fact, GRP94 displays a preference for interacting with non-secretable proteins (Y. Yang & Li, 2005). Several studies have documented GRP94's capacity to bind to folding intermediates so as to prevent them from degradation. GA treatment reduces both intracellular and secreted amounts of bile salt-dependent lipase (BSDL), suggesting that dissociation of BSDL from GRP94 reverts this protein from the secretory to the degradation pathway (Nganga, Bruneau, Sbarra, Lombardo, & Le Petit-Thevenin, 2000), and similar observations were made for another client, p185-erB2 (Mimnaugh, Chavany, & Neckers, 1996). In contrast, IL-22BPi1 joins mutant a1-antitrypsin (Christianson et al., 2008) and γ-aminobutyric acid type A receptors (Di et al., 2016) in revealing GRP94 as a crucial factor for sequestering misfolded proteins in the ER, positively regulating their ERAD.

The effect of GA analogues, together with that of CsA, highlights that an orchestrated ERAD response comprising different ER resident chaperones is needed for IL-22BPi1 degradation and that perturbance of this multimeric chaperone complex by pharmacologically targeting its specific components leads isoform 1 to 'reroute' from the ERAD to the

secretory pathway. Deglycosylation analysis revealed that IL-22BPi1 is secreted as a mixture of high-mannose and complex-type glycoforms, which validates its use in the classical secretory route. Decreased secretion of IL-22BPi2 and IL-22BPi3 in the presence of CsA may be related to changes in ER oxidative pathways (Stocki et al., 2014) or peptidylprolyl isomerase activity. In conclusion, PPIB and GRP94 ATPase activity may be co-involved in the ER sequestration and ERAD of IL-22BPi1, with pharmacological impairment of these enzymatic activities by GA analogues or CsA inducing secretion of IL-22BPi1.

We further investigated whether co-expression of IL-22BP isoforms with their natural ligand, IL-22, may alleviate degradation of the former through enhanced secretion via assembly-induced folding. Such a process has been documented in detail for IL-15, which is pre-assembled in complex with IL-15Rα in the ER/Golgi of DCs. IL-15Rα acts as a chaperone for unstable IL-15, inhibiting its degradation through the proteasome (Bergamaschi et al., 2009; Mortier et al., 2008). A different but related process takes place in eosinophils, where an intracellular pool of IL-4Rα enhances the secretory trafficking of IL-4 for rapid mobilization into secretory vesicles prior to secretion (Spencer et al., 2006). For IL-12 and IL-23, co-expression of the shared β-subunit (p40) inhibits misfolding of the poorly secreted α-subunits (p35 and p19), thereby facilitating secretion of the functional heterodimers (Jalah et al., 2013; Reitberger, Haimerl, Aschenbrenner, Esser-von Bieren, & Feige, 2017). In line with these studies, we found that co-expression of IL-22 enhanced the secretory transit of IL- 22BPi2 and IL-22BPi3, resulting in much higher levels of secreted proteins. This was not seen for IL-22BPi1, whose secretion levels were unaffected by IL-22 co-expression. We were not able to detect expression of IL-22 in immature or mature moDCs by qPCR; therefore, whether IL-22–IL-22BPi2 assembly-induced folding takes place in any other natural producer cell types, such as $CD4^+$ T lymphocytes (Pelczar et al., 2016), remains to be determined. However, together with bioactivity measurements, which showed that IL- 22BPi2 but not IL-22BPi1, when used at similar concentrations, inhibited STAT3 phosphorylation by IL-22, it appears that IL- 22BPi1 is naturally incapable

of interacting with IL-22. This finding contradicts the hypothesis that Lim and colleagues (Lim et al., 2016) made where the lack of secretion of IL-22BPi1 was thought to be the principal reason that this isoform fails to significantly alter IL-22 signalling. This discrepancy was likely because the researchers were unable to perform this assay with sufficient amounts of secreted IL-22BPi1. This incapacity to neutralize IL-22 is in accordance with the location of residues critical for the binding of IL-22BPi2 to IL-22, especially Lys65 and Tyr67, close to the position of insertion of the alternatively spliced exon in IL- 22BPi1 (de Moura et al., 2009; B. C. Jones et al., 2008), and it also coincides with what was anticipated from the *in silico* predictions. Dumoutier et al. (Dumoutier, Leemans, et al., 2001) demonstrated that of the IL-10-type homologues including IL-19, IL-20, and IL-24, only IL-22 was able to bind to IL-22BPi2. These observations render the potential for any residual interaction between IL-10- type cytokines and IL-22BPi1 that may 'rescue' its misfolding highly unlikely.

We also tested the capacity of IL-22BP isoforms to activate ER stress signalling via induction of UPR through an accumulation of misfolded protein (Malhotra & Kaufman, 2007). IL-22BPi1 strongly upregulated expression of UPR genes, resulting in increased GRP78 and GRP94 protein levels, thus suggesting that under these experimental conditions, ERAD alone is insufficient to restore ER folding capacity (Molinari & Sitia, 2006). In contrast, IL-22BPi2 did not augment GRP78 and GRP94 protein levels, indicating that its more balanced export from the ER through either secretion or ERAD may eliminate the need for UPR induction. Mirroring the findings in recombinant cells, the work not presented in this thesis, but also done by our group, found that the silencing of *IL22RA2* expression in immature $CD14^{+}$ moDCs coincided with reduced GRP78 expression (Gómez-Fernández et al., 2018).

The alternatively spliced exon of IL22RA2v1 evolved from a retrotransposon of the mammalian apparent long terminal repeat (MaLR) family specific to the great ape lineage that became active consequential to a single mutation (AT➔GT) in the proto-splice site (Piriyapongsa et al., 2007). Exonization processes such as this one have been described as mechanisms that act by adding disordered regions to proteins,

contributing to evolution and linked to new roles in protein-protein interactions associated with signalling and regulatory functions (Buljan et al., 2010). We performed a computational structure prediction of the three mature IL-22BP isoforms; it showed that the only region with a high profile of intrinsic disorder is the one coded by this exon, coinciding with the concept that exonization contributes with disordered regions. Therefore, the failure of IL-22BPi1 to fold may be partially due to the general tendency of alternatively spliced exons to encode intrinsically disordered protein segments (R. van der Lee et al., 2014). Moreover, the sequence and conformation of IL-22BPi2 have phenotypically evolved for high-affinity binding to and neutralization of IL- 22, and the presence of the extra exon in IL-22BPi1 breaks this selection pressure. We cannot exclude the possibility that specific beneficial interactions with IL-22BPi1 occur with as yet undetermined partners within natural producer cells, in specific tissues, or in the extracellular milieu. Our work suggests that one benefit of co-expression of IL-22BPi1 with IL-22BPi2 may reside in its ability, through UPR induction, to augment GRP78 and GRP94 levels. Since both of these chaperones are instrumental in the folding of IL-22BPi2, enhanced secretion levels of IL-22BPi2 by moDCs could thus constitute a positive selectable trait. It has also been described that tissue-specific alternative splicing contributing with intrinsically disordered segments might rewire molecular interactions in specific tissues, conferring functional versatility to proteins and increasing interaction network diversity across tissues (Buljan et al., 2013). In this regard, considering that the placenta is the tissue that exhibits the highest expression of *IL22RA2* splice variant 1 and high levels of the other two variants (Gruenberg et al., 2001; Lim et al., 2016), and that moderated and regulated UPR plays an essential role in early placental development (Bastida-Ruiz, Aguilar, Ditisheim, Yart, & Cohen, 2017; Ghosh et al., 2010; Iwawaki, Akai, Yamanaka, & Kohno, 2009), the function of IL-22BPi1 in this tissue could be implicated in the embryo implantation and placentation process as well as in the modulation of the immune response. A constant increase in IL-22BP protein levels (without mention of which isoform) in maternal plasma during gestation has recently been

reported (Romero et al., 2017); those levels likely correspond to IL-22BPi2 and IL-22BPi3, which, as mentioned before, could be beneficiated by co-expression with IL-22BPi1. As previously stated, this long isoform emerged in the evolution of great apes earlier than the divergence of orangutans and humans (~14 M.Y.; Piriyapongsa et al., 2007). The differences in placentation between gibbons and Old World monkeys (not expressing this isoform) on the one hand and the great apes on the other, such as the deep extravillous trophoblast invasion and spiral artery remodelling characteristic in the human placenta shared within the great ape line (Crosley, Elliot, Christians, & Crespi, 2013), should be considered for future functional studies of this isoform in the placental tissue. Further research should be done to investigate which cells in the placenta express this isoform as well as when during pregnancy. Research regarding isoform-specific expression will also contribute to the understanding of their role in that tissue. Gene-editing techniques, such as CRISP-CAS9, to abolish IL-22BP1 expression in the natural producer cells will aid in the evaluation of its function. Finally, pending further investigation, constitutively higher levels of ER chaperones may prepare the ER of immature moDCs for the enhanced processing potential of secretory and membrane proteins, including MHC receptors, integrins, and cytokines, which are massively expressed immediately upon receipt of TLR ligands or other maturation triggers (Wolk et al., 2008).

Finally, the functional study of the effect of the rare MS risk-associated variant in *IL22RA2* (rs28385692) revealed reducing secreted IL-22BP levels in HEK293 cells. This SNP, located in exon 2 of *IL22RA2*, changes the amino acid in position 16 of the protein SP from leucine to proline. *In silico* prediction methods diverged in their capacity to assign to this variant a functionally relevant effect on the protein function. However, various *in silico* structural assessment methods coincided in predicting a modification to the SP by the 16P residue that may influence the precise location of the cleavage site with the mature portion of the IL-22BP proteins. Furthermore, using transfected cells, *in vitro* assessment of the rs28385692 effect showed experimentally that the L16P mutation significantly reduced the secreted levels of the IL-22BPi1, IL-22BPi2, and

IL-22BPi3 isoforms. Specifically, the risk allele of L16P lowers the secretion levels of each isoform to around 50–60% of those of the respective wild-type forms as quantified using ELISA. The literature documents several examples of similar changes in SPs that have been proven to affect secretion and are related to human diseases or traits: a Leu→Pro mutation in the SP of COL5A1 (Alpha 1 Type V Collagen), which is a subunit of type V collagen, caused retention of this subunit in the ER and was associated with Ehler-Danlos syndrome, a heritable connective tissue disease, in two unrelated families (Symoens et al., 2009). In addition, a common SNP causing a Leu→Pro mutation in the prohormone region of NPY (Neuropeptide Y) caused an increased secretion of this protein in chromaffin cells (Mitchell, Wang, Ramamoorthy, & Whim, 2008). The inverse case (i.e., a change from proline to leucine) has also been reported to affect protein secretion: a Pro→Leu mutation in the SP of Dentin Sialophosphoprotein (DSPP) resulted in a defective secretion of this protein and was associated with dentinogenesis imperfecta type III in a Korean family (S.-K. Lee et al., 2013). Finally, a Thr→Pro variant associated with coronary artery disease risk, located in the SP of the lysosomal acid lipase gene (*LIPA*), yields reduced LIPA protein levels and activity due to enhanced degradation (Morris et al., 2017). Functional research on this variant will certainly provide insight into the role of this gene in MS and a better understanding of the still fairly unexplored function of IL-22BP isoforms in the immune system.

The intriguing biological and differential activities of each IL-22BP isoform may assign new functions to *IL22RA2* genetic polymorphisms that have been associated with inflammatory and autoimmune diseases. Important next steps would be: firstly, to determine the biological function of isoform 1, which seems to be far from blocking IL-22; secondly, to determine the expression of each isoform in human diseases; and thirdly, to understand the homeostatic subtle balance that IL-22BP exerts together with IL-22.

7. Bibliography

7 Bibliography

Abbas, A. K., Lichtman, A. H., & Pillai, S. (2012). *Cellular and molecular immunology*. Elsevier/Saunders.

Adamczak, R., Porollo, A., & Meller, J. (2004). Accurate prediction of solvent accessibility using neural networks-based regression. *Proteins: Structure, Function, and Bioinformatics*, *56*(4), 753–767. https://doi.org/10.1002/prot.20176

Adzhubei, I. A., Schmidt, S., Peshkin, L., Ramensky, V. E., Gerasimova, A., Bork, P., Kondrashov, A. S., & Sunyaev, S. R. (2010). A method and server for predicting damaging missense mutations. *Nature Methods*, *7*(4), 248–249. https://doi.org/10.1038/nmeth0410-248

Adzhubei, I., Jordan, D. M., & Sunyaev, S. R. (2013). *Predicting functional effect of human missense mutations using PolyPhen-2*. *Current Protocols in Human Genetics*. https://doi.org/10.1002/0471142905.hg0720s76

Aggarwal, S., Xie, M. H., Maruoka, M., Foster, J., & Gurney, A. L. (2001). Acinar cells of the pancreas are a target of interleukin-22. *Journal of Interferon & Cytokine Research : The Official Journal of the International Society for Interferon and Cytokine Research*, *21*(12), 1047–1053. https://doi.org/10.1089/107999001317205178

Almagro Armenteros, J. J., Tsirigos, K. D., Sønderby, C. K., Petersen, T. N., Winther, O., Brunak, S., von Heijne, G., & Nielsen, H. (2019). SignalP 5.0 improves signal peptide predictions using deep neural networks. *Nature Biotechnology*, *37*(4), 420–423. https://doi.org/10.1038/s41587-019-0036-z

Almolda, B., Costa, M., Montoya, M., González, B., & Castellano, B. (2011). Increase in Th17 and T-reg Lymphocytes and Decrease of IL22 Correlate with the Recovery Phase of Acute EAE IN Rat. *PLoS ONE*, *6*(11), e27473. https://doi.org/10.1371/journal.pone.0027473

Andoh, A., Zhang, Z., Inatomi, O., Fujino, S., Deguchi, Y., Araki, Y., Tsujikawa, T., Kitoh, K., Kim–Mitsuyama, S., Takayanagi, A., Shimizu, N., & Fujiyama, Y. (2005). Interleukin-22, a Member of the IL-10 Subfamily, Induces Inflammatory Responses in Colonic Subepithelial Myofibroblasts. *Gastroenterology*, *129*(3), 969–984. https://doi.org/10.1053/j.gastro.2005.06.071

Arloth, J., Eraslan, G., Andlauer, T. F. M., Martins, J., Iurato, S., Kühnel, B., Waldenberger, M., Frank, J., Gold, R., Hemmer, B., Luessi, F., Nischwitz, S., Paul, F., Wiendl, H., Gieger, C., Heilmann-Heimbach, S., Kacprowski, T., Laudes, M., Meitinger, T., Peters, A., Rawal, R., Strauch, K., Lucae, S., Müller-Myhsok, B., Rietschel, M., Theis, F. J., Binder, E. B., & Mueller, N. S. (2020). DeepWAS: Multivariate genotype-phenotype associations by directly integrating regulatory information using deep learning. *PLoS Computational Biology*, *16*(2), e1007616. https://doi.org/10.1371/journal.pcbi.1007616

Aujla, S. J., Chan, Y. R., Zheng, M., Fei, M., Askew, D. J., Pociask, D. A., Reinhart, T. A., McAllister, F., Edeal, J., Gaus, K., Husain, S., Kreindler, J. L., Dubin, P. J., Pilewski, J. M., Myerburg, M. M., Mason, C. A., Iwakura, Y., & Kolls, J. K. (2008). IL-22 mediates mucosal host defense against Gram-negative bacterial pneumonia. *Nature Medicine*, *14*(3), 275–281. https://doi.org/10.1038/nm1710

Babu, M. M. (2016). The contribution of intrinsically disordered regions to protein function, cellular complexity, and human disease. *Biochemical Society Transactions*, *44*(5), 1185–1200. https://doi.org/10.1042/BST20160172

Badr, A. M. M., Farag, Y., Abdelshafy, M., & Riad, N. M. (2017). Urinary interleukin 22 binding protein as a marker of lupus nephritis in Egyptian children with juvenile systemic lupus erythematosus. *Clinical Rheumatology*. https://doi.org/10.1007/s10067-017-3812-5

Baecher-Allan, C., Kaskow, B. J., & Weiner, H. L. (2018). Multiple Sclerosis: Mechanisms and Immunotherapy. *Neuron*, *97*(4), 742–768. https://doi.org/10.1016/j.neuron.2018.01.021

Bahlo, M., Booth, D. R., Broadley, S. A., Brown, M. A., Foote, S. J., Griffiths, L. R., Kilpatrick, T. J., Lechner-Scott, J., Moscato, P., Perreau, V. M., Rubio, J. P., Scott, R. J., Stankovich, J., Stewart, G. J., Taylor, B. V, Wiley, J., Brown, M. A., Booth, D. R., Clarke, G., Cox, M. B., Csurhes, P. A., Danoy, P., Drysdale, K., Field, J., Foote, S. J., Greer, J. M., Griffiths, L. R., Guru, P., Hadler, J., McMorran, B. J., Jensen, C. J., Johnson, L. J., McCallum, R., Merriman, M., Merriman, T., Pryce, K., Scott, R. J., Stewart, G. J., Tajouri, L., Wilkins, E. J., Rubio, J. P., Bahlo, M., Brown, M. A., Browning, B. L., Browning, S. R., Perera, D., Rubio, J. P., Stankovich, J., Broadley, S., Butzkueven, H., Carroll, W. M., Chapman, C., Kermode, A. G., Marriott, M., Mason, D., Heard, R. N., Pender, M. P., Slee, M., Tubridy, N., Lechner-Scott, J., Taylor, B. V, Willoughby, E., & Kilpatrick, T. J. (2009). Genome-wide association study identifies new multiple sclerosis susceptibility loci on chromosomes 12 and 20. *Nature Genetics*, *41*(7), 824–828. https://doi.org/10.1038/ng.396

Bao, W., Jin, L., Fu, H. jing, Shen, Y. nian, Lu, G. xia, Mei, H., Cao, X. zhi, Wang, H. sheng, & Liu, W. da. (2013). Interleukin-22 Mediates Early Host Defense against Rhizomucor pusilluscan Pathogens. *PLoS ONE*, *8*(6). https://doi.org/10.1371/journal.pone.0065065

Baranzini, S. E., & Oksenberg, J. R. (2017). The Genetics of Multiple Sclerosis: From 0 to 200 in 50 Years. *Trends in Genetics*, *33*(12), 960–970. https://doi.org/10.1016/j.tig.2017.09.004

Baranzini, S. E., Wang, J., Gibson, R. A., Galwey, N., Naegelin, Y., Barkhof, F., Radue, E. W., Lindberg, R. L. P., Uitdehaag, B. M. G., Johnson, M. R., Angelakopoulou, A., Hall, L., Richardson, J. C., Prinjha, R. K., Gass, A., Geurts, J. J. G., Kragt, J., Sombekke, M., Vrenken, H., Qualley, P., Lincoln, R. R., Gomez, R., Caillier, S. J., George, M. F., Mousavi, H., Guerrero, R., Okuda, D. T., Cree, B. A. C., Green, A. J., Waubant, E., Goodin, D. S., Pelletier, D., Matthews, P. M., Hauser, S. L., Kappos, L., Polman, C. H., & Oksenberg, J. R. (2009). Genome-wide association analysis of susceptibility and clinical phenotype in multiple sclerosis. *Human Molecular Genetics*, *18*(4), 767–778.

https://doi.org/10.1093/hmg/ddn388

Bastida-Ruiz, D., Aguilar, E., Ditisheim, A., Yart, L., & Cohen, M. (2017). Endoplasmic reticulum stress responses in placentation - A true balancing act. *Placenta*, *57*, 163–169. https://doi.org/10.1016/j.placenta.2017.07.004

Beecham, A. H., Patsopoulos, N. A., Xifara, D. K., Davis, M. F., Kemppinen, A., Cotsapas, C., Shah, T. S., Spencer, C., Booth, D., Goris, A., Oturai, A., Saarela, J., Fontaine, B., Hemmer, B., Martin, C., Zipp, F., D'Alfonso, S., Martinelli-Boneschi, F., Taylor, B., Harbo, H. F., Kockum, I., Hillert, J., Olsson, T., Ban, M., Oksenberg, J. R., Hintzen, R., Barcellos, L. F., Agliardi, C., Alfredsson, L., Alizadeh, M., Anderson, C., Andrews, R., Søndergaard, H. B., Baker, A., Band, G., Baranzini, S. E., Barizzone, N., Barrett, J., Bellenguez, C., Bergamaschi, L., Bernardinelli, L., Berthele, A., Biberacher, V., Binder, T. M. C., Blackburn, H., Bomfim, I. L., Brambilla, P., Broadley, S., Brochet, B., Brundin, L., Buck, D., Butzkueven, H., Caillier, S. J., Camu, W., Carpentier, W., Cavalla, P., Celius, E. G., Coman, I., Comi, G., Corrado, L., Cosemans, L., Cournu-Rebeix, I., Cree, B. A. C., Cusi, D., Damotte, V., Defer, G., Delgado, S. R., Deloukas, P., Di Sapio, A., Dilthey, A. T., Donnelly, P., Dubois, B., Duddy, M., Edkins, S., Elovaara, I., Esposito, F., Evangelou, N., Fiddes, B., Field, J., Franke, A., Freeman, C., Frohlich, I. Y., Galimberti, D., Gieger, C., Gourraud, P. A., Graetz, C., Graham, A., Grummel, V., Guaschino, C., Hadjixenofontos, A., Hakonarson, H., Halfpenny, C., Hall, G., Hall, P., Hamsten, A., Harley, J., Harrower, T., Hawkins, C., Hellenthal, G., Hillier, C., Hobart, J., Hoshi, M., Hunt, S. E., Jagodic, M., Jelcic, I., Jochim, A., Kendall, B., Kermode, A., Kilpatrick, T., Koivisto, K., Konidari, I., Korn, T., Kronsbein, H., Langford, C., Larsson, M., Lathrop, M., Lebrun-Frenay, C., Lechner-Scott, J., Lee, M. H., Leone, M. A., Leppä, V., Liberatore, G., Lie, B. A., Lill, C. M., Lindén, M., Link, J., Luessi, F., Lycke, J., Macciardi, F., Männistö, S., Manrique, C. P., Martin, R., Martinelli, V., Mason, D., Mazibrada, G., McCabe, C., Mero, I. L., Mescheriakova, J., Moutsianas, L., Myhr, K. M., Nagels, G., Nicholas, R., Nilsson, P., Piehl, F., Pirinen, M., Price, S. E., Quach, H., Reunanen, M., Robberecht, W., Robertson, N. P., Rodegher, M., Rog, D., Salvetti, M., Schnetz-Boutaud, N. C., Sellebjerg, F., Selter, R. C., Schaefer, C., Shaunak, S., Shen, L., Shields, S., Siffrin, V., Slee, M., Sorensen, P. S., Sorosina, M., Sospedra, M., Spurkland, A., Strange, A., Sundqvist, E., Thijs, V., Thorpe, J., Ticca, A., Tienari, P., Van Duijn, C., Visser, E. M., Vucic, S., Westerlind, H., Wiley, J. S., Wilkins, A., Wilson, J. F., Winkelmann, J., Zajicek, J., Zindler, E., Haines, J. L., Pericak-Vance, M. A., Ivinson, A. J., Stewart, G., Hafler, D., Hauser, S. L., Compston, A., McVean, G., De Jager, P., Sawcer, S. J., & McCauley, J. L. (2013). Analysis of immune-related loci identifies 48 new susceptibility variants for multiple sclerosis. *Nature Genetics*, *45*(11), 1353–1362. https://doi.org/10.1038/ng.2770

Behnke, J., Mann, M. J., Scruggs, F.-L., Feige, M. J., & Hendershot, L. M. (2016). Members of the Hsp70 Family Recognize Distinct Types of Sequences to Execute ER Quality Control. *Molecular Cell*, *63*(5), 739–752. https://doi.org/10.1016/j.molcel.2016.07.012

Bendl, J., Stourac, J., Salanda, O., Pavelka, A., Wieben, E. D., Zendulka, J., Brezovsky, J., & Damborsky, J. (2014). PredictSNP: Robust and Accurate Consensus Classifier for

Prediction of Disease-Related Mutations. *PLoS Computational Biology*, *10*(1), e1003440. https://doi.org/10.1371/journal.pcbi.1003440

Bendtsen, J. D., Nielsen, H., von Heijne, G., & Brunak, S. (2004). Improved prediction of signal peptides: SignalP 3.0. *Journal of Molecular Biology*, *340*(4), 783–795. https://doi.org/10.1016/j.jmb.2004.05.028

Bergamaschi, C., Jalah, R., Kulkarni, V., Rosati, M., Zhang, G.-M., Alicea, C., Zolotukhin, A. S., Felber, B. K., & Pavlakis, G. N. (2009). Secretion and biological activity of short signal peptide IL-15 is chaperoned by IL-15 receptor alpha in vivo. *Journal of Immunology (Baltimore, Md. : 1950)*, *183*(5), 3064–3072. https://doi.org/10.4049/jimmunol.0900693

Bernasconi, R., Soldà, T., Galli, C., Pertel, T., Luban, J., & Molinari, M. (2010). Cyclosporine A-Sensitive, Cyclophilin B-Dependent Endoplasmic Reticulum-Associated Degradation. *PLoS ONE*, *5*(9), e13008. https://doi.org/10.1371/journal.pone.0013008

Bertrams, J., & Kuwert, E. (1972). HL-A Antigen Frequencies in Multiple Sclerosis. *European Neurology*, *7*(1–2), 74–78. https://doi.org/10.1159/000114414

Beyeen, A. D., Adzemovic, M. Z., Ockinger, J., Stridh, P., Becanovic, K., Laaksonen, H., Lassmann, H., Harris, R. A., Hillert, J., Alfredsson, L., Celius, E. G., Harbo, H. F., Kockum, I., Jagodic, M., & Olsson, T. (2010). IL-22RA2 Associates with Multiple Sclerosis and Macrophage Effector Mechanisms in Experimental Neuroinflammation. *The Journal of Immunology*, *185*(11), 6883–6890. https://doi.org/10.4049/jimmunol.1001392

Bleicher, L., de Moura, P. R., Watanabe, L., Colau, D., Dumoutier, L., Renauld, J. C., & Polikarpov, I. (2008). Crystal structure of the IL-22/IL-22R1 complex and its implications for the IL-22 signaling mechanism. *FEBS Letters*, *582*(20), 2985–2992. https://doi.org/10.1016/j.febslet.2008.07.046

Boniface, K., Bernard, F.-X., Garcia, M., Gurney, A. L., Lecron, J.-C., & Morel, F. (2005). IL-22 inhibits epidermal differentiation and induces proinflammatory gene expression and migration of human keratinocytes. *Journal of Immunology (Baltimore, Md. : 1950)*, *174*(6), 3695–3702. https://doi.org/10.4049/jimmunol.174.6.3695

Brand, S., Beigel, F., Olszak, T., Zitzmann, K., Eichhorst, T., Otte, J., Diepolder, H., Marquardt, A., Jagla, W., Popp, A., Herrmann, K., Seiderer, J., Ochsenku, T., Auernhammer, C. J., Dambacher, J., Mar-, A., Herr-, K., & Go, B. (2006). IL-22 is increased in active Crohn's disease and promotes proinflammatory gene expression and intestinal epithelial cell migration. *Am J Physiol Gastrointest Liver Physiol*, *290*, G827-838. https://doi.org/10.1152/ajpgi.00513.2005.

Brias, S. G., Stack, G., Stacey, M. A., Redwood, A. J., & Humphreys, I. R. (2016). The role of IL-22 in viral infections: Paradigms and paradoxes. *Frontiers in Immunology*, *7*(MAY), 1–9. https://doi.org/10.3389/fimmu.2016.00211

Brito-Zerón, P., Baldini, C., Bootsma, H., Bowman, S. J., Jonsson, R., Mariette, X., Sivils, K., Theander, E., Tzioufas, A., & Ramos-Casals, M. (2016). Sjögren syndrome. *Nature Reviews Disease Primers*, *2*(July), 1–20. https://doi.org/10.1038/nrdp.2016.47

Bromberg, Y., & Rost, B. (2007). SNAP: predict effect of non-synonymous polymorphisms on function. *Nucleic Acids Research*, *35*(11), 3823–3835. https://doi.org/10.1093/nar/gkm238

Buchan, D. W. A. A., Minneci, F., Nugent, T. C. O. O., Bryson, K., & Jones, D. T. (2013). Scalable web services for the PSIPRED Protein Analysis Workbench. *Nucleic Acids Research*, *41*(Web Server issue), 349–357. https://doi.org/10.1093/nar/gkt381

Buchan, D. W. A., & Jones, D. T. (2019). The PSIPRED Protein Analysis Workbench: 20 years on. *Nucleic Acids Research*, *47*(8), 4068–4085. https://doi.org/10.1093/nar/gkz297

Buljan, M., Chalancon, G., Dunker, A. K., Bateman, A., Balaji, S., Fuxreiter, M., & Babu, M. M. (2013). Alternative splicing of intrinsically disordered regions and rewiring of protein interactions. *Current Opinion in Structural Biology*, *23*(3), 443–450. https://doi.org/10.1016/j.sbi.2013.03.006

Buljan, M., Frankish, A., & Bateman, A. (2010). Quantifying the mechanisms of domain gain in animal proteins. *Genome Biology*, *11*(7), R74. https://doi.org/10.1186/gb-2010-11-7-r74

Bulleid, N. J. (2012). Disulfide bond formation in the mammalian endoplasmic reticulum. *Cold Spring Harbor Perspectives in Biology*, *4*(11), 1–12. https://doi.org/10.1101/cshperspect.a013219

Buonocore, S., Ahern, P. P., Uhlig, H. H., Ivanov, I. I., Littman, D. R., Maloy, K. J., & Powrie, F. (2010). Innate lymphoid cells drive interleukin-23-dependent innate intestinal pathology. *Nature*, *464*(7293), 1371–1375. https://doi.org/10.1038/nature08949

Capriotti, E., Calabrese, R., & Casadio, R. (2006). Predicting the insurgence of human genetic diseases associated to single point protein mutations with support vector machines and evolutionary information. *Bioinformatics*, *22*(22), 2729–2734. https://doi.org/10.1093/bioinformatics/btl423

Capriotti, Emidio, Altman, R. B., & Bromberg, Y. (2013). Collective judgment predicts disease-associated single nucleotide variants. *BMC Genomics*, *14*(Suppl 3), S2. https://doi.org/10.1186/1471-2164-14-S3-S2

Cella, M., Fuchs, A., Vermi, W., Facchetti, F., Otero, K., Lennerz, J. K. M., Doherty, J. M., Mills, J. C., & Colonna, M. (2009). A human natural killer cell subset provides an innate source of IL-22 for mucosal immunity. *Nature*, *457*(7230), 722–725. https://doi.org/10.1038/nature07537

Chang, Y., Al-Alwan, L., Risse, P.-A., Halayko, A. J., Martin, J. G., Baglole, C. J., Eidelman, D. H., & Hamid, Q. (2012). Th17-associated cytokines promote human airway smooth muscle

cell proliferation. *The FASEB Journal*, *26*(12), 5152–5160. https://doi.org/10.1096/fj.12-208033

Chen, F., Cao, A., Yao, S., Evans-Marin, H. L., Liu, H., Wu, W., Carlsen, E. D., Dann, S. M., Soong, L., Sun, J., Zhao, Q., & Cong, Y. (2016). mTOR Mediates IL-23 Induction of Neutrophil IL-17 and IL-22 Production. *The Journal of Immunology*, *196*(10), 4390–4399. https://doi.org/10.4049/jimmunol.1501541

Cheng, F., Guo, Z., Xu, H., Yan, D., & Li, Q. (2009). Decreased plasma IL22 levels, but not increased IL17 and IL23 levels, correlate with disease activity in patients with systemic lupus erythematosus. *Annals of the Rheumatic Diseases*, *68*(4), 604–606. https://doi.org/10.1136/ard.2008.097089

Cheng, J., Saigo, H., & Baldi, P. (2005). Large-scale prediction of disulphide bridges using kernel methods, two-dimensional recursive neural networks, and weighted graph matching. *Proteins: Structure, Function, and Bioinformatics*, *62*(3), 617–629. https://doi.org/10.1002/prot.20787

Christianson, J. C., Shaler, T. A., Tyler, R. E., & Kopito, R. R. (2008). OS-9 and GRP94 deliver mutant alpha1-antitrypsin to the Hrd1-SEL1L ubiquitin ligase complex for ERAD. *Nature Cell Biology*, *10*(3), 272–282. https://doi.org/10.1038/ncb1689

Chung, Y., Yang, X., Chang, S. H., Ma, L., Tian, Q., & Dong, C. (2006). Expression and regulation of IL-22 in the IL-17-producing CD4+ T lymphocytes. *Cell Research*, *16*(11), 902–907. https://doi.org/10.1038/sj.cr.7310106

Ciccia, F., Guggino, G., Rizzo, A., Bombardieri, M., Raimondo, S., Carubbi, F., Cannizzaro, A., Sireci, G., Dieli, F., Campisi, G., Giacomelli, R., Cipriani, P., De Leo, G., Alessandro, R., & Triolo, G. (2015). Interleukin (IL)-22 receptor 1 is over-expressed in primary Sjogren's syndrome and Sjögren-associated non-Hodgkin lymphomas and is regulated by IL-18. *Clinical and Experimental Immunology*, *181*(2), 219–229. https://doi.org/10.1111/cei.12643

Ciccia, Francesco, Guggino, G., Rizzo, A., Ferrante, A., Raimondo, S., Giardina, A., Dieli, F., Campisi, G., Alessandro, R., & Triolo, G. (2012). Potential involvement of IL-22 and IL-22-producing cells in the inflamed salivary glands of patients with Sjögren's syndrome. *Annals of the Rheumatic Diseases*, *71*(2), 295–301. https://doi.org/10.1136/ard.2011.154013

Ciric, B., El-behi, M., Cabrera, R., Zhang, G.-X., & Rostami, A. (2009). IL-23 Drives Pathogenic IL-17-Producing CD8+ T Cells. *The Journal of Immunology*, *182*(9), 5296–5305. https://doi.org/10.4049/jimmunol.0900036

Collin, M., & Bigley, V. (2018). Human dendritic cell subsets: an update. *Immunology*, *154*(1), 3–20. https://doi.org/10.1111/imm.12888

Collin, M., Bigley, V., Haniffa, M., & Hambleton, S. (2011). Human dendritic cell deficiency: The

missing ID? *Nature Reviews Immunology*, *11*(9), 575–583. https://doi.org/10.1038/nri3046

Comabella, M., Craig, D. W., Camiña-Tato, M., Morcillo, C., Lopez, C., Navarro, A., Rio, J., Montalban, X., & Martin, R. (2008). Identification of a Novel Risk Locus for Multiple Sclerosis at 13q31.3 by a Pooled Genome-Wide Scan of 500,000 Single Nucleotide Polymorphisms. *PLoS ONE*, *3*(10), e3490. https://doi.org/10.1371/journal.pone.0003490

Crosley, E. J., Elliot, M. G., Christians, J. K., & Crespi, B. J. (2013). Placental invasion, preeclampsia risk and adaptive molecular evolution at the origin of the great apes: Evidence from genome-wide analyses. *Placenta*, *34*(2), 127–132. https://doi.org/10.1016/j.placenta.2012.12.001

Cunningham, F., Achuthan, P., Akanni, W., Allen, J., Amode, M. R., Armean, I. M., Bennett, R., Bhai, J., Billis, K., Boddu, S., Cummins, C., Davidson, C., Dodiya, K. J., Gall, A., Girón, C. G., Gil, L., Grego, T., Haggerty, L., Haskell, E., Hourlier, T., Izuogu, O. G., Janacek, S. H., Juettemann, T., Kay, M., Laird, M. R., Lavidas, I., Liu, Z., Loveland, J. E., Marugán, J. C., Maurel, T., McMahon, A. C., Moore, B., Morales, J., Mudge, J. M., Nuhn, M., Ogeh, D., Parker, A., Parton, A., Patricio, M., Abdul Salam, A. I., Schmitt, B. M., Schuilenburg, H., Sheppard, D., Sparrow, H., Stapleton, E., Szuba, M., Taylor, K., Threadgold, G., Thormann, A., Vullo, A., Walts, B., Winterbottom, A., Zadissa, A., Chakiachvili, M., Frankish, A., Hunt, S. E., Kostadima, M., Langridge, N., Martin, F. J., Muffato, M., Perry, E., Ruffier, M., Staines, D. M., Trevanion, S. J., Aken, B. L., Yates, A. D., Zerbino, D. R., & Flicek, P. (2019). Ensembl 2019. *Nucleic Acids Research*, *47*(D1), D745–D751. https://doi.org/10.1093/nar/gky1113

da Rocha, L. F., Duarte, Â. L. B. P., Dantas, A. T., Mariz, H. A., Pitta, I. da R., Galdino, S. L., & Pitta, M. G. da R. (2012). Increased serum interleukin 22 in patients with rheumatoid arthritis and correlation with disease activity. *The Journal of Rheumatology*, *39*(7), 1320–1325. https://doi.org/10.3899/jrheum.111027

De Jager, P. L., Jia, X., Wang, J., de Bakker, P. I. W., Ottoboni, L., Aggarwal, N. T., Piccio, L., Raychaudhuri, S., Tran, D., Aubin, C., Briskin, R., Romano, S., Baranzini, S. E., McCauley, J. L., Pericak-Vance, M. A., Haines, J. L., Gibson, R. A., Naeglin, Y., Uitdehaag, B., Matthews, P. M., Kappos, L., Polman, C., McArdle, W. L., Strachan, D. P., Evans, D., Cross, A. H., Daly, M. J., Compston, A., Sawcer, S. J., Weiner, H. L., Hauser, S. L., Hafler, D. A., & Oksenberg, J. R. (2009). Meta-analysis of genome scans and replication identify CD6, IRF8 and TNFRSF1A as new multiple sclerosis susceptibility loci. *Nature Genetics*, *41*(7), 776–782. https://doi.org/10.1038/ng.401

De Luca, A., Zelante, T., D'Angelo, C., Zagarella, S., Fallarino, F., Spreca, A., Iannitti, R. G., Bonifazi, P., Renauld, J. C., Bistoni, F., Puccetti, P., & Romani, L. (2010). IL-22 defines a novel immune pathway of antifungal resistance. *Mucosal Immunology*, *3*(4), 361–373. https://doi.org/10.1038/mi.2010.22

de Moura, P. R., Watanabe, L., Bleicher, L., Colau, D., Dumoutier, L., Lemaire, M. M., Renauld,

J.-C., & Polikarpov, I. (2009). Crystal structure of a soluble decoy receptor IL-22BP bound to interleukin-22. *FEBS Letters*, *583*(7), 1072–1077. https://doi.org/10.1016/j.febslet.2009.03.006

Dendrou, C. A., Fugger, L., & Friese, M. A. (2015). Immunopathology of multiple sclerosis. *Nature Reviews Immunology*, *15*(9), 545–558. https://doi.org/10.1038/nri3871

Dersh, D., Jones, S. M., Eletto, D., Christianson, J. C., & Argon, Y. (2014). OS-9 facilitates turnover of nonnative GRP94 marked by hyperglycosylation. *Molecular Biology of the Cell*, *25*(15), 2220–2234. https://doi.org/10.1091/mbc.E14-03-0805

Di, X.-J., Wang, Y.-J., Han, D.-Y., Fu, Y.-L., Duerfeldt, A. S., Blagg, B. S. J., & Mu, T.-W. (2016). Grp94 Protein Delivers γ-Aminobutyric Acid Type A (GABA A) Receptors to Hrd1 Protein-mediated Endoplasmic Reticulum-associated Degradation. *Journal of Biological Chemistry*, *291*(18), 9526–9539. https://doi.org/10.1074/jbc.M115.705004

Didonna, A., & Oksenberg, J. R. (2015). Genetic determinants of risk and progression in multiple sclerosis. *Clinica Chimica Acta*, *449*, 16–22. https://doi.org/10.1016/j.cca.2015.01.034

Doisne, J.-M., Soulard, V., Becourt, C., Amniai, L., Henrot, P., Havenar-Daughton, C., Blanchet, C., Zitvogel, L., Ryffel, B., Cavaillon, J.-M., Marie, J. C., Couillin, I., & Benlagha, K. (2011). Cutting Edge: Crucial Role of IL-1 and IL-23 in the Innate IL-17 Response of Peripheral Lymph Node NK1.1- Invariant NKT Cells to Bacteria. *The Journal of Immunology*, *186*(2), 662–666. https://doi.org/10.4049/jimmunol.1002725

Dong, Chen, & Martinez, G. J. (2010). T cells : the usual subsets. Retrieved from https://www.nature.com/nri/posters/tcellsubsets/index.html

Dong, Chengliang, Wei, P., Jian, X., Gibbs, R., Boerwinkle, E., Wang, K., & Liu, X. (2015). Comparison and integration of deleteriousness prediction methods for nonsynonymous SNVs in whole exome sequencing studies. *Human Molecular Genetics*, *24*(8), 2125–2137. https://doi.org/10.1093/hmg/ddu733

Donnelly, R. P., Sheikh, F., Kotenko, S. V., & Dickensheets, H. (2004). The expanded family of class II cytokines that share the IL-10 receptor-2 (IL-10R2) chain. *Journal of Leukocyte Biology*, *76*(2), 314–321. https://doi.org/10.1189/jlb.0204117

Drozdetskiy, A., Cole, C., Procter, J., & Barton, G. J. (2015). JPred4: A protein secondary structure prediction server. *Nucleic Acids Research*, *43*(W1), W389–W394. https://doi.org/10.1093/nar/gkv332

Dudakov, J. A., Hanash, A. M., Brink, M. R. M. van den, & van den Brink, M. R. M. (2015). Interleukin-22: Immunobiology and Pathology. *Annual Review of Immunology*, *33*(1), 747–785. https://doi.org/10.1146/annurev-immunol-032414-112123

Duerfeldt, A. S., Peterson, L. B., Maynard, J. C., Ng, C. L., Eletto, D., Ostrovsky, O., Shinogle, H.

E., Moore, D. S., Argon, Y., Nicchitta, C. V, & Blagg, B. S. J. (2012). Development of a Grp94 inhibitor. *Journal of the American Chemical Society*, *134*(23), 9796–9804. https://doi.org/10.1021/ja303477g

Duhen, T., Geiger, R., Jarrossay, D., Lanzavecchia, A., & Sallusto, F. (2009). Production of interleukin 22 but not interleukin 17 by a subset of human skin-homing memory T cells. *Nature Immunology*, *10*(8), 857–863. https://doi.org/10.1038/ni.1767

Dumoutier, L., de Meester, C., Tavernier, J., & Renauld, J.-C. (2009). New Activation Modus of STAT3. *Journal of Biological Chemistry*, *284*(39), 26377–26384. https://doi.org/10.1074/jbc.M109.007955

Dumoutier, L., Leemans, C., Lejeune, D., Kotenko, S. V., & Renauld, J.-C. (2001). Cutting Edge: STAT Activation By IL-19, IL-20 and mda-7 Through IL-20 Receptor Complexes of Two Types. *The Journal of Immunology*, *167*(7), 3545–3549. https://doi.org/10.4049/jimmunol.167.7.3545

Dumoutier, L., Lejeune, D., Colau, D., & Renauld, J.-C. (2001). Cloning and Characterization of IL-22 Binding Protein, a Natural Antagonist of IL-10-Related T Cell-Derived Inducible Factor/IL-22. *The Journal of Immunology*, *166*(12), 7090–7095. https://doi.org/10.4049/jimmunol.166.12.7090

Dumoutier, L., Louahed, J., & Renauld, J.-C. (2000). Cloning and Characterization of IL-10-Related T Cell-Derived Inducible Factor (IL-TIF), a Novel Cytokine Structurally Related to IL-10 and Inducible by IL-9. *The Journal of Immunology*, *164*(4), 1814–1819. https://doi.org/10.4049/jimmunol.164.4.1814

Dumoutier, L., Van Roost, E., Ameye, G., Michaux, L., & Renauld, J. C. (2000). IL-TIF/IL-22: genomic organization and mapping of the human and mouse genes. *Genes and Immunity*, *1*(8), 488–494. https://doi.org/10.1038/sj.gene.6363716

Dumoutier, L., Van Roost, E., Colau, D., & Renauld, J. C. (2000). Human interleukin-10-related T cell-derived inducible factor: molecular cloning and functional characterization as an hepatocyte-stimulating factor. *Proceedings of the National Academy of Sciences of the United States of America*, *97*(18), 10144–10149. https://doi.org/10.1073/pnas.170291697

Dyment, D. A., Yee, I. M. L., Ebers, G. C., & Sadovnick, A. D. (2006). Multiple sclerosis in stepsiblings: Recurrence risk and ascertainment. *Journal of Neurology, Neurosurgery and Psychiatry*, *77*(2), 258–259. https://doi.org/10.1136/jnnp.2005.063008

Dyson, H. J., & Wright, P. E. (2005). Intrinsically unstructured proteins and their functions. *Nature Reviews Molecular Cell Biology*, *6*(3), 197–208. https://doi.org/10.1038/nrm1589

Ebbo, M., Crinier, A., Vély, F., & Vivier, E. (2017). Innate lymphoid cells: Major players in inflammatory diseases. *Nature Reviews Immunology*, *17*(11), 665–678.

https://doi.org/10.1038/nri.2017.86

Ebers, G. C., Sadovnick, A. D., & Risch, N. J. (1995). A genetic basis for familial aggregation in multiple sclerosis. *Nature*, *377*(6545), 150–151. https://doi.org/10.1038/377150a0

Ebers, G. C., Yee, I. M. L., Sadovnick, A. D., & Duquette, P. (2000). Conjugal multiple sclerosis: Population-based prevalence and recurrence risks in offspring. *Annals of Neurology*, *48*(6), 927–931. https://doi.org/10.1002/1531-8249(200012)48:6<927::AID-ANA14>3.0.CO;2-F

Ebers, George C. (2008). Environmental factors and multiple sclerosis. *The Lancet Neurology*, *7*(3), 268–277. https://doi.org/10.1016/S1474-4422(08)70042-5

Eken, A., Singh, A. K., Treuting, P. M., & Oukka, M. (2014). IL-23R+innate lymphoid cells induce colitis via interleukin-22-dependent mechanism. *Mucosal Immunology*, *7*(1), 143–154. https://doi.org/10.1038/mi.2013.33

Eletto, D., Dersh, D., & Argon, Y. (2010). GRP94 in ER quality control and stress responses. *Seminars in Cell & Developmental Biology*, *21*(5), 479–485. https://doi.org/10.1016/j.semcdb.2010.03.004

Fagnani, C., Neale, M. C., Nisticò, L., Stazi, M. A., Ricigliano, V. A., Buscarinu, M. C., Salvetti, M., & Ristori, G. (2015). Twin studies in multiple sclerosis: A meta-estimation of heritability and environmentality. *Multiple Sclerosis*, *21*(11), 1404–1413. https://doi.org/10.1177/1352458514564492

Fantou, A., Abidi, A., Delbos, L., Podevin, J., Jarry, A., Heslan, M., Martin, J., Bourreille, A., & Josien, R. (2019). P089 Extensive characterisation of cellular sources of IL-22BP in inflammatory bowel diseases indicates that T cells do not express IL-22BP. In *Journal of Crohn's and Colitis* (Vol. 13, pp. S130–S130). Narnia. https://doi.org/10.1093/ecco-jcc/jjy222.213

Fard, N. A., Azizi, G., & Mirshafiey, A. (2016). The potential role of T helper cell 22 and IL-22 in immunopathogenesis of multiple sclerosis. *Innovations in Clinical Neuroscience*, *13*(7–8), 30–36.

Fass, D. (2012). Disulfide Bonding in Protein Biophysics. *Annual Review of Biophysics*, *41*(1), 63–79. https://doi.org/10.1146/annurev-biophys-050511-102321

Fearon, P., Lonsdale-Eccles, A. A., Ross, O. K., Todd, C., Sinha, A., Allain, F., & Reynolds, N. J. (2011). Keratinocyte Secretion of Cyclophilin B via the Constitutive Pathway Is Regulated through Its Cyclosporin-Binding Site. *Journal of Investigative Dermatology*, *131*(5), 1085–1094. https://doi.org/10.1038/jid.2010.415

Felix, J., & Savvides, S. N. (2017). Mechanisms of immunomodulation by mammalian and viral decoy receptors: insights from structures. *Nature Reviews Immunology*, *17*(2), 112–129. https://doi.org/10.1038/nri.2016.134

Filippi, M., Rocca, M. A., Ciccarelli, O., De Stefano, N., Evangelou, N., Kappos, L., Rovira, A., Sastre-Garriga, J., Tintorè, M., Frederiksen, J. L., Gasperini, C., Palace, J., Reich, D. S., Banwell, B., Montalban, X., & Barkhof, F. (2016). MRI criteria for the diagnosis of multiple sclerosis: MAGNIMS consensus guidelines. *The Lancet Neurology*, *15*(3), 292–303. https://doi.org/10.1016/S1474-4422(15)00393-2

Franz, J., Jerome, J., Lear, T., Gong, Q., & Weathington, N. M. (2015). The human IL-22 receptor is regulated through the action of the novel E3 ligase subunit FBXW12, which functions as an epithelial growth suppressor. *Journal of Immunology Research*, *2015*. https://doi.org/10.1155/2015/912713

Fukaya, T., Fukui, T., Uto, T., Takagi, H., Nasu, J., Miyanaga, N., Arimura, K., Nakamura, T., Koseki, H., Choijookhuu, N., Hishikawa, Y., & Sato, K. (2018). Pivotal Role of IL-22 Binding Protein in the Epithelial Autoregulation of Interleukin-22 Signaling in the Control of Skin Inflammation. *Frontiers in Immunology*, *9*(June), 1–13. https://doi.org/10.3389/fimmu.2018.01418

Fukui, H., Zhang, X., Sun, C., Hara, K., Kikuchi, S., Yamasaki, T., Kondo, T., Tomita, T., Oshima, T., Watari, J., Imura, J., Fujimori, T., Sasako, M., & Miwa, H. (2014). IL-22 produced by cancer-associated fibroblasts promotes gastric cancer cell invasion via STAT3 and ERK signaling. *British Journal of Cancer*, *111*(4), 763–771. https://doi.org/10.1038/bjc.2014.336

Fumagalli, S., Torri, A., Papagna, A., Citterio, S., Mainoldi, F., & Foti, M. (2016). IL-22 is rapidly induced by Pathogen Recognition Receptors Stimulation in Bone-Marrow-derived Dendritic Cells in the Absence of IL-23. *Scientific Reports*, *6*(September), 1–15. https://doi.org/10.1038/srep33900

Gaut, J. R., & Hendershot, L. M. (1993). Mutations within the nucleotide binding site of immunoglobulin-binding protein inhibit ATPase activity and interfere with release of immunoglobulin heavy chain. *The Journal of Biological Chemistry*, *268*(10), 7248–7255. Retrieved from http://www.ncbi.nlm.nih.gov/pubmed/8463260

Geijtenbeek, T. B., Torensma, R., van Vliet, S. J., van Duijnhoven, G. C., Adema, G. J., van Kooyk, Y., & Figdor, C. G. (2000). Identification of DC-SIGN, a novel dendritic cell-specific ICAM-3 receptor that supports primary immune responses. *Cell*, *100*(5), 575–585. Retrieved from https://www.cell.com/action/showPdf?pii=S0092-8674%2800%2980693-5

Gessner, M. A., Werner, J. L., Lilly, L. M., Nelson, M. P., Metz, A. E., Dunaway, C. W., Chan, Y. R., Ouyang, W., Brown, G. D., Weaver, C. T., & Steele, C. (2012). Dectin-1-dependent interleukin-22 contributes to early innate lung defense against aspergillus fumigatus. *Infection and Immunity*, *80*(1), 410–417. https://doi.org/10.1128/IAI.05939-11

Gewirth, D. T. (2016). Paralog Specific Hsp90 Inhibitors - A Brief History and a Bright Future. *Current Topics in Medicinal Chemistry*, *16*(25), 2779–2791. https://doi.org/10.2174/1568026616666160413141154

Ghosh, R., Lipson, K. L., Sargent, K. E., Mercurio, A. M., Hunt, J. S., Ron, D., & Urano, F. (2010). Transcriptional regulation of VEGF-A by the unfolded protein response pathway. *PLoS ONE*, *5*(3). https://doi.org/10.1371/journal.pone.0009575

Ginhoux, F., & Jung, S. (2014). Monocytes and macrophages : developmental pathways and tissue homeostasis. *Nature Publishing Group*, *14*(6), 392–404. https://doi.org/10.1038/nri3671

Goger, B., Halden, Y., Rek, A., Mösl, R., Pye, D., Gallagher, J., & Kungl, A. J. (2002). Different Affinities of Glycosaminoglycan Oligosaccharides for Monomeric and Dimeric Interleukin-8: A Model for Chemokine Regulation at Inflammatory Sites †. *Biochemistry*, *41*(5), 1640–1646. https://doi.org/10.1021/bi011944j

Gómez-Fernández, P., Lopez de Lapuente Portilla, A., Astobiza, I., Mena, J., Urtasun, A., Altmann, V., Matesanz, F., Otaegui, D., Urcelay, E., Antigüedad, A., Malhotra, S., Montalban, X., Castillo-Triviño, T., Espino-Paisán, L., Aktas, O., Buttmann, M., Chan, A., Fontaine, B., Gourraud, P.-A., Hecker, M., Hoffjan, S., Kubisch, C., Kümpfel, T., Luessi, F., Zettl, U. K., Zipp, F., Alloza, I., Comabella, M., Lill, C. M., & Vandenbroeck, K. (2020). The Rare IL22RA2 Signal Peptide Coding Variant rs28385692 Decreases Secretion of IL-22BP Isoform-1, -2 and -3 and Is Associated with Risk for Multiple Sclerosis. *Cells*, *9*(1), 175. https://doi.org/10.3390/cells9010175

Gómez-Fernández, P., Urtasun, A., Paton, A. W., Paton, J. C., Borrego, F., Dersh, D., Argon, Y., Alloza, I., & Vandenbroeck, K. (2018). Long Interleukin-22 Binding Protein Isoform-1 Is an Intracellular Activator of the Unfolded Protein Response. *Frontiers in Immunology*, *9*, 2934. https://doi.org/10.3389/fimmu.2018.02934

Goto, Y., Obata, T., Kunisawa, J., Sato, S., Ivanov, I. I., Lamichhane, A., Takeyama, N., Kamioka, M., Sakamoto, M., Matsuki, T., Setoyama, H., Imaoka, A., Uematsu, S., Akira, S., Domino, S. E., Kulig, P., Becher, B., Renauld, J.-C., Sasakawa, C., Umesaki, Y., Benno, Y., & Kiyono, H. (2014). Innate lymphoid cells regulate intestinal epithelial cell glycosylation. *Science*, *345*(6202), 1254009–1254009. https://doi.org/10.1126/science.1254009

Greb, J. E., Goldminz, A. M., Elder, J. T., Lebwohl, M. G., Gladman, D. D., Wu, J. J., Mehta, N. N., Finlay, A. Y., & Gottlieb, A. B. (2016). Psoriasis. *Nature Reviews Disease Primers*, *2*. https://doi.org/10.1038/nrdp.2016.82

Gruenberg, B. H., Schoenemeyer, A., Weiss, B., Toschi, L., Kunz, S., Wolk, K., Asadullah, K., & Sabat, R. (2001). A novel, soluble homologue of the human IL-10 receptor with preferential expression in placenta. *Genes and Immunity*, *2*(6), 329–334. https://doi.org/10.1038/sj.gene.6363786

Guilliams, M., Ginhoux, F., Jakubzick, C., Naik, S. H., Onai, N., Schraml, B. U., Segura, E., Tussiwand, R., & Yona, S. (2014). Dendritic cells, monocytes and macrophages: a unified nomenclature based on ontogeny. *Nature Reviews Immunology*, *14*(8), 571–578.

https://doi.org/10.1038/nri3712

Gupta, R., Jung, E., & Brunak, S. (2004). Prediction of N-glycosylation sites in human proteins, *46*, 203–206.

Halim, T. Y. F., Steer, C. A., Mathä, L., Gold, M. J., Martinez-Gonzalez, I., McNagny, K. M., McKenzie, A. N. J., & Takei, F. (2014). Group 2 innate lymphoid cells are critical for the initiation of adaptive T helper 2 cell-mediated allergic lung inflammation. *Immunity*, *40*(3), 425–435. https://doi.org/10.1016/j.immuni.2014.01.011

Hamada, H., Garcia-Hernandez, M. d. l. L., Reome, J. B., Misra, S. K., Strutt, T. M., McKinstry, K. K., Cooper, A. M., Swain, S. L., & Dutton, R. W. (2009). Tc17, a Unique Subset of CD8 T Cells That Can Protect against Lethal Influenza Challenge. *The Journal of Immunology*, *182*(6), 3469–3481. https://doi.org/10.4049/jimmunol.0801814

Hansson, M., Silverpil, E., Lindén, A., & Glader, P. (2013). Interleukin-22 produced by alveolar macrophages during activation of the innate immune response. *Inflammation Research*, *62*(6), 561–569. https://doi.org/10.1007/s00011-013-0608-1

Harter, C., & Wieland, F. (1996). The secretory pathway: mechanisms of protein sorting and transport. *Biochimica et Biophysica Acta (BBA) - Reviews on Biomembranes*, *1286*(2), 75–93. https://doi.org/10.1016/0304-4157(96)00003-2

Hassan, M. S., Shaalan, A. A., Dessouky, M. I., Abdelnaiem, A. E., Abdel-Haleem, D. A., & ElHefnawi, M. (2018). Predicting Non-Synonymous Single Nucleotide Variants Pathogenic Effects in Human Diseases. In *Encyclopedia of Bioinformatics and Computational Biology* (pp. 400–409). Amserdam, Netherlands: Elsevier Ltd. https://doi.org/10.1016/b978-0-12-809633-8.90692-7

Hebert, K. D., Mclaughlin, N., Galeas-Pena, M., Zhang, Z., Eddens, T., Govero, A., Pilewski, J. M., Kolls, J. K., & Pociask, D. A. (2020). Targeting the IL-22/IL-22BP axis enhances tight junctions and reduces inflammation during influenza infection. *Mucosal Immunology*, *13*(1), 64–74. https://doi.org/10.1038/s41385-019-0206-9

Hernandez, P., Gronke, K., & Diefenbach, A. (2018). A catch-22: Interleukin-22 and cancer. *European Journal of Immunology*, *48*(1), 15–31. https://doi.org/10.1002/eji.201747183

Hetz, C. (2012). The unfolded protein response: controlling cell fate decisions under ER stress and beyond. *Nature Reviews Molecular Cell Biology*, *13*(2), 89–102. https://doi.org/10.1038/nrm3270

Hiller, K., Grote, A., Scheer, M., Munch, R., & Jahn, D. (2004). PrediSi: prediction of signal peptides and their cleavage positions. *Nucleic Acids Research*, *32*(Web Server), W375–W379. https://doi.org/10.1093/nar/gkh378

Holden, P., & Horton, W. A. (2009). Crude subcellular fractionation of cultured mammalian cell

lines. *BMC Research Notes*, *2*(1), 243. https://doi.org/10.1186/1756-0500-2-243

Hu, G., Wang, K., Groenendyk, J., Barakat, K., Mizianty, M. J., Ruan, J., Michalak, M., & Kurgan, L. (2014). Human structural proteome-wide characterization of Cyclosporine a targets. *Bioinformatics*, *30*(24), 3561–3566. https://doi.org/10.1093/bioinformatics/btu581

Hubank, M., & Schatz, D. G. (1994). Identifying differences in mRNA expression by\rrepresentational difference analysis of cDNA. *Nucleic Acids Research*, *22*(25), 5640–5648.

Huber, S., Gagliani, N., Zenewicz, L. A., Huber, F. J., Bosurgi, L., Hu, B., Hedl, M., Zhang, W., O'Connor, W., Murphy, A. J., Valenzuela, D. M., Yancopoulos, G. D., Booth, C. J., Cho, J. H., Ouyang, W., Abraham, C., & Flavell, R. A. (2012). IL-22BP is regulated by the inflammasome and modulates tumorigenesis in the intestine. *Nature*, *491*(7423), 259–263. https://doi.org/10.1038/nature11535

Igawa, D., Sakai, M., & Savan, R. (2006). An unexpected discovery of two interferon gamma-like genes along with interleukin (IL)-22 and -26 from teleost: IL-22 and -26 genes have been described for the first time outside mammals. *Molecular Immunology*, *43*(7), 999–1009. https://doi.org/10.1016/j.molimm.2005.05.009

Ikeuchi, H., Kuroiwa, T., Hiramatsu, N., Kaneko, Y., Hiromura, K., Ueki, K., & Nojima, Y. (2005). Expression of interleukin-22 in rheumatoid arthritis: Potential role as a proinflammatory cytokine. *Arthritis & Rheumatism*, *52*(4), 1037–1046. https://doi.org/10.1002/art.20965

Ioannidis, N. M., Rothstein, J. H., Pejaver, V., Middha, S., McDonnell, S. K., Baheti, S., Musolf, A., Li, Q., Holzinger, E., Karyadi, D., Cannon-Albright, L. A., Teerlink, C. C., Stanford, J. L., Isaacs, W. B., Xu, J., Cooney, K. A., Lange, E. M., Schleutker, J., Carpten, J. D., Powell, I. J., Cussenot, O., Cancel-Tassin, G., Giles, G. G., MacInnis, R. J., Maier, C., Hsieh, C.-L., Wiklund, F., Catalona, W. J., Foulkes, W. D., Mandal, D., Eeles, R. A., Kote-Jarai, Z., Bustamante, C. D., Schaid, D. J., Hastie, T., Ostrander, E. A., Bailey-Wilson, J. E., Radivojac, P., Thibodeau, S. N., Whittemore, A. S., & Sieh, W. (2016). REVEL: An Ensemble Method for Predicting the Pathogenicity of Rare Missense Variants. *The American Journal of Human Genetics*, *99*(4), 877–885. https://doi.org/10.1016/j.ajhg.2016.08.016

Iwawaki, T., Akai, R., Yamanaka, S., & Kohno, K. (2009). Function of IRE1 alpha in the placenta is essential for placental development and embryonic viability. *Proceedings of the National Academy of Sciences of the United States of America*, *106*(39), 16657–16662. https://doi.org/10.1073/pnas.0903775106

Jakkula, E., Leppä, V., Sulonen, A.-M., Varilo, T., Kallio, S., Kemppinen, A., Purcell, S., Koivisto, K., Tienari, P., Sumelahti, M.-L., Elovaara, I., Pirttilä, T., Reunanen, M., Aromaa, A., Oturai, A. B., Søndergaard, H. B., Harbo, H. F., Mero, I.-L., Gabriel, S. B., Mirel, D. B., Hauser, S. L., Kappos, L., Polman, C., De Jager, P. L., Hafler, D. A., Daly, M. J., Palotie, A.,

Saarela, J., & Peltonen, L. (2010). Genome-wide association study in a high-risk isolate for multiple sclerosis reveals associated variants in STAT3 gene. *American Journal of Human Genetics*, *86*(2), 285–291. https://doi.org/10.1016/j.ajhg.2010.01.017

Jalah, R., Rosati, M., Ganneru, B., Pilkington, G. R., Valentin, A., Kulkarni, V., Bergamaschi, C., Chowdhury, B., Zhang, G.-M., Beach, R. K., Alicea, C., Broderick, K. E., Sardesai, N. Y., Pavlakis, G. N., & Felber, B. K. (2013). The p40 Subunit of Interleukin (IL)-12 Promotes Stabilization and Export of the p35 Subunit. *Journal of Biological Chemistry*, *288*(9), 6763–6776. https://doi.org/10.1074/jbc.M112.436675

Jansen, G., Määttänen, P., Denisov, A. Y., Scarffe, L., Schade, B., Balghi, H., Dejgaard, K., Chen, L. Y., Muller, W. J., Gehring, K., & Thomas, D. Y. (2012). An Interaction Map of Endoplasmic Reticulum Chaperones and Foldases. *Molecular & Cellular Proteomics*, *11*(9), 710–723. https://doi.org/10.1074/mcp.M111.016550

Javed, M. J., Richmond, T. D., & Barber, D. L. (2010). Cytokine Receptor Signaling. In *Handbook of Cell Signaling* (Second Edi, Vol. 2, pp. 451–466). Elsevier. https://doi.org/10.1016/B978-0-12-374145-5.00063-2

Jia, L., & Wu, C. (2014). The Biology and Functions of Th22 Cells. In B. Sun (Ed.), *T Helper Cell Differentiation and Their Function* (Vol. 841, pp. 209–230). Dordrecht: Springer Netherlands. https://doi.org/10.1007/978-94-017-9487-9

Jinnohara, T., Kanaya, T., Hase, K., Sakakibara, S., Kato, T., Tachibana, N., Sasaki, T., Hashimoto, Y., Sato, T., Watarai, H., Kunisawa, J., Shibata, N., Williams, I. R., Kiyono, H., & Ohno, H. (2017). IL-22BP dictates characteristics of Peyer ' s patch follicle- associated epithelium for antigen uptake. *J. Exp. Med*. https://doi.org/10.1084/jem.20160770

Johnson, M., Zaretskaya, I., Raytselis, Y., Merezhuk, Y., McGinnis, S., & Madden, T. L. (2008). NCBI BLAST: a better web interface. *Nucleic Acids Research*, *36*(Web Server), W5–W9. https://doi.org/10.1093/nar/gkn201

Jones, B. C., Logsdon, N. J., & Walter, M. R. (2008). Structure of IL-22 Bound to Its High-Affinity IL-22R1 Chain. *Structure*, *16*(9), 1333–1344. https://doi.org/10.1016/j.str.2008.06.005

Jones, D. T., & Cozzetto, D. (2015). DISOPRED3: precise disordered region predictions with annotated protein-binding activity. *Bioinformatics*, *31*(6), 857–863. https://doi.org/10.1093/bioinformatics/btu744

Julenius, K., Mølgaard, A., Gupta, R., & Brunak, S. (2005). Prediction, conservation analysis, and structural characterization of mammalian mucin-type O-glycosylation sites. *Glycobiology*, *15*(2), 153–164. https://doi.org/10.1093/glycob/cwh151

Justa, S., Zhou, X., & Sarkar, S. (2014). Endogenous IL-22 plays a dual role in arthritis: Regulation of established arthritis via IFN-γ responses. *PLoS ONE*, *9*(3), 1–12.

https://doi.org/10.1371/journal.pone.0093279

Kaech, S. M., & Cui, W. (2012). Transcriptional control of effector and memory CD8+ T cell differentiation. *Nature Reviews Immunology*, *12*(11), 749–761. https://doi.org/10.1038/nri3307

Kall, L., Krogh, A., & Sonnhammer, E. L. L. (2007). Advantages of combined transmembrane topology and signal peptide prediction--the Phobius web server. *Nucleic Acids Research*, *35*(Web Server), W429–W432. https://doi.org/10.1093/nar/gkm256

Kamanaka, M., Huber, S., Zenewicz, L. A., Gagliani, N., Rathinam, C., O'Connor, W., Wan, Y. Y., Nakae, S., Iwakura, Y., Hao, L., & Flavell, R. A. (2011). Memory/effector (CD45RB ^{lo}) CD4 T cells are controlled directly by IL-10 and cause IL-22–dependent intestinal pathology. *The Journal of Experimental Medicine*, *208*(5), 1027–1040. https://doi.org/10.1084/jem.20102149

Kaser, A., Zeissig, S., & Blumberg, R. S. (2010). Inflammatory Bowel Disease. *Annual Review of Immunology*, *28*(1), 573–621. https://doi.org/10.1146/annurev-immunol-030409-101225

Kaul, A., Gordon, C., Crow, M. K., Touma, Z., Urowitz, M. B., Van Vollenhoven, R., Ruiz-Irastorza, G., & Hughes, G. (2016). Systemic lupus erythematosus. *Nature Reviews Disease Primers*, *2*(June), 1–22. https://doi.org/10.1038/nrdp.2016.39

Kebir, H., Kreymborg, K., Ifergan, I., Dodelet-Devillers, A., Cayrol, R., Bernard, M., Giuliani, F., Arbour, N., Becher, B., & Prat, A. (2007). Human TH17 lymphocytes promote blood-brain barrier disruption and central nervous system inflammation. *Nature Medicine*, *13*(10), 1173–1175. https://doi.org/10.1038/nm1651

Kempski, J., Giannou, A. D., Riecken, K., Zhao, L., Steglich, B., Lücke, J., Garcia-Perez, L., Karstens, K.-F., Wöstemeier, A., Nawrocki, M., Pelczar, P., Witkowski, M., Nilsson, S., Konczalla, L., Shiri, A. M., Kempska, J., Wahib, R., Brockmann, L., Huber, P., Gnirck, A.-C., Turner, J.-E., Zazara, D. E., Arck, P. C., Stein, A., Simon, R., Daubmann, A., Meiners, J., Perez, D., Strowig, T., Koni, P., Kruglov, A. A., Sauter, G., Izbicki, J. R., Guse, A. H., Roesch, T., Lohse, A. W., Flavell, R. A., Gagliani, N., & Huber, S. (2020). IL22BP Mediates the Anti-Tumor Effects of Lymphotoxin Against Colorectal Tumors in Mice and Humans. *Gastroenterology*. https://doi.org/10.1053/j.gastro.2020.06.033

Kihara, D. (Ed. . (2017). *Protein Function Prediction. Methods in Molecular Biology*. https://doi.org/10.1007/978-1-4939-7015-5

Kim, J., Choi, T. G., Ding, Y., Kim, Y., Ha, K. S., Lee, K. H., Kang, I., Ha, J., Kaufman, R. J., Lee, J., Choe, W., & Kim, S. S. (2008). Overexpressed cyclophilin B suppresses apoptosis associated with ROS and Ca2+ homeostasis after ER stress. *Journal of Cell Science*, *121*(21), 3636–3648. https://doi.org/10.1242/jcs.028654

Kirchberger, S., Royston, D. J., Boulard, O., Thornton, E., Franchini, F., Szabady, R. L., Harrison, O., & Powrie, F. (2013). Innate lymphoid cells sustain colon cancer through production of interleukin-22 in a mouse model. *The Journal of Experimental Medicine*, *210*(5), 917–931. https://doi.org/10.1084/jem.20122308

Kleinschmidt, D., Giannou, A. D., McGee, H. M., Kempski, J., Steglich, B., Huber, F. J., Ernst, T. M., Shiri, A. M., Wegscheid, C., Tasika, E., Hübener, P., Huber, P., Bedke, T., Steffens, N., Agalioti, T., Fuchs, T., Noll, J., Lotter, H., Tiegs, G., Lohse, A. W., Axelrod, J. H., Galun, E., Flavell, R. A., Gagliani, N., & Huber, S. (2017). A Protective Function of IL-22BP in Ischemia Reperfusion and Acetaminophen-Induced Liver Injury. *The Journal of Immunology*, *199*(12), 4078–4090. https://doi.org/10.4049/jimmunol.1700587

Klose, C. S. N., Flach, M., Möhle, L., Rogell, L., Hoyler, T., Ebert, K., Fabiunke, C., Pfeifer, D., Sexl, V., Fonseca-Pereira, D., Domingues, R. G., Veiga-Fernandes, H., Arnold, S. J., Busslinger, M., Dunay, I. R., Tanriver, Y., & Diefenbach, A. (2014). Differentiation of type 1 ILCs from a common progenitor to all helper-like innate lymphoid cell lineages. *Cell*, *157*(2), 340–356. https://doi.org/10.1016/j.cell.2014.03.030

Kolaczkowska, E., & Kubes, P. (2013). Neutrophil recruitment and function. *Nature Reviews Immunology*, *13*(3), 159–175. https://doi.org/10.1038/nri3399

Kong, X., Feng, D., Wang, H., Hong, F., Bertola, A., Wang, F.-S., & Gao, B. (2012). Interleukin-22 induces hepatic stellate cell senescence and restricts liver fibrosis in mice. *Hepatology*, *56*(3), 1150–1159. https://doi.org/10.1002/hep.25744

Kotenko, S. V., Izotova, L. S., Mirochnitchenko, O. V., Esterova, E., Dickensheets, H., Donnelly, R. P., & Pestka, S. (2001a). Identification, Cloning, and Characterization of a Novel Soluble Receptor That Binds IL-22 and Neutralizes Its Activity. *The Journal of Immunology*, *166*(12), 7096–7103. https://doi.org/10.4049/jimmunol.166.12.7096

Kotenko, S. V., Izotova, L. S., Mirochnitchenko, O. V., Esterova, E., Dickensheets, H., Donnelly, R. P., & Pestka, S. (2001b). Identification of the functional interleukin-22 (IL-22) receptor complex: the IL-10R2 chain (IL-10Rbeta) is a common chain of both the IL-10 and IL-22 (IL-10-related T cell-derived inducible factor, IL-TIF) receptor complexes. *The Journal of Biological Chemistry*, *276*(4), 2725–2732. https://doi.org/10.1074/jbc.M007837200

Kreymborg, K., Etzensperger, R., Dumoutier, L., Haak, S., Rebollo, A., Buch, T., Frank, L., Heppner, F. L. L., Renauld, J. J.-C., & Becher, B. (2007). IL-22 Is Expressed by Th17 Cells in an IL-23-Dependent Fashion, but Not Required for the Development of Autoimmune Encephalomyelitis. *The Journal of Immunology*, *179*(12), 8098–8104. https://doi.org/10.4049/jimmunol.179.12.8098

Krogh, A., Larsson, B., Von Heijne, G., & Sonnhammer, E. L. L. (2001). Predicting transmembrane protein topology with a hidden Markov model: Application to complete genomes. *Journal of Molecular Biology*, *305*(3), 567–580. https://doi.org/10.1006/jmbi.2000.4315

Kronenberger, B., Rudloff, I., Bachmann, M., Brunner, F., Kapper, L., Filmann, N., Waidmann, O., Herrmann, E., Pfeilschifter, J., Zeuzem, S., Piiper, A., & Mühl, H. (2012). Interleukin-22 predicts severity and death in advanced liver cirrhosis: a prospective cohort study. *BMC Medicine*, *10*(1), 102. https://doi.org/10.1186/1741-7015-10-102

Kryczek, I., Lin, Y., Nagarsheth, N., Peng, D., Zhao, L., Zhao, E., & Vatan, L. (2013). Article Stemness via STAT3 Transcription Factor Activation and Induction of the Methyltransferase DOT1L. *Immunity*, *40*(5), 772–784. https://doi.org/10.1016/j.immuni.2014.03.010

Küçükali, C. İ., Kürtüncü, M., Çoban, A., Çebi, M., & Tüzün, E. (2015). Epigenetics of Multiple Sclerosis: An Updated Review. *NeuroMolecular Medicine*, *17*(2), 83–96. https://doi.org/10.1007/s12017-014-8298-6

Kulkarni, O. P., Hartter, I., Mulay, S. R., Hagemann, J., Darisipudi, M. N., Kumar VR, S., Romoli, S., Thomasova, D., Ryu, M., Kobold, S., & Anders, H.-J. (2014). Toll-Like Receptor 4-Induced IL-22 Accelerates Kidney Regeneration. *Journal of the American Society of Nephrology*, *25*(5), 978–989. https://doi.org/10.1681/ASN.2013050528

Kulshreshtha, S., Chaudhary, V., Goswami, G. K., & Mathur, N. (2016). Computational approaches for predicting mutant protein stability. *Journal of Computer-Aided Molecular Design*, *30*(5), 401–412. https://doi.org/10.1007/s10822-016-9914-3

Kumar, P., Thakar, M. S., Ouyang, W., & Malarkannan, S. (2013). IL-22 from conventional NK cells is epithelial regenerative and inflammation protective during influenza infection. *Mucosal Immunology*, *6*(1), 69–82. https://doi.org/10.1038/mi.2012.49

Kumar, Prateek, Henikoff, S., & Ng, P. C. (2009). Predicting the effects of coding non-synonymous variants on protein function using the SIFT algorithm. *Nature Protocols*, *4*(7), 1073–1081. https://doi.org/10.1038/nprot.2009.86

Kumar, R., Kumari, B., & Kumar, M. (2017). Prediction of endoplasmic reticulum resident proteins using fragmented amino acid composition and support vector machine. *PeerJ*, *5*, e3561. https://doi.org/10.7717/peerj.3561

Kumar, S. (2018). Cellular and molecular pathways of renal repair after acute kidney injury. *Kidney International*, *93*(1), 27–40. https://doi.org/10.1016/j.kint.2017.07.030

Laaksonen, H., Guerreiro-Cacais, A. O., Adzemovic, M. Z., Parsa, R., Zeitelhofer, M., Jagodic, M., & Olsson, T. (2014). The multiple sclerosis risk gene IL22RA2 contributes to a more severe murine autoimmune neuroinflammation. *Genes and Immunity*, *15*(7), 457–465. https://doi.org/10.1038/gene.2014.36

Lacy, P., & Stow, J. L. (2018). Review article Cytokine release from innate immune cells : association with diverse membrane trafficking pathways, *118*(1), 9–19.

https://doi.org/10.1182/blood-2010-08-265892.

Lavoie, T. N., Stewart, C. M., Berg, K. M., Li, Y., & Nguyen, C. Q. (2011). Expression of Interleukin-22 in Sjögren's Syndrome: Significant correlation with disease parameters. *Scandinavian Journal of Immunology*, *74*(4), 377–382. https://doi.org/10.1111/j.1365-3083.2011.02583.x

Lebien, T. W., & Tedder, T. F. (2008). ASH 50th anniversary review B lymphocytes : how they develop and function. *The American Society of Hematology*, *112*(5), 1570–1580. https://doi.org/10.1182/blood-2008-02-078071.

Lee, S.-K., Lee, K.-E., Song, S. J., Hyun, H.-K., Lee, S.-H., & Kim, J.-W. (2013). A DSPP Mutation Causing Dentinogenesis Imperfecta and Characterization of the Mutational Effect. *BioMed Research International*, *2013*, 1–7. https://doi.org/10.1155/2013/948181

Leipe, J., Schramm, M. A., Grunke, M., Baeuerle, M., Dechant, C., Nigg, A. P., Witt, M. N., Vielhauer, V., Reindl, C. S., Schulze-Koops, H., & Skapenko, A. (2011). Interleukin 22 serum levels are associated with radiographic progression in rheumatoid arthritis. *Annals of the Rheumatic Diseases*, *70*(8), 1453–1457. https://doi.org/10.1136/ard.2011.152074

Lejeune, D., Dumoutier, L., Constantinescu, S., Kruijer, W., Schuringa, J. J., & Renauld, J.-C. (2002). Interleukin-22 (IL-22) activates the JAK/STAT, ERK, JNK, and p38 MAP kinase pathways in a rat hepatoma cell line. Pathways that are shared with and distinct from IL-10. *The Journal of Biological Chemistry*, *277*(37), 33676–33682. https://doi.org/10.1074/jbc.M204204200

Levine, S. J. (2008). Molecular mechanisms of soluble cytokine receptor generation. *The Journal of Biological Chemistry*, *283*(21), 14177–14181. https://doi.org/10.1074/jbc.R700052200

Li, J., Tomkinson, K. N., Tan, X. Y., Wu, P., Yan, G., Spaulding, V., Deng, B., Annis-Freeman, B., Heveron, K., Zollner, R., De Zutter, G., Wright, J. F., Crawford, T. K., Liu, W., Jacobs, K. A., Wolfman, N. M., Ling, V., Pittman, D. D., Veldman, G. M., & Fouser, L. A. (2004). Temporal associations between interleukin 22 and the extracellular domains of IL-22R and IL-10R2. *International Immunopharmacology*, *4*(5), 693–708. https://doi.org/10.1016/j.intimp.2004.01.010

Li, Z., Galvin, B. D., Raverdy, S., & Carlow, C. K. S. (2011). Identification and characterization of the cofactor-independent phosphoglycerate mutases of Dirofilaria immitis and its Wolbachia endosymbiont. *Veterinary Parasitology*, *176*(4), 350–356. https://doi.org/10.1016/j.vetpar.2011.01.020

Liang, S. C., Nickerson-Nutter, C., Pittman, D. D., Carrier, Y., Goodwin, D. G., Shields, K. M., Lambert, A.-J., Schelling, S. H., Medley, Q. G., Ma, H.-L., Collins, M., Dunussi-Joannopoulos, K., & Fouser, L. A. (2010). IL-22 Induces an Acute-Phase Response. *The Journal of Immunology*, *185*(9), 5531–5538. https://doi.org/10.4049/jimmunol.0904091

Liang, Spencer C., Tan, X.-Y., Luxenberg, D. P., Karim, R., Dunussi-Joannopoulos, K., Collins, M., & Fouser, L. A. (2006). Interleukin (IL)-22 and IL-17 are coexpressed by Th17 cells and cooperatively enhance expression of antimicrobial peptides. *The Journal of Experimental Medicine*, *203*(10), 2271–2279. https://doi.org/10.1084/jem.20061308

Lill, C. M. (2014). Recent advances and future challenges in the genetics of multiple sclerosis. *Frontiers in Neurology*, *5 JUL*(July), 1–5. https://doi.org/10.3389/fneur.2014.00130

Lill, C. M., Schilling, M., Ansaloni, S., Schröder, J., Jaedicke, M., Luessi, F., Schjeide, B.-M. M., Mashychev, A., Graetz, C., Akkad, D. A., Gerdes, L.-A., Kroner, A., Blaschke, P., Hoffjan, S., Winkelmann, A., Dörner, T., Rieckmann, P., Steinhagen-Thiessen, E., Lindenberger, U., Chan, A., Hartung, H.-P., Aktas, O., Lohse, P., Buttmann, M., Kümpfel, T., Kubisch, C., Zettl, U. K., Epplen, J. T., Zipp, F., & Bertram, L. (2014). Assessment of microRNA-related SNP effects in the 3′ untranslated region of the IL22RA2 risk locus in multiple sclerosis. *Neurogenetics*, *15*(2), 129–134. https://doi.org/10.1007/s10048-014-0396-y

Lim, C., Hong, M., & Savan, R. (2016). Human IL-22 binding protein isoforms act as a rheostat for IL-22 signaling. *Science Signaling*, *9*(447), ra95–ra95. https://doi.org/10.1126/scisignal.aad9887

Lindahl, H. (2017). *INTERLEUKIN-22 BINDING PROTEIN IN MULTIPLE SCLEROSIS AND EXPERIMENTAL INFLAMMATION MODELS*. Karolinska Instituet.

Lindahl, H., Guerreiro-Cacais, A. O., Bedri, S. K., Linnerbauer, M., Lindén, M., Abdelmagid, N., Tandre, K., Hollins, C., Irving, L., Glover, C., Jones, C., Alfredsson, L., Rönnblom, L., Kockum, I., Khademi, M., Jagodic, M., & Olsson, T. (2019). IL-22 Binding Protein Promotes the Disease Process in Multiple Sclerosis. *The Journal of Immunology*, *203*(4), 888–898. https://doi.org/10.4049/jimmunol.1900400

Liu, J., Farmer, J. D., Lane, W. S., Friedman, J., Weissman, I., & Schreiber, S. L. (1991). Calcineurin is a common target of cyclophilin-cyclosporin A and FKBP-FK506 complexes. *Cell*, *66*(4), 807–815. https://doi.org/10.1016/0092-8674(91)90124-H

Liu, M., Chen, Z., & Chen, L. (2016). Endoplasmic reticulum stress: a novel mechanism and therapeutic target for cardiovascular diseases. *Acta Pharmacologica Sinica*, *37*(4), 425–443. https://doi.org/10.1038/aps.2015.145

Liu, Y., Yang, B., Ma, J., Wang, H., Huang, F., Zhang, J., Chen, H., & Wu, C. (2011). Interleukin-21 induces the differentiation of human Tc22 cells via phosphorylation of signal transducers and activators of transcription. *Immunology*, *132*(4), 540–548. https://doi.org/10.1111/j.1365-2567.2010.03399.x

Liu, Y., Yang, B., Zhou, M., Li, L., Zhou, H., Zhang, J., Chen, H., & Wu, C. (2009). Memory IL-22-producing CD4+T cells specific for Candida albicans are present in humans. *European Journal of Immunology*, *39*(6), 1472–1479. https://doi.org/10.1002/eji.200838811

Logsdon, N. J., Jones, B. C., Allman, J. C., Izotova, L., Schwartz, B., Pestka, S., & Walter, M. R. (2004). The IL-10R2 Binding Hot Spot on IL-22 is Located on the N-terminal Helix and is Dependent on N-linked Glycosylation. *Journal of Molecular Biology*, *342*(2), 503–514. https://doi.org/10.1016/j.jmb.2004.07.069

Logsdon, N. J., Jones, B. C., Josephson, K., Cook, J., & Walter, M. R. (2002). Comparison of Interleukin-22 and Interleukin-10 Soluble Receptor Complexes. *Journal of Interferon & Cytokine Research*, *22*(11), 1099–1112. https://doi.org/10.1089/10799900260442520

Lowes, M. A., Suárez-Fariñas, M., & Krueger, J. G. (2014). Immunology of psoriasis. *Annual Review of Immunology*, *32*, 227–255. https://doi.org/10.1146/annurev-immunol-032713-120225

Lublin, F. D., Reingold, S. C., Cohen, J. a, Cutter, G. R., Sorensen, P. S., Thompson, A. J., Wolinsky, J. S., Balcer, L. J., Banwell, B., Barkhof, F., Bebo, B., Calabresi, P. A., Clanet, M., Comi, G., Fox, R. J., Freedman, M. S., Goodman, A. D., Inglese, M., Kappos, L., Kieseier, B. C., Lincoln, J. A., Lubetzki, C., Miller, A. E., Montalban, X., O'Connor, P. W., Petkau, J., Pozzilli, C., Rudick, R. A., Sormani, M. P., Stuve, O., Waubant, E., & Polman, C. H. (2014). Defining the clinical course of multiple sclerosis: The 2013 revisions. *Neurology*, *83*(3), 278–286. https://doi.org/10.1212/WNL.0000000000000560

Malhotra, J. D., & Kaufman, R. J. (2007). The endoplasmic reticulum and the unfolded protein response. *Seminars in Cell & Developmental Biology*, *18*(6), 716–731. https://doi.org/10.1016/j.semcdb.2007.09.003

Marijnissen, R. J., Koenders, M. I., Smeets, R. L., Stappers, M. H. T., Nickerson-Nutter, C., Joosten, L. A. B., Boots, A. M. H., & Van Den Berg, W. B. (2011). Increased expression of interleukin-22 by synovial Th17 cells during late stages of murine experimental arthritis is controlled by interleukin-1 and enhances bone degradation. *Arthritis and Rheumatism*, *63*(10), 2939–2948. https://doi.org/10.1002/art.30469

Martin, B., Hirota, K., Cua, D. J., Stockinger, B., & Veldhoen, M. (2009). Interleukin-17-Producing γδ T Cells Selectively Expand in Response to Pathogen Products and Environmental Signals. *Immunity*, *31*(2), 321–330. https://doi.org/10.1016/j.immuni.2009.06.020

Martin, J. C., Bériou, G., Heslan, M., Bossard, C., Jarry, A., Abidi, A., Hulin, P., Ménoret, S., Thinard, R., Anegon, I., Jacqueline, C., Lardeux, B., Halary, F., Renauld, J.-C., Bourreille, A., & Josien, R. (2016). IL-22BP is produced by eosinophils in human gut and blocks IL-22 protective actions during colitis. *Mucosal Immunology*, *9*(2), 539–549. https://doi.org/10.1038/mi.2015.83

Martin, J. C., Bériou, G., Heslan, M., Chauvin, C., Utriainen, L., Aumeunier, A., Scott, C. L., Mowat, A., Cerovic, V., Houston, S. a, Leboeuf, M., Hubert, F. X., Hémont, C., Merad, M., Milling, S., & Josien, R. (2014). Interleukin-22 binding protein (IL-22BP) is constitutively expressed by a subset of conventional dendritic cells and is strongly induced by retinoic

acid. *Mucosal Immunology*, *7*(1), 101–113. https://doi.org/10.1038/mi.2013.28

Martin, J. C., Wolk, K., Bériou, G., Abidi, A., Witte-Händel, E., Louvet, C., Kokolakis, G., Drujont, L., Dumoutier, L., Renauld, J.-C., Sabat, R., & Josien, R. (2017). Limited Presence of IL-22 Binding Protein, a Natural IL-22 Inhibitor, Strengthens Psoriatic Skin Inflammation. *The Journal of Immunology*, *198*(9), 3671–3678. https://doi.org/https://doi.org/10.4049/jimmunol.1700021

Martin, P., McGovern, A., Massey, J., Schoenfelder, S., Duffus, K., Yarwood, A., Barton, A., Worthington, J., Fraser, P., Eyre, S., & Orozco, G. (2016). Identifying causal genes at the multiple sclerosis associated region 6q23 using capture Hi-C. *PLoS ONE*, *11*(11), 1–15. https://doi.org/10.1371/journal.pone.0166923

Marzec, M., Eletto, D., & Argon, Y. (2012). GRP94: An HSP90-like protein specialized for protein folding and quality control in the endoplasmic reticulum. *Biochimica et Biophysica Acta (BBA) - Molecular Cell Research*, *1823*(3), 774–787. https://doi.org/10.1016/j.bbamcr.2011.10.013

Marzec, M., Hawkes, C. P., Eletto, D., Boyle, S., Rosenfeld, R., Hwa, V., Wit, J. M., van Duyvenvoorde, H. A., Oostdijk, W., Losekoot, M., Pedersen, O., Yeap, B. B., Flicker, L., Barzilai, N., Atzmon, G., Grimberg, A., & Argon, Y. (2016). A Human Variant of Glucose-Regulated Protein 94 That Inefficiently Supports IGF Production. *Endocrinology*, *157*(5), 1914–1928. https://doi.org/10.1210/en.2015-2058

Mashiko, S., Bouguermouh, S., Rubio, M., Baba, N., Bissonnette, R., & Sarfati, M. (2015). Human mast cells are major IL-22 producers in patients with psoriasis and atopic dermatitis. *Journal of Allergy and Clinical Immunology*, *136*(2), 351-359.e1. https://doi.org/10.1016/j.jaci.2015.01.033

McLaren, W., Gil, L., Hunt, S. E., Riat, H. S., Ritchie, G. R. S., Thormann, A., Flicek, P., & Cunningham, F. (2016). The Ensembl Variant Effect Predictor. *Genome Biology*, *17*(1), 122. https://doi.org/10.1186/s13059-016-0974-4

McLaughlin, M., & Vandenbroeck, K. (2011). The endoplasmic reticulum protein folding factory and its chaperones: new targets for drug discovery? *British Journal of Pharmacology*, *162*(2), 328–345. https://doi.org/10.1111/j.1476-5381.2010.01064.x

Medzhitov, R. (2007). Recognition of microorganisms and activation of the immune response. *Nature*, *449*(7164), 819–826. https://doi.org/10.1038/nature06246

Men, K., Huang, R., Zhang, X., Zhang, R., Zhang, Y., Peng, Y., Tong, R., Yang, L., Wei, Y., & Duan, X. (2018). Delivery of interleukin-22 binding protein (IL-22BP) gene by cationic micelle for colon cancer gene therapy. *RSC Advances*, *8*(30), 16537–16548. https://doi.org/10.1039/c8ra02580k

Meunier, L., Usherwood, Y.-K., Chung, K. T., & Hendershot, L. M. (2002). A Subset of Chaperones and Folding Enzymes Form Multiprotein Complexes in Endoplasmic Reticulum to Bind Nascent Proteins. *Molecular Biology of the Cell*, *13*(12), 4456–4469. https://doi.org/10.1091/mbc.e02-05-0311

Mimnaugh, E. G., Chavany, C., & Neckers, L. (1996). Polyubiquitination and Proteasomal Degradation of the p185 c- erb B-2 Receptor Protein-tyrosine Kinase Induced by Geldanamycin. *Journal of Biological Chemistry*, *271*(37), 22796–22801. https://doi.org/10.1074/jbc.271.37.22796

Minagar, A., & Alexander, J. S. (2003). Blood-brain barrier disruption in multiple sclerosis. *Multiple Sclerosis*, *9*(6), 540–549. https://doi.org/10.1191/1352458503ms965oa

Mitchell, G. C., Wang, Q., Ramamoorthy, P., & Whim, M. D. (2008). A Common Single Nucleotide Polymorphism Alters the Synthesis and Secretion of Neuropeptide Y. *Journal of Neuroscience*, *28*(53), 14428–14434. https://doi.org/10.1523/JNEUROSCI.0343-08.2008

Mittrücker, H.-W., Visekruna, A., & Huber, M. (2014). Heterogeneity in the Differentiation and Function of CD8+ T Cells. *Archivum Immunologiae et Therapiae Experimentalis*, *62*(6), 449–458. https://doi.org/10.1007/s00005-014-0293-y

Molinari, M., & Sitia, R. (2006). The secretory capacity of a cell depends on the efficiency of endoplasmic reticulum-associated degradation. In E. Wiertz & M. Kikkert (Eds.), *Dislocation and Degradation of Proteins from the Endoplasmic Reticulum. CTMI* (Vol. 300, pp. 1–15). Springer-Verlag Berlin Heidelberg. https://doi.org/10.1007/3-540-28007-3_1

Montaldo, E., Juelke, K., & Romagnani, C. (2015). Group 3 innate lymphoid cells (ILC3s): Origin, differentiation, and plasticity in humans and mice. *European Journal of Immunology*, *45*(8), 2171–2182. https://doi.org/10.1002/eji.201545598

Monteleone, I., Rizzo, A., Sarra, M., Sica, G., Sileri, P., Biancone, L., MacDonald, T. T., Pallone, F., & Monteleone, G. (2011). Aryl Hydrocarbon Receptor-Induced Signals Up-regulate IL-22 Production and Inhibit Inflammation in the Gastrointestinal Tract. *Gastroenterology*, *141*(1), 237-248.e1. https://doi.org/10.1053/j.gastro.2011.04.007

Morris, G. E., Braund, P. S., Moore, J. S., Samani, N. J., Codd, V., & Webb, T. R. (2017). Coronary Artery Disease–Associated LIPA Coding Variant rs1051338 Reduces Lysosomal Acid Lipase Levels and Activity in Lysosomes. *Arteriosclerosis, Thrombosis, and Vascular Biology*, *37*(6), 1050–1057. https://doi.org/10.1161/ATVBAHA.116.308734

Mortier, E., Woo, T., Advincula, R., Gozalo, S., & Ma, A. (2008). IL-15Rα chaperones IL-15 to stable dendritic cell membrane complexes that activate NK cells via trans presentation. *The Journal of Experimental Medicine*, *205*(5), 1213–1225. https://doi.org/10.1084/jem.20071913

Msif. (2013). Atlas of MS 2013: Mapping Multiple Sclerosis Around the World. *Multiple Sclerosis International Federation*, 1–28. https://doi.org/10.1093/brain/awm236

Muls, N., Nasr, Z., Dang, H. A., Sindic, C., & Van Pesch, V. (2017). IL-22, GM-CSF and IL-17 in peripheral CD4+T cell subpopulations during multiple sclerosis relapses and remission. Impact of corticosteroid therapy. *PLoS ONE*, *12*(3), 1–16. https://doi.org/10.1371/journal.pone.0173780

Nagalakshmi, M. L., Murphy, E., McClanahan, T., & de Waal Malefyt, R. (2004). Expression patterns of IL-10 ligand and receptor gene families provide leads for biological characterization. *International Immunopharmacology*, *4*(5), 577–592. https://doi.org/10.1016/j.intimp.2004.01.007

Nagalakshmi, M. L., Rascle, A., Zurawski, S., Menon, S., & de Waal Malefyt, R. (2004). Interleukin-22 activates STAT3 and induces IL-10 by colon epithelial cells. *International Immunopharmacology*, *4*(5), 679–691. https://doi.org/10.1016/j.intimp.2004.01.008

Nagem, R. A. P., Colau, D., Dumoutier, L., Renauld, J.-C., Ogata, C., & Polikarpov, I. (2002). Crystal Structure of Recombinant Human Interleukin-22. *Structure*, *10*(8), 1051–1062. https://doi.org/10.1016/S0969-2126(02)00797-9

Naito, S. (1972). Multiple Sclerosis : Association with HL-A3, (March 1971), 1–4.

Nganga, A., Bruneau, N., Sbarra, V., Lombardo, D., & Le Petit-Thevenin, J. (2000). Control of pancreatic bile-salt-dependent-lipase secretion by the glucose-regulated protein of 94 kDa (Grp94). *The Biochemical Journal*, *352 Pt 3*, 865–874. Retrieved from http://www.ncbi.nlm.nih.gov/pubmed/11104697

Nograles, K. E., Zaba, L. C., Shemer, A., Fuentes-Duculan, J., Cardinale, I., Kikuchi, T., Ramon, M., Bergman, R., Krueger, J. G., & Guttman-Yassky, E. (2009). IL-22-producing "T22" T cells account for upregulated IL-22 in atopic dermatitis despite reduced IL-17-producing TH17 T cells. *Journal of Allergy and Clinical Immunology*, *123*(6), 1244-1252.e2. https://doi.org/10.1016/j.jaci.2009.03.041

O'Gorman, C., Lucas, R., & Taylor, B. (2012). Environmental risk factors for multiple sclerosis: A review with a focus on molecular mechanisms. *International Journal of Molecular Sciences*, *13*(9), 11718–11752. https://doi.org/10.3390/ijms130911718

Okabe, Y., & Medzhitov, R. (2016). Tissue biology perspective on macrophages. *Nature Publishing Group*, *17*(1), 9–17. https://doi.org/10.1038/ni.3320

Olsson, T., Barcellos, L. F., & Alfredsson, L. (2016). Interactions between genetic, lifestyle and environmental risk factors for multiple sclerosis. *Nature Reviews Neurology*, *13*(1), 26–36. https://doi.org/10.1038/nrneurol.2016.187

Otero, J. H., Lizák, B., & Hendershot, L. M. (2010). Life and death of a BiP substrate. *Seminars in*

Cell & Developmental Biology, *21*(5), 472–478. https://doi.org/10.1016/j.semcdb.2009.12.008

Owji, H., Nezafat, N., Negahdaripour, M., Hajiebrahimi, A., & Ghasemi, Y. (2018). A comprehensive review of signal peptides: Structure, roles, and applications. *European Journal of Cell Biology*, *97*(6), 422–441. https://doi.org/10.1016/j.ejcb.2018.06.003

Paget, C., Ivanov, S., Fontaine, J., Renneson, J., Blanc, F., Pichavant, M., Dumoutier, L., Ryffel, B., Renauld, J. C., Gosset, P. P., Gosset, P. P., Si-Tahar, M., Faveeuw, C., & Trottein, F. (2012). Interleukin-22 is produced by invariant natural killer T lymphocytes during influenza A virus infection: Potential role in protection against lung epithelial damages. *Journal of Biological Chemistry*, *287*(12), 8816–8829. https://doi.org/10.1074/jbc.M111.304758

Pan, H. F., Ye, D. Q., & Li, X. P. (2008). Type 17 T-helper cells might be a promising therapeutic target for systemic lupus erythematosus. *Nature Clinical Practice Rheumatology*, *4*(7), 352–353. https://doi.org/10.1038/ncprheum0815

Pan, H. F., Zhao, X. F., Yuan, H., Zhang, W. H., Li, X. P., Wang, G. H., Wu, G. C., Tang, X. W., Li, W. X., Li, L. H., Feng, J. B., Hu, C. S., & Ye, D. Q. (2009). Decreased serum IL-22 levels in patients with systemic lupus erythematosus. *Clinica Chimica Acta*, *401*(1–2), 179–180. https://doi.org/10.1016/j.cca.2008.11.009

Park, O., Wang, H., Weng, H., Feigenbaum, L., Li, H., Yin, S., Ki, S. H., Yoo, S. H., Dooley, S., Wang, F.-S., Young, H. A., & Gao, B. (2011). In vivo consequences of liver-specific interleukin-22 expression in mice: Implications for human liver disease progression. *Hepatology*, *54*(1), 252–261. https://doi.org/10.1002/hep.24339

Park, S. W., & Ozcan, U. (2013). Potential for therapeutic manipulation of the UPR in disease. *Seminars in Immunopathology*, *35*(3), 351–373. https://doi.org/10.1007/s00281-013-0370-z

Patsopoulos, N., Baranzini, S. E., Santaniello, A., Shoostari, P., Cotsapas, C., Wong, G., Beecham, A. H., James, T., Replogle, J., Vlachos, I., McCabe, C., Pers, T., Brandes, A., White, C., Keenan, B., Cimpean, M., Winn, P., Panteliadis, I.-P., Robbins, A., Andlauer, T. F. M., Zarzycki, O., Dubois, B., Goris, A., Bach Sondergaard, H., Sellebjerg, F., Soelberg Sorensen, P., Ullum, H., Wegner Thoerner, L., Saarela, J., Cournu-Rebeix, I., Damotte, V., Fontaine, B., Guillot-Noel, L., Lathrop, M., Vukusik, S., Berthele, A., Biberacher, V., Buck, D., Gasperi, C., Graetz, C., Grummel, V., Hemmer, B., Hoshi, M., Knier, B., Korn, T., Lill, C. M., Luessi, F., Muhlau, M., Zipp, F., Dardiotis, E., Agliardi, C., Amoroso, A., Barizzone, N., Benedetti, M. D., Bernardinelli, L., Cavalla, P., Clarelli, F., Comi, G., Cusi, D., Esposito, F., Ferre, L., Galimberti, D., Guaschino, C., Leone, M. A., Martinelli, V., Moiola, L., Salvetti, M., Sorosina, M., Vecchio, D., Zauli, A., Santoro, S., Zuccala, M., Mescheriakova, J., van Duijn, C., Bos, S. D., Celius, E. G., Spurkland, A., Comabella, M., Montalban, X., Alfredsson, L., Bomfim, I. L., Gomez-Cabrero, D., Hillert, J., Jagodic, M., Linden, M., Piehl, F., Jelcic, I., Martin, R., Sospedra, M., Baker, A., Ban, M., Hawkins, C., Hysi, P., Kalra, S., Karpe, F., Khadake, J., Lachance, G., Molyneux, P., Neville, M., Thorpe, J., Bradshaw, E., Caillier, S. J., Calabresi, P., Cree, B. A. C., Cross, A., Davis, M. F., de Bakker, P., Delgado,

S., Dembele, M., Edwards, K., Fitzgerald, K., Frohlich, I. Y., Gourraud, P.-A., Haines, J. L., Hakonarson, H., Kimbrough, D., Isobe, N., Konidari, I., Lathi, E., Lee, M. H., Li, T., An, D., Zimmer, A., Lo, A., Madireddy, L., Manrique, C. P., Mitrovic, M., Olah, M., Patrick, E., Pericak-Vance, M. A., Piccio, L., Schaefer, C., Weiner, H., Lage, K., Compston, A., Hafler, D., Harbo, H. F., Hauser, S. L., Stewart, G., D'Alfonso, S., Hadjigeorgiou, G., Taylor, B., Barcellos, L. F., Booth, D., Hintzen, R., Kockum, I., Martinelli-Boneschi, F., McCauley, J. L., Oksenberg, J. R., Oturai, A., Sawcer, S., Ivinson, A. J., Olsson, T., De Jager, P. L., & Jager, P. L. De. (2017). The Multiple Sclerosis Genomic Map: Role of peripheral immune cells and resident microglia in susceptibility. *BioRxiv*, 1–43. https://doi.org/https://doi.org/10.1101/143933

Pelczar, P., Witkowski, M., Perez, L. G., Kempski, J., Hammel, A. G., Brockmann, L., Kleinschmidt, D., Wende, S., Haueis, C., Bedke, T., Witkowski, M., Krasemann, S., Steurer, S., Booth, C. J., Busch, P., König, A., Rauch, U., Benten, D., Izbicki, J. R., Rösch, T., Lohse, A. W., Strowig, T., Gagliani, N., Flavell, R. A., & Huber, S. (2016). A pathogenic role for T cell–derived IL-22BP in inflammatory bowel disease. *Science*, *354*(6310), 358–362. https://doi.org/10.1126/science.aah5903

Pepper, M., & Jenkins, M. K. (2011). Origins of CD4+ effector and central memory T cells. *Nature Immunology*, *12*(6), 467–471. https://doi.org/10.1038/ni.2038

Perriard, G., Mathias, A., Enz, L., Canales, M., Schluep, M., Gentner, M., Schaeren-Wiemers, N., & Du Pasquier, R. A. (2015). Interleukin-22 is increased in multiple sclerosis patients and targets astrocytes. *Journal of Neuroinflammation*, *12*(1), 119. https://doi.org/10.1186/s12974-015-0335-3

Petersen, T. N., Brunak, S., von Heijne, G., & Nielsen, H. (2011). SignalP 4.0: discriminating signal peptides from transmembrane regions. *Nature Methods*, *8*(10), 785–786. https://doi.org/10.1038/nmeth.1701

Pham, T. A. N., Clare, S., Goulding, D., Arasteh, J. M., Stares, M. D., Browne, H. P., Keane, J. A., Page, A. J., Kumasaka, N., Kane, L., Mottram, L., Harcourt, K., Hale, C., Arends, M. J., Gaffney, D. J., Dougan, G., & Lawley, T. D. (2014). Epithelial IL-22RA1-mediated fucosylation promotes intestinal colonization resistance to an opportunistic pathogen. *Cell Host and Microbe*, *16*(4), 504–516. https://doi.org/10.1016/j.chom.2014.08.017

Pickert, G., Neufert, C., Leppkes, M., Zheng, Y., Wittkopf, N., Warntjen, M., Lehr, H.-A., Hirth, S., Weigmann, B., Wirtz, S., Ouyang, W., Neurath, M. F., & Becker, C. (2009). STAT3 links IL-22 signaling in intestinal epithelial cells to mucosal wound healing. *The Journal of Experimental Medicine*, *206*(7), 1465–1472. https://doi.org/10.1084/jem.20082683

Piriyapongsa, J., Polavarapu, N., Borodovsky, M., & McDonald, J. (2007). Exonization of the LTR transposable elements in human genome. *BMC Genomics*, *8*(1), 291. https://doi.org/10.1186/1471-2164-8-291

Plank, M. W., Kaiko, G. E., Maltby, S., Weaver, J., Tay, H. L., Shen, W., Wilson, M. S., Durum, S. K., & Foster, P. S. (2017). Th22 Cells Form a Distinct Th Lineage from Th17 Cells In Vitro with Unique Transcriptional Properties and Tbet-Dependent Th1 Plasticity. *The Journal of Immunology*, *198*(5), 2182–2190. https://doi.org/10.4049/jimmunol.1601480

Ponath, G., Park, C., & Pitt, D. (2018). The role of astrocytes in multiple sclerosis. *Frontiers in Immunology*, *9*(FEB), 1–12. https://doi.org/10.3389/fimmu.2018.00217

Porollo, A. A., Adamczak, R., & Meller, J. (2004). POLYVIEW: A flexible visualization tool for structural and functional annotations of proteins. *Bioinformatics*, *20*(15), 2460–2462. https://doi.org/10.1093/bioinformatics/bth248

Price, E. R., Jin, M., Lim, D., Pati, S., Walsh, C. T., & McKeon, F. D. (1994). Cyclophilin B trafficking through the secretory pathway is altered by binding of cyclosporin A. *Proceedings of the National Academy of Sciences*, *91*(9), 3931–3935. https://doi.org/10.1073/pnas.91.9.3931

Radaeva, S., Sun, R., Pan, H.-N., Hong, F., & Gao, B. (2004). Interleukin 22 (IL-22) plays a protective role in T cell-mediated murine hepatitis: IL-22 is a survival factor for hepatocytes via STAT3 activation. *Hepatology*, *39*(5), 1332–1342. https://doi.org/10.1002/hep.20184

Rajendran, V., Kalita, P., Shukla, H., Kumar, A., & Tripathi, T. (2018). Aminoacyl-tRNA synthetases: Structure, function, and drug discovery. *International Journal of Biological Macromolecules*, *111*, 400–414. https://doi.org/10.1016/j.ijbiomac.2017.12.157

Ramensky, V. (2002). Human non-synonymous SNPs: server and survey. *Nucleic Acids Research*, *30*(17), 3894–3900. https://doi.org/10.1093/nar/gkf493

Randow, F., & Seed, B. (2001). Endoplasmic reticulum chaperone gp96 is required for innate immunity but not cell viability. *Nature Cell Biology*, *3*(10), 891–896. https://doi.org/10.1038/ncb1001-891

Raphael, I., Nalawade, S., Eagar, T. N., & Forsthuber, T. G. (2015). T cell subsets and their signature cytokines in autoimmune and inflammatory diseases. *Cytokine*, *74*(1), 5–17. https://doi.org/10.1016/j.cyto.2014.09.011

Reitberger, S., Haimerl, P., Aschenbrenner, I., Esser-von Bieren, J., & Feige, M. J. (2017). Assembly-induced folding regulates interleukin 12 biogenesis and secretion. *Journal of Biological Chemistry*, *292*(19), 8073–8081. https://doi.org/10.1074/jbc.M117.782284

Relloso, M., Puig-Kroger, A., Pello, O. M., Rodriguez-Fernandez, J. L., de la Rosa, G., Longo, N., Navarro, J., Munoz-Fernandez, M. A., Sanchez-Mateos, P., Corbi, A. L., Puig-Kröger, A., Pello, O. M., Rodríguez-Fernández, J. L., de la Rosa, G., Longo, N., Navarro, J., Muñoz-Fernández, M. A., Sánchez-Mateos, P., & Corbí, A. L. (2002). DC-SIGN (CD209)

expression is IL-4 dependent and is negatively regulated by IFN, TGF-beta, and anti-inflammatory agents. *Journal of Immunology (Baltimore, Md. : 1950)*, *168*(6), 2634–2643. https://doi.org/10.4049/jimmunol.168.6.2634

Renauld, J.-C. (2003). Class II cytokine receptors and their ligands: Key antiviral and inflammatory modulators. *Nature Reviews Immunology*, *3*(8), 667–676. https://doi.org/10.1038/nri1153

Rentzsch, P., Witten, D., Cooper, G. M., Shendure, J., & Kircher, M. (2019). CADD: predicting the deleteriousness of variants throughout the human genome. *Nucleic Acids Research*, *47*(D1), D886–D894. https://doi.org/10.1093/nar/gky1016

Reva, B., Antipin, Y., & Sander, C. (2011). Predicting the functional impact of protein mutations: application to cancer genomics. *Nucleic Acids Research*, *39*(17), e118–e118. https://doi.org/10.1093/nar/gkr407

Rivas, A., Vidal, R. L., & Hetz, C. (2015). Targeting the unfolded protein response for disease intervention. *Expert Opinion on Therapeutic Targets*, *19*(9), 1203–1218. https://doi.org/10.1517/14728222.2015.1053869

Robertson, F. C., Berzofsky, J. A., & Terabe, M. (2014). NKT cell networks in the regulation of tumor immunity. *Frontiers in Immunology*, *5*(OCT), 1–12. https://doi.org/10.3389/fimmu.2014.00543

Robertson, N. P., Fraser, M., Deans, J., Clayton, D., Walker, N., & Compston, D. A. S. (1996). Age-adjusted recurrence risks for relatives of patients with multiple sclerosis. *Brain*, *119*(2), 449–455. https://doi.org/10.1093/brain/119.2.449

Rolla, S., Bardina, V., De Mercanti, S., Quaglino, P., De Palma, R., Gned, D., Brusa, D., Durelli, L., Novelli, F., & Clerico, M. (2014). Th22 cells are expanded in multiple sclerosis and are resistant to IFN- . *Journal of Leukocyte Biology*, *96*(6), 1155–1164. https://doi.org/10.1189/jlb.5A0813-463RR

Romero, R., Erez, O., Maymon, E., Chaemsaithong, P., Xu, Z., Pacora, P., Chaiworapongsa, T., Done, B., Hassan, S. S., & Tarca, A. L. (2017). The maternal plasma proteome changes as a function of gestational age in normal pregnancy: a longitudinal study. *American Journal of Obstetrics and Gynecology*, *217*(1), 67.e1-67.e21. https://doi.org/10.1016/j.ajog.2017.02.037

Rosati, G. (2001). The prevalence of multiple sclerosis in the world: An update. *Neurological Sciences*, *22*(2), 117–139. https://doi.org/10.1007/s100720170011

Rose, A. S., Bradley, A. R., Valasatava, Y., Duarte, J. M., Prlić, A., & Rose, P. W. (2018). NGL viewer: web-based molecular graphics for large complexes. *Bioinformatics*, *34*(21), 3755–3758. https://doi.org/10.1093/bioinformatics/bty419

Roy, A., Kucukural, A., & Zhang, Y. (2010). I-TASSER: a unified platform for automated protein

structure and function prediction. *Nature Protocols*, *5*(4), 725–738. https://doi.org/10.1038/nprot.2010.5

Rutz, S., Eidenschenk, C., & Ouyang, W. (2013). IL-22, not simply a Th17 cytokine. *Immunological Reviews*, *252*(1), 116–132. https://doi.org/10.1111/imr.12027

Rutz, S., Wang, X., & Ouyang, W. (2014). The IL-20 subfamily of cytokines — from host defence to tissue homeostasis. *Nature Reviews Immunology*, *14*(12), 783–795. https://doi.org/10.1038/nri3766

Sa, S. M., Valdez, P. A., Wu, J., Jung, K., Zhong, F., Hall, L., Kasman, I., Winer, J., Modrusan, Z., Danilenko, D. M., & Ouyang, W. (2007). The effects of IL-20 subfamily cytokines on reconstituted human epidermis suggest potential roles in cutaneous innate defense and pathogenic adaptive immunity in psoriasis. *Journal of Immunology (Baltimore, Md. : 1950)*, *178*(4), 2229–2240. https://doi.org/10.4049/jimmunol.178.4.2229

Sabat, R., Ouyang, W., & Wolk, K. (2013). Therapeutic opportunities of the IL-22–IL-22R1 system. *Nature Reviews Drug Discovery*, *13*(1), 21–38. https://doi.org/10.1038/nrd4176

Sadovnick, A. D., Armstrong, H. ., Rice, G. P. A. ., Bulman, D. ., Hashimoto, L. ., Paty, D. W. ., Hashimoto, S. A. ., Warren, S. ., Hader, W. ., Murray, T. J. ., Seland, T. P. ., Metz, L. ., Bell, R. ., Duquette, P. ., Gray, T. ., Nelson, R., & Weinshenker B, Brunet D, E. G. (1993). A Population-Based Study of Multiple Sclerosis in Twins. *Annals of Neurology*, *33*, 281–285. https://doi.org/10.1056/NEJM198612253152603

Sadovnick, A. D., & Baird, P. A. (1988). The familial nature of multiple sclerosis: age-corrected empiric recurrence risks for children and siblings of patients. *Neurology*, *38*(6), 990–991.

Sadovnick, A. D., & Macleod, P. M. (1981). The familial nature of multiple sclerosis: empiric recurrence risks for first, second-, and third-degree relatives of patients. *Neurology*, *31*(8), 1039–1041. Retrieved from http://www.ncbi.nlm.nih.gov/pubmed/3368082

Sakamoto, K., Kim, Y.-G., Hara, H., Kamada, N., Caballero-Flores, G., Tolosano, E., Soares, M. P., Puente, J. L., Inohara, N., & Núñez, G. (2017). IL-22 controls iron-dependent nutritional immunity against systemic bacterial infections. *Science Immunology*, *2*(8), eaai8371. https://doi.org/10.1126/sciimmunol.aai8371

Sanos, S. L., Bui, V. L., Mortha, A., Oberle, K., Heners, C., Johner, C., & Diefenbach, A. (2009). RORgammat and commensal microflora are required for the differentiation of mucosal interleukin 22-producing NKp46+ cells. *Nature Immunology*, *10*(1), 83–91. https://doi.org/10.1038/ni.1684

Savage, A. K., Liang, H.-E., & Locksley, R. M. (2017). The Development of Steady-State Activation Hubs between Adult LTi ILC3s and Primed Macrophages in Small Intestine. *The Journal of Immunology*, *199*(5), 1912–1922. https://doi.org/10.4049/jimmunol.1700155

Sawcer, S. (2008). The complex genetics of multiple sclerosis: Pitfalls and prospects. *Brain*, *131*(12), 3118–3131. https://doi.org/10.1093/brain/awn081

Sawcer, S., Franklin, R. J. M., & Ban, M. (2014). Multiple sclerosis genetics. *The Lancet Neurology*, *13*(7), 700–709. https://doi.org/10.1016/S1474-4422(14)70041-9

Sawcer, S., Hellenthal, G., Pirinen, M., Spencer, C. C. A., Patsopoulos, N. A., Moutsianas, L., Dilthey, A., Su, Z., Freeman, C., Hunt, S. E., Edkins, S., Gray, E., Booth, D. R., Potter, S. C., Goris, A., Band, G., Bang Oturai, A., Strange, A., Saarela, J., Bellenguez, C., Fontaine, B., Gillman, M., Hemmer, B., Gwilliam, R., Zipp, F., Jayakumar, A., Martin, R., Leslie, S., Hawkins, S., Giannoulatou, E., D'alfonso, S., Blackburn, H., Martinelli Boneschi, F., Liddle, J., Harbo, H. F., Perez, M. L., Spurkland, A., Waller, M. J., Mycko, M. P., Ricketts, M., Comabella, M., Hammond, N., Kockum, I., McCann, O. T., Ban, M., Whittaker, P., Kemppinen, A., Weston, P., Hawkins, C., Widaa, S., Zajicek, J., Dronov, S., Robertson, N., Bumpstead, S. J., Barcellos, L. F., Ravindrarajah, R., Abraham, R., Alfredsson, L., Ardlie, K., Aubin, C., Baker, A., Baker, K., Baranzini, S. E., Bergamaschi, L., Bergamaschi, R., Bernstein, A., Berthele, A., Boggild, M., Bradfield, J. P., Brassat, D., Broadley, S. A., Buck, D., Butzkueven, H., Capra, R., Carroll, W. M., Cavalla, P., Celius, E. G., Cepok, S., Chiavacci, R., Clerget-Darpoux, F., Clysters, K., Comi, G., Cossburn, M., Cournu-Rebeix, I., Cox, M. B., Cozen, W., Cree, B. A. C., Cross, A. H., Cusi, D., Daly, M. J., Davis, E., de Bakker, P. I. W., Debouverie, M., D'hooghe, M. B., Dixon, K., Dobosi, R., Dubois, B., Ellinghaus, D., Elovaara, I., Esposito, F., Fontenille, C., Foote, S., Franke, A., Galimberti, D., Ghezzi, A., Glessner, J., Gomez, R., Gout, O., Graham, C., Grant, S. F. A., Rosa Guerini, F., Hakonarson, H., Hall, P., Hamsten, A., Hartung, H.-P., Heard, R. N., Heath, S., Hobart, J., Hoshi, M., Infante-Duarte, C., Ingram, G., Ingram, W., Islam, T., Jagodic, M., Kabesch, M., Kermode, A. G., Kilpatrick, T. J., Kim, C., Klopp, N., Koivisto, K., Larsson, M., Lathrop, M., Lechner-Scott, J. S., Leone, M. A., Leppä, V., Liljedahl, U., Lima Bomfim, I., Lincoln, R. R., Link, J., Liu, J., Lorentzen, Å. R., Lupoli, S., Macciardi, F., Mack, T., Marriott, M., Martinelli, V., Mason, D., McCauley, J. L., Mentch, F., Mero, I.-L., Mihalova, T., Montalban, X., Mottershead, J., Myhr, K.-M., Naldi, P., Ollier, W., Page, A., Palotie, A., Pelletier, J., Piccio, L., Pickersgill, T., Piehl, F., Pobywajlo, S., Quach, H. L., Ramsay, P. P., Reunanen, M., Reynolds, R., Rioux, J. D., Rodegher, M., Roesner, S., Rubio, J. P., Rückert, I.-M., Salvetti, M., Salvi, E., Santaniello, A., Schaefer, C. A., Schreiber, S., Schulze, C., Scott, R. J., Sellebjerg, F., Selmaj, K. W., Sexton, D., Shen, L., Simms-Acuna, B., Skidmore, S., Sleiman, P. M. A., Smestad, C., Sørensen, P. S., Søndergaard, H. B., Stankovich, J., Strange, R. C., Sulonen, A.-M., Sundqvist, E., Syvänen, A.-C., Taddeo, F., Taylor, B., Blackwell, J. M., Tienari, P., Bramon, E., Tourbah, A., Brown, M. A., Tronczynska, E., Casas, J. P., Tubridy, N., Corvin, A., Vickery, J., Jankowski, J., Villoslada, P., Markus, H. S., Wang, K., Mathew, C. G., Wason, J., Palmer, C. N. A., Wichmann, H.-E., Plomin, R., Willoughby, E., Rautanen, A., Winkelmann, J., Wittig, M., Trembath, R. C., Yaouanq, J., Viswanathan, A. C., Zhang, H., Wood, N. W., Zuvich, R., Deloukas, P., Langford, C., Duncanson, A., Oksenberg, J. R., Pericak-Vance, M. A., Haines, J. L., Olsson, T., Hillert, J., Ivinson, A. J., De Jager, P. L., Peltonen, L., Stewart, G. J., Hafler, D. A., Hauser, S. L., McVean, G., Donnelly, P., & Compston, A. (2011). Genetic risk and a primary role for cell-mediated immune mechanisms in multiple sclerosis. *Nature*, *476*(7359), 214–219.

https://doi.org/10.1038/nature10251

Schaefer, L. (2014). Complexity of danger: The diverse nature of damage-associated molecular patterns. *Journal of Biological Chemistry*, *289*(51), 35237–35245. https://doi.org/10.1074/jbc.R114.619304

Schaid, D. J., Chen, W., & Larson, N. B. (2018). From genome-wide associations to candidate causal variants by statistical fine-mapping. *Nature Reviews Genetics*, *19*(8), 491–504. https://doi.org/10.1038/s41576-018-0016-z

Schmechel, S., Konrad, A., Diegelmann, J., Glas, J., Wetzke, M., Paschos, E., Lohse, P., Göke, B., & Brand, S. (2008). Linking genetic susceptibility to Crohn's disease with Th17 cell function: IL-22 serum levels are increased in Crohn's disease and correlate with disease activity and IL23R genotype status. *Inflammatory Bowel Diseases*, *14*(2), 204–212. https://doi.org/10.1002/ibd.20315

Sekikawa, A., Fukui, H., Suzuki, K., Karibe, T., Fujii, S., Ichikawa, K., Tomita, S., Imura, J., Shiratori, K., Chiba, T., & Fujimori, T. (2010). Involvement of the IL-22/REG Iα axis in ulcerative colitis. *Laboratory Investigation*, *90*(3), 496–505. https://doi.org/10.1038/labinvest.2009.147

Sertorio, M., Hou, X., Carmo, R. F., Dessein, H., Cabantous, S., Abdelwahed, M., Romano, A., Albuquerque, F., Vasconcelos, L., Carmo, T., Li, J., Varoquaux, A., Arnaud, V., Oliveira, P., Hamdoun, A., He, H., Adbelmaboud, S., Mergani, A., Zhou, J., Monis, A., Pereira, L. B., Halfon, P., Bourlière, M., Parana, R., dos Reis, M., Gonnelli, D., Moura, P., Elwali, N. E., Argiro, L., Li, Y., & Dessein, A. (2015). IL-22 and IL-22 binding protein (IL-22BP) regulate fibrosis and cirrhosis in hepatitis C virus and schistosome infections. *Hepatology*, *61*(4), 1321–1331. https://doi.org/10.1002/hep.27629

Sheikh, F., Baurin, V. V., Lewis-Antes, A., Shah, N. K., Smirnov, S. V., Anantha, S., Dickensheets, H., Dumoutier, L., Renauld, J.-C., Zdanov, A., Donnelly, R. P., & Kotenko, S. V. (2004). Cutting Edge: IL-26 Signals through a Novel Receptor Complex Composed of IL-20 Receptor 1 and IL-10 Receptor 2. *The Journal of Immunology*, *172*(4), 2006–2010. https://doi.org/10.4049/jimmunol.172.4.2006

Shental-Bechor, D., & Levy, Y. (2008). Effect of glycosylation on protein folding: A close look at thermodynamic stabilization. *Proceedings of the National Academy of Sciences*, *105*(24), 8256–8261. https://doi.org/10.1073/pnas.0801340105

Shevchenko, A., Wilm, M., Vorm, O., & Mann, M. (1996). Mass Spectrometric Sequencing of Proteins from Silver-Stained Polyacrylamide Gels. *Analytical Chemistry*, *68*(5), 850–858. https://doi.org/10.1021/ac950914h

Shioya, M., Andoh, A., Kakinoki, S., Nishida, A., & Fujiyama, Y. (2008). Interleukin 22 receptor 1 expression in pancreas islets. *Pancreas*, *36*(2), 197–199.

https://doi.org/10.1097/MPA.0b013e3181594258

Shishido, S. N., Varahan, S., Yuan, K., Li, X., & Fleming, S. D. (2012). Humoral innate immune response and disease. *Clinical Immunology*, *144*(2), 142–158. https://doi.org/10.1016/j.clim.2012.06.002

Sievers, F., Wilm, A., Dineen, D., Gibson, T. J., Karplus, K., Li, W., Lopez, R., McWilliam, H., Remmert, M., Söding, J., Thompson, J. D., & Higgins, D. G. (2011). Fast, scalable generation of high-quality protein multiple sequence alignments using Clustal Omega. *Molecular Systems Biology*, *7*(1), 539. https://doi.org/10.1038/msb.2011.75

Simpson, S., Blizzard, L., Otahal, P., Van Der Mei, I., & Taylor, B. (2011). Latitude is significantly associated with the prevalence of multiple sclerosis: A meta-analysis. *Journal of Neurology, Neurosurgery and Psychiatry*, *82*(10), 1132–1141. https://doi.org/10.1136/jnnp.2011.240432

Smith, M. H., Ploegh, H. L., & Weissman, J. S. (2011). Road to Ruin: Targeting Proteins for Degradation in the Endoplasmic Reticulum. *Science*, *334*(6059), 1086–1090. https://doi.org/10.1126/science.1209235

Smolen, J. S., Aletaha, D., Barton, A., Burmester, G. R., Emery, P., Firestein, G. S., Kavanaugh, A., McInnes, I. B., Solomon, D. H., Strand, V., & Yamamoto, K. (2018). Rheumatoid arthritis. *Nature Reviews Disease Primers*, *4*, 1–23. https://doi.org/10.1038/nrdp.2018.1

Snijders, A., Kalinski, P., Hilkens, C. M., & Kapsenberg, M. L. (1998). High-level IL-12 production by human dendritic cells requires two signals. *International Immunology*, *10*(11), 1593–1598. https://doi.org/10.1093/intimm/10.11.1593

Sokol, C. L., & Luster, A. D. (2015). The Chemokine System in Innate Immunity. *Cold Spring Harbor Perspectives in Biology*, *7*(5), a016303. https://doi.org/10.1101/cshperspect.a016303

Spencer, L. A., Melo, R. C. N., Perez, S. A. C., Bafford, S. P., Dvorak, A. M., & Weller, P. F. (2006). Cytokine receptor-mediated trafficking of preformed IL-4 in eosinophils identifies an innate immune mechanism of cytokine secretion. *Proceedings of the National Academy of Sciences*, *103*(9), 3333–3338. https://doi.org/10.1073/pnas.0508946103

Spits, H., Artis, D., Colonna, M., Diefenbach, A., Di Santo, J. P., Eberl, G., Koyasu, S., Locksley, R. M., McKenzie, A. N. J., Mebius, R. E., Powrie, F., & Vivier, E. (2013). Innate lymphoid cells-a proposal for uniform nomenclature. *Nature Reviews Immunology*, *13*(2), 145–149. https://doi.org/10.1038/nri3365

Spits, H., & Cupedo, T. (2012). Innate Lymphoid Cells: Emerging Insights in Development, Lineage Relationships, and Function. *Annual Review of Immunology*, *30*(1), 647–675. https://doi.org/10.1146/annurev-immunol-020711-075053

Stocki, P., Chapman, D. C., Beach, L. A., & Williams, D. B. (2014). Depletion of cyclophilins B and C Leads to dysregulation of endoplasmic reticulum redox homeostasis. *Journal of*

Biological Chemistry, *289*(33), 23086–23096. https://doi.org/10.1074/jbc.M114.570911

Stone, E. A., & Sidow, A. (2005). Physicochemical constraint violation by missense substitutions mediates impairment of protein function and disease severity. *Genome Research*, *15*(7), 978–986. https://doi.org/10.1101/gr.3804205

Stone, K. D., Prussin, C., & Metcalfe, D. D. (2010). IgE, mast cells, basophils, and eosinophils. *Journal of Allergy and Clinical Immunology*, *125*(2), S73–S80. https://doi.org/10.1016/j.jaci.2009.11.017

Støy, S., Laursen, T. L., Glavind, E., Eriksen, P. L., Terczynska-Dyla, E., Magnusson, N. E., Hamilton-Dutoit, S., Mortensen, F. V., Veidal, S. S., Rigbolt, K., Riggio, O., Deleuran, B., Vilstrup, H., & Sandahl, T. D. (2020). Low Interleukin-22 Binding Protein Is Associated With High Mortality in Alcoholic Hepatitis and Modulates Interleukin-22 Receptor Expression. *Clinical and Translational Gastroenterology*, *11*(8), e00197. https://doi.org/10.14309/ctg.0000000000000197

Sugimoto, K., Ogawa, A., Mizoguchi, E., Shimomura, Y., Andoh, A., Bhan, A. K., Blumberg, R. S., Xavier, R. J., & Mizoguchi, A. (2008). IL-22 ameliorates intestinal inflammation in a mouse model of ulcerative colitis. *Journal of Clinical Investigation*, *118*(2), 534–544. https://doi.org/10.1172/JCI33194

Sutton, C. E., Lalor, S. J., Sweeney, C. M., Brereton, C. F., Lavelle, E. C., & Mills, K. H. G. (2009). Interleukin-1 and IL-23 Induce Innate IL-17 Production from γδ T Cells, Amplifying Th17 Responses and Autoimmunity. *Immunity*, *31*(2), 331–341. https://doi.org/10.1016/j.immuni.2009.08.001

Symoens, S., Malfait, F., Renard, M., André, J., Hausser, I., Loeys, B., Coucke, P., & De Paepe, A. (2009). COL5A1 signal peptide mutations interfere with protein secretion and cause classic Ehlers-Danlos syndrome. *Human Mutation*, *30*(2), 395–403. https://doi.org/10.1002/humu.20887

The International Multiple Sclerosis Genetics Consortium (IMSGC). (2010). Evidence for Polygenic Susceptibility to Multiple Sclerosis-The Shape of Things to Come. *American Journal of Human Genetics*, *86*(4), 621–625. https://doi.org/10.1016/j.ajhg.2010.02.027

The International Multiple Sclerosis Genetics Consortium (IMSGC). (2019a). A systems biology approach uncovers cell-specific gene regulatory effects of genetic associations in multiple sclerosis. *Nature Communications*, *10*(1), 2236. https://doi.org/10.1038/s41467-019-09773-y

The International Multiple Sclerosis Genetics Consortium (IMSGC). (2019b). Multiple sclerosis genomic map implicates peripheral immune cells and microglia in susceptibility. *Science*, *365*(6460), eaav7188. https://doi.org/10.1126/science.aav7188

The UniProt Consortium. (2019). UniProt: a worldwide hub of protein knowledge. *Nucleic Acids*

Research, *47*(D1), D506–D515. https://doi.org/10.1093/nar/gky1049

Thessen Hedreul, M., Gillett, A., Olsson, T., Jagodic, M., & Harris, R. A. (2009). Characterization of Multiple Sclerosis candidate gene expression kinetics in rat experimental autoimmune encephalomyelitis. *Journal of Neuroimmunology*, *210*(1–2), 30–39. https://doi.org/10.1016/j.jneuroim.2009.02.010

Thomas, P. D., & Kejariwal, A. (2004). Coding single-nucleotide polymorphisms associated with complex vs. Mendelian disease: Evolutionary evidence for differences in molecular effects. *Proceedings of the National Academy of Sciences*, *101*(43), 15398–15403. https://doi.org/10.1073/pnas.0404380101

Thompson, C. L., Plummer, S. J., Tucker, T. C., Casey, G., & Li, L. (2010). Interleukin-22 genetic polymorphisms and risk of colon cancer. *Cancer Causes & Control*, *21*(8), 1165–1170. https://doi.org/10.1007/s10552-010-9542-5

Trevejo-Nunez, G., Elsegeiny, W., Aggor, F. E. Y., Tweedle, J. L., Kaplan, Z., Gandhi, P., Castillo, P., Ferguson, A., Alcorn, J. F., Chen, K., Kolls, J. K., & Gaffen, S. L. (2019). Interleukin-22 (IL-22) Binding Protein Constrains IL-22 Activity, Host Defense, and Oxidative Phosphorylation Genes during Pneumococcal Pneumonia. *Infection and Immunity*, *87*(11), 1–11. https://doi.org/10.1128/IAI.00550-19

Trifari, S., Kaplan, C. D., Tran, E. H., Crellin, N. K., & Spits, H. (2009). Identification of a human helper T cell population that has abundant production of interleukin 22 and is distinct from TH-17, TH1 and TH2 cells. *Nature Immunology*, *10*(8), 864–871. https://doi.org/10.1038/ni.1770

Trivella, D. B. B., Ferreira-Júnior, J. R., Dumoutier, L., Renauld, J.-C., & Polikarpov, I. (2010). Structure and function of interleukin-22 and other members of the interleukin-10 family. *Cellular and Molecular Life Sciences*, *67*(17), 2909–2935. https://doi.org/10.1007/s00018-010-0380-0

Uhlen, M., Fagerberg, L., Hallstrom, B. M., Lindskog, C., Oksvold, P., Mardinoglu, A., Sivertsson, A., Kampf, C., Sjostedt, E., Asplund, A., Olsson, I., Edlund, K., Lundberg, E., Navani, S., Szigyarto, C. A.-K., Odeberg, J., Djureinovic, D., Takanen, J. O., Hober, S., Alm, T., Edqvist, P.-H., Berling, H., Tegel, H., Mulder, J., Rockberg, J., Nilsson, P., Schwenk, J. M., Hamsten, M., von Feilitzen, K., Forsberg, M., Persson, L., Johansson, F., Zwahlen, M., von Heijne, G., Nielsen, J., & Ponten, F. (2015). Tissue-based map of the human proteome. *Science*, *347*(6220), 1260419–1260419. https://doi.org/10.1126/science.1260419

van der Lee, R., Buljan, M., Lang, B., Weatheritt, R. J., Daughdrill, G. W., Dunker, A. K., Fuxreiter, M., Gough, J., Gsponer, J., Jones, D. T., Kim, P. M., Kriwacki, R. W., Oldfield, C. J., Pappu, R. V., Tompa, P., Uversky, V. N., Wright, P. E., & Babu, M. M. (2014). Classification of Intrinsically Disordered Regions and Proteins. *Chemical Reviews*, *114*(13), 6589–6631. https://doi.org/10.1021/cr400525m

Vandenbroeck, K., Alvarez, J., Swaminathan, B., Alloza, I., Matesanz, F., Urcelay, E., Comabella, M., Alcina, A., Fedetz, M., Ortiz, M. A., Izquierdo, G., Fernandez, O., Rodriguez-Ezpeleta, N., Matute, C., Caillier, S., Arroyo, R., Montalban, X., Oksenberg, J. R., Antigüedad, A., & Aransay, A. (2012). A cytokine gene screen uncovers SOCS1 as genetic risk factor for multiple sclerosis. *Genes and Immunity*, *13*(1), 21–28. https://doi.org/10.1038/gene.2011.44

Vandenbroeck, Koen, Martens, E., & Alloza, I. (2006). Multi-chaperone complexes regulate the folding of interferon-gamma in the endoplasmic reticulum. *Cytokine*, *33*(5), 264–273. https://doi.org/10.1016/j.cyto.2006.02.004

Vantourout, P., & Hayday, A. (2013). Six-of-the-best: Unique contributions of γδ T cells to immunology. *Nature Reviews Immunology*, *13*(2), 88–100. https://doi.org/10.1038/nri3384

Vilariño-Güell, C., Zimprich, A., Martinelli-Boneschi, F., Herculano, B., Wang, Z., Matesanz, F., Urcelay, E., Vandenbroeck, K., Leyva, L., Gris, D., Massaad, C., Quandt, J. A., Traboulsee, A. L., Encarnacion, M., Bernales, C. Q., Follett, J., Yee, I. M., Criscuoli, M. G., Deutschländer, A., Reinthaler, E. M., Zrzavy, T., Mascia, E., Zauli, A., Esposito, F., Alcina, A., Izquierdo, G., Espino-Paisán, L., Mena, J., Antigüedad, A., Urbaneja-Romero, P., Ortega-Pinazo, J., Song, W., & Sadovnick, A. D. (2019). *Exome sequencing in multiple sclerosis families identifies 12 candidate genes and nominates biological pathways for the genesis of disease*. *PLoS Genetics* (Vol. 15). https://doi.org/10.1371/journal.pgen.1008180

Visscher, P. M., Brown, M. A., McCarthy, M. I., & Yang, J. (2012). Five years of GWAS discovery. *American Journal of Human Genetics*, *90*(1), 7–24. https://doi.org/10.1016/j.ajhg.2011.11.029

Vivier, E., Raulet, D. H., Moretta, A., Caligiuri, M. A., Zitvogel, L., Lanier, L. L., Yokoyama, W. M., & Ugolini, S. (2011). Innate or Adaptive Immunity? The Example of Natural Killer Cells. *Science*, *331*(6013), 44–49. https://doi.org/10.1126/science.1198687

Vliet, S. J. Van, Duijnhoven, G. C. F. Van, Grabovsky, V., Alon, R., Figdor, C. G., & Kooyk, Y. Van. (2000). DC-SIGN – ICAM-2 interaction medi- ates dendritic cell trafficking, *1*(4).

Voglis, S., Moos, S., Kloos, L., Wanke, F., Zayoud, M., Pelczar, P., Giannou, A. D., Pezer, S., Albers, M., Luessi, F., Huber, S., Schäkel, K., & Kurschus, F. C. (2018). Regulation of IL-22BP in psoriasis. *Scientific Reports*, *8*(1), 5085. https://doi.org/10.1038/s41598-018-23510-3

Volpe, E., Servant, N., Zollinger, R., Bogiatzi, S. I., Hupé, P., Barillot, E., & Soumelis, V. (2008). A critical function for transforming growth factor-β, interleukin 23 and proinflammatory cytokines in driving and modulating human TH-17 responses. *Nature Immunology*, *9*(6), 650–657. https://doi.org/10.1038/ni.1613

Wade, R., Di Bernardo, M. C., Richards, S., Rossi, D., Crowther-Swanepoel, D., Gaidano, G., Oscier, D. G., Catovsky, D., & Houlston, R. S. (2011). Association between single nucleotide polymorphism-genotype and outcome of patients with chronic lymphocytic leukemia in a randomized chemotherapy trial. *Haematologica*, *96*(10), 1496–1503.

https://doi.org/10.3324/haematol.2011.043471

Walter, M. R. (2011). Interleukin-26: An IL-10-related cytokine produced by Th17 cells. *Cytokine Growth Factor Rev*, *21*(5), 393–401. https://doi.org/10.1016/j.cytogfr.2010.09.001.Interleukin-26

Wang, B., Han, D., Li, F., Hou, W., Wang, L., Meng, L., Mou, K., Lu, S., Zhu, W., & Zhou, Y. (2020). Elevated IL-22 in psoriasis plays an anti-apoptotic role in keratinocytes through mediating Bcl-xL/Bax. *Apoptosis*, (0123456789). https://doi.org/10.1007/s10495-020-01623-3

Wang, K., Song, F., Fernandez-Escobar, A., Luo, G., Wang, J., & Sun, Y. (2018). The Properties of Cytokine in Multiple Sclerosis: Pros and Cons. *The American Journal of the Medical Sciences*. https://doi.org/10.1016/j.amjms.2018.08.018

Wang, S., Li, W., Liu, S., & Xu, J. (2016). RaptorX-Property: a web server for protein structure property prediction. *Nucleic Acids Research*, *44*(W1), W430–W435. https://doi.org/10.1093/nar/gkw306

Wang, Y., Mumm, J. B., Herbst, R., Kolbeck, R., & Wang, Y. (2017). IL-22 Increases Permeability of Intestinal Epithelial Tight Junctions by Enhancing Claudin-2 Expression. *The Journal of Immunology*, *199*(9), 3316–3325. https://doi.org/10.4049/jimmunol.1700152

Watanabe, L., de Moura, P. R., Nascimento, A. S., Colau, D., Dumoutier, L., Renauld, J. C., & Polikarpov, I. (2009). Crystallization and preliminary X-ray diffraction analysis of human IL-22 bound to its soluble decoy receptor IL-22BP. *Acta Crystallographica. Section F, Structural Biology and Crystallization Communications*, *65*(Pt 2), 102–104. https://doi.org/10.1107/S1744309108042309

Watchmaker, P. B., Lahl, K., Lee, M., Baumjohann, D., Morton, J., Kim, S. J., Zeng, R., Dent, A., Ansel, K. M., Diamond, B., Hadeiba, H., & Butcher, E. C. (2014). Comparative transcriptional and functional profiling defines conserved programs of intestinal DC differentiation in humans and mice. *Nature Immunology*, *15*(1), 98–108. https://doi.org/10.1038/ni.2768

Weathington, N. M., Snavely, C. A., Chen, B. B., Zhao, J., Zhao, Y., & Mallampalli, R. K. (2014). Glycogen synthase kinase-3?? stabilizes the interleukin (IL)-22 receptor from proteasomal degradation in murine lung epithelia. *Journal of Biological Chemistry*, *289*(25), 17610–17619. https://doi.org/10.1074/jbc.M114.551747

Weber, G. F., Schlautkötter, S., Kaiser-Moore, S., Altmayr, F., Holzmann, B., & Weighardt, H. (2007). Inhibition of interleukin-22 attenuates bacterial load and organ failure during acute polymicrobial sepsis. *Infection and Immunity*, *75*(4), 1690–1697. https://doi.org/10.1128/IAI.01564-06

Wei, C.-C., Ho, T.-W., Liang, W.-G., Chen, G.-Y., & Chang, M.-S. (2003). Cloning and characterization of mouse IL-22 binding protein. *Genes & Immunity*, *4*(3), 204–211. https://doi.org/10.1038/sj.gene.6363947

Wei, J., Gaut, J. R., & Hendershot, L. M. (1995). In vitro dissociation of BiP-peptide complexes requires a conformational change in BiP after ATP binding but does not require ATP hydrolysis. *Journal of Biological Chemistry*, *270*(44), 26677–26682. https://doi.org/10.1074/jbc.270.44.26677

Weiss, B., Wolk, K., Grünberg, B. H., Volk, H.-D., Sterry, W., Asadullah, K., & Sabat, R. (2004). Cloning of murine IL-22 receptor alpha 2 and comparison with its human counterpart. *Genes and Immunity*, *5*(5), 330–336. https://doi.org/10.1038/sj.gene.6364104

Whittington, H. A., Armstrong, L., Uppington, K. M., & Millar, A. B. (2004). Interleukin-22: a potential immunomodulatory molecule in the lung. *American Journal of Respiratory Cell and Molecular Biology*, *31*(2), 220–226. https://doi.org/10.1165/rcmb.2003-0285OC

Willer, C. J., Dyment, D. A., Risch, N. J., Sadovnick, A. D., & Ebers, G. C. (2003). Twin concordance and sibling recurrence rates in multiple sclerosis. *Proceedings of the National Academy of Sciences*, *100*(22), 12877–12882. https://doi.org/10.1073/pnas.1932604100

Williams, D. B. (2006). Beyond lectins: the calnexin/calreticulin chaperone system of the endoplasmic reticulum. *Journal of Cell Science*, *119*(Pt 4), 615–623. https://doi.org/10.1242/jcs.02856

Wolfram, L., Fischbeck, A., Frey-Wagner, I., Wojtal, K. A., Lang, S., Fried, M., Vavricka, S. R., Hausmann, M., & Rogler, G. (2013). Regulation of the Expression of Chaperone gp96 in Macrophages and Dendritic Cells. *PLoS ONE*, *8*(10), e76350. https://doi.org/10.1371/journal.pone.0076350

Wolk, K., Haugen, H. S., Xu, W., Witte, E., Waggie, K., Anderson, M., Vom Baur, E., Witte, K., Warszawska, K., Philipp, S., Johnson-Leger, C., Volk, H. D., Sterry, W., & Sabat, R. (2009). IL-22 and IL-20 are key mediators of the epidermal alterations in psoriasis while IL-17 and IFN-γ are not. *Journal of Molecular Medicine*, *87*(5), 523–536. https://doi.org/10.1007/s00109-009-0457-0

Wolk, K., Kunz, S., Asadullah, K., & Sabat, R. (2002). Cutting Edge: Immune Cells as Sources and Targets of the IL-10 Family Members? *The Journal of Immunology*, *168*(11), 5397–5402. https://doi.org/10.4049/jimmunol.168.11.5397

Wolk, K., Kunz, S., Witte, E., Friedrich, M., Asadullah, K., & Sabat, R. (2004). IL-22 Increases the Innate Immunity of Tissues. *Immunity*, *21*(2), 241–254. https://doi.org/10.1016/j.immuni.2004.07.007

Wolk, K., Witte, E., Hoffmann, U., Doecke, W.-D. W.-D. W.-D., Endesfelder, S., Asadullah, K.,

Sterry, W., Volk, H.-D. H.-D. H.-D., Wittig, B. M., & Sabat, R. (2007). IL-22 Induces Lipopolysaccharide-Binding Protein in Hepatocytes: A Potential Systemic Role of IL-22 in Crohn's Disease. *The Journal of Immunology*, *178*(9), 5973–5981. https://doi.org/10.4049/jimmunol.178.9.5973

Wolk, K., Witte, E., Reineke, U., Witte, K., Friedrich, M., Sterry, W., Asadullah, K., Volk, H.-D., & Sabat, R. (2005). Is there an interaction between interleukin-10 and interleukin-22? *Genes & Immunity*, *6*(1), 8–18. https://doi.org/10.1038/sj.gene.6364144

Wolk, K., Witte, E., Wallace, E., Döcke, W.-D., Kunz, S., Asadullah, K., Volk, H.-D., Sterry, W., & Sabat, R. (2006). IL-22 regulates the expression of genes responsible for antimicrobial defense, cellular differentiation, and mobility in keratinocytes: a potential role in psoriasis. *European Journal of Immunology*, *36*(5), 1309–1323. https://doi.org/10.1002/eji.200535503

Wolk, K., Witte, K., Witte, E., Proesch, S., Schulze-Tanzil, G., Nasilowska, K., Thilo, J., Asadullah, K., Sterry, W., Volk, H.-D., & Sabat, R. (2008). Maturing dendritic cells are an important source of IL-29 and IL-20 that may cooperatively increase the innate immunity of keratinocytes. *Journal of Leukocyte Biology*, *83*(5), 1181–1193. https://doi.org/10.1189/jlb.0807525

Wong, C. K., Ho, C. Y., Li, E., & Lam, C. (2000). Elevation of proinflammatory cytokine (IL-18, IL-17, IL-12) and Th2 cytokine (IL-4) concentrations in patients with systemic lupus erythematosus. *Lupus*, *9*(8), 589–593. https://doi.org/10.1191/096120300678828703

Worbs, T., Hammerschmidt, S. I., & Förster, R. (2017). Dendritic cell migration in health and disease. *Nature Reviews Immunology*, *17*(1), 30–48. https://doi.org/10.1038/nri.2016.116

Wu, L.-Y., Liu, S., Liu, Y., Guo, C., Li, H., Li, W., Jin, X., Zhang, K., Zhao, P., Wei, L., & Zhao, J. (2015). Up-regulation of interleukin-22 mediates liver fibrosis via activating hepatic stellate cells in patients with hepatitis C. *Clinical Immunology*, *158*(1), 77–87. https://doi.org/10.1016/j.clim.2015.03.003

Wu, P. W., Li, J., Kodangattil, S. R., Luxenberg, D. P., Bennett, F., Martino, M., Collins, M., Dunussi-Joannopoulos, K., Gill, D. S., Wolfman, N. M., & Fouser, L. A. (2008). IL-22R, IL-10R2, and IL-22BP Binding Sites Are Topologically Juxtaposed on Adjacent and Overlapping Surfaces of IL-22. *Journal of Molecular Biology*, *382*(5), 1168–1183. https://doi.org/10.1016/j.jmb.2008.07.046

Wu, S., Hong, F., Gewirth, D., Guo, B., Liu, B., & Li, Z. (2012). The molecular chaperone gp96/GRP94 interacts with Toll-like receptors and integrins via its C-terminal hydrophobic domain. *The Journal of Biological Chemistry*, *287*(9), 6735–6742. https://doi.org/10.1074/jbc.M111.309526

Xie, M.-H., Aggarwal, S., Ho, W.-H., Foster, J., Zhang, Z., Stinson, J., Wood, W. I., Goddard, A.

D., & Gurney, A. L. (2000). Interleukin (IL)-22, a Novel Human Cytokine That Signals through the Interferon Receptor-related Proteins CRF2–4 and IL-22R. *Journal of Biological Chemistry*, *275*(40), 31335–31339. https://doi.org/10.1074/jbc.M005304200

Xu, T., Logsdon, N. J., & Walter, M. R. (2004). Crystallization and X-ray diffraction analysis of insect-cell-derived IL-22. *Acta Crystallographica Section D: Biological Crystallography*, *60*(7), 1295–1298. https://doi.org/10.1107/S0907444904010492

Xu, T., Logsdon, N. J., & Walter, M. R. (2005). Structure of insect-cell-derived IL-22. *Acta Crystallographica Section D: Biological Crystallography*, *61*(7), 942–950. https://doi.org/10.1107/S0907444905009601

Xu, Wen, Li, R., Dai, Y., Wu, A., Wang, H., Cheng, C., Qiu, W., Lu, Z., Zhong, X., Shu, Y., Kermode, A. G., & Hu, X. (2013). IL-22 secreting CD4+ T cells in the patients with neuromyelitis optica and multiple sclerosis. *Journal of Neuroimmunology*, *261*(1–2), 87–91. https://doi.org/10.1016/j.jneuroim.2013.04.021

Xu, Wenfeng, Presnell, S. R., Parrish-Novak, J., Kindsvogel, W., Jaspers, S., Chen, Z., Dillon, S. R., Gao, Z., Gilbert, T., Madden, K., Schlutsmeyer, S., Yao, L., Whitmore, T. E., Chandrasekher, Y., Grant, F. J., Maurer, M., Jelinek, L., Storey, H., Brender, T., Hammond, A., Topouzis, S., Clegg, C. H., & Foster, D. C. (2001). A soluble class II cytokine receptor, IL-22RA2, is a naturally occurring IL-22 antagonist. *Proceedings of the National Academy of Sciences*, *98*(17), 9511–9516. https://doi.org/10.1073/pnas.171303198

Yam-Puc, J. C., Zhang, L., Zhang, Y., & Toellner, K.-M. (2018). Role of B-cell receptors for B-cell development and antigen-induced differentiation. *F1000Research*, *7*(0), 429. https://doi.org/10.12688/f1000research.13567.1

Yang, X., Gao, Y., Wang, H., Zhao, X., Gong, X., Wang, Q., & Zhang, X. (2014). Increased urinary interleukin 22 binding protein levels correlate with lupus nephritis activity. *Journal of Rheumatology*, *41*(9), 1793–1800. https://doi.org/10.3899/jrheum.131292

Yang, Y., & Li, Z. (2005). Roles of heat shock protein gp96 in the ER quality control: redundant or unique function. *Mol Cells*, *20*(2), 173–182.

Yoon, S. il, Jones, B. C., Logsdon, N. J., Harris, B. D., Deshpande, A., Radaeva, S., Halloran, B. A., Gao, B., & Walter, M. R. (2010). Structure and mechanism of receptor sharing by the IL-10R2 common chain. *Structure*, *18*(5), 638–648. https://doi.org/10.1016/j.str.2010.02.009

Zenewicz, L. A. (2018). IL-22: There Is a Gap in Our Knowledge. *ImmunoHorizons*, *2*(6), 198–207. https://doi.org/10.4049/immunohorizons.1800006

Zenewicz, L. A., Yancopoulos, G. D., Valenzuela, D. M., Murphy, A. J., Stevens, S., & Flavell, R. A. (2008). Innate and Adaptive Interleukin-22 Protects Mice from Inflammatory Bowel Disease. *Immunity*, *29*(6), 947–957. https://doi.org/10.1016/j.immuni.2008.11.003

Zenewicz, L. A., Yin, X., Wang, G., Elinav, E., Hao, L., Zhao, L., & Flavell, R. A. (2013). IL-22 Deficiency Alters Colonic Microbiota To Be Transmissible and Colitogenic. *The Journal of Immunology*, *190*(10), 5306–5312. https://doi.org/10.4049/jimmunol.1300016

Zhang, J., & Herscovitz, H. (2003). Nascent lipidated apolipoprotein B is transported to the Golgi as an incompletely folded intermediate as probed by its association with network of endoplasmic reticulum molecular chaperones, GRP94, ERp72, BiP, calreticulin, and cyclophilin B. *Journal of Biological Chemistry*, *278*(9), 7459–7468. https://doi.org/10.1074/jbc.M207976200

Zhang, L., Li, J. M., Liu, X. G., Ma, D. X., Hu, N. W., Li, Y. G., Li, W., Hu, Y., Yu, S., Qu, X., Yang, M. X., Feng, A. L., & Wang, G. H. (2011). Elevated Th22 cells correlated with Th17 cells in patients with rheumatoid arthritis. *Journal of Clinical Immunology*, *31*(4), 606–614. https://doi.org/10.1007/s10875-011-9540-8

Zhang, W., Chen, Y., Wei, H., Zheng, C., Sun, R., Zhang, J., & Tian, Z. (2008). Antiapoptotic activity of autocrine interleukin-22 and therapeutic effects of interleukin-22-small interfering RNA on human lung cancer xenografts. *Clinical Cancer Research*, *14*(20), 6432–6439. https://doi.org/10.1158/1078-0432.CCR-07-4401

Zhang, Y.-Z., & Shen, H.-B. (2017). Signal-3L 2.0: A Hierarchical Mixture Model for Enhancing Protein Signal Peptide Prediction by Incorporating Residue-Domain Cross-Level Features. *Journal of Chemical Information and Modeling*, *57*(4), 988–999. https://doi.org/10.1021/acs.jcim.6b00484

Zheng, Y., Danilenko, D. M., Valdez, P., Kasman, I., Eastham-Anderson, J., Wu, J., & Ouyang, W. (2007). Interleukin-22, a TH17 cytokine, mediates IL-23-induced dermal inflammation and acanthosis. *Nature*, *445*(7128), 648–651. https://doi.org/10.1038/nature05505

Zheng, Y., Valdez, P. a, Danilenko, D. M., Hu, Y., Sa, S. M., Gong, Q., Abbas, A. R., Modrusan, Z., Ghilardi, N., de Sauvage, F. J., & Ouyang, W. (2008). Interleukin-22 mediates early host defense against attaching and effacing bacterial pathogens. *Nature Medicine*, *14*(3), 282–289. https://doi.org/10.1038/nm1720

Zhong, W., Zhao, L., Liu, T., & Jiang, Z. (2017). IL-22-producing CD4+T cells in the treatment response of rheumatoid arthritis to combination therapy with methotrexate and leflunomide. *Scientific Reports*, *7*(January), 1–11. https://doi.org/10.1038/srep41143

Zhou, L. J., & Tedder, T. F. (1996). CD14+ blood monocytes can differentiate into functionally mature CD83+ dendritic cells. *Proceedings of the National Academy of Sciences*, *93*(6), 2588–2592. https://doi.org/10.1073/pnas.93.6.2588

Zhou, Y., Simpson, S., Holloway, A. F., Charlesworth, J., van der Mei, I., & Taylor, B. V. (2014). The potential role of epigenetic modifications in the heritability of multiple sclerosis. *Multiple Sclerosis Journal*, *20*(2), 135–140. https://doi.org/10.1177/1352458514520911

Zindl, C. L., Lai, J.-F., Lee, Y. K., Maynard, C. L., Harbour, S. N., Ouyang, W., Chaplin, D. D., & Weaver, C. T. (2013). IL-22-producing neutrophils contribute to antimicrobial defense and restitution of colonic epithelial integrity during colitis. *Proceedings of the National Academy of Sciences*, *110*(31), 12768–12773. https://doi.org/10.1073/pnas.1300318110

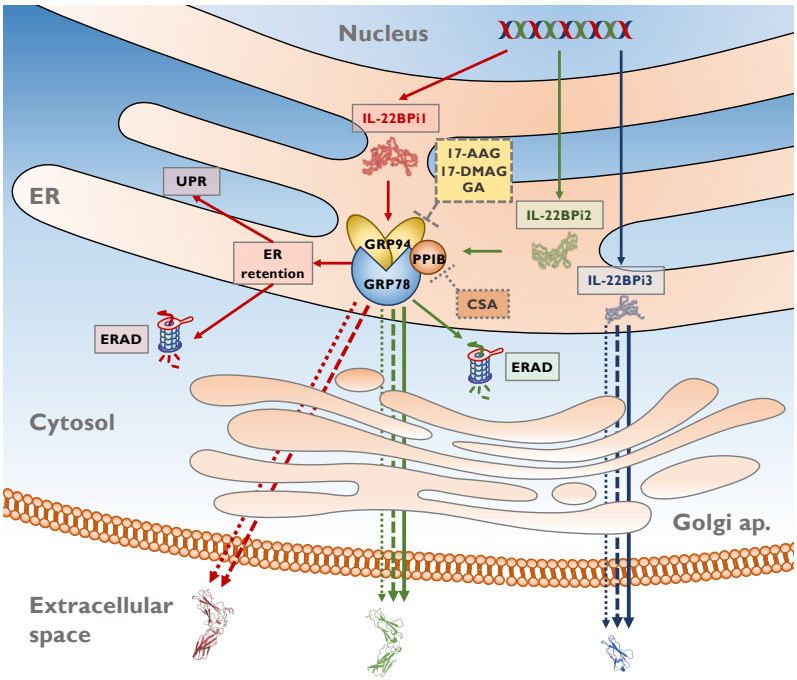

Departamento de Neurociencias, Facultad de Medicina y Enfermería

Universidad del País Vasco, EHU/UPV